The role of PHIST proteins in cytoadherence of *P. falciparum*

INAUGURALDISSERTATION

zur

Erlangung der Würde eines Doktors der Philosophie

vorgelegt der

Philosophisch-Naturwissenschaftlichen Fakultät

der Universität Basel

von

Alexander Oliver Oberli

aus

Münchenstein (BL)

Basel, 2016

Genehmigt von der Philosophisch-Naturwissenschaftlichen Fakultät auf Antrag von Prof. Dr. Hans-Peter Beck und Prof. Dr. Kai Matuschewski

Basel, den 08. Dezember 2015

_____

Prof. Dr. Jörg Schibler
Dekan der Philosophisch-
Naturwissenschaftlichen Fakultät

Summary

Plasmodium falciparum, the causative agent of malaria, is responsible for over half a million deaths each year and approximately 50% of the world population lives in malaria endemic areas. Despite strategies to reduce the burden of infection like transmission control and development of drugs and vaccines, malaria remains a major public health concern.

A characteristic of *P. falciparum* infected red blood cells (iRBC) is the ability to avoid splenic clearance by adhering to the vascular endothelium. This pathologic feature is a major contributor to the severity of malaria tropica and as a consequence of the cytoadherence of iRBCs, a high number of parasites are sequestered to different tissues leading to vascular occlusion and inflammation. The major ligand for this cytoadhesion is the *P. falciparum* erythrocyte membrane protein 1 (PfEMP1), anchored in the erythrocyte membrane in knob structures. The semi-conserved intracellular acidic terminal segment (ATS) domain anchors P*f*EMP1 to the host cell, whereas the highly variable ectodomain is responsible for endothelial receptor binding of iRBCs. Recently, the ATS domain of PfEMP1 was found to be a conserved protein interaction epitope and was shown to interact *in vitro* with the PHIST domain of PFI1780w, a member of the *Plasmodium* helical interspersed sub-telomeric (PHIST) protein family. The initial identification of this large gene family counted 72 paralogs in *P. falciparum*, which are organized into three subgroups (PHISTa, PHISTb, PHISTc). All PHIST proteins contain a conserved domain of approximately 150 amino acids, predicted to consist of four consecutive alpha helices. It is proposed that PHIST domains facilitate protein interactions and that the semi-conserved ATS epitope may be involved in the parasite`s cytoadherence.

To date, little is known about the role of PHIST proteins but recent data indicate that they might be implicated in knob formation, in altered host cell rigidity, in transport of PfEMP1 and in adhesion of iRBCs in the brain microvasculature. Moreover, members of the PHIST family were found to localize to the iRBC periphery, to bind to cytoskeletal components of the host cell, and were found in detergent-resistant membrane fractions indicating an important role of PHIST proteins in host cell refurbishment.

The aim of this thesis was to gain insight into the functional role of a subset of exported PHIST proteins with a focus on PFE1605w, a protein of the PHISTb subclass which showed significant higher binding affinity to PfEMP1 than PFI1780w. By immunofluorescence and

immunoelectron microscopy we were able to show that PFE1605w is exported to the RBC membrane, co-migrates with P*f*EMP1 and localizes to knobs. NMR and fluorescence polarization experiments revealed that its PHIST domain binds directly to the C-terminus of the ATS. Polarization experiments using PFE1605w and a set of ATS domains from different PfEMP1 molecules showed substantial variation in affinity across the different ATS domains, suggesting that different PHIST proteins might have been optimized for interacting with different PfEMP1 variants. Moreover, in collaboration we resolved the first crystallographic structure of a PHIST domain and derived a partial model of the PHIST-PfEMP1 interaction from nuclear magnetic resonance measures.

Inducible down regulation of PFE1605w levels using the FKBP destabilisation domain but also controlled tethering at Maurer's clefts with the knocksideways technique resulted in absence of PFE1605w in knobs and led to strongly reduced adhesion properties of iRBC to the endothelial receptor CD36. To assess the specific selection of a PHIST protein for a particular PfEMP1 molecule, we selected iRBCs through binding to different host receptors thus selectively switching to different PfEMP1 molecules. Interestingly, adhesion to other endothelial receptors was less affected or even unaltered by PFE1605w depletion, suggesting that PFE1605w is optimized for a particular subset of PfEMP1 molecules. Moreover, absence of PFE1605w in knobs did not ablate PfEMP1 surface exposure, thus suggesting no role of PFE1605w in PfEMP1 transport.

Co-immunoprecipitation (Co-IP) assays with two constructs which covered only the C-terminal ATS fragment of each of the two main subtypes of PfEMP1 molecules but lacked a TM domain allowed the determination of any *in vivo* interaction of PFE1605w with both ATS-C fragments. In a next step, Co-IP experiments with the full-length PFE1605w-HA fusion protein revealed a small number of host integral membrane proteins and components of the erythrocyte cytoskeleton as putative protein interaction partners of PFE1605w. These findings allowed us to perform reverse Co-IP experiments with specific antibodies against several of the detected host cell proteins. Reverse Co-IP experiments with antibodies against band 4.2 identified other components of the band 3 complex, including band 3, band 4.2 and α- and β-chains of spectrin, and ankyrin but no other *P. falciparum* protein except PFE1605w, clearly suggesting that PFE1605w interacts with one or several components of

the band 3 complex. From this, it would be possible to map the exact interaction epitope where PFE1605w is interacting with the band 3 complex.

On a side-line of this project we investigated the *var* gene expression and binding phenotypes of 3D7 parasites selected to bind to ICAM-1 and showed that ICAM-1 binding selects for parasites expressing PFL0020w and PF07_0050, both group B PfEMP1 molecules. With a single PfEMP1 expressing parasite population we were able to show that PFL0020w binds recombinant ICAM-1 through the DBLβ domain. Furthermore, a dual binding affinity of PFL0020w to different endothelial receptors was detected.

In summary, in this thesis we show for the first time that a member of the PHIST protein family exercises its functional role in knobs and interacts both with key molecules of the cytoadherence complex and the host cytoskeleton. We therefore propose that the functional role of PFE1605w is to anchor a variety of PfEMP1 molecules to the host cytoskeleton. It remains to be elucidated how other PHIST proteins and other key molecules of the cytoadherence complex further contribute to anchoring of PfEMP1 within the knob structure. These results clearly demonstrate the important role of the expanded PHIST protein family in *P. falciparum* and suggest avenues for innovative interactions.

Zusammenfassung

Plasmodium falciparum ist der Erreger der Malaria und verursacht jährlich über 500,000 Todesfälle. Heute lebt etwa die Hälfte der Weltbevölkerung in Malariarisikogebieten. Trotz diversen Anstrengungen die Häufigkeit von Malariainfektionen mittels Kontrolle der Erregerübertragung oder durch die Entwicklung von Medikamenten und Impfstoffen zu reduzieren, bleibt Malaria ein grosses Gesundheitsproblem in Endemiegebieten.

Eine Besonderheit des von *P. falciparum* infizierten Erythrozyten ist die Fähigkeit an Endothelzellrezeptoren der Kapillaren zu binden um so der Filtrierung durch die Milz zu entgehen. Dieser Prozess der Sequestration von infizierten Erythrozyten in verschiedenen Organen führt zu Gefässverstopfungen und Entzündungen und ist hauptverantwortlich für die gefährlichste Form der Malaria. Der bedeutendste Ligand für diese Zytoadhärenz ist das *P. falciparum* Erythrozyten Membran-Protein 1 (PfEMP1), welches in der Erythrozyten-membran in sogenannten Knob Strukturen verankert ist. Dabei bindet die semi-konservierte, intrazelluläre ATS Domäne das PfEMP1 Molekül an die Wirtszelle, wohingegen der variable, extrazelluläre Teil für die Anhaftung der infizierten Erythrozyten an die Wirtsrezeptoren zuständig ist. Vor kurzem fand man heraus, dass die ATS Domäne des PfEMP1 Moleküls ein konserviertes Epitop für Proteininteraktionen ist und es wurde eine *in vitro* Interaktion mit der PHIST Domäne von PFI1780w, einem Mitglied der Plasmodium Helical Interspersed Sub-Telomeric (PHIST) Proteinfamile nachgewiesen. Diese grosse Proteinfamilie zählt 72 Paraloge in *P. falciparum*, welche in drei Untergruppen (PHISTa, PHISTb, PHISTc) aufgeteilt sind. Alle PHIST Proteine besitzen eine ungefähr 150 Aminosäuren lange, konservierte Domäne, welche voraussichtlich eine Struktur von vier Alpha-Helices einnimmt.

Zurzeit ist wenig über die Funktion der verschiedenen PHIST Proteine bekannt, jedoch weisen neuste Daten daraufhin, dass diese in der Bildung der Knob Strukturen, im Transport von PfEMP1 und in der Adhärenz von infizierten Erythrozyten in den Mikrogefässen des Gehirns eine Rolle spielen. Des Weiteren fand man heraus, dass einige PHIST Proteine in der Peripherie der Wirtszelle lokalisiert sind, an Komponenten des Wirtszellzytoskeleton binden sowie in detergentienunlöslichen Membranfraktionen zu finden sind. Diese Erkenntnisse deuten auf eine wichtige Funktion der PHIST Proteine in der Modifikation der Wirtszelle hin.

Das Ziel dieser Arbeit war es, einen besseren Einblick in die funktionelle Rolle von einigen PHIST Proteinen zu bekommen. Dabei wurde der Fokus auf das PHISTb Protein PFE1605w gerichtet, welches verglichen mit PFI1780w eine stärkere Bindungsaffinität zu PfEMP1 aufzeigte. Mittels Immunofluoreszenz- und Elektronenmikroskopie konnte gezeigt werden, dass PFE1605w gleichzeitig mit PfEMP1 exportiert wird und schlussendlich in den Knob Strukturen zu finden ist. Experimente mithilfe NMR und Fluoreszenzpolarisation zeigten eine direkte Interaktion der PFE1605w PHIST Domäne mit dem C-Terminus der ATS Domäne. Weitere Polarisationsexperimente mit der PFE1605w PHIST Domäne und verschiedenen ATS Domänen von einigen PfEMP1 Molekülen zeigten beträchtliche Unterschiede in den Bindungsaffinitäten auf, was darauf hinweist, dass verschiedene PHIST Proteine eine optimierte Bindungsaffinität zu verschiedenen PfEMP1 Molekülen entwickelt haben. In einer Kollaboration konnten wir ausserdem die erste Kristallstruktur einer PHIST Domäne auflösen und daraus ein Modell für die PHIST-PfEMP1 Interaktion entwickeln.

Eine induzierte Reduktion von PFE1605w mithilfe einer destabilisierenden FKBP Domäne und kontrolliertes Anhalten von PFE1605w an den Maurer'schen Spalten mittels einer neuartigen Verankerungsmethode, führte zu einer Abwesenheit von PFE1605w in den Knob Strukturen und zu einer stark reduzierten Fähigkeit der infizierten Erythrozyten an den Endothelrezeptor CD36 zu binden. Um die spezifische Auswahl eines PHIST Proteins für ein bestimmtes PfEMP1 Molekül zu bestimmen, wurden infizierte Erythrozyten für eine Bindung an ein bestimmtes Rezeptormolekül selektioniert und somit wurde gleichzeitig für die Expression eines spezifischen PfEMP1 Moleküls selektioniert. Interessanterweise war die Adhäsion an andere Endothelrezeptoren nach der induzierten Reduktion von PFE1605w nur leicht oder sogar gar nicht betroffen. Dieses Ergebnis deutet darauf hin, dass PFE1605w für die Bindung an spezifische PfEMP1 Moleküle optimiert wurde. Da die Abwesenheit von PFE1605w in den Knob Strukturen die Oberflächenpräsenz von PfEMP1 nicht beeinflusst, kann angenommen werden, dass PFE1605w keine Rolle im Transport von PfEMP1 spielt.

Co-Immunopräzipitation (Co-IP) Experimente mit zwei Konstrukten, welche nur den C-terminalen Teil der ATS Domänen von zwei PfEMP1 Molekülen umfassen, jedoch keine Transmembrandomänen, erlaubten die Bestimmung der *in vivo* Proteininteraktion von PFE1605w mit beiden C-terminalen Fragmenten der ATS Domänen.

In einem weiteren Schritt ermöglichten Co-IP Experimente mit PFE1605w als HA-Fusionsprotein die Identifikation diverser integraler Membranproteine und verschiedener Bestandteile des Zytoskeletts der Wirtszelle als potentielle Interaktionspartner von PFE1605w. Diese Resultate ermöglichten die Durchführung von inversen Co-IP Experimenten mit spezifischen Antikörpern, welche die vorher detektierten Wirtszellproteine erkennen und binden. Inverse Co-IP Experimente mit α-Bande 4.2 Antikörper identifizierten weitere Komponenten des Bande 3 Komplexes wie Bande 3, Bande 4.2 und α- und β-Spektrin sowie Ankyrin. Neben den genannten Wirtszellproteinen wurde PFE1605w als einziges *P. falciparum* Protein identifiziert was deutlich darauf hinweist, dass PFE1605w mit einer oder mehreren Komponenten des Bande 3 Komplexes interagiert. Diese Resultate ermöglichen nun die genaue Identifikation der PFE1605w Bindungsstelle innerhalb des Bande 3 Komplexes.

In einem Nebenprojekt wurden die *var* Genexpression und der Bindungsphänotyp von 3D7 Parasiten, welche vorher für eine Bindung an das Rezeptormolekül ICAM-1 selektioniert wurden, untersucht. Die selektionierten Parasiten exprimieren PFL0020w und PF07_0050, beides PfEMP1 Moleküle, welche zur Gruppe B PfEMP1 Moleküle gehören. Mittels Selektion einer Parasitenpopulation welche nur ein PfEMP1 Molekül exprimiert, konnten wir zeigen, dass das Rezeptormolekül ICAM-1 durch die DBLβ Domäne von PFL0020w gebunden wird. Des Weiteren konnten wir für PFL0020w Bindungsaffinitäten für zwei verschiedene Arten von Rezeptormolekülen aufzeigen.

Zusammenfassend konnte in dieser Arbeit zum ersten Mal gezeigt werden, dass ein Mitglied der PHIST Proteinfamilie seine Funktion in den Knob Strukturen ausübt und dabei mit Hauptkomponenten des Zytoadhärenzkomplexes aber auch mit Komponenten des Zytoskeletts der Wirtszelle interagieren. Aus diesem Grund nehmen wir an, dass die Funktion von PFE1605w darin besteht, verschiedene PfEMP1 Moleküle an das Zytoskeleton zu binden und somit die Verankerung von PfEMP1 in den Knob Strukturen zu gewährleisten. Es ist in Zukunft zu klären wie weitere PHIST Proteine und andere Hauptkomponenten des Zytoadhärenzkomplexes zur Verankerung von PfEMP1 in den Knob Strukturen beitragen. Die Resultate dieser Arbeit zeigen deutlich die wichtige Funktion der PHIST Proteinfamilie in *P. falciparum* auf und deuten auf einen Beitrag zur Entwicklung von neuen Interventionsstrategien.

Acknowledgements

This dissertation was carried out at the Swiss Tropical and Public Health Institute in Basel from March 2012 until December 2015. All work presented in this thesis would not have been possible without the advice and support of many great colleagues and friends.

First, and foremost I would like to say a very big thank you to my supervisor Hans-Peter Beck for providing me the opportunity and support throughout this project. Your valuable inputs, ideas and confidence decisively influenced this project and made my PhD studies a very interesting and educational time. I truly enjoyed the time in the lab but also the numerous city-trips to London, Berlin, Aachen, Heidelberg and Hamburg.

I am very grateful to Kai Matuschewski and Tobias Spielmann for joining my PhD committee and for the inspiring conversation and hospitality during the annual PhD committee meetings. Furthermore I would like to express my gratitude to Tobias for acquiring me with plenty of molecular tools and knowledge during my master studies in his lab.

A big thank goes to Till Voss for giving helpful inputs, providing plasmids and antibodies, helping with the microarray experiments and for chairing my PhD defense. I also thank Ingrid Felger for her input and advice during the weekly lab meetings and the stimulated scientific discussions during coffee breaks.

I am very thankful to Ioannis Vakonakis for his support, all the stimulated discussions and teleconferences and his patience in answering all questions about structural biology. Without our fruitful collaboration many projects and approaches in this thesis would not have been possible. Many thanks also to all people of the Vakonakis lab, especially Leanne Slater, Erin Cutts, Dirk Reiter and Jemma Day.

A very special thank goes to all the current and former lab members of the Molecular Parasitology group at the Swiss TPH for the amazing working environment, for feeding my parasites during holidays (exceptional and rare cases), for the numerous and extensive coffee breaks and for the intense barbeque and after-work beer evenings. You all contributed a lot that I had a great time at the Swiss TPH and that I will never forget this amazing time. Many thanks Sebastian Rusch (the guy who knows everything), Esther Mundwiler-Pachlatko (Miss MAHRPle), Oliver Dietz (Dr. 007), Francoise Brand (Mrs. Tokuyasu), Jan Warncke, Beatrice Schibler (Dachterassen-Bea), Armin Passegger (Der

Östereicher), Laura Zurbrügg (s Miggeli) , Eva Hitz (Pilz-Evi), Serej Ley, Maira Bholla, Moussa Maganga, Adrian Najer, Martin Chichi Maire and Tereza Vieira de Rezende.

I am also very grateful to the Gene Regulation and Molecular Diagnostic groups next door: Nicole Bertschi, Igor Niederwieser, Michael Filarsky (it was a great trip to New York!), Nicolas Brancucci, Hai Bui, Sylwia Panek and Rahel Wampfler, Natalie Hofmann, Lincoln Timinao, Felista Mwingira and Pricila Thihara.

I also thank all the great people outside the lab that strayed through the basement and the institute: Matthias Rottman (Matze), Christian Scheurer (Scheuri), Sergio Wittlin, Pascal Mäser, Susi Gyoerffy, Yvette Endriss, Beatrice Wäckerlin, Myriam Baume, Dirk Stoll (many thanks for parts of the carneval costume), Thierry Brun, Fabien Haas, Paul Haas, Amanda Ross (statistical support) and the IT crew.

Furthermore I want to thank numerous people at the Swiss TPH for sharing lunch and coffee breaks, student parties, Thursday evening fondues, unpredictable carnival evenings and for sharing an amazing time. It was a pleasure of meeting you and I will always remember the wonderful time I spent here. Many thanks Raphi (Inkubieri), Fabrice (Fabe), Pheppu (Lüdin), Remo, Sämi, Tobi, Philipp, Pierre, Henry, Beni, Urs, Wendelin and Nadja.

I am also very thankful to the Image Core Facility at the Biozentrum for giving me the opportunity to use the confocal and high resolution microscope and Alexia Ferrand for her support.

I am grateful to the Swiss Society of Tropical Medicine and Parasitology (SSTMP) and the Basler Stiftung für Experimentelle Zoologie for their financial support to enable the participation at the Molecular Parasitology Meeting (MPM) in Woods Hole.

Special thank goes to my family. I am deeply grateful to my parents for the continuous support during my academic studies and my life.

Many thanks to all of you (and to the one I unfortunately forgot to mention…)!

Table of contents

Summary I

Zusammenfassung IV

Acknowledgements VII

Table of contents IX

Abbreviations XI

Chapter 1 : Introduction 1

1.1. Malaria 2

1.1.1. Prevalence 2
1.1.2. The agent of malaria 2
1.1.3. Pathophysiology of malaria infection 4
1.1.4. Anti-malaria drugs and vaccines 5
1.1.5. The lifecycle of Plasmodium 6
1.1.6. The asexual life cycle 8

1.2. Host cell modifications 9

1.2.1. New permeation pathways 11
1.2.2. Maurer's clefts 11
1.2.3. The cytoadherence complex 12

1.3. Protein export in *P. falciparum* 13

1.3.1. Signal sequences for export 15
1.3.2. Transport through the PVM 16

1.4. *Plasmodium falciparum* erythrocyte membrane protein 1 17

1.4.1. The ATS domain of PfEMP1 19
1.4.2. The ectodomain of PfEMP1 19
1.4.3. Export of PfEMP1 to the surface of the iRBC 20

1.5. PHIST protein family 21

1.5.1. The PHISTa subfamily 23
1.5.2. The PHISTb subfamily 23
1.5.3. The PHISTc subfamily 25

1.6. The human red blood cell 25

1.6.1. The structural organization of the RBC membrane 26
1.6.2. Interactions with the host erythrocyte cytoskeleton 27

1.7. Outline of the thesis 30

1.8. References 31

Chapter 2 : A *Plasmodium falciparum* PHIST protein binds the virulence factor PfEMP1 and comigrates to knobs on the host cell surface 47

Chapter 3 : *Plasmodium falciparum Plasmodium* helical interspersed subtelomeric proteins contribute to cytoadherence and anchor *P. falciparum* erythrocyte membrane protein 1 to the host cell 67

Chapter 4 : *Plasmodium falciparum* blood stage parasites selected for binding to ICAM-1 express var group B PfEMP1 89

Chapter 5: General discussion 104

Outlook 121

Appendix 123

Curriculum vitae ..... Fehler! Textmarke nicht definiert.

Abbreviations

aa	amino acids
ACT	artemisinin combination therapy
ATS	acidic terminal sequence
BSD	blasticidin S deaminase
CD36	cluster of differentiation 36
CM	cerebral malaria
Co-IP	co-immunoprecipitation
CSA	chondroitin sulphate A
C-terminus	carboxy-terminus
DAPI	4`,6`-diamidino-2-phenylindole
DBL	Duffy binding-like
DD	destabilization domain
DIC	differential interference contrast
DHFR	dihydrofolate reductase
EM	electron microscopy
EPCR	endothelial protein C receptor
ER	endoplasmic reticulum
EXP2	exported protein 2
FKBP	FK506-binding protein
FRB	FKBP-rapamycin-binding
GAPDH	glyceraldehyde 3-phosphate dehydrogenase
GFP	green fluorescent protein
GPC	glycophorin C
HA	influenza hemaglutinin
HDMEC	human dermal microvascular endothelial cells
hpi	hours post infection
HSP	heat shock protein
ICAM-1	intercellular adhesion molecule 1
IFA	immunofluorescence assay
IOVs	inside-out vesicles
iRBC	infected red blood cell
KAHRP	knob associated histidine-rich protein
LC-MS/MS	liquid chromatography-mass spectrometry/ mass spectrometry
MAHRP1,2	membrane associated histidine-rich protein 1,2
MC	Maurer's cleft
MEC	MESA erythrocyte cytoskeleton-binding motif
MESA	mature parasite-infected erythrocyte surface antigen
MS	mass spectrometry

NPPs	new permeation pathways
N-terminus	amino-terminus
ORF	open reading frame
PCR	polymerase chain reaction
PEXEL	*Plasmodium* export element
PfEMP1,3	*Plasmodium* falciparum erythrocyte membrane protein 1,3
PHIST	Plasmodium helical interspersed sub-telomeric protein
PM5	Plasmepsin V
PNEP	PEXEL-negative exported protein
PPM	parasite plasma membrane
PTEX	*Plasmodium* translocon of exported proteins
PTP	PfEMP1 transport protein
PV	parasitophorous vacuole
PVM	parasitophorous vacuolar membrane
RAP	rapalog/rapamycin
RBC	red blood cell
RESA	ring-infected erythrocyte surface antigen
RIFIN	repetitive interspersed family
SDS	sodiumdodecylsulfate
SEM	scanning electron microscopy
SP	signal peptide
STEVOR	subtelomeric variable open reading frame
TM	transmembrane
TRX2	thioredoxin 2
TVN	tubovesicular network
VTS	vacuolar transport signal
WHO	World Health Organization

Chapter 1

Introduction:

Malaria and the cell biology of *Plasmodium falciparum*

Introduction

1.1. Malaria

1.1.1. Prevalence

More than 135 years after the military physician Charles Louis Alphonse Laveran observed malaria parasites in blood from soldiers, malaria still represents one of the most devastating human diseases (Cox, 2010). Besides HIV/AIDS and tuberculosis, malaria belongs to the big three infectious diseases and caused estimated 200 million clinical cases and approximately 580,000 deaths annually (WHO, 2014), mostly in sub-Saharan Africa. Almost 90% of all malaria-associated fatal cases occur in children younger than five years old (Snow et al., 2005). Nowadays, malaria is restricted to tropical and sub-tropical zones but in ancient times it also occurred in northern temperate zones including Canada, the United States of America, Russia and Europe. Due to large eradication strategies, economic progress and health improvement, malaria was eliminated from most of the Northern hemisphere (Greenwood et al., 2008). Nevertheless, climate change may favour the resurgence of malaria in previously malaria-free areas, albeit this topic is frequently debated (Caminade et al., 2014; Gething et al., 2010).

According to the WHO, currently 3.3 billion people are at risk of being infected with malaria and African countries south of the Sahara bear the highest burden with nearly 90% of the worldwide incidence. In these areas this widespread disease has a dramatic impact on the socio-economic development and the public health (Sachs & Malaney, 2002).

1.1.2. The agent of malaria

Plasmodium, the causative agent of malaria, belongs to the phylum Apicomplexa, which further includes other important pathogens such as *Babesia*, *Cryptosporidium*, *Eimeria*, *Theileria* and *Toxoplasma* (Baldauf, 2000). Apicomplexa, a diverse group of unicellular protozoans, is characterized by an electron dense structure at the apical pole of the merozoite, the invasive form of the parasite, which allows the parasite to invade host cells and to establish itself therein. Moreover, most apicomplexan parasites possess an apicoplast, a vestigial plasmid of secondary endosymbiotic origin, which harbours essential biochemical pathways and is indispensable for growth of the parasite (Lim & McFadden,

2010). The absence of these prokaryote-specific pathways in humans makes the apicoplast an attractive target for chemotherapeutic interventions (McFadden & Roos, 1999).

To date, there are more than 200 *Plasmodium* species described of which only five cause disease in humans: *P. falciparum*, *P. vivax*, *P. malariae*, *P. ovale* and *P. knowlesi*. The latter, a malaria parasite infecting macaque monkey, has been known to infect humans a while ago (Fong et al., 1971) but it only has arisen epidemically recently due to displacement of monkeys into human settlements (Rayner et al., 2011). Depending on the *Plasmodium* subspecies infecting humans, the severity of malaria differs. The most severe form of human malaria, *falciparum* malaria or malaria tropica is caused by *P. falciparum* and accounts for the majority of malaria-associated deaths whereas *P. vivax*, *P. ovale* and *P. malariae* have long been thought to cause only benign malaria. However, increasing numbers of severe *P. vivax* malaria infections suggest a more prominent role of *P. vivax* in severe disease (Anstey et al., 2009; Genton et al., 2008; Tjitra et al., 2008). Both, *P. vivax* and *P. ovale* can form hypnozoites, dormant liver stages that can lead to reoccurring disease relapses a long time after the primary infection. In contrast, *P. malaria* and *P. falciparum* do not form hypnozoites but relapses of permanent disposable blood stages have been reported for *P. malariae* (Cogswell, 1992). In regions with high *P. falciparum* transmission malaria tropica often becomes chronic, as after repeated infections a person may develop a protective semi-immunity. Such semi-immune persons often carry parasites but may not develop severe disease and frequently lack any typical malaria symptoms. The long-lasting dormant stages or chronic infections have a tremendous influence on eradication programs (Wells et al., 2010).

The *Plasmodium* parasite is transmitted to the human host during a blood meal of the female *Anopheles spp.* mosquito. There are more than 30 *Anopheles* subspecies that can transmit *Plasmodium* parasites but the most important subspecies that accounts for the highest transmission rate in Africa is *A. gambiae* and *A. funestus* (Tuteja, 2007). In other malaria endemic regions such as Asia or Latin America different *Anopheles* subspecies contribute equally to the transmission of the parasite.

1.1.3. Pathophysiology of malaria infection

The incubation time of the human pathogenic *Plasmodium* subspecies varies from approximately 6-12 days for malaria tropica (*P. falciparum*), 12-18 days for malaria tertiana (*P. vivax* / *P. ovale*) and 15-50 days for malaria quartana (*P. malariae*) respectively.

All clinical symptoms of malaria are caused by the asexual blood stage of *Plasmodium* parasites and the three different etiopathologies can be distinguished in infected patients. However they all share classical symptoms of periodic fever peaks, except for *P. falciparum* which causes asynchronous fever attacks due to unsynchronized egress with persistent fever at high temperatures (Miller et al., 2002). The characteristic reoccurring fever periods can be explained by the synchronous intraerythrocytic life cycle of *Plasmodium*. All three etiopathologies can cause anaemia, caused by multifactorial reasons such as removal of circulating red blood cells (RBCs), reduced production of RBCs in the bone marrow, polymorphisms in cytokines but also destruction of RBCs by the parasite upon host cell rupture (Haldar & Mohandas, 2009). The increase of body temperature during the fever periods is a reaction to the activation of the immune system upon contact to hemozoin and glycosylphosphatidylinositol (GPI) molecules covalently linked to merozoite surface antigens, such as the merozoite surface protein (MSP-1) (Schofield & Hackett, 1993; Shio et al., 2010). Hence, innate and adaptive immune responses such as pro-inflammatory cytokine release by activated macrophages or T-cell activation and antibody production are triggered (Engwerda & Good, 2005). Nevertheless, the interplay between the parasite and the host immune system upon infection is highly complex and still subject of current research (Chua et al., 2013).

The main reason that *P. falciparum* causes the most severe symptoms among all human pathogenic *Plasmodium* subspecies is the distinct feature of the *P. falciparum* infected RBCs (iRBCs) to avoid splenic clearance by adhering to the vascular endothelium. This pathologic feature is a major contributor to the severity of malaria tropica (Ockenhouse et al., 1992). A result of the cytoadhesion is the sequestration of a high number of parasites in different tissues of the human body leading to local hypoxia and inflammation. Affecting the brain, it leads to cerebral malaria and can result in coma and death (Medana & Turner, 2006). Other severe pathologic outcomes are severe anaemia, respiratory distress and renal and general organ failure (Miller et al., 2002). Especially pregnant women face high risk of severe malaria

as massive sequestration of iRBCs in the placenta has a devastating effect during pregnancy such as maternal morbidity, low bird weight, preterm delivery and infant mortality (Desai et al., 2007).

1.1.4. Anti-malaria drugs and vaccines

Today, a broad variety of medical treatments are available to combat malaria infections. After World War II, chloroquine, a drug based on a derivate from the alkaloid quinine, was a widely distributed, cheap and effective anti-malaria drug. Subsequently, the first cases of chloroquine resistant parasites were reported from the Thai-Cambodian border in 1957 (Wellems & Plowe, 2001). It took about 20 years until the resistance was carried over to Africa and ended the successful story of this drug. Until recently, resistance has emerged against all known classes of anti-malarial drugs except the artemisinins and its derivates. Artemisinin is a sesquiterpene extracted from the wormwood *Artemisia annua*. After being discovered as an anti-malaria drug, a variety of derivates such as artesunate, artemether and dihydroartemisinin have been synthesized. To reduce the probability of parasite resistance against artemisinins, the WHO recommended the application of artemisinins as a combination therapy (ACT) with a second anti-malaria drug (Aregawi et al., 2010). Nevertheless, first reports in 2009 of increased clearance time using artemisinin pointed to an emerging resistance in the parasite population (Dondorp et al., 2009). Today, increased tolerance to ACTs has been confirmed in several countries of the Greater Mekong subregion and mutations in the Kelch 13 (K13) propeller protein were shown to be associated with delayed parasite clearance *in vitro* and *in vivo* (Ariey et al., 2013; Dondorp et al., 2009; Noedl et al., 2008). This molecular marker can now enable a mapping of possible resistance as the spread or independent emergence of artemisinin resistance in other parts of the world would pose a major health risk as no anti-malaria treatment is available at present with the same efficacy and applicability as artemisinin combination therapy.

A recently identified new class of compunds termed spiroindolones raises hope for a new malaria treatment (Rottmann et al., 2010; Yeung et al., 2010). The optimized candidate NITD609 displayed good pharmacokinetic properties and was highly active against both *P. falciparum* and *P. vivax* field isolates but also against drug resistant *P. falciparum* strains. Moreover, the molecular target and the potential mutations involved in resistance

development were identified, potentially enabling structural optimization of the compound in case of occurring resistance.

Besides the long endeavour to discover new chemotherapeutic agents, the development of an efficient vaccine is an important field in malaria research. In recent decades a remarkable number of different vaccines was developed targeting a variety of parasite stages and surface proteins and many vaccine candidates are currently in the clinical phase pipeline. However, so far the most advanced vaccine candidate is RTS,S, also known as Mosquirix^{TM}, a hybrid of the amino acids 207-395 of the live stage specific circumsporozoite surface protein (CSP) from the NF54 strain of *P. falciparum* and the hepatitis B surface antigen HBsAg containing known B- and T-cell epitopes. The phase III efficacy and safety trial of RTS,S was carried out at 11 sites in seven African countries with 15,459 infants and young children participating. The final results showed that vaccination with a three dose series reduced clinical malaria cases by 28% in young children (5-17 months) and 18% in infants (6-12 weeks) to the end of the study (RTS, 2015). A booster dose of RTS,S received 18 months after primary series reduced the number of clinical malaria cases in young children by 36% and in infants by 26% to the end of the study (RTS, 2015).

Besides the identification and evaluation of new antigenic targets, approaches for next-generation vaccines include whole-sporozoites vaccines, virosome- and nanoparticle-based combination vaccines and the use of different adjuvants and prime-boost strategies (Alonso & Tanner, 2013).

1.1.5. The lifecycle of Plasmodium

The *P. falciparum* parasite enters the human body during a blood meal of a female mosquito of the genus *Anopheles* (Fig. 1). The mosquito injects the infective sporozoites into the human dermis where they are transported to the liver via the bloodstream (Amino et al., 2006). Before the infection of hepatocytes, the sporozoites need to cross the sinusoidal endothelial cell layer by traversing Kuppfer or endothelial cells (Mota, 2001; Tavares et al., 2013). After the transit of several hepatocytes the sporozoite invades a final hepatocyte by the use of surface proteins for invasion (e.g. circumsporozoite protein and thrombospondin-related adhesins), which specifically bind heparin sulfate proteoglycans on hepatocytes (Frevert et al., 1993). During invasion, a parasitophorous vacuole (PV) is build wherein the parasite undergoes asexual replication resulting in thousands of infective merozoites

(Prudêncio & Mota, 2007). To initiate the blood stage the newly build merozoites are packed into merosomes which are released into the blood stream and after rupture, the released merozoites are ready to invade red blood cells (Sturm et al., 2006).

Compared to *P. vivax*, which is restricted to infect reticulocytes, *P. falciparum* is able invade all types of red blood cells, independent of age. Directly after invasion of a red blood cell the parasites immediately start to remodel its host cell to establish a suitable niche for growth and replication (Fig. 2). This stage of the life cycle is solely responsible for all symptoms observed in malaria and the asexual life cycle is discussed in detail in section 1.1.6.

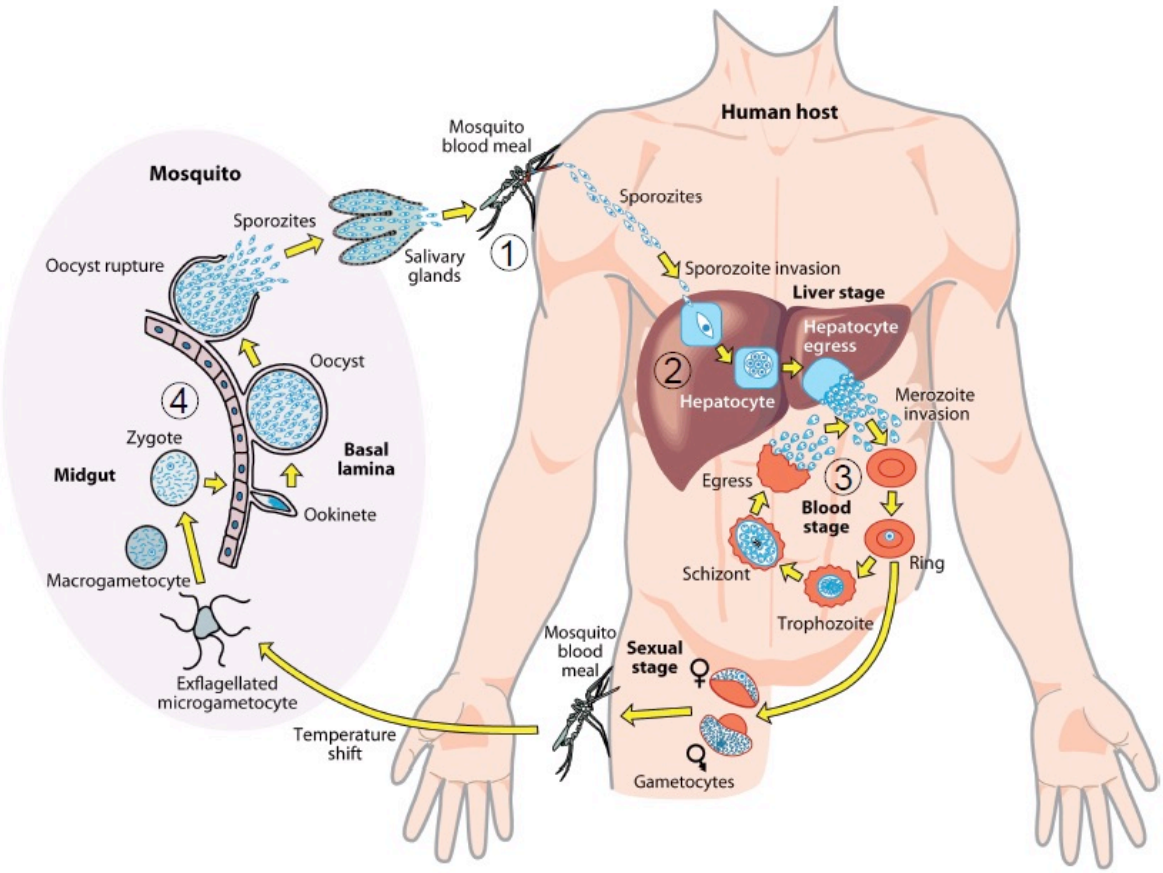

Figure 1: Life cycle of *P. falciparum*

Sporozoites injected during a blood meal of a female *Anopheles* mosquito (1) migrate to the liver where they invade hepatocytes, multiply and release thousands of merozoites (2). Parasites enter the asexual intraerythrocytic life cycle and develop from the ring, via the trophozoite to the schizont stage (3). Some parasites differentiate to sexual forms and are taken up during a blood meal of a mosquito. The sexual development resulting in sporozoite stages occurs in the midgut and the basal lamina of the mosquito (4). Figure modified from (Boddey & Cowman, 2013).

While the asexual development occurs in the human body, the sexual development takes place in the female *Anopheles* mosquito. During the red blood cell cycle a small number of merozoites differentiate into male and female gametocytes, the sexual precursor forms of *P. falciparum* gamets. With a blood meal of the female mosquito the gametocytes are taken up and the subsequent drop in temperature or the presence of xanthurenic acid triggers gametocyte activation. After reaching the mosquito midgut, the female macrogametocytes form haploid macrogametes, whereas male microgametocytes undergo rapid nuclear division resulting in eight motile microgametes. After fertilization of one macrogamete by a microgamete, a diploid zygote is formed. 18-24 hours later, the zygote further develops into a mobile ookinete and migrates through the midgut epithelium to the extracellular space between the midgut epithelium and the basal lamina where it arrests and develops into an oocyst. When the proliferation is completed, the oocyst ruptures and thousands of infective sporozoites are released. After migration and penetration into the salivary gland of the mosquito, the sporozoites are ready to be injected into the human skin to start a new infection. Usually, the motile sporozoites are present in the mosquito salivary gland from 10-18 days after the initial blood meal and remain infective for 1-2 months (Tuteja, 2007).

1.1.6. The asexual life cycle

Within the 48 hour intraerythrocytic life cycle, merozoite, ring, trophozoite and schizont stage parasite can be microscopically distinguished (Bannister et al., 2000; Grüring et al., 2011). The non-motile merozoites invade RBCs through a first contact via proteins located on the merozoite surface and the subsequent use of an actin-myosin dependent machinery (Baum et al., 2008). The invasion of the RBC occurs within minutes to minimize contact with the host immune system. During invasion the invagination of the RBC membrane and the formation of a parasitophorous vacuole membrane (PVM) forming the parasitophorous vacuole (PV) builds the environment for the further development of the parasite. After invasion, the parasite turns into the ring stage and induces the first steps of the host cell modification. Therefore the parasite exports a variety of proteins inducing structures like Maurer's clefts (section 1.2.2) or the tubovesicular network (TVN) (Atkinson & Aikawa, 1990). Within the PV the parasite proliferates from the ring to the trophozoite stage and increases its metabolism in order to create an appropriate niche for intraerythrocytic survival. To gain space for growth and for amino acid supply the parasite proteolytically

degrades haemoglobin and the toxic haematin by-product is converted into a crystalline form, known as haemozoin, and stored in the food vacuole (Goldberg, 2013). Moreover, during the trophozoite stage which lasts approximately 22 to 36 hours post invasion, the parasite initiates DNA replication, the number of ribosomes increases and the endoplasmatic reticulum (ER) prolongs. After 36 hours post invasion the parasite turns into a schizont stage parasite and occupies most of the host cell. In this stage nuclear division continues until the parasite ends up with 8-32 new nuclei. Finally, a process called schizogony assembles mono-nucleated merozoites, each containing a nucleus, mitochondrion and plastid. After 48 hours post invasion the host cell ruptures and the released merozoites invade new RBCs.

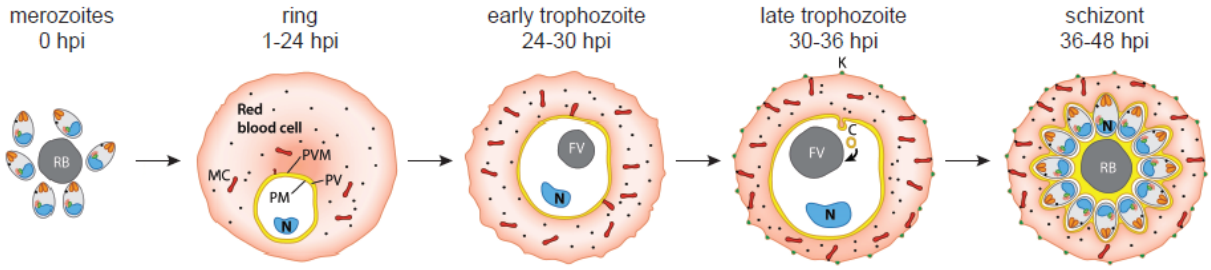

Figure 2: The blood stage cycle of *P. falciparum*

During invasion the parasite encases itself in a parasitophorous vacuole membrane. The ring stage parasite exports proteins and generates Maurer's clefts. Cytostomes, emarginations in the parasite periphery, indicate hemoglobin uptake and hemozoin christals are observed in the food vacuole. The host cell remoldeling continues as MCs are tethered to the RBC membrane, formation of knobs occurs and PfEMP1 is displayed on the surface of the RBC. Up to 32 new merozoites are produced and their egress allows the invasion of new RBCs. Abbreviations: **hpi**: hours post invasion; **RB**: residual body; **N**: nucleus; **PM**: parasite membrane; **PV**: parasitophorous vacuole; **PVM**: parasitophorous vacuolar membrane; **MC**: Maurer's cleft; **FV**: food vacuole; **C**: cytostome. Figure modified from (Boddey & Cowman, 2013).

1.2. Host cell modifications

Besides the apicomplexan parasites *Plasmodium*, *Babesia* and *Theileria* (Dobbelaere & Küenzi, 2004; Gohil et al., 2010) also two bacteria *Anaplasma* and *Bartonella* (Dehio, 2004; Kocan et al., 2010) use the RBC as an environment for survival. Indeed, there are many advantages for parasites to choose the RBC as a host cell. The most striking advantage is that RBCs are not able to present antigens on MHC molecules and therefore the iRBC is less obvious to the immune system. Moreover, the absence of a lysosomal degradation system

protects the parasites from degradation, a threat that many intracellular pathogens are facing (Rohde et al., 2007). However, the parasite also deals with major problems, as the RBC is a highly differentiated cell lacking much of the cellular machinery (like a nucleus and the secretory system) and associated processes (protein synthesis and trafficking) that the parasite could hijack. In the case of *P. falciparum,* the parasite extensively refurbishes its host cell marked by changes in the permeability, rigidity, and cytoadhesive properties in order to proliferate and replicate within the RBC. An overview of the most obvious host cell modifications is depicted in Fig. 3 and in the sections 1.2.1 – 1.2.3.

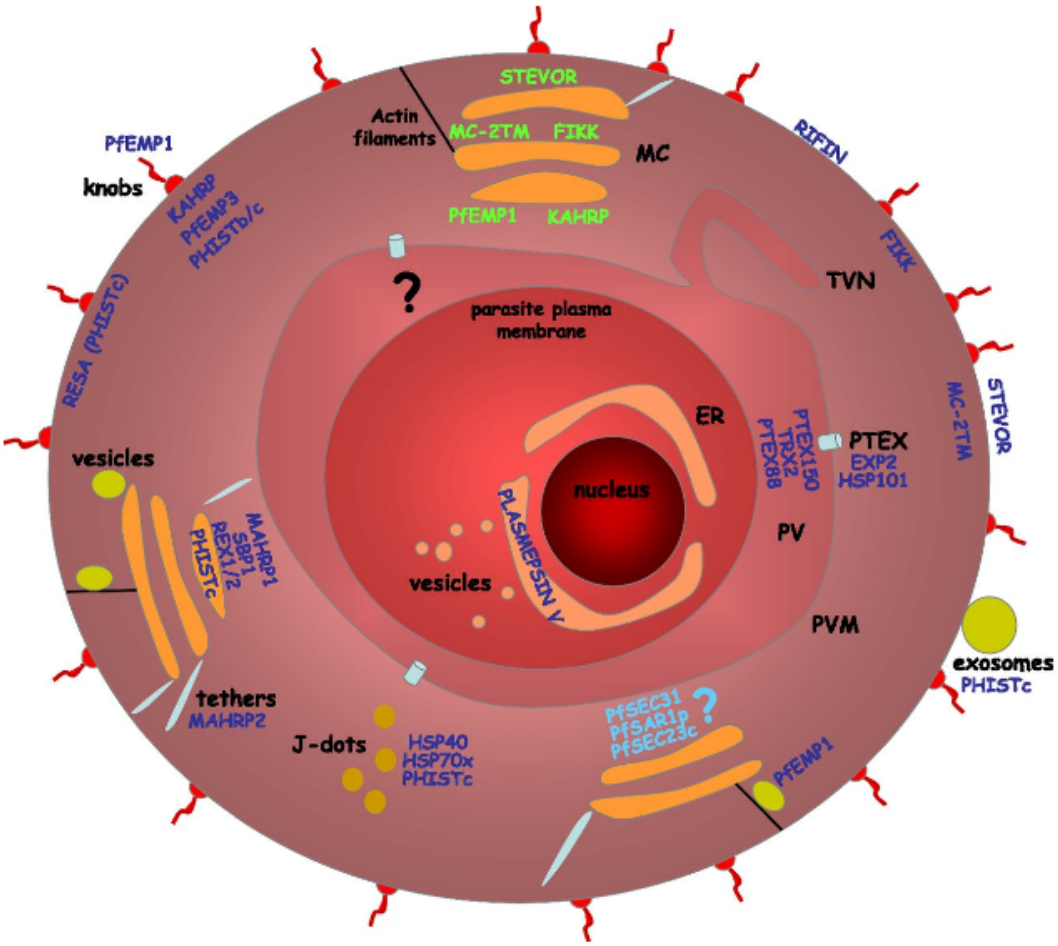

Figure 3: Schematic view of an infected red blood cell

Illustration of parasite-derived structures and proteins involved in protein translocation into the iRBC. Abbreviations: **ER**: endoplasmatic reticulum; **PV**: parasitophorous vacuole; **PVM**: parasitophorous vacuolar membrane; **TVN**: tubovesicular network; **PTEX**: *Plasmodium* translocon of exported proteins. Protein names indicated in blue represents resident protein of the respective organelle, names in green represent transient localization to the indicated organelle and names in light blue indicates unknown subcellular localization (Mundwiler-Pachlatko & Beck, 2013).

1.2.1. New permeation pathways

During maturation the parasite facilitates nutrient uptake by the formation of new permeation pathways (NPPs). Although not well characterized on a molecular level the RBC membrane permeability for charged and neutral solutes increases during maturation of the parasite. It is still debated whether the proteins mediating transport across the RBC membrane are parasite derived or represent activation of previously silent RBC transporters (Huber et al., 2002; Staines et al., 2007). It was suggested that NPP formation is actively mediated by proteins secreted beyond the parasite (Baumeister et al., 2006). The NPP is also termed plasmodial surface anion channel and is linked to the expression of either of the two exported proteins CLAG3.1/3.2 which are inserted into the RBC membrane during merozoite invasion (Nguitragool et al., 2011).

1.2.2. Maurer's clefts

Another striking modification of iRBCs is the appearance of parasite induced membranous structures in the RBC cytoplasm, called Maurer's clefts (Aikawa, 1971; Hanssen et al., 2007; Tilley et al., 2007; Wickert & Krohne, 2007). First described by Georg Maurer in 1902 in *P. falciparum* iRBCs as dots stained with alkaline methylene blue (Maurer, 1902), Maurer's clefts are today known to be a disk-shaped cistern of about 500 nm width and 30 nm height, bordered by a single membrane (Bannister et al., 2000; Hanssen et al., 2007; Lanzer et al., 2006). Maurer's clefts are heterogenous in size and morphology, although the overall heterogeneity is dependent on the *P. falciparum* strain. In early stage parasites the Maurer's clefts are very motile and get arrested before the parasite develops to the trophozoite stage at around 22 hours post invasion (Grüring et al., 2011; McMillan et al., 2013). The sudden arrest of Maurer's clefts requires a fast anchoring process and the discovery of tether-like extensions connecting Maurer's clefts to the RBC membrane or to the PVM suggest an involvement of these tubular structures in the immobilization event. To date only the membrane-associated histidine-rich protein 2 (MAHRP2) was found to localize specifically to tethers (Pachlatko et al., 2010) and it remains to be determined whether MAHRP2 is responsible for Maurer's clefts immobilization or actin-like filaments (Haeggstrom, 2004) are involved in this process.

The genesis of Maurer's clefts has only vaguely been described but it is thought to occur through budding from the PVM (Goldberg & Cowman, 2010; Spycher et al., 2006). Different

mechanisms for protein trafficking to and from clefts have been proposed including diffusion of proteins during MC genesis at the PVM, vesicular transport but also transport via chaperone-mediated soluble complexes (Mundwiler-Pachlatko & Beck, 2013). Recently, it was shown that some proteins arrive at already existing Maurer's clefts suggesting that not all Maurer's cleft proteins are loaded into the clefts when they are formed at the PVM but rather a continuous cargo to Maurer's clefts exists (Grüring et al., 2011; McMillan et al., 2013).

With the identification of the protein export motif *Plasmodium* export element (PEXEL) (section 1.3.1) the list of parasite proteins exported beyond the parasite's confines increased extensively. Out of these proteins a considerable number localize or transiently associate with Maurer's clefts. The skeleton binding protein 1 (SBP1), membrane-associated histidine-rich protein 1 (MAHRP1) and ring-exported protein 1 and 2 (REX1/2) reside within the Maurer's clefts and are involved in Maurer's clefts architecture and PfEMP1 transport (Dixon et al., 2011) (Fig. 3 & Fig. 9). Others, such as PfEMP1, PfEMP3, KAHRP and members of the subtelomeric variable open reading frame family (STEVOR) are transiently associated with Maurer's clefts. Overall, a remarkable number of studies imply that Maurer's clefts function as sorting stations for proteins destined to the erythrocyte membrane.

1.2.3. The cytoadherence complex

During the asexual lifecycle the parasite's maturation is accompanied by remarkable changes in the topography and membrane architecture of the iRBC (section 1.6.2, Fig. 4, Fig. 9). A peculiar modification is the formation of ~100 nm electron dense protrusions termed knobs during the second half of the asexual lifecycle, which mainly comprise the knob-associated histidine-rich protein 1 (KAHRP) (Taylor et al., 1987) (Fig. 4). *Plasmodium falciparum* erythrocyte membrane protein (PfEMP1), the major ligand for binding of iRBC to host receptors on vascular endothelium is anchored in the iRBC membrane within the knobs (Baruch et al., 1995; Smith et al., 1995; Su et al., 1995). Knockout of KAHRP leads to absence of knobs and diffuse surface distribution of PfEMP1 over the iRBC membrane, leading to greatly reduced cytoadhesive properties under flow conditions (Crabb et al., 1997; Waller et al., 1999). This suggests that although the protein is dispensable for PfEMP1 trafficking, the physical interaction of KAHRP is important for the proper presentation of the adhesin. Nevertheless, Horrocks and colleagues suggest that this reduction may occur due to reduced

level of surface exposed PfEMP1 rather than failure of PfEMP1 clustering in the knob structure (Horrocks, 2005).

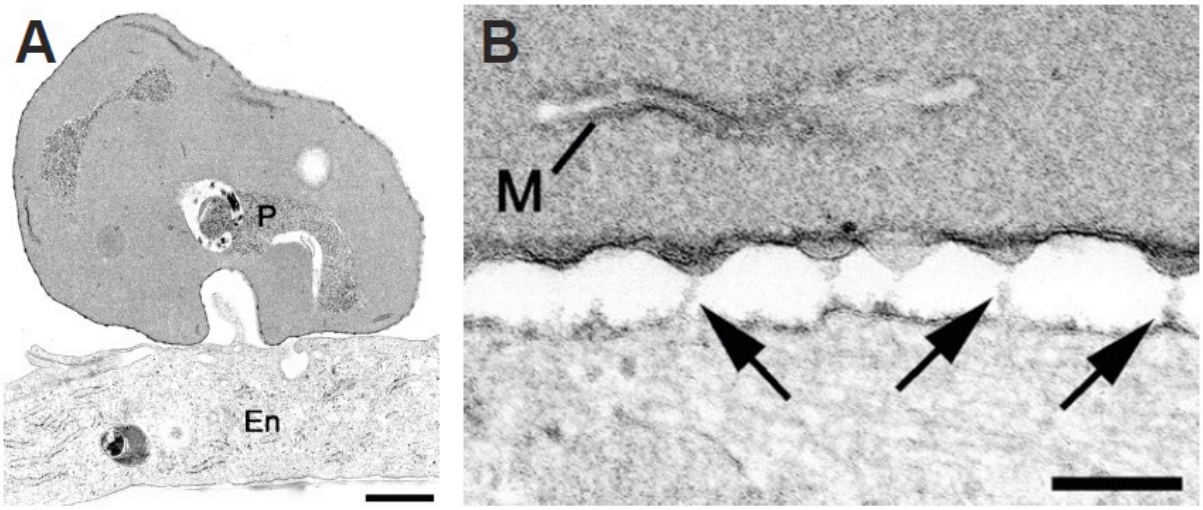

Figure 4: Transmission electron micrograph of an iRBC with knobs adhering to a microvascular endothelial cell. (A) *P. falciparum* iRBC (P) adhering to the surface of a microvascular endothelial cell (En). Scale bar is 1 µm. (B) Detailed view of the interface between an iRBC and an endothelial cell. Arrows indicate electron dense connective material located at knobs. A Maurer's cleft is located close to the iRBC surface (M). Scale bar is 100 nm. Figure modified from (Horrocks, 2005).

1.3. Protein export in *P. falciparum*

By invading a RBC, the *P. falciparum* parasite faces a conceptual problem as it has to install the capacity for protein secretion to the host cell de novo. Even though most of the genes of the classical secretion pathway were found in the *P. falciparum* genome, some features are specific to the parasite, such as the rudimentary Golgi apparatus. The fact that parasite proteins that are exported beyond the parasite's confines have to pass through the parasite plasma membrane (PPM), the parasitophorous vacuolar membrane (PVM) and some proteins even traverse the RBC membrane suggests that the parasite developed and induced a highly complex transport mechanism for protein secretion within the host cell. Some of the exported proteins even do not contain a N-terminal ER targeting signal peptide, which in general guides translocation of the proteins into the endoplasmatic reticulum (ER) (Crabb et al., 2010; Haase & de Koning-Ward, 2010; Lingelbach & Przyborski, 2006; Spielmann & Gilberger, 2010, 2015).

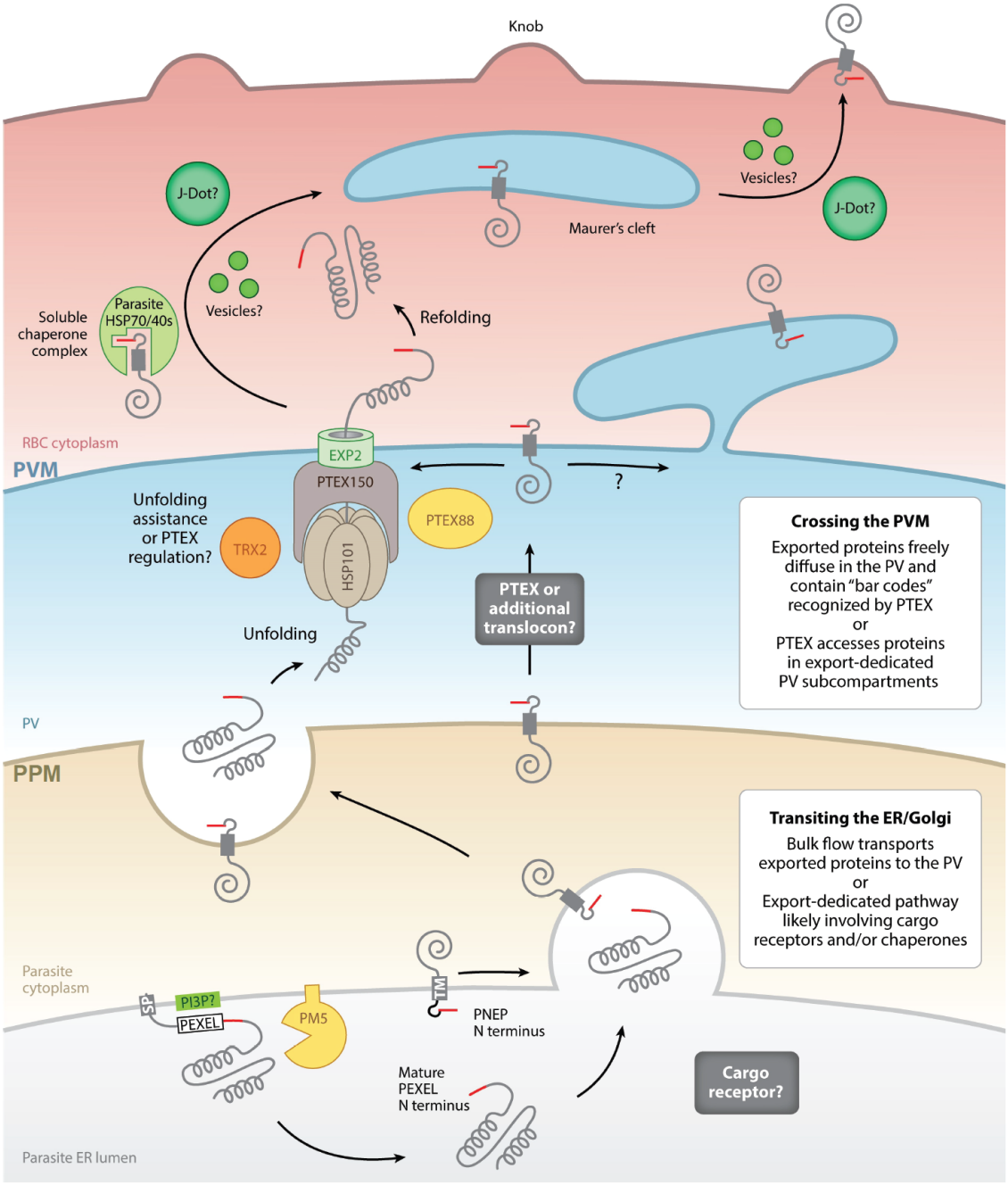

Figure 5: Schematic model of the protein transport mechanisms in *P. falciparum*

After signal sequence cleavage, PI3P binding and plasmepsin-cleavage may initiate transport of PEXEL proteins to the PPM possibly involving a vesicular pathway. After migration through the secretory pathway, the mature PEXEL protein is released to the PV. This process may involve a bulk flow transport or cargo receptors or/and chaperone molecules. In the PV the proteins are unfolded and pass the PTEX. PNEPs are either transported with the same vesicular transport or are trafficked independently to the PPM with a first translocon releasing the PNEPs to the PV or directly to the PTEX or another translocon. Once arrived in the RBC cytoplasm the exported proteins refold and most proteins are transported to the Maurer's clefts to reach their final destination. This step may involve exported parasite chaperones associate with J-dots or vesicles. Figure modified from (Spillman et al., 2015).

1.3.1. Signal sequences for export

A milestone in deciphering the export mechanism of *P. falciparum* was the discovery of a conserved amino acid motif close to the N-terminus in a large group of exported proteins and led to the prediction of the *Plasmodium* exportome (Hiller et al., 2004; Marti et al., 2004; van Ooij et al., 2008; Sargeant et al., 2006). The *Plasmodium* export element (PEXEL) (Marti et al., 2004) or vacuolar transport signal (VTS) (Hiller et al., 2004) consists of the pentameric consensus RxLxE/Q/D whereas x represents any non-charged amino acid. Most PEXEL proteins also contain an N-terminal signal sequence (SS) that mediates co- or post-translational insertion into the endoplasmatic reticulum (ER). Generally, this hydrophobic stretch is located up to 80 amino acids from the N-terminus. It was suggested that in the ER the aspartic protease plasmepsin V (PM5) cleaves the PEXEL after the leucine residue (Klemba & Goldberg, 2005), prior to N-terminal acetylation (Boddey et al., 2009, 2010; Chang et al., 2008; Osborne et al., 2010; Russo et al., 2010) (Fig. 5). The enzyme responsible for acetylation has not been identified so far and the importance of the modification of the export process is unknown. However, N-acetylation on its own is not sufficient to mediate protein export (Boddey et al., 2009; Tarr et al., 2013). The PEXEL motif has also been reported to mediate phosphatidylinositol 3-phosphate (PI3P) binding in the ER, binding PEXEL proteins to a unique trafficking pathway and PM5 to facilitate release from the membrane (Bhattacharjee et al., 2012a). However, recent data do no support this hypothesis (Bhattacharjee et al., 2012b; Sleebs et al., 2014; Tarr et al., 2013). The presence of PEXEL proteins not only seems to be restricted to asexual blood stages as members of the PHIST protein family (section 1.5.1) have an implicated functional role in gametocytogenesis (Silvestrini et al., 2010).

Proteins which do not contain an N-terminal hydrophobic signal sequence, a PEXEL motiv, or other conserved export sequences are referred to as PEXEL-negative exported proteins and are not substrates for PM5 (Boddey et al., 2013). The first PNEP discovered was SBP1 (Blisnick et al., 2000) even though at this time the PEXEL motif had not yet been described.

With the discovery of further PNEPs, namely REX1 (Hawthorne et al., 2004), REX2 (Spielmann et al., 2006), MAHRP1 (Spycher et al., 2003) and MAHRP2 (Pachlatko et al., 2010) it became apparently that the *Plasmodium* exportome comprises more proteins than previously estimated. Typical PNEPs contain a transmembrane domain and lack a classical

signal peptide but recent work identified a variety of PNEPs including soluble and TM proteins with or without SS (Heiber et al., 2013). Detailed studies with a set of different chimeric reporter proteins suggests that the N-terminus of PNEPs can function similarly to mature PEXEL within the ER and that PNEP TM domains mediate ER entry in the absence of a SS peptide (Grüring et al., 2012).

Even though the function of many PNEPs has not yet been described, knockout studies of REX1, SBP1 and MAHRP1 suggest that they play an important role in Maurer's clefts morphology (REX1) and the transport of PfEMP1 to the surface of the iRBC (SBP1, MAHRP1) (Cooke, 2006; Hanssen et al., 2008; Maier et al., 2007; Spycher et al., 2008).

The absence of a distinct export sequence prevented the identification of further PNEPs which may account for an even larger number of exported proteins, especially in other *Plasmodium* subspecies, that lack the PEXEL-containing genes families present in *P. falciparum*. Sensitivity to brefeldin A suggests a shared trafficking mechanism for both PEXEL proteins and PNEPs (Grüring et al., 2012). The elucidation of such a mechanism and the characterization of key molecules for routing to the PV for export would further shed light into the complex transport mechanism of exported proteins in *Plasmodium*.

1.3.2. Transport through the PVM

To reach the RBC cytosol exported proteins need to traverse the parasitophorous vacuolar membrane (PVM). This process was assumed to involve an ATP-powered translocon apparatus and that unfolding of both soluble PEXEL proteins and PNEPs is required (Ansorge et al., 1996; Gehde et al., 2009; Heiber et al., 2013). The subsequent discovery of a protein complex termed *Plasmodium* translocon of exported proteins (PTEX) was the first indication of the presence of a PVM translocon (de Koning-Ward et al., 2009) (Fig. 6). The PTEX complex comprises the single membrane protein component exported protein 2 (EXP2) (Fischer et al., 1998) which is suggested to form a protein-conducting channel. The second core component, consistent with the requirement of ATP, is HSP101, an AAA+ ATPase serving as a power source for the translocation process. The third core component of the PTEX complex PTEX150 is less characterized so far and seems to be restricted to *Plasmodium* species. Further components of the PTEX complex are PTEX88 and thioredoxin2 (TRX2) (Boucher et al., 2006) representing a smaller proportion of the complex. TRX2 is an active thioredoxin and may help facilitate protein unfolding or reducing intramolecular disulfide

bonds (Sharma et al., 2011). Both TRX2 and PTEX88 are non-essential accessory components of the PTEX translocon as both genes can be deleted in *P. berghei* (Matthews et al., 2013; Matz et al., 2013). Further, knockdown experiments of PTEX150 in *P. falciparum* and HSP101 in *P. berghei* arrested parasite development in early trophozoite stage and blocked protein export (Elsworth et al., 2014). Indcucible regulation of HSP101 in *P. falciparum* resulted in a similar growth arrest and soluble exported proteins accumulated in the PV lumen (Beck et al., 2014). Remarkably, both studies showed a block in protein export for all classes of exported proteins including soluble and TM proteins of both PEXEL proteins and PNEPs, suggesting the PTEX to be a universal translocon for various classes of exported proteins.

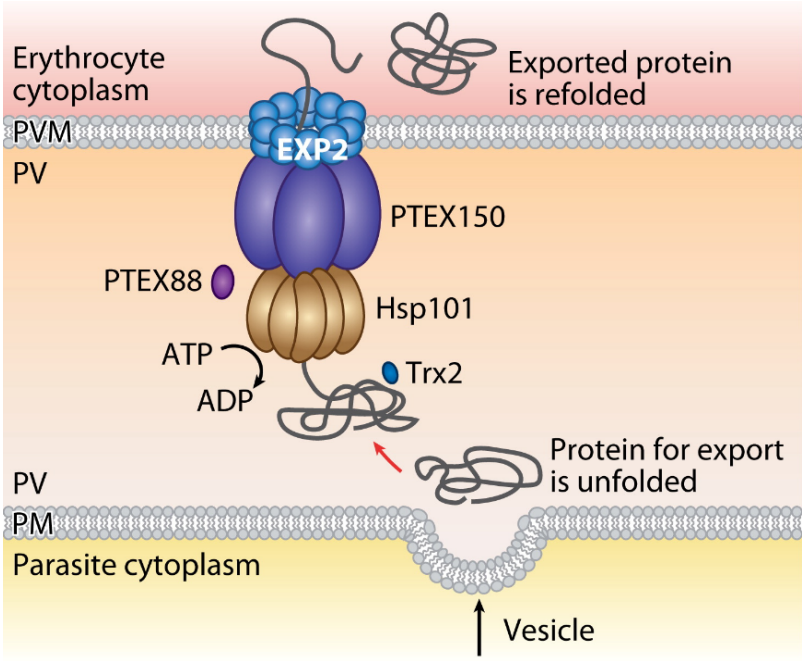

Figure 6: Schematic view of the putative PTEX. The protein destined for the RBC cytoplasm is transported to the parasitophorous vacuole (PV) by fusion of a vesicle at the parasite membrane (PM). The unfolded protein is fed through the Hsp101-PTEX150 complex to EXP2 which has been proposed to be the translocation pore. The translocated protein is again refolded, possibly with chaperones involved. (Boddey & Cowman, 2013).

1.4. *Plasmodium falciparum* erythrocyte membrane protein 1

Plasmodium falciparum erythrocyte membrane protein 1 (PfEMP1) is a family of high-molecular weight (200-400kDa) proteins, which are exported to the surface of the iRBC where they mediate adhesion to the vascular endothelium allowing the parasite to avoid splenic clearance. They are encoded by different members of the *var* multi-copy gene family, which are mostly localized in subtelomeric regions but also in central regions of the 14 chromosomes. All 59 *var* genes in the haploid *P. falciparum* genome consist of two exons

separated by a conserved intron (Gardner et al., 2002). Exon 1 encodes the extracellular part of the PfEMP1 molecule, while the TM domain and the intracellular part are encoded by exon 2 (Fig. 7). Based on the chromosomal location, upstream promoter sequence (ups) and direction of transcription, *var* genes can be divided into 3 major groups A (10 genes in *P. falciparum* 3D7), B (22 genes), C (13 genes) and intermediate groups B/A (4 genes) or B/C (9 genes) (Gardner et al., 2002; Lavstsen et al., 2003). Work with parasite field isolates from endemic regions revealed that mostly group A and B *var* genes are differentially transcribed in patients with severe malaria compared with uncomplicated malaria (Jensen, 2004; Rottmann et al., 2006).

It has been shown that the mutually exclusive expression of a single *var* gene and the silent state of the rest of the family members is epigenetically controlled and linked to histone modifications (Chookajorn et al., 2007; Lopez-Rubio et al., 2007). Previous work demonstrated that of the hyper variable repertoire of *var* genes only a single PfEMP1 molecule is transcribed and expressed on the surface of the iRBC at each life cycle (Dzikowski et al., 2006; Voss et al., 2005). However, recent data reported parasites that co-express two different PfEMP1 antigens at the surface of iRBCs (Joergensen et al., 2010).

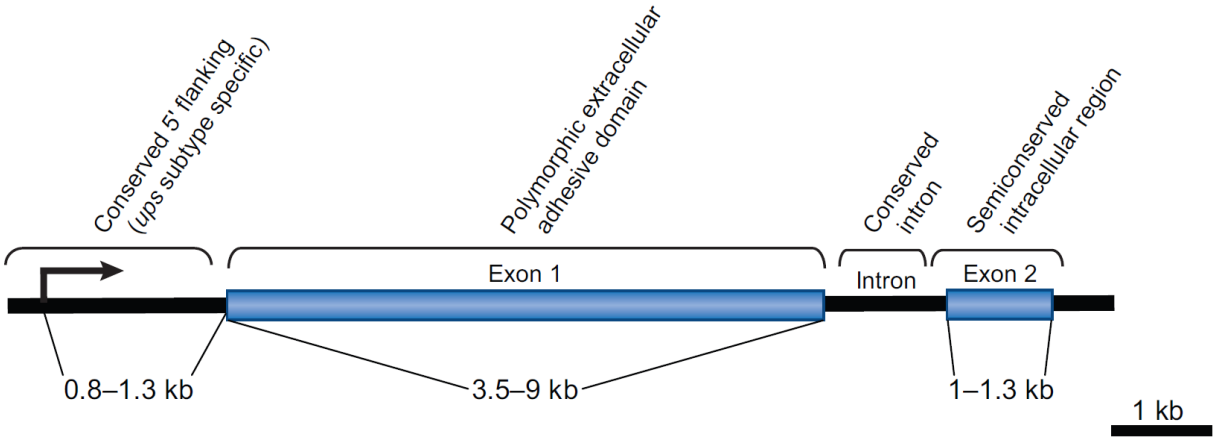

Figure 7: Common features of the var gene family

The members of the *var* gene family consist of two exons separated by a single conserved intron. Exon 1 encodes the variable extracellular domain including the N-terminal sequence (NTS), Duffy binding like domains (DBL), cysteine-rich interdomains (CIDR) and a transmembrane domain (TM). Exon 2 encodes the semi-conserved intracellular amino acidic terminal segment (ATS). Figure modified from (Scherf et al., 2008).

1.4.1. The ATS domain of PfEMP1

Exon II encodes for the semi-conserved cytoplasmic tail of PfEMP1 with an acidic terminal sequence (ATS). The intracellular ATS domain is semi-conserved across the PfEMP1 family (Lavstsen et al., 2003), shares a unique molecular architecture with a minimal folded core and three flexible segments and is thought to be a conserved protein interaction epitope for anchoring PfEMP1 within the knob structure on the surface of the iRBC (Mayer et al., 2012). The high level of sequence conservation of the ATS domains within the 59 PfEMP1 variants in the *P. falciparum* 3D7 isolate suggests that parts of the ATS domain are a generalized feature in the PfEMP1 family (Mayer et al., 2012). Moreover it has been shown that the ATS domain associates with the PHIST domain of PFI1780w, a member of the *Plasmodium* helical interspersed sub-telomeric (PHIST) protein family (Mayer et al., 2012).

Recombinant KAHRP is shown to interact with the ATS fragments when bound and immobilized on a surface (Oh et al., 2000; Waller et al., 1999). Therefore the KAHRP-ATS interaction is well accepted in the malaria field, even though no biophysical studies were performed. Conversely, recent NMR studies do not support the KAHRP-ATS interaction although a very weak interaction could not be excluded (Mayer et al., 2012).

1.4.2. The ectodomain of PfEMP1

In contrast to the semi-conserved exon II, there is an extensive polymorphism for exon I within single genomes but also between genomes. Due to frequent recombination or rearrangement events a vast repertoire of *var* genes is generated in nature. However, the overall function of PfEMP1 in adhesion to endothelial receptors is conserved.

The highly variable extracellular part of PfEMP1 usually includes an N-terminal segment (NTS), multiple copies of duffy binding like domains (DBL), 1-2 cysteine rich interdomain regions (CIDR) and a transmembrane domain (TM) (Gardner et al., 2002). The length of each *var* gene depends on the number and types of domains in the sequence. Based on sequence similarities the DBL domains can be further categorized into DBL α, β, γ, ε, δ, ζ and five smaller classes (Rask et al., 2010; Smith et al., 2000). Similar to that, CIDR domains can be divided into α, β, γ, δ and pam subclasses (Rask et al., 2010; Smith et al., 2000). Each of these subclasses can be further subdivided into 147 subtypes (e.g. DBL$\alpha_{1.3}$).

The binding specificity to endothelial receptors is closely related to the structural characteristics of PfEMP1 molecules. Despite the enormous diversity of PfEMP1 molecules

only a few endothelial surface molecules have been confirmed to act as receptors of iRBC adhesion. Therefore it is assumed that a number of PfEMP1 molecules must have a binding affinity for the same receptor. A recent study indicated that receptor specificity is mediated by a combination of different domains referred to as domain cassette (DC) (Rask et al., 2010). The binding sites of some receptors can be mapped to specific CIDR and DBL domains of PfEMP1 (Baruch et al., 1997; Joergensen et al., 2010). For instance parts of the CIDR1α domain of group B and C PfEMP1 molecules revealed strong binding to multiple receptors including CD36 and ICAM-1 (Chen et al., 2000; Robinson et al., 2003). Concomitant, iRBCs bind to ICAM-1 via the DBLβ3 domain of group A PfEMP1 molecules and the DBLβ-C2 domains of group B and C PfEMP1 molecules (Bengtsson et al., 2013; Howell et al., 2007).

1.4.3. Export of PfEMP1 to the surface of the iRBC

To date the transport process of PfEMP1 to the RBC membrane is poorly understood. PfEMP1 does not possess a SS but a TM domain in the C-terminal region, which bears resemblance to the PEXEL motiv and seems to be essential for PfEMP1 transport (Knuepfer, 2005; Marti et al., 2004). Moreover the semi-conserved head region (NTS, DBL1 and CIDR domains) and the TM domain with the cytoplasmic part of the molecule are required for proper export and display of PfEMP1 on the iRBC (Melcher et al., 2010).

PfEMP1 is found at the parasite surface after 8-11 hours post-invasion, trafficked to MC's and simultaneously with the arrest of Maurer's clefts mobility appears on the surface of the iRBC (Grüring et al., 2011; Kriek et al., 2003; Papakrivos et al., 2004; Wickham et al., 2001). Some studies suggest that PfEMP1 is transported through a vesicle-dependent process (Taraschi, 2003), whereas other studies indicate a possible role for a soluble chaperone complex (Knuepfer, 2005; Papakrivos et al., 2004). Disruption of resident Maurer's clefts proteins including MAHRP1 (Spycher et al., 2008), SBP1 (Cooke, 2006; Maier et al., 2007), *P. falciparum* antigen 332 (Glenister et al., 2009) and deletion of REX1 or the coiled-coil region of REX1 (Dixon et al., 2011; McHugh et al., 2015) abolished PfEMP1 display on the iRBC surface. Recently, six PEXEL proteins, namely PfEMP1-trafficking proteins 1-6 (PTP1-6) were identified to play a role in PfEMP1 transport (Maier et al., 2008). Disruption of PTP3, PTP4 and PTP6 expression in *P. falciparum* resulted in decreased PfEMP1 level on the iRBC surface, whereas lack of PTP1, PTP2 and PTP3 abolished PfEMP1 iRBC surface display suggesting they are all required for proper subcellular localization of PfEMP1. Moreover

PTP1 has shown to play a role for proper Maurer's clefts formation and links other proteins to the iRBC actin cytoskeleton (Rug et al., 2014). Recent work has suggested that haemoglobinopathies HbS and HbC protected carriers from severe malaria by interfering with parasite-induced host actin remodeling, thereby preventing the parasite to establish its own actin cytoskeleton (Cyrklaff et al., 2011, 2012). As a result Maurer's clefts movement was altered, PfEMP1 failed to reach the host cell surface and cytoadherence of iRBC was reduced (Cholera et al., 2008; Fairhurst et al., 2003). A recent study showed that hemoglobinophatic iRBCs displayed a reduced amount and slower parasite-derived protein transport compared to wild type iRBCs (Kilian et al., 2015).

1.5. PHIST protein family

A multi-gene family that is expanded in human-infective *Plasmodium* species and greatly expanded in *P. falciparum* is the recently identified *Plasmodium* helical interspersed subtelomeric (PHIST) family (Sargeant et al., 2006). Initial sequence alignments indicated the presence of a conserved domain of approximately 150 amino acids in length and the domain is predicted to consist of four consecutive alpha helices without any similarities to other known protein sequences. A recent study revealed 67 *P. falciparum* specific proteins containing a conserved *Plasmodium* RESA N-terminal (PRESAN) domain and structure predictions of the core domain assumed six conserved helical segments (Oakley et al., 2007). Noteworthy, the newly discovered multi-gene family underwent a dramatic lineage-specific proliferation only in *P. falciparum* and both studies suggested a role in host cell modification and an interaction epitope for cytoplasmic protein interactions. A typical PHIST protein includes a two exon gene structure, whereat the first exon encodes a SS and the second exon encodes a PEXEL motif, a PHIST domain and other additional amino acid residues. The genes encoding PHIST proteins are primarily encoded in subtelomeric regions of all chromosomes, except chromosome 3 and generally show transcriptional peaks in late schizont and ring stages (Le Roch et al., 2004; Sargeant et al., 2006). A large number of PHIST members also show variation in expression during the parasite life cycle and among parasite isolates (Flueck et al., 2009; Lopez-Rubio et al., 2009; Rovira-Graells et al., 2012; Salcedo-Amaya et al., 2009). The primal identification of the PHIST family revealed 72 paralogs in *P. falciparum,* 39 in *P. vivax*, 27 in *P. knowlesi* and *P. cynomolgi*, 3 in *P. gallinaceum* and one

each in *P. yoelli*, *P. berghei* and *P. chabaudi* (Sargeant et al., 2006) (Fig. 8). To date only one member of the PHIST family has been identified in the four rodent parasite genomes, indicating radiation of the *phist* gene family in primate parasites. Although sharing a common core domain, the PHIST domain clusters into three distinct subgroups (PHISTa, PHISTb, PHISTc), distinguished by the presence and position of several conserved tryptophan residues. Moreover, the three subfamilies have expanded differentially in *Plasmodia* species (Fig. 8).

A recent comparative analysis and classification of variant surface antigens (VSA) from seven *Plasmodium* genomes including the *phist* gene family revealed 22 full-length proteins that are currently not annotated as *phist* family members, including four *P. falciparum* genes (Frech & Chen, 2013). Moreover the *phist* cluster was shown to be closely related to a *P. vivax* gene family of 44 genes called *rad* (pv-fam-e) (Carlton et al., 2008).

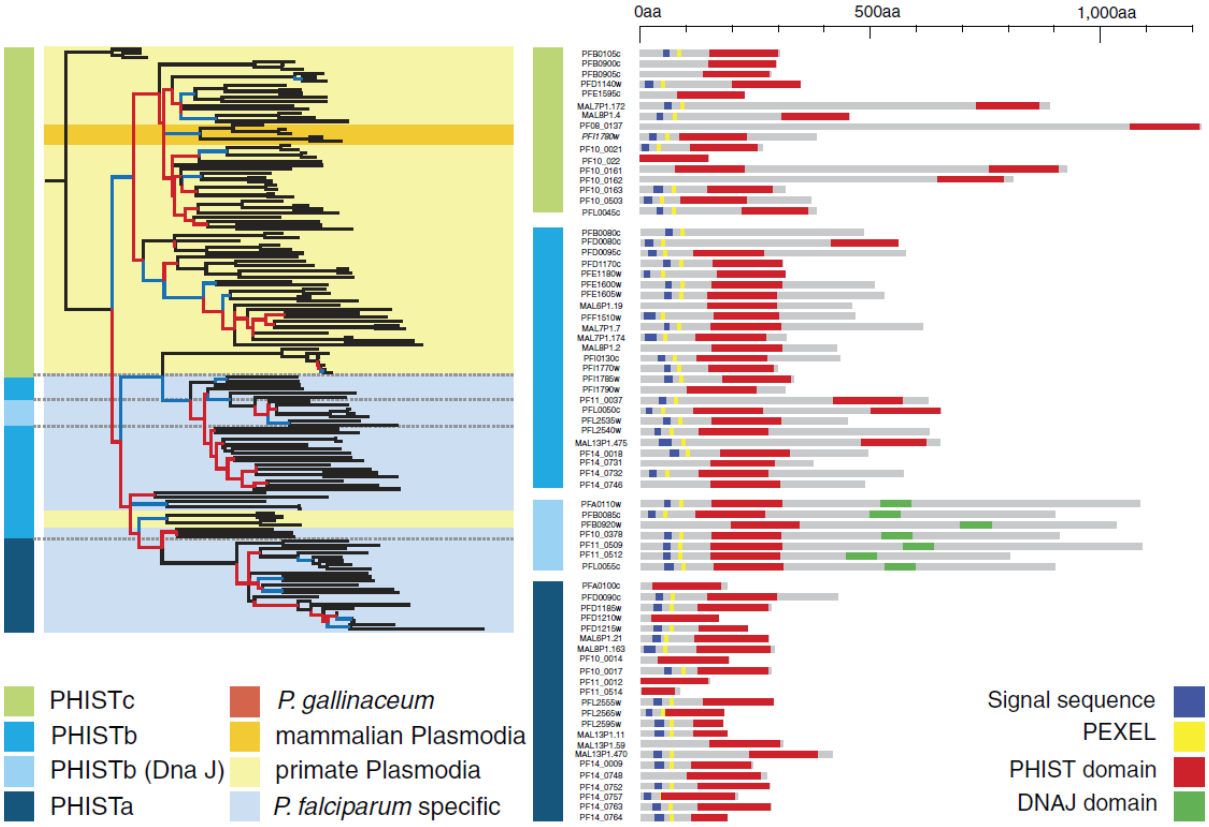

Figure 8: The PHIST protein family

(Left) Phylogenetic tree illustrates the conservation of the PHIST domain across *Plasmodium*. Subfamilies and species conservation are visualized in colours. (Right) Domain map depicts members of the PHIST family and illustrates organisatorial differences between subfamilies. Characterized domains are highlighted in colours. Figure modified from (Sargeant et al., 2006).

As the number of identified members, the classification into subgroups, and the criteria to cluster the PHIST family greatly varies between recent publications, an elaborate and comprehensive analysis of all potential and suggested members of this highly divergent protein family is urgently needed.

1.5.1. The PHISTa subfamily

PHISTa proteins are very short in size and some consist only of a signal sequence, a PEXEL motif and a PHIST domain (Sargeant et al., 2006). In contrast to the PHISTb and PHISTc subfamilies, PHISTa is specific to the *P. falciparum* lineage. PHISTa appear to be transcriptionally silent in 3D7 parasites with two exeptions, PFD0090c and PFL2565w (Sargeant et al., 2006; Scholz & Fraunholz, 2008). In contrast, whole transcriptional studies from venous blood of different patients highlighted *phist-a* transcript upregulation and suggested a role in iRBC adhesion in the brain microvasculature and potentially cerebral malaria (Claessens et al., 2012; Daily et al., 2005; Mok et al., 2007). Moreover, the differential expression of *phist-a* genes in these studies further supported the findings that some PHIST members are mutually exclusive expressed (Rovira-Graells et al., 2012) as originally postulated (Sargeant et al., 2006)

With a yeast two-hybrid screen an interaction between the PHIST domain of PFD0090c and the erythrocyte cytoskeleton component band 4.1 was identified, even though the subcellular localization of the endogenous protein at the PVM suggests a different role of this protein (Parish et al., 2013).

PHISTa proteins may also play a role in gametocytogenesis, as two *phist-a* genes, namely PF14_0744 and PF14_0748 were upregulated in gametocytes (Eksi et al., 2005; Silvestrini et al., 2005, 2010). The proteins were either localizing in the gametocyte PV or the iRBC cytosol indicating that exported PHISTa proteins may be involved in the formation of sexual stages.

1.5.2. The PHISTb subfamily

The PHISTb subfamily displays length variability at the C-terminus after the PHIST domain and a subset of PHISTb proteins including the ring infected surface antigen (RESA) and the RESA-like proteins contain a DnaJ domain at the C-terminus. Most of the *phist-b* genes show transcriptional peaks mainly in early asexual stages (Scholz & Fraunholz, 2008) but a number

of genes of this subfamily are specifically upregulated in early gametocyte stages (Eksi et al., 2005; Silvestrini et al., 2005; Young et al., 2005).

RESA was shown to interact directly with the erythrocyte cytoskeleton by binding to spectrin tetramers, resulting in increased resistance to shear stress and thermal damage (Mills et al., 2007; Pei et al., 2007; Da Silva et al., 1994; Silva et al., 2005). In a large-scale knockout approach, several functions have been assigned to PHISTb proteins although the localization of the proteins has not been determined (Maier et al., 2008). Disruption of PFB0920w resulted in an increased rigidity of iRBCs, whereas disruption of PF14_0018 or RESA lead to a decrease in cell rigidity (Maier et al., 2008; Mills et al., 2007). Moreover, deletion of PFD1170c resulted in loss of knob structures on the surface of iRBCs and a partial reduction of cytoadherence under flow conditions (Maier et al., 2008). Interestingly, in parasite isolates from placenta, the PFI1785w transcript is specifically upregluated (Francis et al., 2007; Tuikue Ndam et al., 2008).

Nine PHISTb proteins including PFD1170c were recently shown to localize to the iRBC periphery and detergent insolubility further supports a cytoskeleton association of these proteins (Tarr et al., 2014). Additionally, the region N-terminal to the PHIST domain together with the PHIST domain contributes to a functional peripheral targeting domain in PHISTb proteins. PHISTb homologues in *P. vivax* and *P. knowlesi* exhibit an iRBC peripheral localization indicating a conserved feature in multiple human malaria parasite species.

Kilili et al. reported that the MESA erythrocyte cytoskeleton-binding (MEC) domain is present in at least 14 different exported *P. falciparum* proteins, among which nine belong to the PHISTb subfamily (Kilili & LaCount, 2011). A subset of these proteins bound to inside-out vesicles and co-precipitated full-length human erythrocyte band 4.1 suggesting the MEC domain facilitates binding to the erythrocyte cytoskeleton.

Recent work by Proellocks and colleages identified the function of PFE1605w, termed lysine-rich membrane-associated PHISTb (LyMP). With inside-out vesicles experiments LyMP was shown to be associated directly with the cytoskeleton of iRBC and deletion of LyMP reduced the adhesion of iRBCs to CD36 by 55% (Proellocks et al., 2014).

Overall it seems that most PHISTb proteins localize to the periphery of the RBC and interact with the cytoskeleton suggesting a role in the refurbishment and rigidification of the host cell.

1.5.3. The PHISTc subfamily

The PHISTc subfamily is the most diverse group of PHIST proteins and the PHIST domain is mostly located at the very C-terminus. They are commonly found in different *Plasmodium* subspecies and it seems that the PHISTc subfamily has evolved before the two lineages *P. falciparum* and *P. vivax* diverged, as disclosed by the presence of PHISTc orthologs in both subspecies and also in other subspecies like *P. knowlesi* (Prajapati & Singh, 2013; Sargeant et al., 2006; Scholz and Fraunholz, 2008). Some proteins containing a PHISTc domain have been shown to be essential for survival of *P. falciparum* (Maier et al., 2008) and *P.vivax* (Akinyi et al., 2012) as targeted gene disruption failed. A PHISTc protein, MAL7P1.172 or also termed PfEMP1 trafficking protein 2 (PTP2) was shown to localize in the MC's lumen and gene disruption resulted in a reduced level of PfEMP1 on the surface of iRBCs (Maier et al., 2008). Further, a follow-up study revealed that MAL7P1.172 localizes to exosomes and mediates cell-cell communication by plasmid transfer between iRBCs (Regev-Rudzki et al., 2013).

Very recently, the PHISTc termed *Plasmodium falciparum* Gametocyte Exported Protein-5 (PfGEXP5) has been shown to be exported into the host cell cytoplasm after 14 hour post invasion of sexually committed merozoites therefore representing the earliest post-invasion gametocyte marker described to date (Tiburcio et al., 2015).

Biophysical protein interaction studies identified the ATS domain of PfEMP1 to be a conserved protein interaction epitope and demonstrated an ATS interaction with the PHIST domain of PFI1780w (Mayer et al., 2012). Therefore the PHIST domain is proposed to facilitate protein interactions and may be involved in the parasite cytoadherence system.

1.6. The human red blood cell

The human red blood cell is a biconcave disk-shaped cell lacking a nucleus or intracellular organelles and contains approximately 450 mg/ml hemoglobin in the cytoplasm for O_2/CO_2 exchange. As the RBC repeatedly passes narrow capillaries in the peripheral tissue vessels it is remarkably deformable and extremely stable. The plasma membrane is composed of a bilayer of cholesterol and phospholipids which are anchored to a 2 dimensional elastic network of skeletal proteins via interactions with the cytoplasmic domains of TM proteins embedded in the lipid bilayer (Mohandas & Evans, 1994). The lipid bilayer consists of equal ratios of cholesterol and phospholipids. Cholesterol is suggested to be equally distributed

between the two leaflets of the RBC membrane but the ratio of the four different major phospholipids varies (Zwaal & Schroit, 1997). This asymmetry is suggested to be controlled by scramblases and flippases (Sims & Wiedmer, 2001) and is of functional relevance as phospholipids interact with skeletal proteins such as spectrin and protein 4.1R.

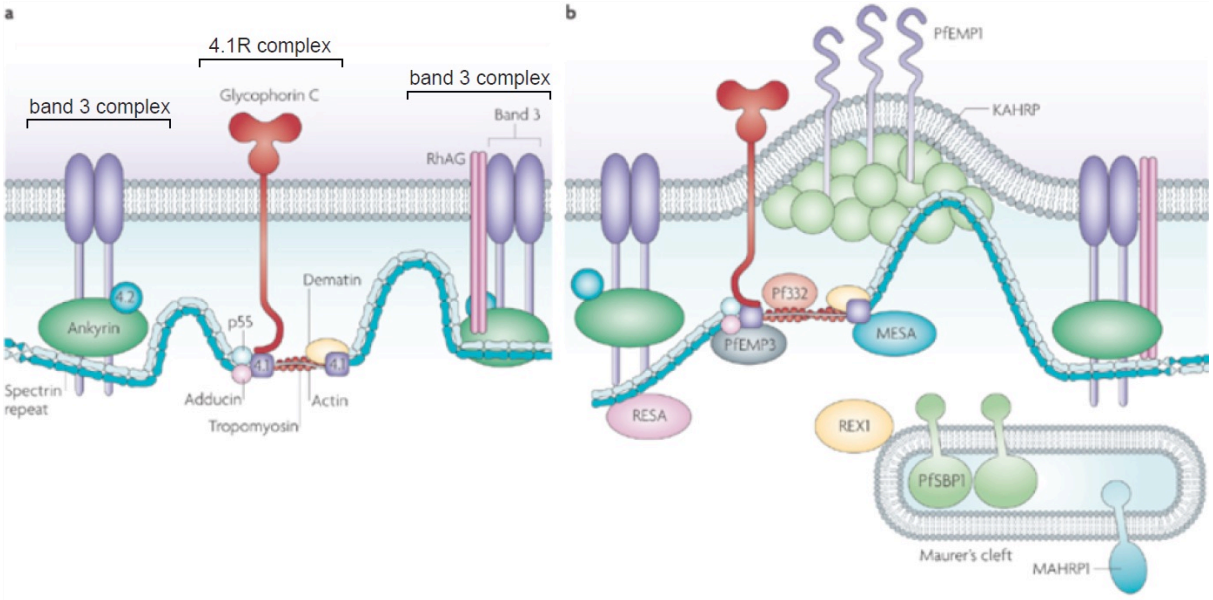

Figure 9: The membrane organization of uninfected and *P. falciparum* infected RBCs

(a) Uninfected RBC. The band 3 complex is anchored via ankyrin to the spectrin tetramer. The membrane skeletal protein 4.2 has binding affinity to both band 3 and ankyrin. The protein 4.1R or junctional complex is comprised of the ternary complex of spectrin, F-actin and 4.1R and the actin binding proteins adducing, dermatin, tropomodulin and tropomyosin. The adaptor protein 4.1R ternary binds GPC and p55. (b) Infected RBC. RESA associates with spectrin and stabilizes and protects the band 3 complex. KAHRP self-associates and binds ankyrin and spectrin. PfEMP1 localizes in knobs and is thought to interact with the cytosolic domain to spectrin. Pf322 and MESA are thought to bind to the 4.1R complex whilst PfEMP3 binds to spectrin. REX1, MAHRP1 and SBP1 are Mauer's cleft proteins. Figure modified from (Maier et al., 2009).

1.6.1. The structural organization of the RBC membrane

The RBC owes its mechanical flexibility to the membrane-associates protein skeleton which is composed of spectrin tetramers, formed by self-assembly of α-/β-spectrin heterodimers. This 2-dimensional spectrin-based membrane skeleton is attached to the lipid bilayer through two well characterized linkages, the band 3 complex and the junctional 4.1R complex (Fig. 9).

The more prominent and well characterized band 3 complex forms a bridge from the integral membrane protein band 3 via ankyrin to spectrin and involves a variety of well characterized high affinity protein-protein interactions (Mohandas & Gallagher, 2008; Steck, 1974). Defects or deficiencies of the band 3 anion transport protein or the adaptor protein ankyrin lead to a reduced coherence between the membrane skeleton and the lipid bilayer resulting in sphere-shaped RBCs, a pathology termed spherocytosis (Costa et al., 1990; Stefanovic et al., 2007). Disruption of the band 3 complex by addition of competing fragments of either band 3 or ankyrin or specific monoclonal antibodies led to membrane deformation and emphasizes the importance of the band 3 complex-spectrin bridge in the maintenance of the RBC membrane integrity (Van Dort et al., 2001).

The second bridge of the membrane bilayer to the spectrin/actin skeleton involves the transmembrane protein glycophorin C (GPC), which is anchored to spectrin through binding to the adapter protein 4.1 (Marfatia et al., 1994). As actin weakly interacts with the N-terminus of β-spectrin, this interaction is enhanced by protein 4.1R binding and the ternary spectrin-actin-protein 4.1R complex is an important regulator of mechanical membrane integrity (Ohanian et al., 1984). The cytoskeletal protein complex comprised of actin, adducin, dematin, protein 4.1, tropomodulin and tropomyosin builds the junctional complex and spectrin tetramers extending to a two dimensional grid allows mechanical stability to the RBC membrane. GPC-deficient RBCs showed a decrease in the mechanical stability suggesting the GPC protein 4.1 bridge is essential for RBC integrity (Gascard & Cohen, 1994; Reid et al., 1990).

Together, these two major protein complexes with the bridge to the spectrin/actin cytoskeleton are likely to be responsible for the structural and mechanical properties of the highly specialized and differentiated red blood cell.

1.6.2. Interactions with the host erythrocyte cytoskeleton

Uninfected RBCs possess a highly ordered but flexible cytoskeleton. A consequence of *P. falciparum* infection is the reorganization of the cytoskeletal network resulting in increased rigidity of the host cell and dramatic changes in fluidity, permeability and adhesiveness. This improves the ability of the iRBC to cytoadhere to host receptors but also leads to blocking of the microcapillaries of organs resulting in the major pathology of malaria. Molecular protein-protein interactions of exported *Plasmodium* proteins with the RBC cytoskeleton lead to

crosslinking of cytoskeletal proteins that can increase the rigidity of the iRBC. Even though the mechanism leading to decreased deformability of the iRBC is not understood to date, the contribution of exported parasite-derived proteins to increase rigidity can most likely be ascribed to direct or indirect interactions with the RBC cytoskeleton.

One of the first proteins exported to the RBC is RESA which binds β-spectrin and is thought to stabilize the band 3 complex against thermal disruption (Mills et al., 2007; Pei et al., 2007; Silva et al., 2005). These findings are further supported as disruption of RESA resulted in a reduced rigidity of the iRBCs (Maier et al., 2008). KAHRP is known to associate with spectrin, ankyrin and actin in the RBC cytoskeleton and is suggested to crosslink spectrin resulting in increased rigidity of the membrane (Pei et al., 2005; Weng et al., 2014). Moreover, KAHRP is thought to anchor PfEMP1 to the RBC membrane through an interaction of KAHRP with the C-terminus of PfEMP1 (Waller et al., 1999) although a recent study did not shown evidence for this interaction in solution experiments under physiological conditions (Mayer et al., 2012). In case of a physiological relevant interaction of KAHRP with PfEMP1, which is inserted in the RBC membrane through a TM domain, this would cause an additional increase in rigidity of the iRBC. The cytoplasmic domain of PfEMP1 was also shown to bind spectrin, actin band 4.1 and full length KAHRP *in vitro* (Oh et al., 2000). The mature parasite-infected erythrocyte surface antigen (MESA) interacts with the N-terminal domain of protein 4.1R, it competes with p55 for binding to 4.1R, and therefore may modulate the 4.1R-p55 interaction *in vivo* (Waller, 2003). The PHISTa protein PFD0090c has also been shown to interact with the regulator protein band 4.1 (Parish et al., 2013).

Several exported proteins have been implicated in the alteration of the RBC mechanical properties but the exact function or interaction epitopes have not yet been elucidated. Disruption of the *P. falciparum* antigen 332 (Pf322), glycophorin binding protein 130, PTP3, PF13_0073, PFB0920w and PF10_0159 lead to increase in rigidity of the iRBCs (Glenister et al., 2009; Maier et al., 2008), whereas reduced levels of MAL8P1.154, PF14_0018 and FIKK4.2 resulted in a decrease in rigidity (Kats et al., 2014; Maier et al., 2008). STEVOR and RIFIN proteins measureable contribute to the rigidity of the iRBC, although it cannot be excluded that this effect is an indirect consequence of STEVOR/RIFIN export to the iRBC membrane (Sanyal et al., 2012).

A recent study suggested that parasite-induced actin remodeling leads to reorganization of the cytoskeletal network (Cyrklaff et al., 2011). In addition to the exported proteins which directly interact with the host cytoskeleton there are also exported proteins which post-translationally modify cytoskeletal components. Recently, FIKK4.1 (PFD1165w) has been shown to phosphorylate band 4.9 at the spectrin actin interface (Brandt & Bailey, 2013).

1.7. Outline of the thesis

The main aim of this thesis was to gain insight into the function of a subset of exported *P. falciparum* PHIST proteins in host cell refurbishment, their influence on the transport of the major virulence factor PfEMP1 to the iRBC surface and to reveal potential protein-protein interactions at the parasite-host interface. The specific objectives of this thesis were:

(i) Identification of the subcellular localization of PFE1605w within the iRBC and investigation of a potential association of the PFE1605w PHIST domain with the ATS domain of different PfEMP1 molecules (chapter 2 & 3).

(ii) Investigation of the function of PFE1605w using different approaches to deplete PFE1605w in its functional compartment and identification of potential protein interactions with parasite-derived or host cell proteins (chapter 3).

(iii) Investigation of the *var* expression and binding phenotypes of ICAM-1 selected 3D7 parasite lines (chapter 4).

1.8. References

Aikawa, M. (1971). Plasmodium: The fine structure of malarial parasites. Exp. Parasitol. *30*, 284–320.

Akinyi, S., Hanssen, E., Meyer, E.V.S., Jiang, J., Korir, C.C., Singh, B., Lapp, S., Barnwell, J.W., Tilley, L., and Galinski, M.R. (2012). A 95 kDa protein of Plasmodium vivax and P. cynomolgi visualized by three-dimensional tomography in the caveola-vesicle complexes (Schüffner's dots) of infected erythrocytes is a member of the PHIST family: Plasmodium caveola-vesicle complex structure. Mol. Microbiol. *84*, 816–831.

Alonso, P.L., and Tanner, M. (2013). Public health challenges and prospects for malaria control and elimination. Nat. Med. *19*, 150–155.

Amino, R., Thiberge, S., Shorte, S., Frischknecht, F., and Ménard, R. (2006). Quantitative imaging of Plasmodium sporozoites in the mammalian host. Défis Microbiol. Mal. Infect. Microbiol. Infect. Dis. *329*, 858–862.

Ansorge, I., Benting, J., Bhakdi, S., and Lingelbach, K. (1996). Protein sorting in Plasmodium falciparum-infected red blood cells permeabilized with the pore-forming protein streptolysin O. Biochem J *315*, 307–314.

Anstey, N.M., Russell, B., Yeo, T.W., and Price, R.N. (2009). The pathophysiology of vivax malaria. Trends Parasitol. *25*, 220–227.

Aregawi, M., Cibulskis, R.E., Kita, Y., Otten, M., Williams, R., World Health Organization, and Global Malaria Programme (2010). World malaria report 2010. (Geneva: World Health Organization).

Ariey, F., Witkowski, B., Amaratunga, C., Beghain, J., Langlois, A.-C., Khim, N., Kim, S., Duru, V., Bouchier, C., Ma, L., et al. (2013). A molecular marker of artemisinin-resistant Plasmodium falciparum malaria. Nature *505*, 50–55.

Atkinson, C., and Aikawa, M. (1990). Ultrastructure of malaria-infected erythrocytes. Blood Cells *16*, 351–368.

Baldauf, S.L. (2000). A Kingdom-Level Phylogeny of Eukaryotes Based on Combined Protein Data. Science *290*, 972–977.

Bannister, L.., Hopkins, J.., Fowler, R.., Krishna, S., and Mitchell, G.. (2000). A Brief Illustrated Guide to the Ultrastructure of Plasmodium falciparum Asexual Blood Stages. Parasitol. Today *16*, 427–433.

Baruch, D.I., Pasloske, B.L., Singh, H.B., Bi, X., Ma, X.C., Feldman, M., Taraschi, T.F., and Howard, R.J. (1995). Cloning the P. falciparum gene encoding PfEMP1, a malarial variant antigen and adherence receptor on the surface of parasitized human erythrocytes. Cell *82*, 77–87.

Baruch, D.I., Ma, X.C., Singh, H.B., Bi, X., Pasloske, B.L., and Howard, R.J. (1997). Identification of a region of PfEMP1 that mediates adherence of Plasmodium falciparum infected erythrocytes to CD36: conserved function with variant sequence. Blood *90*, 3766–3775.

Baum, J., Gilberger, T.-W., Frischknecht, F., and Meissner, M. (2008). Host-cell invasion by malaria parasites: insights from Plasmodium and Toxoplasma. Trends Parasitol. *24*, 557–563.

Baumeister, S., Winterberg, M., Duranton, C., Huber, S.M., Lang, F., Kirk, K., and Lingelbach, K. (2006). Evidence for the involvement of Plasmodium falciparum proteins in the formation of new permeability pathways in the erythrocyte membrane. Mol. Microbiol. *60*, 493–504.

Beck, J.R., Muralidharan, V., Oksman, A., and Goldberg, D.E. (2014). PTEX component HSP101 mediates export of diverse malaria effectors into host erythrocytes. Nature *511*, 592–595.

Bengtsson, A., Joergensen, L., Rask, T.S., Olsen, R.W., Andersen, M.A., Turner, L., Theander, T.G., Hviid, L., Higgins, M.K., Craig, A., et al. (2013). A Novel Domain Cassette Identifies Plasmodium falciparum PfEMP1 Proteins Binding ICAM-1 and Is a Target of Cross-Reactive, Adhesion-Inhibitory Antibodies. J. Immunol. Author Choice *190*, 240–249.

Bhattacharjee, S., Stahelin, R.V., Speicher, K.D., Speicher, D.W., and Haldar, K. (2012a). Endoplasmic Reticulum PI(3)P Lipid Binding Targets Malaria Proteins to the Host Cell. Cell *148*, 201–212.

Bhattacharjee, S., Speicher, K.D., Stahelin, R.V., Speicher, D.W., and Haldar, K. (2012b). PI(3)P-independent and -dependent pathways function together in a vacuolar translocation sequence to target malarial proteins to the host erythrocyte. Mol. Biochem. Parasitol. *185*, 106–113.

Blisnick, T., Betoulle, M.E.M., Barale, J.-C., Uzureau, P., Berry, L., Desroses, S., Fujioka, H., Mattei, D., and Breton, C.B. (2000). Pfsbp1, a Maurer's cleft Plasmodium falciparum protein, is associated with the erythrocyte skeleton. Mol. Biochem. Parasitol. *111*, 107–121.

Boddey, J.A., and Cowman, A.F. (2013). Plasmodium Nesting: Remaking the Erythrocyte from the Inside Out. Annu. Rev. Microbiol. *67*, 243–269.

Boddey, J.A., Moritz, R.L., Simpson, R.J., and Cowman, A.F. (2009). Role of the *Plasmodium* Export Element in Trafficking Parasite Proteins to the Infected Erythrocyte. Traffic *10*, 285–299.

Boddey, J.A., Hodder, A.N., Günther, S., Gilson, P.R., Patsiouras, H., Kapp, E.A., Pearce, J.A., de Koning-Ward, T.F., Simpson, R.J., Crabb, B.S., et al. (2010). An aspartyl protease directs malaria effector proteins to the host cell. Nature *463*, 627–631.

Boddey, J.A., Carvalho, T.G., Hodder, A.N., Sargeant, T.J., Sleebs, B.E., Marapana, D., Lopaticki, S., Nebl, T., and Cowman, A.F. (2013). Role of Plasmepsin V in Export of Diverse Protein Families from the *Plasmodium falciparum* Exportome: Substrate Specificity of Plasmepsin V. Traffic *14*, 532–550.

Boucher, I.W., McMillan, P.J., Gabrielsen, M., Akerman, S.E., Brannigan, J.A., Schnick, C., Brzozowski, A.M., Wilkinson, A.J., and Muller, S. (2006). Structural and biochemical characterization of a mitochondrial peroxiredoxin from Plasmodium falciparum. Mol. Microbiol. *61*, 948–959.

Bozdech, Z., Llinás, M., Pulliam, B.L., Wong, E.D., Zhu, J., and DeRisi, J.L. (2003). The Transcriptome of the Intraerythrocytic Developmental Cycle of Plasmodium falciparum. PLoS Biol *1*, e5.

Brandt, G.S., and Bailey, S. (2013). Dematin, a human erythrocyte cytoskeletal protein, is a substrate for a recombinant FIKK kinase from Plasmodium falciparum. Mol. Biochem. Parasitol. *191*, 20–23.

Caminade, C., Kovats, S., Rocklov, J., Tompkins, A.M., Morse, A.P., Colón-González, F.J., Stenlund, H., Martens, P., and Lloyd, S.J. (2014). Impact of climate change on global malaria distribution. Proc. Natl. Acad. Sci. *111*, 3286–3291.

Carlton, J.M., Adams, J.H., Silva, J.C., Bidwell, S.L., Lorenzi, H., Caler, E., Crabtree, J., Angiuoli, S.V., Merino, E.F., Amedeo, P., et al. (2008). Comparative genomics of the neglected human malaria parasite Plasmodium vivax. Nature *455*, 757–763.

Chang, H.H., Falick, A.M., Carlton, P.M., Sedat, J.W., DeRisi, J.L., and Marletta, M.A. (2008). N-terminal processing of proteins exported by malaria parasites. Mol. Biochem. Parasitol. *160*, 107–115.

Chen, Q., Heddini, A., Barragan, A., Fernandez, V., Pearce, S.F.A., and Wahlgren, M. (2000). The semiconserved head structure of Plasmodium falciparum erythrocyte membrane protein 1 mediates binding to multiple independent host receptors. J. Exp. Med. *192*, 1–10.

Cholera, R., Brittain, N.J., Gillrie, M.R., Lopera-Mesa, T.M., Diakité, S.A.S., Arie, T., Krause, M.A., Guindo, A., Tubman, A., Fujioka, H., et al. (2008). Impaired cytoadherence of Plasmodium falciparum-infected erythrocytes containing sickle hemoglobin. Proc. Natl. Acad. Sci. *105*, 991–996.

Chookajorn, T., Dzikowski, R., Frank, M., Li, F., Jiwani, A.Z., Hartl, D.L., and Deitsch, K.W. (2007). Epigenetic memory at malaria virulence genes. Proc. Natl. Acad. Sci. U. S. A. *104*, 899–902.

Chua, C.L.L., Brown, G., Hamilton, J.A., Rogerson, S., and Boeuf, P. (2013). Monocytes and macrophages in malaria: protection or pathology? Trends Parasitol. *29*, 26–34.

Claessens, A., Adams, Y., Ghumra, A., Lindergard, G., Buchan, C.C., Andisi, C., Bull, P.C., Mok, S., Gupta, A.P., Wang, C.W., et al. (2012). A subset of group A-like var genes encodes the malaria parasite ligands for binding to human brain endothelial cells. Proc. Natl. Acad. Sci. *109*, E1772–E1781.

Cogswell, F.B. (1992). The hypnozoite and relapse in primate malaria. Clin. Microbiol. Rev. *5*, 26–35.

Cooke, B.M. (2006). A Maurer's cleft-associated protein is essential for expression of the major malaria virulence antigen on the surface of infected red blood cells. J. Cell Biol. *172*, 899–908.

Costa, F.F., Agre, P., Watkins, P.C., Winkelmann, J.C., Tang, T.K., John, K.M., Lux, S.E., and Forget, B.G. (1990). Linkage of Dominant Hereditary Spherocytosis to the Gene for the Erythrocyte Membrane-Skeleton Protein Ankyrin. N. Engl. J. Med. *323*, 1046–1050.

Cox, F.E. (2010). History of the discovery of the malaria parasites and their vectors. Parasit Vectors *3*, 5.

Crabb, B.S., Cooke, B.M., Reeder, J.C., Waller, R.F., Caruana, S.R., Davern, K.M., Wickham, M.E., Brown, G.V., Coppel, R.L., and Cowman, A.F. (1997). Targeted gene disruption shows that knobs enable malaria-infected red cells to cytoadhere under physiological shear stress. Cell *89*, 287–296.

Crabb, B.S., de Koning-Ward, T.F., and Gilson, P.R. (2010). Protein export in Plasmodium parasites: From the endoplasmic reticulum to the vacuolar export machine. Int. J. Parasitol. *40*, 509–513.

Cyrklaff, M., Sanchez, C.P., Kilian, N., Bisseye, C., Simpore, J., Frischknecht, F., and Lanzer, M. (2011). Hemoglobins S and C Interfere with Actin Remodeling in Plasmodium falciparum–Infected Erythrocytes. Science *334*, 1283–1286.

Cyrklaff, M., Sanchez, C.P., Frischknecht, F., and Lanzer, M. (2012). Host actin remodeling and protection from malaria by hemoglobinopathies. Trends Parasitol. *28*, 479–485.

Daily, J.P., Le Roch, K.G., Sarr, O., Ndiaye, D., Lukens, A., Zhou, Y., Ndir, O., Mboup, S., Sultan, A., Winzeler, E.A., et al. (2005). In Vivo Transcriptome of *Plasmodium falciparum* Reveals Overexpression of Transcripts That Encode Surface Proteins. J. Infect. Dis. *191*, 1196–1203.

Dehio, C. (2004). Molecular and Cellular Basis of *Bartonella* Pathogenesis. Annu. Rev. Microbiol. *58*, 365–390.

Desai, M., ter Kuile, F.O., Nosten, F., McGready, R., Asamoa, K., Brabin, B., and Newman, R.D. (2007). Epidemiology and burden of malaria in pregnancy. Lancet Infect. Dis. *7*, 93–104.

Dixon, M.W.A., Kenny, S., McMillan, P.J., Hanssen, E., Trenholme, K.R., Gardiner, D.L., and Tilley, L. (2011). Genetic ablation of a Maurer's cleft protein prevents assembly of the Plasmodium falciparum virulence complex: REX1 is required for PfEMP1 trafficking. Mol. Microbiol. *81*, 982–993.

Dobbelaere, D.A., and Küenzi, P. (2004). The strategies of the Theileria parasite: a new twist in host–pathogen interactions. Curr. Opin. Immunol. *16*, 524–530.

Dondorp, A.M., Nosten, F., Yi, P., Das, D., Phyo, A.P., Tarning, J., Lwin, K.M., Ariey, F., Hanpithakpong, W., Lee, S.J., et al. (2009). Artemisinin Resistance in *Plasmodium falciparum* Malaria. N. Engl. J. Med. *361*, 455–467.

Van Dort, H.M., Knowles, D.W., Chasis, J.A., Lee, G., Mohandas, N., and Low, P.S. (2001). Analysis of Integral Membrane Protein Contributions to the Deformability and Stability of the Human Erythrocyte Membrane. J. Biol. Chem. *276*, 46968–46974.

Dzikowski, R., Frank, M., and Deitsch, K. (2006). Mutually Exclusive Expression of Virulence Genes by Malaria Parasites Is Regulated Independently of Antigen Production. PLoS Pathog. *2*, e22.

Eksi, S., Haile, Y., Furuya, T., Ma, L., Su, X., and Williamson, K.C. (2005). Identification of a subtelomeric gene family expressed during the asexual–sexual stage transition in Plasmodium falciparum. Mol. Biochem. Parasitol. *143*, 90–99.

Elsworth, B., Matthews, K., Nie, C.Q., Kalanon, M., Charnaud, S.C., Sanders, P.R., Chisholm, S.A., Counihan, N.A., Shaw, P.J., Pino, P., et al. (2014). PTEX is an essential nexus for protein export in malaria parasites. Nature *511*, 587–591.

Engwerda, C.R., and Good, M.F. (2005). Interactions between malaria parasites and the host immune system. Curr. Opin. Immunol. *17*, 381–387.

Fairhurst, R.M., Fujioka, H., Hayton, K., Collins, K.F., and Wellems, T.E. (2003). Aberrant development of Plasmodium falciparum in hemoglobin CC red cells: implications for the malaria protective effect of the homozygous state. Blood *101*, 3309–3315.

Fischer, K., Marti, T., Rick, B., Johnson, D., Benting, J., Baumeister, S., Helmbrecht, C., Lanzer, M., and Lingelbach, K. (1998). Characterization and cloning of the gene encoding the vacuolar membrane protein EXP-2 from Plasmodium falciparum. Mol. Biochem. Parasitol. *92*, 47–57.

Flueck, C., Bartfai, R., Volz, J., Niederwieser, I., Salcedo-Amaya, A.M., Alako, B.T.F., Ehlgen, F., Ralph, S.A., Cowman, A.F., Bozdech, Z., et al. (2009). Plasmodium falciparum Heterochromatin Protein 1 Marks Genomic Loci Linked to Phenotypic Variation of Exported Virulence Factors. PLoS Pathog. *5*, e1000569.

Fong, Y.L., Cadigan, F.C., and Robert Coatney, G. (1971). A presumptive case of naturally occurring Plasmodium knowlesi malaria in man in Malaysia. Trans. R. Soc. Trop. Med. Hyg. *65*, 839–840.

Francis, S.E., Malkov, V.A., Oleinikov, A.V., Rossnagle, E., Wendler, J.P., Mutabingwa, T.K., Fried, M., and Duffy, P.E. (2007). Six Genes Are Preferentially Transcribed by the Circulating and Sequestered Forms of Plasmodium falciparum Parasites That Infect Pregnant Women. Infect. Immun. *75*, 4838–4850.

Frech, C., and Chen, N. (2013). Variant surface antigens of malaria parasites: functional and evolutionary insights from comparative gene family classification and analysis. BMC Genomics *14*, 427.

Frevert, U., Sinnis, P., Cerami, C., Shreffler, W., Takacs, B., and Nussenzweig, V. (1993). Malaria circumsporozoite protein binds to heparan sulfate proteoglycans associated with the surface membrane of hepatocytes. J. Exp. Med. *177*, 1287–1298.

Gardner, M.J., Hall, N., Fung, E., White, O., Berriman, M., Hyman, R.W., Carlton, J.M., Pain, A., Nelson, K.E., Bowman, S., et al. (2002). Genome sequence of the human malaria parasite Plasmodium falciparum. Nature *419*, 498–511.

Gascard, P., and Cohen, C. (1994). Absence of high-affinity band 4.1 binding sites from membranes of glycophorin C- and D-deficient (Leach phenotype) erythrocytes. Blood *83*, 1102–1108.

Gehde, N., Hinrichs, C., Montilla, I., Charpian, S., Lingelbach, K., and Przyborski, J.M. (2009). Protein unfolding is an essential requirement for transport across the parasitophorous vacuolar membrane of *Plasmodium falciparum*. Mol. Microbiol. *71*, 613–628.

Genton, B., D'Acremont, V., Rare, L., Baea, K., Reeder, J.C., Alpers, M.P., and Muller, I. (2008). Plasmodium vivax and mixed infections are associated with severe malaria in children: a prospective cohort study from Papua New Guinea. PLoS Med *5*, e127.

Gething, P.W., Smith, D.L., Patil, A.P., Tatem, A.J., Snow, R.W., and Hay, S.I. (2010). Climate change and the global malaria recession. Nature *465*, 342–345.

Glenister, F.K., Fernandez, K.M., Kats, L.M., Hanssen, E., Mohandas, N., Coppel, R.L., and Cooke, B.M. (2009). Functional alteration of red blood cells by a megadalton protein of Plasmodium falciparum. Blood *113*, 919–928.

Gohil, S., Kats, L.M., Sturm, A., and Cooke, B.M. (2010). Recent insights into alteration of red blood cells by Babesia bovis: moovin' forward. Trends Parasitol. *26*, 591–599.

Goldberg, D.E. (2013). Complex nature of malaria parasite hemoglobin degradation. Proc. Natl. Acad. Sci. *110*, 5283–5284.

Goldberg, D.E., and Cowman, A.F. (2010). Moving in and renovating: exporting proteins from Plasmodium into host erythrocytes. Nat. Rev. Microbiol. *8*, 617–621.

Greenwood, B.M., Fidock, D.A., Kyle, D.E., Kappe, S.H.I., Alonso, P.L., Collins, F.H., and Duffy, P.E. (2008). Malaria: progress, perils, and prospects for eradication. J. Clin. Invest. *118*, 1266–1276.

Grüring, C., Heiber, A., Kruse, F., Ungefehr, J., Gilberger, T.-W., and Spielmann, T. (2011). Development and host cell modifications of Plasmodium falciparum blood stages in four dimensions. Nat. Commun. *2*, 165.

Grüring, C., Heiber, A., Kruse, F., Flemming, S., Franci, G., Colombo, S.F., Fasana, E., Schoeler, H., Borgese, N., Stunnenberg, H.G., et al. (2012). Uncovering Common Principles in Protein Export of Malaria Parasites. Cell Host Microbe *12*, 717–729.

Haase, S., and de Koning-Ward, T.F. (2010). New insights into protein export in malaria parasites. Cell. Microbiol. *12*, 580–587.

Haeggstrom, M. (2004). Common trafficking pathway for variant antigens destined for the surface of the Plasmodium falciparum-infected erythrocyte. Mol. Biochem. Parasitol. *133*, 1–14.

Haldar, K., and Mohandas, N. (2009). Malaria, erythrocytic infection, and anemia. Hematology *2009*, 87–93.

Hanssen, E., Sougrat, R., Frankland, S., Deed, S., Klonis, N., Lippincott-Schwartz, J., and Tilley, L. (2007). Electron tomography of the Maurer's cleft organelles of Plasmodium falciparum-infected erythrocytes reveals novel structural features: Electron tomography of malaria parasite structures. Mol. Microbiol. *67*, 703–718.

Hanssen, E., Hawthorne, P., Dixon, M.W.A., Trenholme, K.R., McMillan, P.J., Spielmann, T., Gardiner, D.L., and Tilley, L. (2008). Targeted mutagenesis of the ring-exported protein-1 of *Plasmodium falciparum* disrupts the architecture of Maurer's cleft organelles. Mol. Microbiol. *69*, 938–953.

Hawthorne, P.L., Trenholme, K.R., Skinner-Adams, T.S., Spielmann, T., Fischer, K., Dixon, M.W.A., Ortega, M.R., Anderson, K.L., Kemp, D.J., and Gardiner, D.L. (2004). A novel Plasmodium falciparum ring stage protein, REX, is located in Maurer's clefts. Mol. Biochem. Parasitol. *136*, 181–189.

Heiber, A., Kruse, F., Pick, C., Grüring, C., Flemming, S., Oberli, A., Schoeler, H., Retzlaff, S., Mesén-Ramírez, P., Hiss, J.A., et al. (2013). Identification of New PNEPs Indicates a Substantial Non-PEXEL Exportome and Underpins Common Features in Plasmodium falciparum Protein Export. PLoS Pathog. *9*, e1003546.

Hiller, N.L., Bhattacharjee, S., van Ooij, C., Liolios, K., Harrison, T., Lopez-Estrano, C., and Haldar, K. (2004). A host-targeting signal in virulence proteins reveals a secretome in malarial infection. Science *306*, 1934–1937.

Horrocks, P. (2005). PfEMP1 expression is reduced on the surface of knobless Plasmodium falciparum infected erythrocytes. J. Cell Sci. *118*, 2507–2518.

Howell, D.P.-G., Levin, E.A., Springer, A.L., Kraemer, S.M., Phippard, D.J., Schief, W.R., and Smith, J.D. (2007). Mapping a common interaction site used by Plasmodium falciparum Duffy binding-like domains to bind diverse host receptors: Interaction site for DBLβ−C2 and ICAM-1. Mol. Microbiol. *67*, 78–87.

Huber, S.M., Uhlemann, A.-C., Gamper, N.L., Duranton, C., Kremsner, P.G., and Lang, F. (2002). Plasmodium falciparum activates endogenous Cl(–) channels of human erythrocytes by membrane oxidation. EMBO J. *21*, 22–30.

Jensen, A.T.R. (2004). Plasmodium falciparum Associated with Severe Childhood Malaria Preferentially Expresses PfEMP1 Encoded by Group A var Genes. J. Exp. Med. *199*, 1179–1190.

Joergensen, L., Bengtsson, D.C., Bengtsson, A., Ronander, E., Berger, S.S., Turner, L., Dalgaard, M.B., Cham, G.K.K., Victor, M.E., Lavstsen, T., et al. (2010). Surface Co-Expression of Two Different PfEMP1 Antigens on Single Plasmodium falciparum-Infected Erythrocytes Facilitates Binding to ICAM1 and PECAM1. PLoS Pathog. *6*, e1001083.

Kats, L.M., Fernandez, K.M., Glenister, F.K., Herrmann, S., Buckingham, D.W., Siddiqui, G., Sharma, L., Bamert, R., Lucet, I., Guillotte, M., et al. (2014). An exported kinase (FIKK4.2) that mediates virulence-associated changes in Plasmodium falciparum-infected red blood cells. Int. J. Parasitol. *44*, 319–328.

Kilian, N., Srismith, S., Dittmer, M., Ouermi, D., Bisseye, C., Simpore, J., Cyrklaff, M., Sanchez, C.P., and Lanzer, M. (2015). Hemoglobin S and C affect protein export in Plasmodium falciparum-infected erythrocytes. Biol. Open *4*, 400–410.

Kilili, G.K., and LaCount, D.J. (2011). An Erythrocyte Cytoskeleton-Binding Motif in Exported Plasmodium falciparum Proteins. Eukaryot. Cell *10*, 1439–1447.

Klemba, M., and Goldberg, D.E. (2005). Characterization of plasmepsin V, a membrane-bound aspartic protease homolog in the endoplasmic reticulum of Plasmodium falciparum. Mol. Biochem. Parasitol. *143*, 183–191.

Knuepfer, E. (2005). Trafficking of the major virulence factor to the surface of transfected P falciparum-infected erythrocytes. Blood *105*, 4078–4087.

Kocan, K.M., de la Fuente, J., Blouin, E.F., Coetzee, J.F., and Ewing, S.A. (2010). The natural history of Anaplasma marginale. Vet. Parasitol. *167*, 95–107.

De Koning-Ward, T.F., Gilson, P.R., Boddey, J.A., Rug, M., Smith, B.J., Papenfuss, A.T., Sanders, P.R., Lundie, R.J., Maier, A.G., Cowman, A.F., et al. (2009). A newly discovered protein export machine in malaria parasites. Nature *459*, 945–949.

Kriek, N., Tilley, L., Horrocks, P., Pinches, R., Elford, B.C., Ferguson, D.J.P., Lingelbach, K., and Newbold, C.I. (2003). Characterization of the pathway for transport of the cytoadherence-mediating protein, PfEMP1, to the host cell surface in malaria parasite-infected erythrocytes: Trafficking of PfEMP1 in P. falciparum. Mol. Microbiol. *50*, 1215–1227.

Lanzer, M., Wickert, H., Krohne, G., Vincensini, L., and Braun Breton, C. (2006). Maurer's clefts: A novel multi-functional organelle in the cytoplasm of Plasmodium falciparum-infected erythrocytes. Int. J. Parasitol. *36*, 23–36.

Lavstsen, T., Salanti, A., Jensen, A.T., Arnot, D.E., and Theander, T.G. (2003). Sub-grouping of Plasmodium falciparum 3D7 var genes based on sequence analysis of coding and non-coding regions. Malar. J. *2*, 27.

Lim, L., and McFadden, G.I. (2010). The evolution, metabolism and functions of the apicoplast. Philos. Trans. R. Soc. B Biol. Sci. *365*, 749–763.

Lingelbach, K., and Przyborski, J.M. (2006). The long and winding road: Protein trafficking mechanisms in the Plasmodium falciparum infected erythrocyte. Mol. Biochem. Parasitol. *147*, 1–8.

Lopez-Rubio, J.J., Gontijo, A.M., Nunes, M.C., Issar, N., Hernandez Rivas, R., and Scherf, A. (2007). 5' flanking region of var genes nucleate histone modification patterns linked to phenotypic inheritance of virulence traits in malaria parasites. Mol. Microbiol. *0*, 071119190133003

Lopez-Rubio, J.-J., Mancio-Silva, L., and Scherf, A. (2009). Genome-wide Analysis of Heterochromatin Associates Clonally Variant Gene Regulation with Perinuclear Repressive Centers in Malaria Parasites. Cell Host Microbe *5*, 179–190.

Maier, A.G., Rug, M., O'Neill, M.T., Beeson, J.G., Marti, M., Reeder, J., and Cowman, A.F. (2007). Skeleton-binding protein 1 functions at the parasitophorous vacuole membrane to traffic PfEMP1 to the Plasmodium falciparum–infected erythrocyte surface. Blood *109*, 1289–1297.

Maier, A.G., Rug, M., O'Neill, M.T., Brown, M., Chakravorty, S., Szestak, T., Chesson, J., Wu, Y., Hughes, K., Coppel, R.L., et al. (2008). Exported Proteins Required for Virulence and Rigidity of Plasmodium falciparum-Infected Human Erythrocytes. Cell *134*, 48–61.

Maier, A.G., Cooke, B.M., Cowman, A.F., and Tilley, L. (2009). Malaria parasite proteins that remodel the host erythrocyte. Nat. Rev. Microbiol. *7*, 341–354.

Marfatia, S., Lue, R., Branton, D., and Chishti, A. (1994). In vitro binding studies suggest a membrane-associated complex between erythroid p55, protein 4.1, and glycophorin C. J. Biol. Chem. *269*, 8631—8634.

Marti, M., Good, R.T., Rug, M., Knuepfer, E., and Cowman, A.F. (2004). Targeting malaria virulence and remodeling proteins to the host erythrocyte. Science *306*, 1930–1933.

Matthews, K., Kalanon, M., Chisholm, S.A., Sturm, A., Goodman, C.D., Dixon, M.W.A., Sanders, P.R., Nebl, T., Fraser, F., Haase, S., et al. (2013). The *Plasmodium* translocon of exported proteins (PTEX) component thioredoxin-2 is important for maintaining normal blood-stage growth: Characterization of PTEX in *P. berghei*. Mol. Microbiol. *89*, 1167–1186.

Matz, J.M., Matuschewski, K., and Kooij, T.W.A. (2013). Two putative protein export regulators promote Plasmodium blood stage development in vivo. Mol. Biochem. Parasitol. *191*, 44–52.

Maurer, G. (1902). Die malaria perniciosa. Cent. F Bakt Abt Orig *32*, 695–719.

Mayer, C., Slater, L., Erat, M.C., Konrat, R., and Vakonakis, I. (2012). Structural Analysis of the Plasmodium falciparum Erythrocyte Membrane Protein 1 (PfEMP1) Intracellular Domain Reveals a Conserved Interaction Epitope. J. Biol. Chem. *287*, 7182–7189.

McFadden, G.I., and Roos, D.S. (1999). Apicomplexan plastids as drug targets. Trends Microbiol. *7*, 328–333.

McHugh, E., Batinovic, S., Hanssen, E., McMillan, P.J., Kenny, S., Griffin, M.D.W., Crawford, S., Trenholme, K.R., Gardiner, D.L., Dixon, M.W.A., et al. (2015). A repeat sequence domain of the ring-exported protein-1 of Plasmodium falciparum controls export machinery architecture and virulence protein trafficking. Mol. Microbiol.

McMillan, P.J., Millet, C., Batinovic, S., Maiorca, M., Hanssen, E., Kenny, S., Muhle, R.A., Melcher, M., Fidock, D.A., Smith, J.D., et al. (2013). Spatial and temporal mapping of the PfEMP1 export pathway in *Plasmodium falciparum*: PfEMP1 export via the exomembrane system. Cell. Microbiol. *15*, 1401–1418.

Medana, I.M., and Turner, G.D.H. (2006). Human cerebral malaria and the blood–brain barrier. Int. J. Parasitol. *36*, 555–568.

Melcher, M., Muhle, R.A., Henrich, P.P., Kraemer, S.M., Avril, M., Vigan-Womas, I., Mercereau-Puijalon, O., Smith, J.D., and Fidock, D.A. (2010). Identification of a role for the PfEMP1 semi-conserved head structure in protein trafficking to the surface of Plasmodium falciparum infected red blood cells: Red blood cell surface expression of recombinant PfEMP1. Cell. Microbiol. *12*, 1446–1462.

Miller, L.H., Baruch, D.I., Marsh, K., and Doumbo, O.K. (2002). The pathogenic basis of malaria. Nature *415*, 673–679.

Mills, J.P., Diez-Silva, M., Quinn, D.J., Dao, M., Lang, M.J., Tan, K.S.W., Lim, C.T., Milon, G., David, P.H., Mercereau-Puijalon, O., et al. (2007). Effect of plasmodial RESA protein on deformability of human red blood cells harboring Plasmodium falciparum. Proc. Natl. Acad. Sci. *104*, 9213–9217.

Mohandas, N., and Evans, E. (1994). Mechanical properties of the red cell membrane in relation to molecular structure and genetic defects. Annu. Rev. Biophys. Biomol. Struct. *23*, 787–818.

Mohandas, N., and Gallagher, P.G. (2008). Red cell membrane: past, present, and future. Blood *112*, 3939–3948.

Mok, B.W., Ribacke, U., Winter, G., Yip, B.H., Tan, C.-S., Fernandez, V., Chen, Q., Nilsson, P., and Wahlgren, M. (2007). Comparative transcriptomal analysis of isogenic Plasmodium falciparum clones of distinct antigenic and adhesive phenotypes. Mol. Biochem. Parasitol. *151*, 184–192.

Mota, M.M. (2001). Migration of Plasmodium Sporozoites Through Cells Before Infection. Science *291*, 141–144.

Mundwiler-Pachlatko, E., and Beck, H.-P. (2013). Maurer's clefts, the enigma of Plasmodium falciparum. Proc. Natl. Acad. Sci. *110*, 19987–19994.

Nguitragool, W., Bokhari, A.A.B., Pillai, A.D., Rayavara, K., Sharma, P., Turpin, B., Aravind, L., and Desai, S.A. (2011). Malaria Parasite clag3 Genes Determine Channel-Mediated Nutrient Uptake by Infected Red Blood Cells. Cell *145*, 665–677.

Noedl, H., Se, Y., Schaecher, K., Smith, B.L., Socheat, D., and Fukuda, M.M. (2008). Evidence of Artemisinin-Resistant Malaria in Western Cambodia. N. Engl. J. Med. *359*, 2619–2620.

Oakley, M.S.M., Kumar, S., Anantharaman, V., Zheng, H., Mahajan, B., Haynes, J.D., Moch, J.K., Fairhurst, R., McCutchan, T.F., and Aravind, L. (2007). Molecular Factors and Biochemical Pathways Induced by Febrile Temperature in Intraerythrocytic Plasmodium falciparum Parasites. Infect. Immun. *75*, 2012–2025.

Ockenhouse, C.F., Tegoshi, T., Maeno, Y., Benjamin, C., Ho, M., Kan, K.E., Thway, Y., Win, K., Aikawa, M., and Lobb, R.R. (1992). Human vascular endothelial cell adhesion receptors for Plasmodium falciparum-infected erythrocytes: roles for endothelial leukocyte adhesion molecule 1 and vascular cell adhesion molecule 1. J. Exp. Med. *176*, 1183–1189.

Oh, S.S., Voigt, S., Fisher, D., Yi, S.J., LeRoy, P.J., Derick, L.H., Liu, S.-C., and Chishti, A.H. (2000). Plasmodium falciparum erythrocyte membrane protein 1 is anchored to the actin–spectrin junction and knob-associated histidine-rich protein in the erythrocyte skeleton. Mol. Biochem. Parasitol. *108*, 237–247.

Ohanian, V., Wolfe, L.C., John, K.M., Pinder, J.C., Lux, S.E., and Gratzer, W.B. (1984). Analysis of the ternary interaction of the red cell membrane skeletal proteins, spectrin, actin, and 4.1. Biochemistry (Mosc.) *23*, 4416–4420.

Van Ooij, C., Tamez, P., Bhattacharjee, S., Hiller, N.L., Harrison, T., Liolios, K., Kooij, T., Ramesar, J., Balu, B., Adams, J., et al. (2008). The Malaria Secretome: From Algorithms to Essential Function in Blood Stage Infection. PLoS Pathog. *4*, e1000084.

Osborne, A.R., Speicher, K.D., Tamez, P.A., Bhattacharjee, S., Speicher, D.W., and Haldar, K. (2010). The host targeting motif in exported Plasmodium proteins is cleaved in the parasite endoplasmic reticulum. Mol. Biochem. Parasitol. *171*, 25–31.

Pachlatko, E., Rusch, S., Müller, A., Hemphill, A., Tilley, L., Hanssen, E., and Beck, H.-P. (2010). MAHRP2, an exported protein of Plasmodium falciparum, is an essential component of Maurer's cleft tethers: MAHRP2 is a component of P. falciparum tethers. Mol. Microbiol. *77*, 1136–1152.

Painter, H., Altenhofen, L., Kafsack, B.C., and Llinás, M. (2013). Whole-Genome Analysis of Plasmodium spp. Utilizing a New Agilent Technologies DNA Microarray Platform. In Malaria, R. Ménard, ed. (Humana Press), pp. 213–219.

Papakrivos, J., Newbold, C.I., and Lingelbach, K. (2004). A potential novel mechanism for the insertion of a membrane protein revealed by a biochemical analysis of the Plasmodium falciparum cytoadherence molecule PfEMP-1: Membrane association of PfEMP-1. Mol. Microbiol. *55*, 1272–1284.

Parish, L.A., Mai, D.W., Jones, M.L., Kitson, E.L., and Rayner, J.C. (2013). A member of the Plasmodium falciparum PHIST family binds to the erythrocyte cytoskeleton component band 4.1. Malar. J. *12*, 1–9.

Pei, X., An, X., Guo, X., Tarnawski, M., Coppel, R., and Mohandas, N. (2005). Structural and Functional Studies of Interaction between Plasmodium falciparum Knob-associated Histidine-rich Protein (KAHRP) and Erythrocyte Spectrin. J. Biol. Chem. *280*, 31166–31171.

Pei, X., Guo, X., Coppel, R., Bhattacharjee, S., Haldar, K., Gratzer, W., Mohandas, N., and An, X. (2007). The ring-infected erythrocyte surface antigen (RESA) of Plasmodium falciparum stabilizes spectrin tetramers and suppresses further invasion. Blood *110*, 1036–1042.

Prajapati, S.K., and Singh, O.P. (2013). Remodeling of human red cells infected with Plasmodium falciparum and the impact of PHIST proteins. Blood Cells. Mol. Dis. *51*, 195–202.

Proellocks, N.I., Herrmann, S., Buckingham, D.W., Hanssen, E., Hodges, E.K., Elsworth, B., Morahan, B.J., Coppel, R.L., and Cooke, B.M. (2014). A lysine-rich membrane-associated PHISTb protein involved in alteration of the cytoadhesive properties of Plasmodium falciparum-infected red blood cells. FASEB J. *28*, 3103–3113.

Prudêncio, M., and Mota, M.M. (2007). To Migrate or to Invade: Those Are the Options. Cell Host Microbe *2*, 286–288.

Rask, T.S., Hansen, D.A., Theander, T.G., Gorm Pedersen, A., and Lavstsen, T. (2010). Plasmodium falciparum Erythrocyte Membrane Protein 1 Diversity in Seven Genomes – Divide and Conquer. PLoS Comput. Biol. *6*, e1000933.

Rayner, J.C., Liu, W., Peeters, M., Sharp, P.M., and Hahn, B.H. (2011). A plethora of Plasmodium species in wild apes: a source of human infection? Trends Parasitol. *27*, 222–229.

Regev-Rudzki, N., Wilson, D.W., Carvalho, T.G., Sisquella, X., Coleman, B.M., Rug, M., Bursac, D., Angrisano, F., Gee, M., Hill, A.F., et al. (2013). Cell-Cell Communication between Malaria-Infected Red Blood Cells via Exosome-like Vesicles. Cell *153*, 1120–1133.

Reid, M.E., Takakuwa, Y., Conboy, J., Tchernia, G., and Mohandas, N. (1990). Glycophorin C content of human erythrocyte membrane is regulated by protein 4.1. Blood *75*, 2229–2234.

Robinson, B.A., Welch, T.L., and Smith, J.D. (2003). Widespread functional specialization of Plasmodium falciparum erythrocyte membrane protein 1 family members to bind CD36 analysed across a parasite genome. Mol. Microbiol. *47*, 1265–1278.

Le Roch, K.G., Johnson, J.R., Florens, L., Zhou, Y., Santrosyan, A., Grainger, M., Yan, S.F., Williamson, K.C., Holder, A.A., Carucci, D.J., et al. (2004). Global analysis of transcript and protein levels across the Plasmodium falciparum life cycle. Genome Res. *14*, 2308–2318.

Rohde, K., Yates, R.M., Purdy, G.E., and Russell, D.G. (2007). Mycobacterium tuberculosis and the environment within the phagosome. Immunol. Rev. *219*, 37–54.

Rottmann, M., Lavstsen, T., Mugasa, J.P., Kaestli, M., Jensen, A.T.R., Muller, D., Theander, T., and Beck, H.-P. (2006). Differential Expression of var Gene Groups Is Associated with Morbidity Caused by Plasmodium falciparum Infection in Tanzanian Children. Infect. Immun. *74*, 3904–3911.

Rottmann, M., McNamara, C., Yeung, B.K.S., Lee, M.C.S., Zou, B., Russell, B., Seitz, P., Plouffe, D.M., Dharia, N.V., Tan, J., et al. (2010). Spiroindolones, a Potent Compound Class for the Treatment of Malaria. Science *329*, 1175–1180.

Rovira-Graells, N., Gupta, A.P., Planet, E., Crowley, V.M., Mok, S., Ribas de Pouplana, L., Preiser, P.R., Bozdech, Z., and Cortes, A. (2012). Transcriptional variation in the malaria parasite Plasmodium falciparum. Genome Res. *22*, 925–938.

RTS, S. (2015). Efficacy and safety of RTS, S/AS01 malaria vaccine with or without a booster dose in infants and children in Africa: final results of a phase 3, individually randomised, controlled trial. The Lancet.

Rug, M., Cyrklaff, M., Mikkonen, A., Lemgruber, L., Kuelzer, S., Sanchez, C.P., Thompson, J., Hanssen, E., O'Neill, M., Langer, C., et al. (2014). Export of virulence proteins by malaria-infected erythrocytes involves remodeling of host actin cytoskeleton. Blood *124*, 3459.

Russo, I., Babbitt, S., Muralidharan, V., Butler, T., Oksman, A., and Goldberg, D.E. (2010). Plasmepsin V licenses Plasmodium proteins for export into the host erythrocyte. Nature *463*, 632–636.

Sachs, J., and Malaney, P. (2002). The economic and social burden of malaria. Nature *415*, 680–685.

Salcedo-Amaya, A.M., van Driel, M.A., Alako, B.T., Trelle, M.B., van den Elzen, A.M., Cohen, A.M., Janssen-Megens, E.M., van de Vegte-Bolmer, M., Selzer, R.R., Iniguez, A.L., et al. (2009). Dynamic histone H3 epigenome marking during the intraerythrocytic cycle of Plasmodium falciparum. Proc. Natl. Acad. Sci. *106*, 9655–9660.

Sanyal, S., Egee, S., Bouyer, G., Perrot, S., Safeukui, I., Bischoff, E., Buffet, P., Deitsch, K.W., Mercereau-Puijalon, O., David, P.H., et al. (2012). Plasmodium falciparum STEVOR proteins impact erythrocyte mechanical properties. Blood *119*, e1–e8.

Sargeant, T.J., Marti, M., Caler, E., Carlton, J.M., Simpson, K., Speed, T.P., and Cowman, A.F. (2006). Lineage-specific expansion of proteins exported to erythrocytes in malaria parasites. Genome Biol. *7*, R12.

Scherf, A., Lopez-Rubio, J.J., and Riviere, L. (2008). Antigenic Variation in *Plasmodium falciparum*. Annu. Rev. Microbiol. *62*, 445–470.

Schofield, L., and Hackett, F. (1993). Signal transduction in host cells by a glycosylphosphatidylinositol toxin of malaria parasites. J. Exp. Med. *177*, 145–153.

Scholz, M., and Fraunholz, M. (2008). A computational model of gene expression reveals early transcriptional events at the subtelomeric regions of the malaria parasite, Plasmodium falciparum. Genome Biol. *9*, R88.

Sharma, A., Sharma, A., Dixit, S., and Sharma, A. (2011). Structural insights into thioredoxin-2: a component of malaria parasite protein secretion machinery. Sci. Rep. *1*.

Shio, M.T., Kassa, F.A., Bellemare, M.-J., and Olivier, M. (2010). Innate inflammatory response to the malarial pigment hemozoin. Microbes Infect. *12*, 889–899.

Silva, M.D., Cooke, B.M., Guillotte, M., Buckingham, D.W., Sauzet, J.-P., Scanf, C.L., Contamin, H., David, P., Mercereau-Puijalon, O., and Bonnefoy, S. (2005). A role for the Plasmodium falciparum RESA protein in resistance against heat shock demonstrated using gene disruption: Phenotyping resa-KO Plasmodium falciparum parasites. Mol. Microbiol. *56*, 990–1003.

Da Silva, E., Foley, M., Dluzewski, A.R., Murray, L.J., Anders, R.F., and Tilley, L. (1994). The Plasmodium falciparum protein RESA interacts with the erythrocyte cytoskeleton and modifies erythrocyte thermal stability. Mol. Biochem. Parasitol. *66*, 59–69.

Silvestrini, F., Bozdech, Z., Lanfrancotti, A., Giulio, E.D., Bultrini, E., Picci, L., deRisi, J.L., Pizzi, E., and Alano, P. (2005). Genome-wide identification of genes upregulated at the onset of gametocytogenesis in Plasmodium falciparum. Mol. Biochem. Parasitol. *143*, 100–110.

Silvestrini, F., Lasonder, E., Olivieri, A., Camarda, G., van Schaijk, B., Sanchez, M., Younis, S.Y., Sauerwein, R., and Alano, P. (2010). Protein export marks the early phase of gametocytogenesis of the human malaria parasite Plasmodium falciparum. Mol. Cell. Proteomics *9*, 1437–1448.

Sims, P.J., and Wiedmer, T. (2001). Unraveling the Mysteries of Phospholipid Scrambling. Thromb. Haemost. *86*, 266–275.

Sleebs, B.E., Lopaticki, S., Marapana, D.S., O'Neill, M.T., Rajasekaran, P., Gazdik, M., Günther, S., Whitehead, L.W., Lowes, K.N., Barfod, L., et al. (2014). Inhibition of Plasmepsin V Activity Demonstrates Its Essential Role in Protein Export, PfEMP1 Display, and Survival of Malaria Parasites. PLoS Biol. *12*, e1001897.

Smith, J.D., Chitnis, C.E., Craig, A.G., Roberts, D.J., Hudson-Taylor, D.E., Peterson, D.S., Pinches, R., Newbold, C.I., and Miller, L.H. (1995). Switches in Expression of Plasmodium falciparum var Genes Correlate with Changes in Antigenic and Cytoadherent Phenotypes of Infected Erythrocytes. Cell *82*, 101–110.

Smith, J.D., Subramanian, G., Gamain, B., Baruch, D.I., and Miller, L.H. (2000). Classification of adhesive domains in the Plasmodium falciparum Erythrocyte Membrane Protein 1 family. Mol. Biochem. Parasitol. *110*, 293–310.

Snow, R.W., Guerra, C.A., Noor, A.M., Myint, H.Y., and Hay, S.I. (2005). The global distribution of clinical episodes of Plasmodium falciparum malaria. Nature *434*, 214–217.

Spielmann, T., and Gilberger, T.-W. (2010). Protein export in malaria parasites: do multiple export motifs add up to multiple export pathways? Trends Parasitol. *26*, 6–10.

Spielmann, T., and Gilberger, T.-W. (2015). Critical Steps in Protein Export of Plasmodium falciparum Blood Stages. Trends Parasitol. *31*, 514–525.

Spielmann, T., Hawthorne, P.L., Dixon, M.W., Hannemann, M., Klotz, K., Kemp, D.J., Klonis, N., Tilley, L., Trenholme, K.R., and Gardiner, D.L. (2006). A cluster of ring stage–specific genes linked to a locus implicated in

cytoadherence in Plasmodium falciparum codes for PEXEL-negative and PEXEL-positive proteins exported into the host cell. Mol. Biol. Cell *17*, 3613–3624.

Spillman, N.J., Beck, J.R., and Goldberg, D.E. (2015). Protein Export into Malaria Parasite–Infected Erythrocytes: Mechanisms and Functional Consequences. Annu. Rev. Biochem. *84*, 813–841.

Spycher, C. (2003). MAHRP-1, a Novel Plasmodium falciparum Histidine-rich Protein, Binds Ferriprotoporphyrin IX and Localizes to the Maurer's Clefts. J. Biol. Chem. *278*, 35373–35383.

Spycher, C., Rug, M., Klonis, N., Ferguson, D.J.P., Cowman, A.F., Beck, H.-P., and Tilley, L. (2006). Genesis of and Trafficking to the Maurer's Clefts of Plasmodium falciparum-Infected Erythrocytes. Mol. Cell. Biol. *26*, 4074–4085.

Spycher, C., Rug, M., Pachlatko, E., Hanssen, E., Ferguson, D., Cowman, A.F., Tilley, L., and Beck, H.-P. (2008). The Maurer's cleft protein MAHRP1 is essential for trafficking of PfEMP1 to the surface of Plasmodium falciparum-infected erythrocytes. Mol. Microbiol. *68*, 1300–1314.

Staines, H.M., Alkhalil, A., Allen, R.J., De Jonge, H.R., Derbyshire, E., Egée, S., Ginsburg, H., Hill, D.A., Huber, S.M., Kirk, K., et al. (2007). Electrophysiological studies of malaria parasite-infected erythrocytes: Current status. Int. J. Parasitol. *37*, 475–482.

Steck, T.L. (1974). The organization of proteins in the human red blood cell membrane - A review. J. Cell Biol. *62*, 1–19.

Stefanovic, M., Markham, N.O., Parry, E.M., Garrett-Beal, L.J., Cline, A.P., Gallagher, P.G., Low, P.S., and Bodine, D.M. (2007). An 11-amino acid β-hairpin loop in the cytoplasmic domain of band 3 is responsible for ankyrin binding in mouse erythrocytes. Proc. Natl. Acad. Sci. *104*, 13972–13977.

Sturm, A., Amino, R., Van de Sand, C., Regen, T., Retzlaff, S., Rennenberg, A., Krueger, A., Pollok, J.-M., Menard, R., and Heussler, V.T. (2006). Manipulation of host hepatocytes by the malaria parasite for delivery into liver sinusoids. Science *313*, 1287–1290.

Su, X., Heatwole, V.M., Wertheimer, S.P., Guinet, F., Herrfeldt, J.A., Peterson, D.S., Ravetch, J.A., and Wellems, T.E. (1995). The large diverse gene family var encodes proteins involved in cytoadherence and antigenic variation of plasmodium falciparum-infected erythrocytes. Cell *82*, 89–100.

Taraschi, T.F. (2003). Generation of an erythrocyte vesicle transport system by Plasmodium falciparum malaria parasites. Blood *102*, 3420–3426.

Tarr, S.J., Cryar, A., Thalassinos, K., Haldar, K., and Osborne, A.R. (2013). The C-terminal portion of the cleaved HT motif is necessary and sufficient to mediate export of proteins from the malaria parasite into its host cell: *Plasmodium* protein export mediated by the cleaved HT motif. Mol. Microbiol. *87*, 835–850.

Tarr, S.J., Moon, R.W., Hardege, I., and Osborne, A.R. (2014). A conserved domain targets exported PHISTb family proteins to the periphery of Plasmodium infected erythrocytes. Mol. Biochem. Parasitol. *196*, 29–40.

Tavares, J., Formaglio, P., Thiberge, S., Mordelet, E., Van Rooijen, N., Medvinsky, A., Ménard, R., and Amino, R. (2013). Role of host cell traversal by the malaria sporozoite during liver infection. J. Exp. Med. *210*, 905–915.

Taylor, D.W., Parra, M., Chapman, G.B., Stearns, M.E., Rener, J., Aikawa, M., Uni, S., Aley, S.B., Panton, L.J., and Howard, R.J. (1987). Localization of Plasmodium falciparum histidine-rich protein 1 in the erythrocyte skeleton under knobs. Mol. Biochem. Parasitol. *25*, 165–174.

Tiburcio, M., Dixon, M., Looker, O., Younis, S., Tilley, L., and Alano, P. (2015). Specific expression and export of the Plasmodium falciparum Gametocyte EXported Protein-5 marks the gametocyte ring stage. Malar. J. *14*, 334.

Tilley, L., Sougrat, R., Lithgow, T., and Hanssen, E. (2007). The Twists and Turns of Maurer's Cleft Trafficking in P. falciparum-Infected Erythrocytes. Traffic *9*, 187–197.

Tjitra, E., Anstey, N.M., Sugiarto, P., Warikar, N., Kenangalem, E., Karyana, M., Lampah, D.A., and Price, R.N. (2008). Multidrug-Resistant Plasmodium vivax Associated with Severe and Fatal Malaria: A Prospective Study in Papua, Indonesia. PLoS Med. *5*, e128.

Tuikue Ndam, N., Bischoff, E., Proux, C., Lavstsen, T., Salanti, A., Guitard, J., Nielsen, M.A., Coppée, J.-Y., Gaye, A., Theander, T., et al. (2008). Plasmodium falciparum Transcriptome Analysis Reveals Pregnancy Malaria Associated Gene Expression. PLoS ONE *3*, e1855.

Tuteja, R. (2007). Malaria − an overview. FEBS J. *274*, 4670–4679.

Voss, T.S., Healer, J., Marty, A.J., Duffy, M.F., Thompson, J.K., Beeson, J.G., Reeder, J.C., Crabb, B.S., and Cowman, A.F. (2005). A var gene promoter controls allelic exclusion of virulence genes in Plasmodium falciparum malaria. Nature.

Waller, K.L. (2003). Mature parasite-infected erythrocyte surface antigen (MESA) of Plasmodium falciparum binds to the 30-kDa domain of protein 4.1 in malaria-infected red blood cells. Blood *102*, 1911–1914.

Waller, K.L., Cooke, B.M., Nunomura, W., Mohandas, N., and Coppel, R.L. (1999). Mapping the Binding Domains Involved in the Interaction between the Plasmodium falciparum Knob-associated Histidine-rich Protein (KAHRP) and the Cytoadherence Ligand P. falciparumErythrocyte Membrane Protein 1 (PfEMP1). J. Biol. Chem. *274*, 23808–23813.

Wellems, T.E., and Plowe, C.V. (2001). Chloroquine-resistant malaria. J. Infect. Dis. *184*, 770–776.

Wells, T.N.C., Burrows, J.N., and Baird, J.K. (2010). Targeting the hypnozoite reservoir of Plasmodium vivax: the hidden obstacle to malaria elimination. Trends Parasitol. *26*, 145–151.

Weng, H., Guo, X., Papoin, J., Wang, J., Coppel, R., Mohandas, N., and An, X. (2014). Interaction of Plasmodium falciparum knob-associated histidine-rich protein (KAHRP) with erythrocyte ankyrin R is required for its attachment to the erythrocyte membrane. Biochim. Biophys. Acta BBA - Biomembr. *1838*, 185–192.

Wickert, H., and Krohne, G. (2007). The complex morphology of Maurer's clefts: from discovery to three-dimensional reconstructions. Trends Parasitol. *23*, 502–509.

Wickham, M.E., Rug, M., Ralph, S.A., Klonis, N., McFadden, G.I., Tilley, L., and Cowman, A.F. (2001). Trafficking and assembly of the cytoadherence complex in Plasmodium falciparum-infected human erythrocytes. EMBO J. *20*, 5636–5649.

WHO, Global Malaria Programme, and World Health Organization (2014). World Malaria Report 2014.

Yeung, B.K.S., Zou, B., Rottmann, M., Lakshminarayana, S.B., Ang, S.H., Leong, S.Y., Tan, J., Wong, J., Keller-Maerki, S., Fischli, C., et al. (2010). Spirotetrahydro β-Carbolines (Spiroindolones): A New Class of Potent and Orally Efficacious Compounds for the Treatment of Malaria. J. Med. Chem. *53*, 5155–5164.

Young, J.A., Fivelman, Q.L., Blair, P.L., de la Vega, P., Le Roch, K.G., Zhou, Y., Carucci, D.J., Baker, D.A., and Winzeler, E.A. (2005). The Plasmodium falciparum sexual development transcriptome: A microarray analysis using ontology-based pattern identification. Mol. Biochem. Parasitol. *143*, 67–79.

Zwaal, R.F., and Schroit, A.J. (1997). Pathophysiologic implications of membrane phospholipid asymmetry in blood cells. Blood *89*, 1121–1132.

Chapter 2

A *Plasmodium falciparum* PHIST protein binds the virulence factor PfEMP1 and comigrates to knobs on the host cell surface

Alexander Oberli[1,2,*] , Leanne M. Slater[3,*] , Erin Cutts[3] , Françoise Brand[1,2] , Esther Mundwiler-Pachlatko[1,2] , Sebastian Rusch[1,2] , Martin F. G. Masik[3] , Michèle C. Erat[3] , Hans-Peter Beck[1,2,$] and Ioannis Vakonakis[3,$]

Affiliation of authors:

[1] Swiss Tropical and Public Health Institute, Basel, Switzerland

[2] University of Basel, Basel, Switzerland

[3] Department of Biochemistry, University of Oxford, Oxford, United Kingdom

[*] These authors contributed equally

[$] Shared corresponding authors, to whom inquiries should be addressed:

Department of Biochemistry, South Parks Road, Oxford OX1 3QU, United Kingdom, Tel.: +44 1865 613362, e-mail: ioannis.vakonakis@bioch.ox.ac.uk

Molecular Parasitology Unit, Swiss Tropical and Public Health Institute, Socinstrasse 57, CH 4002 Basel, Switzerland, +41 6128 48116, e-mail: hans-peter.beck@unibas.ch

This article has been published in

FASEB, Volume 28, Issue 10, Pages 4420-4433, October 2014

The FASEB Journal • Research Communication

A *Plasmodium falciparum* PHIST protein binds the virulence factor PfEMP1 and comigrates to knobs on the host cell surface

Alexander Oberli,[*,†,1] Leanne M. Slater,[‡,1] Erin Cutts,[‡] Françoise Brand,[*,†] Esther Mundwiler-Pachlatko,[*,†] Sebastian Rusch,[*,†] Martin F. G. Masik,[‡] Michèle C. Erat,[‡] Hans-Peter Beck,[*,†,2] and Ioannis Vakonakis[‡,2]

*Swiss Tropical and Public Health Institute, Basel, Switzerland; [†]University of Basel, Basel, Switzerland; and [‡]Department of Biochemistry, University of Oxford, Oxford, UK

ABSTRACT **Uniquely among malaria parasites, *Plasmodium falciparum*-infected erythrocytes (iRBCs) develop membrane protrusions, known as knobs, where the parasite adhesion receptor *P. falciparum* erythrocyte membrane protein 1 (PfEMP1) clusters. Knob formation and the associated iRBC adherence to host endothelium are directly linked to the severity of malaria and are functional manifestations of protein export from the parasite to the iRBC. A family of exported proteins featuring *Plasmodium* helical interspersed subtelomeric (PHIST) domains has attracted attention, with members being implicated in host-parasite protein interactions and differentially regulated in severe disease and among parasite isolates. Here, we show that PHIST member PFE1605w binds the PfEMP1 intracellular segment directly with $K_d = 5 \pm 0.6$ μM, comigrates with PfEMP1 during export, and locates in knobs. PHIST variants that do not locate in knobs (MAL8P1.4) or bind PfEMP1 30 times more weakly (PFI1780w) used as controls did not display the same pattern. We resolved the first crystallographic structure of a PHIST protein and derived a partial model of the PHIST-PfEMP1 interaction from nuclear magnetic resonance. We propose that PFE1605w reinforces the PfEMP1-cytoskeletal connection in knobs and discuss the possible role of PHIST proteins as interaction hubs in the parasite exportome.—Oberli, A., Slater, L. M., Cutts, E., Brand, F., Mundwiler-Pachlatko, E., Rusch, S., Masik, M. F. G., Erat, M. C., Beck, H.-P., Vakonakis, I. A *Plasmodium falciparum* PHIST protein binds the virulence factor PfEMP1 and comigrates to knobs on the host cell surface. *FASEB J.* 28, 4420–4433 (2014). www.fasebj.org**

Key Words: cytoadherence · exported proteins · interactions · malaria · protein structure

During the intraerythrocytic cycle, *Plasmodium falciparum* completely refurbishes the human erythrocyte by establishing membranous networks and new permeation pathways (1). This refurbishment involves export of hundreds of proteins into the cytosol of the infected red blood cell (iRBC) and dramatic changes in the host cell membrane. The infected cell increases its permeability (2) and becomes more rigid (3, 4), and electron-dense surface protrusions called knobs form, conveying cytoadherence of mature iRBCs to the endothelial lining (5). The major parasite virulence factor *P. falciparum* erythrocyte membrane protein 1 (PfEMP1) is embedded in these knob structures through a transmembrane helix and comprises a highly variable ectodomain and a semiconserved intracellular segment [acidic terminal segment (ATS)] anchoring the molecule to the host cell (6). The presentation of PfEMP1 on the host cell surface is thought to be a major cause of pathological changes (7).

The importance of parasite-exported proteins in these host cell modifications has been acknowledged, but little is known about their function and interac-

Abbreviations: ATS, acidic terminal segment; AUC, analytical ultracentrifugation; DAPI, 4′,6′-diamidino-2-phenylindole; DTT, dithiothreitol; GAPDH, glyceraldehyde-3-phosphate dehydrogenase; GFP, green fluorescent protein; GST, glutathione *S*-transferase; HA, hemagglutinin; hpi, hours postinfection; IFA, immunofluorescence assay; iRBC, infected red blood cell; MES, 2-(*N*-morpholino)ethanesulfonic acid; NMR, nuclear magnetic resonance; PFA, paraformaldehyde; PfEMP1, *P. falciparum* erythrocyte membrane protein 1; PHIST, *Plasmodium* helical interspersed subtelomeric; PBS, phosphate-buffered saline; RMSD, root mean square deviation

[1] These authors contributed equally to this work.

[2] Correspondence: I.V., Department of Biochemistry, South Parks Road, Oxford OX1 3QU, UK. E-mail: ioannis.vakonakis@bioch.ox.ac.uk; H.-P.B., Molecular Parasitology Unit. Swiss Tropical and Public Health Institute, Socinstrasse 57, CH 4002 Basel, Switzerland. E-mail: hans-peter.beck@unibas.ch

doi: 10.1096/fj.14-256057

This article includes supplemental data. Please visit *http://www.fasebj.org* to obtain this information.

0892-6638/14/0028-4420 © The Author(s)

tions. Transport of proteins through the parasitophorous vacuole into the host cell has been shown to be facilitated by a short amino-terminal sequence termed PEXEL or VTS (8, 9). The majority of exported proteins carry this PEXEL motif, which allowed the establishment of the *P. falciparum* exportome with ~400 members (8). A smaller but unknown number of parasite proteins are exported despite lacking an identifiable motif (10). In both groups, only a few proteins have been studied in detail; these include some constituents of the translocon (11) and, in particular, knob components such as PfEMP1 (12) and others (13–16). More recently, PEXEL-negative proteins localizing in membrane structures formed in the host erythrocyte (Maurer's clefts), such as SBP1 (17) and MAHRP1 (18), have also been studied in greater detail. Maier *et al.* (4) used these predictions and identified through a knockout strategy a number of proteins that were essential for the transport of PfEMP1 to the surface, including members of the *Plasmodium* helical interspersed subtelomeric (PHIST) family. PHIST proteins comprise 72 variants in the *P. falciparum* 3D7 reference genome (19) and are organized into 3 subfamilies according to their species distribution: PHISTa proteins are entirely *P. falciparum* specific, PHISTb proteins are present in *Plasmodium vivax* and *Plasmodium knowlesi* but have extensively expanded in *P. falciparum*, and PHISTc proteins are shared between *P. falciparum* and *P. vivax* and appear as single-copy genes in the *Plasmodium berghei* lineage (19).

To date, no molecular function has been assigned to any of the PHIST proteins despite their wide distribution within infected cells. Yeast 2-hybrid analysis identified PHIST proteins as putative interactors with SBP1 (20) and erythrocyte band 4.1 (21). Transcriptome data suggest differences in PHIST expression during the parasite life cycle (19, 22–24) and among parasite isolates (25) and up-regulation of a specific PHIST member in parasites targeting the brain endothelium (26). Proteome data show a consistent presence of PHIST proteins in iRBC membrane fractions (27–29). Recently, a member of the PHIST family was identified within the Maurer's clefts (4); there is also evidence for a PHIST protein in J dots, and very recently PfPTP2, a PHISTb protein, was shown to be present in exosomes, a newly discovered means of *P. falciparum* communication (30). The PHISTc protein PFI1780w (PF3D7_0936800) has been detected in detergent-resistant membrane fractions (31), and we identified the same variant as an interaction partner with the ATS of PfEMP1, demonstrating the first direct association for a PHIST protein (32).

In this study, we show that another PHIST variant, PFE1605w (PF3D7_0532400), directly binds ATSs with higher affinity than PFI1780w. Both PFI1780w and PFE1605w were shown to localize to the iRBC membrane, but only PFE1605w is transported similar to PfEMP1 in time and space, and it locates specifically to knobs. Finally, we elucidate the first PHIST crystallographic structure from PFI1780w and suggest a partial model for the PHIST-ATS complex. This is the first functional information for any PHIST protein and provides evidence that PHIST proteins might be involved in PfEMP1 function and certainly are constituents of knobs.

MATERIALS AND METHODS

Cloning and protein production

PHIST domains

P. falciparum PFI1780w residues 85–247 or 98–247, PFD1170c residues 132–309, and MAL8P1.163 residues 131–284 were cloned in vector pGEX-6P-2 (GE Healthcare Life Sciences, Glattbrugg, Switzerland), and transformed into *Escherichia coli* BL21(DE3). PFE1605w residues 122–335 and MAL8P1.4 residues 310–456 were cloned in pOPINF vector (Oxford Protein Production Facility, Harwell, UK), and transformed into *E. coli* Rosetta2pLacI. Recombinant MAL8P1.4 for antibody production was derived from a full-length codon-optimized gene cloned into psCodon (Eurogentec, Seraing, Belgium) and expressed in the CherryCodon system (Eurogentec). Cells were grown in Luria-Bertani medium, supplemented with 1% (w/v) glucose for PFE1605w and MAL8P1.4. For nuclear magnetic resonance (NMR) samples, cells were grown in M9 medium supplemented with $^{15}NH_4Cl$ and $^{13}C_6$ D-glucose, and after protein induction were grown for 16 h at 18°C .

Cells were resuspended in phosphate-buffered saline (PBS; 150 mM NaCl and 20 mM Na_2HPO_4, pH 7.4) and lysed by sonication; lysates were spun at 24,000 *g* for 30 min. Lysate supernatants of PHIST domains cloned in pGEX-6P-2 were incubated with glutathione Sepharose resin (GE Healthcare LifeSciences) equilibrated in PBS, and proteins were eluted in a 50 mM Tris-Cl (pH 7.8), 12 mM reduced glutathione buffer. The glutathione *S*-transferase (GST) tag was removed by 3C protease cleavage, followed by buffer exchange to PBS using a Sephadex G-20 column (GE Healthcare LifeSciences). GST was retained by reverse glutathione Sepharose affinity.

Lysate supernatants of pOPNIF-cloned PHIST domains were applied to a Talon HiTrap column (GE Healthcare LifeSciences) equilibrated in 20 mM Na_2HPO_4 (pH 7.4) and 300 mM NaCl and eluted with a gradient to an imidazole-containing buffer (20 mM Na_2HPO_4, pH 7.4; 300 mM NaCl; and 500 mM imidazole). For PFE1605w, the His_6 tag was removed by 3C protease cleavage during dialysis in 50 mM Tris-Cl (pH 7.5), 150 mM NaCl, and 2 mM dithiothreitol (DTT), followed by dialysis in 20 mM 2-(*N*-morpholino)ethanesulfonic acid (MES; pH 6.0), 50 mM NaCl, and 2 mM DTT. PFE1605w was then applied to an SP ion exchange column (GE Healthcare LifeSciences) equilibrated in the dialysis buffer and eluted with a NaCl gradient (20 mM MES, pH 6.0; 1 M NaCl, and 2 mM DTT). For MAL8P1.4, the His_6 tag was removed by 3C protease cleavage, followed by dialysis in 20 mM Na_2HPO_4 (pH 7.0), 150 mM NaCl, and 2 mM DTT.

Final purification of all PHIST domains was performed by size-exclusion chromatography over a Superdex S75 column (GE Healthcare LifeSciences) equilibrated in PBS supplemented with 1 mM DTT or buffer A (50 mM NaCl; 20 mM Na_2HPO_4, pH 7.0; and 1 mM DTT).

PfEMP1 intracellular segments

The cloning and protein production of PfEMP1 intracellular segments, both full-length segments and fragments, and

fluorescent labeling of the PF08_0141 ATS were described earlier (32). A further 5 fluorescent-labeled full-length ATS variants were produced in an analogous manner by substituting single amino acids for cysteines; these are PFF0010 (G156C), PFB1055c (Q161C), PFC1120c (Q182C), PF08_0103 (H154C), and PFF0845c (H159C).

Biophysical characterization

Protein identity was confirmed by matrix-assisted laser desorption ionization-time of flight mass spectrometry. Unless otherwise noted, all biophysical experiments were performed in buffer A, except for analytical ultracentrifugation (AUC) experiments in which 1 mM tris(2-carboxyethyl)phosphine was used instead of DTT. Fluorescence polarization measurements were recorded at 20°C with a 5-FAM label using a PHERAstar FS fluorimeter (λ_{ex}=485 nm, λ_{em}=520 nm; BMG Labtech, Ortenberg, Germany). Differences in fluorescence polarization were fit using a single binding model in the program Origin (OriginLab, Northampton, MA, USA). AUC velocity experiments were performed on 25 μM protein samples using an Optima XL-I analytical ultracentrifuge (Beckman Coulter, Fullerton, CA, USA). Sedimentation velocities were recorded by measuring absorbance at 280 nm, with 200 scans every 4 min at 10°C and 35,000 rpm. Data were processed using SEDPHIT (33). The protein partial specific volume was calculated from the amino acid sequence.

Crystallization and structure determination

Crystals were obtained using the sitting drop vapor-diffusion technique at 20°C. A Mosquito robot (TTP LabTech, Melbourn, UK) was used to set up 200-nl sized drops with a 1:1 ratio of protein to mother liquor. PFI1780w residues 85–247 at a concentration of 4.0 mg/ml were mixed with 0.1 M sodium acetate (pH 4.6) and 2.0 M NaCl buffer. Crystals developed in 7 d were cryoprotected by a brief incubation in mother liquor supplemented with 22.5% (v/v) glycerol, flash-cooled in liquid nitrogen, and diffracted up to 2.35 Å at the Diamond Light Source (Harwell, UK), beamline I04. The space group was determined to be $P3_121$ with 2 molecules/asymmetric unit. For phasing experiments, the crystals were incubated with 250 mM 5-amino-2,4,6-triiodoisophthalic acid (Hampton Research, Aliso Viejo, CA, USA) for 5 min before cooling.

Crystallographic data were integrated in XDS (34) and scaled in SCALA (35). Phase information for PFI1780w was obtained from a 2.44-Å resolution data set collected at a wavelength of 1.6531 Å using the Diamond Light Source, beamline I04. Phasing by single-wavelength anomalous diffraction was performed using PHENIX.autosol (36), which located and refined 27 iodine atoms to produce a density map with initial figure of merit of 0.51. Initial model building was done with PHENIX.autosol (247 residues built and 184 identified). Iterative model building was performed with COOT (37) and refinement against the native 2.35 Å data was performed with BUSTER 2.10 (38).

Crystallographic data processing and refinement statistics are provided in Supplemental Table S1. Model quality was assessed by MolProbity (39). For graphical representation, we used PyMOL (40). The model and associated data have been deposited in the Research Collaboratory for Structural Bioinformatics (RCSB) Protein Data Bank (http://www.rcsb.org) under accession number 4JLE.

ATS structure prediction

CS-Rosetta (41) structure prediction was performed on residues 306–346 of ATSs using backbone ^{15}N, $^{1}H_N$, and $^{13}C'$ chemical shifts recorded in the presence of the PFI1780w PHIST domain and extrapolated to complex saturation. Data were processed by TALOS+ (42) before input in CS-Rosetta for fragment selection and generation of 12,800 models. Model superposition with a 3-Å root mean square deviation (RMSD) cutoff yielded large clusters of which the top 3 had 1313, 943, and 719 members. These clusters showed characteristic β-sheet structures but incomplete convergence due to flexible loops between β strands. Superposition using the most stable secondary structure elements (residues 311–314, 320–324, and 329–333) and 1-Å RMSD cutoff resulted in model convergence as judged by the funnel-shaped plot of model score *vs.* pairwise RMSD.

NMR

Sequence-specific resonance assignments of ATSs have been reported previously (32). Assignments of PFI1780w were performed at 37°C using triple-resonance experiments on a 600-MHz Avance III spectrometer (Bruker, Newark, DE, USA) with a cryogenic probehead. NMR samples for assignments consisted of 0.2 mM $^{13}C/^{15}N$-enriched PFI1780w residues 98–247 in buffer A (pH 6.5) supplemented with 0.1 mM 4,4-dimethyl-4-silapentane-1-sulfonic acid, 0.02% (w/v) NaN_3, and 5% (v/v) D_2O. The limited sample concentration and stability under these conditions (typical lifetime of ~2 d) necessitated the use of multiple samples to obtain a sufficient signal/noise ratio. Assignments have been deposited in BioMagResBank (University of Wisconsin, Madison, WI, USA; http://www.bmrb.wisc.edu/) under accession number 19719.

Perturbations in ^{1}H and ^{15}N chemical shifts were combined as $\Delta\delta(^{1}H,^{15}N)$ using the formula

$$\Delta\delta(^{1}H, ^{15}N) = \{[\delta(^{1}H)_{complex} - \delta(^{1}H)_{free}]^2 + 0.04 * [\Delta\delta(^{15}N)_{complex} - \delta(^{15}N)_{free}]^2\}^{1/2}$$

Similar perturbations of carbonyl ^{13}C resonances were expressed as $\Delta\delta(^{13}C) = \delta(^{13}C)_{free} - \delta(^{13}C)_{complex}$.

***Plasmodium* culture, transfection, and protein analysis**

Full-length PFI1780w and PFE1605w inserts were C-terminally fused either to green fluorescent protein (GFP) into pARL1a-GFP (kindly provided by T. Spielmann, Bernhard Nocht Institut, Hamburg, Germany; ref. 43) or C-terminally to hemagglutinin (HA) into pBcamR_3xHA (44). *P. falciparum* strain 3D7 was cultured in human 0+ erythrocytes according to standard procedures (45). Transfected parasites were drug selected with either 10 nM WR99210 (Jacobs Pharmaceuticals, Cologne, Germany) or 2.5 mg/ml blasticidin (Life Technologies, Zug, Switzerland).

Parasite proteins were obtained through saponin lysis of synchronized parasites (5–10% parasitemia) after 2 sorbitol treatments within 4 h and Percoll purified after 30 h. Parasite aliquots were taken every 8 h. Samples were run on a 12.5% (w/v) SDS-PAGE column with complete protease inhibitor cocktail (Roche, Rozkreuz, Switzerland) and transferred to a nitrocellulose membrane (Hybond-C Extra; GE Healthcare LifeSciences). Antibodies were diluted in 5% (v/v) milk-PBS: mouse monoclonal anti-GFP (1:1000; Roche), rabbit anti-HA (1:20; Invitrogen, Zug, Switzerland), rabbit anti-MAHRP1 (1:5000), rabbit anti-MAHRP2 (1:1000), mouse monoclonal anti-glyceraldehyde-3-phosphate dehydrogenase (GAPDH; 1:20,000), mouse anti-PFE1605w (1:500), mouse anti-PFI1780w (1:500), and mouse anti-MAL8P1.4 (1:500). Binding was made visible by chemiluminescence (SuperSignal West Pico, Thermo Scientific, Reinach, Switzerland). Parasite protein solubility was analyzed as described previously (46).

Immunofluorescence assay (IFA) and live cell imaging

Blood smears of infected parasite cultures were fixed in 100% acetone for 30 min (47) and blocked with 3% (v/w) bovine serum albumin. Primary antibodies, rabbit anti-MAHRP1 (1:500), mouse anti-PFI1780w (1:100), mouse anti-PFE1605w (1:100), mouse anti-MAL8P1.4 (1:200), mouse anti-GFP (1:100, Roche), and mouse anti-ATS (1:50), were incubated for 1 h (48). Secondary antibodies (goat anti-mouse Alexa 488, goat anti-mouse Alexa 594, and goat anti-rabbit Alexa 594; Invitrogen) were incubated with 1 μg/ml 4′,6′-diamidino-2-phenylindole (DAPI; Roche) for 1 h at 1:200 dilution. Alternatively, iRBCs were fixed with 4% paraformaldehyde (PFA)-0.01% glutaraldehyde and permeabilized with 0.1% Triton X-100. Slides were viewed with a Zeiss LSM 700 confocal microscope (Carl Zeiss GmbH, Jena, Germany), with a ×63 oil-immersion lens (1.4 numerical aperture).

Transgenic parasites expressing GFP fusion proteins were imaged as described previously (49). Live parasites were imaged with a Leica DM 5000B fluorescence microscope using a ×100 oil immersion lens (1.4 numerical aperture) with an attached Leica DFC300FX camera and Leica Application Suite software (Leica Microsystems, Heerbrugg, Switzerland).

Immunoelectron microscopy

PFE1605w-HA and PFI1780w-GFP transfected mature parasites were purified by Percoll density gradient, fixed in 2% PFA-0.2% glutaraldehyde in phosphate buffer, and prepared according to Tokuyasu (50). Ultrathin sections (70−90 nm) prepared on an FC7/UC7-ultramicrotome (Leica Microsystems) at −120°C were immunogold-labeled with rabbit anti-HA (1:20; Invitrogen) or rabbit anti-GFP (1:20; Abcam, Cambridge, UK) antibodies and 5 nM protein A-gold (1:70; UMC, Utrecht, The Netherlands). Sections were stained with 4% uranyl acetate-methylcellulose (1:9) and examined with a transmission electron microscope (CM10 or CM100; Philips, Eindhoven, The Netherlands) at 80 kV.

RESULTS

PFE1605w interacts with the PfEMP1 intracellular domain

Previously, we showed that intracellular segments (referred to as ATSs) from members of the PfEMP1 family comprise a stably folded core and 3 flexible regions (32). We demonstrated that the PHISTc protein PFI1780w interacts with moderate strength (K_d~150 μM) with the ATS of PfEMP1 variant PF08_0141. However, it was not clear whether PFI1780w is a physiological partner of PfEMP1. Thus, we produced PHIST domains from proteins that had been reported as important for cytoadherence of iRBCs (PFD1170c; ref. 4), that are adjacent on the genome to the locus of PfEMP1 variant PF08_0141 (MAL8P1.163), or, alternatively, that were identified in proteomic studies on tethers (PFE1605w) and tested them for interactions with the ATS. As a negative control, we produced a PHIST member that was shown not to localize to the iRBC membrane and thus would not be expected to associate with the ATS (MAL8P1.4). Polarization experiments showed that PFE1605w, a PHISTb member, bound fluorescently labeled ATS PF08_0141 with ~30-fold higher affinity (K_d=5±0.6 μM) than PFI1780w (**Fig. 1*A***). NMR experiments suggest that the PHIST interaction occurs at the C terminus of the ATS (see below), and polarization experiments using a fluorescently labeled ATS C-terminal construct (residues 293–392) showed that this fragment is sufficient for strong PFE1605w binding (Fig. 1*D*).

To test whether different PfEMP1 members retain the PFE1605w interaction, we produced fluorescently labeled ATSs from PfEMP1 variants PFF0010, PFB1055c, PFC1120c, PF08_0103, and PFF0845c, which were selected on the basis of sequence divergence (32). Intriguingly, polarization experiments with PFE1605w showed up to 25-fold difference in affinities (K_d range, 2.7–67 μM; Fig. 1*B*) across ATS variants. Similar experiments with PFI1780w showed only ~2.5-fold different affinities between ATS members (Fig. 1*C*). PFF0845c, a C-terminally truncated ATS variant (Supplemental Fig. S1*A*), showed little affinity to either PFE1605w or PFI1780w (Fig. 1*B*, *C*). Whether these differences reflect closer associations of PFE1605w with particular PfEMP1 members *in vivo* remains to be studied; however, time course experiments did suggest a closer association of PFE1605w with PfEMP1 than PFI1780w during transport.

PFI1780w and PFE1605w are membrane associated and exported to the iRBC membrane

To test whether these PHIST proteins are exported and to determine their subcellular localizations, they were C-terminally GFP tagged and episomally expressed in 3D7 parasites under the control of the *crt* promoter. The integrity of the GFP-fusion proteins was shown on Western blots (**Fig. 2*A***). The full-length PFI1780w-GFP was exported to the iRBC cytosol similarly to the previously reported GFP-tagged N terminus (19), but full-length PFI1780w-GFP additionally revealed fluorescence at the periphery of iRBCs (Fig. 2*B*; top panel), suggesting a localization close or adjacent to the erythrocyte membrane (Fig. 2*B*; panel 2). Immunofluorescent 3-dimensional reconstructions of fixed iRBCs with PFI1780w-GFP-expressing parasites showed focal fluorescence in parasite cytosol and uniform fluorescence around the biconcave rim of the iRBC (Fig. 2*C*), confirming this location. From all available GFP-tagged PHIST proteins only PFE1605w-GFP gave a similar fluorescent pattern except that the rim-like fluorescence was observed at discrete foci instead of a uniform signal (Fig. 2*B*, panels 4 and 5), indicating that both PFI1780w and PFE1605w were transported close to the iRBC membrane.

Next, we tested the solubility of these 2 PHIST proteins (ref. 46 and Fig. 2*D*). The soluble parasite protein GAPDH was found as expected in the supernatant after hypotonic lysis, and MAHRP1, an integral Maurer's cleft membrane protein (51), was detected in the Triton X-100 supernatant. Both PFI1780w-GFP and PFE1605w-GFP lack a predicted transmembrane domain and were shown to be membrane-associated proteins by solubilization in sodium carbonate similar to

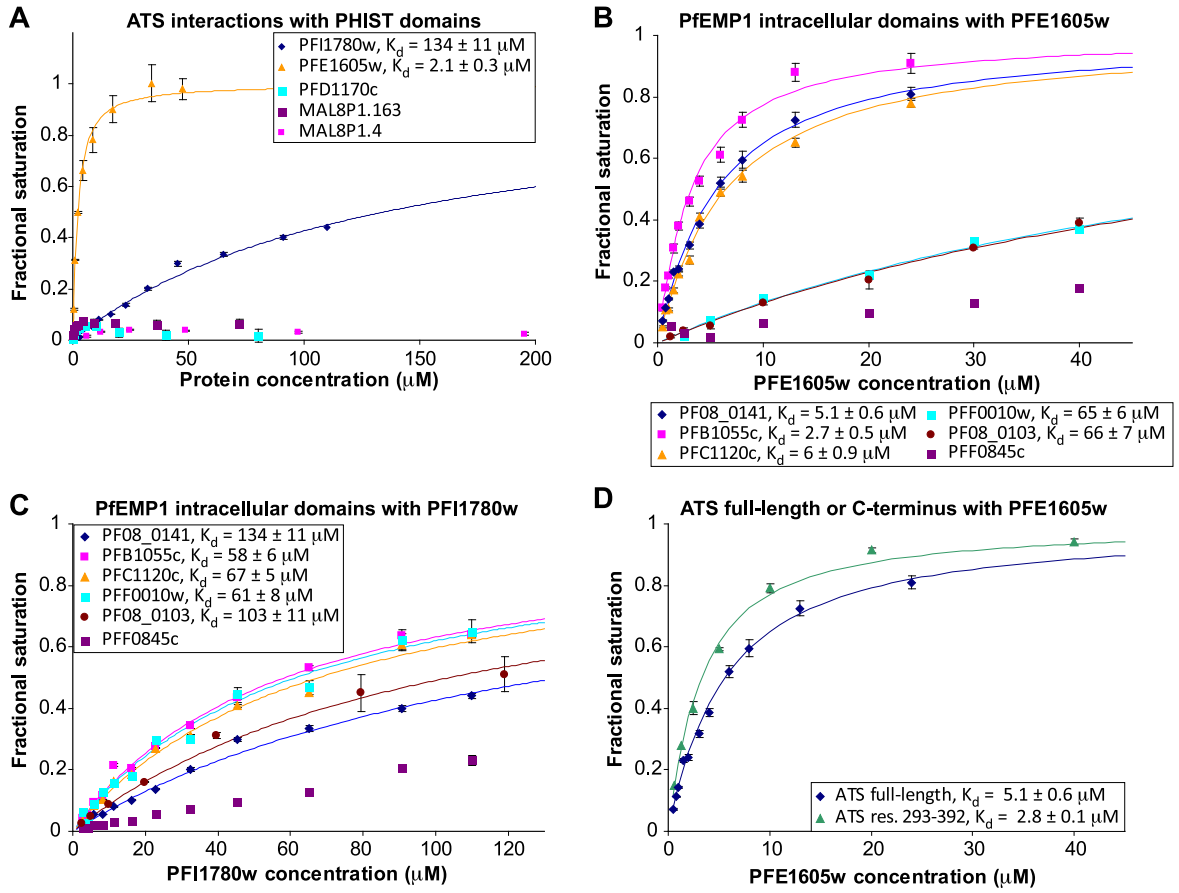

Figure 1. PHIST domains directly interact with ATS. *A*) Fluorescence polarization titrations of labeled ATS PF08_0141 with PHIST domains. Error bars derive from 5 measurements. Solid lines correspond to fits to single-site association models where possible. *B*, *C*) Similar titrations with different labeled PfEMP1 intracellular domains and PFE1605w (*B*) or PFI1780w (*C*). Binding by PfEMP1 variant PFF0845c was weak and could not be fit. In panel *B*, the fits of ATS variants PFF0010w and PF08_0103 overlap closely. *D*) Titrations of ATS PF08_0141 full-length or C-terminal fragment (residues 293–392) with PFE1605w.

MAHRP2, a membrane-associated protein localizing to Maurer's cleft tethers (46). This result was further confirmed by the fluorescent labeling of the iRBC membrane of a ruptured schizont expressing PFI1780w-GFP (Fig. 2*B*, panel 3).

PFI1780w localizes underneath the iRBC membrane and PFE1605w to knob structures

The subcellular localization of both PHIST proteins was shown by postembedding immunoelectron microscopy. Gold labeling of PFI1780w-GFP was found in proximity to the iRBC membrane but was clearly absent from knobs (**Fig. 3*A***) and frequently at Maurer's clefts (Fig. 3*B*). In contrast, PFE1605w-3xHA (Fig. 3*C*) and PFE1605w-GFP were clearly localized in knobs, and in trophozoite stage parasites, PFE1605w-GFP was also frequently found in Maurer's clefts (Fig. 3*D*), suggesting that it localizes underneath the iRBC membrane, whereas PFE1605w localizes to knobs, but both proteins seem to be transiently transported through the Maurer's clefts.

Immunofluorescence reveals a similar trafficking pathway and timing of export for PFE1605w and PfEMP1

Specific antisera against PFI1780w (aa 80–280) recognized a single band of ~45 kDa in agreement with its predicted mass of 45.5 kDa (**Fig. 4*A***), and antisera against PFE1605w (aa 122–335) recognized a band of ~55 kDa and a faint band of 50 kDa. Western blotting using samples from 6 time points of the intraerythrocytic cycle showed that both proteins were present throughout the cycle, which is in agreement with their transcription profile (52, 53). Both proteins were maximally expressed in trophozoite stages (Fig. 4*A*).

We performed IFAs to visualize expression and export of PFE1605w/PFI1780w throughout the intraerythrocytic cycle using tightly synchronized parasites at 6 time points (Fig. 4*B*, *C*) and compared the timing of export of PfEMP1 using anti-ATS antibodies (Fig. 4*D* and ref. 48). PFE1605w was first observed at ~0–8 h postinfection (hpi) in a "necklace of beads" pattern at

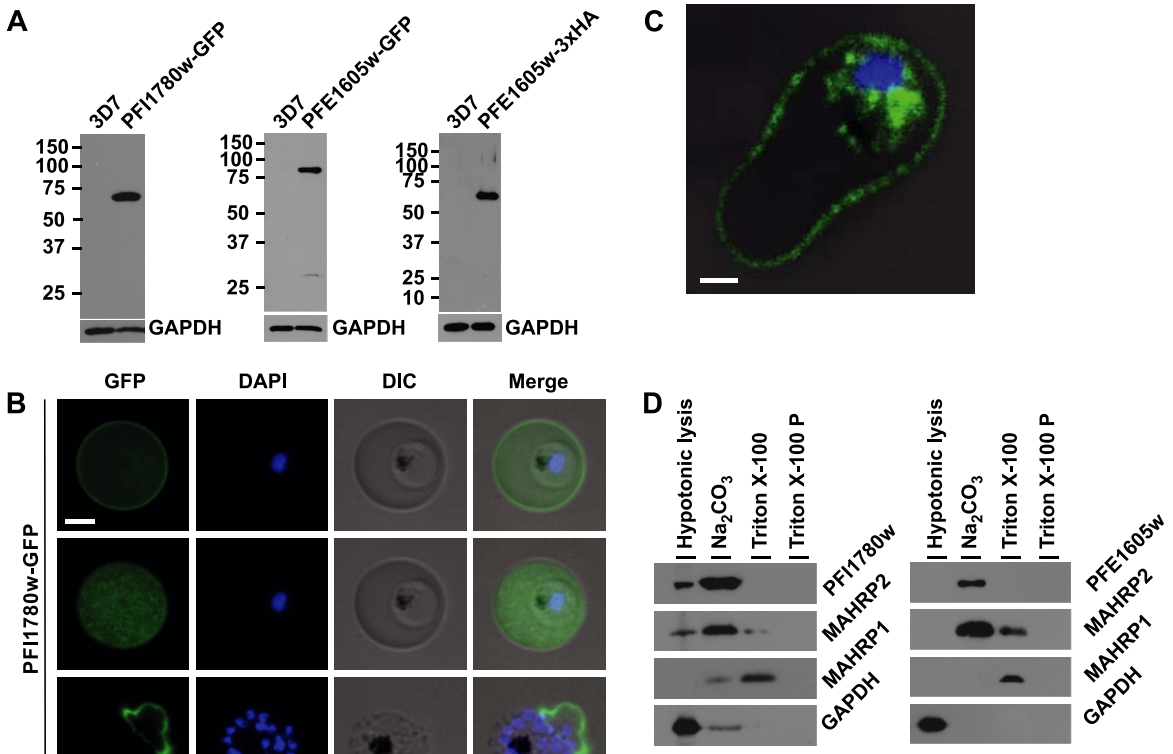

Figure 2. PHIST domains are exported to the iRBC membrane. *A*) Western blots of extracts from cell lines used in this study. All extracts are derived from saponin-released parasites, and the origin is indicated on top. Decoration of the same Western blot with GAPDH as loading control is shown at bottom. *B*) Live cell imaging of 3D7 parasites expressing PFI1780w-GFP and PFE1605w-GFP. For panels 2 and 5, the focal plane of the GFP signal was set on the surface of the iRBC, and the DAPI/differential interference contrast (DIC) microscopy signal was kept on the previous focal plane. Nuclei were stained with DAPI. Scale bar = 2 μm. Panel 3 shows a rare schizont with already ruptured erythrocyte membrane. *C*) Confocal immunofluorescence analysis of 3D7 parasite expressing PFI1780w-GFP. Merge image of GFP/DAPI/DIC channels representing stack 32 of 69 in total. Scale bar = 1 μm. *D*) Western blot of protein fractions of solubility assays of 3D7 parasites expressing PFI1780w-GFP and PFE1605w-GFP. Lane 1, soluble proteins; lane 2, peripheral membrane proteins; lane 3, Triton X-100 extract; lane 4, insoluble pellet.

the parasite surface (Fig. 4*B*; top panel) and in young trophozoites (16–24 hpi) most fluorescence was observed in the parasite with few fluorescent foci beyond the parasite's confines. After 24–32 hpi, the number of fluorescent foci in the iRBC cytosol increased, and faint fluorescence was visible at the iRBC membrane. Schizont stage parasites showed faint fluorescent dots at the iRBC membrane, similar to those seen with live cell images of PFE1605w-GFP (Fig. 2*B*). Bright fluorescent foci indicated that PFE1605w is exported *via* Maurer's clefts to the iRBC membrane and knobs.

PfEMP1 is known to display a necklace of beads pattern at the parasite surface at ~8–11 hpi (54), which was confirmed (Fig. 4*D*) and was similar to the pattern observed for PFE1605w (Fig. 4*B*). Both proteins transiently associated with Maurer's clefts at ~16–24 hpi (ref. 54 and Fig. 4*B*, *D*) before being transferred to the iRBC membrane, suggesting cotransport of PFE1605w with PfEMP1.

In contrast to PFE1605w, PFI1780w was found within the parasite cytosol until ~24–32 hpi with limited focal fluorescence in the iRBC cytosol (Fig. 4*C*). In schizonts, PFI1780w was exported to the iRBC surface as shown in live cell imaging (Fig. 2*B*) with no distinct intermediate locations, although a few fluorescent foci and immunoelectron microscopy data (Fig. 3*B*) suggest that Maurer's clefts are intermediate transport compartments.

To confirm the transient location of PFE1605w at Maurer's clefts, we colocalized the protein with MAHRP1 in ring, trophozoite, and schizont stage parasites. While in ring stages, MAHRP1 already appeared in Maurer's clefts and PFE1605w exclusively localized

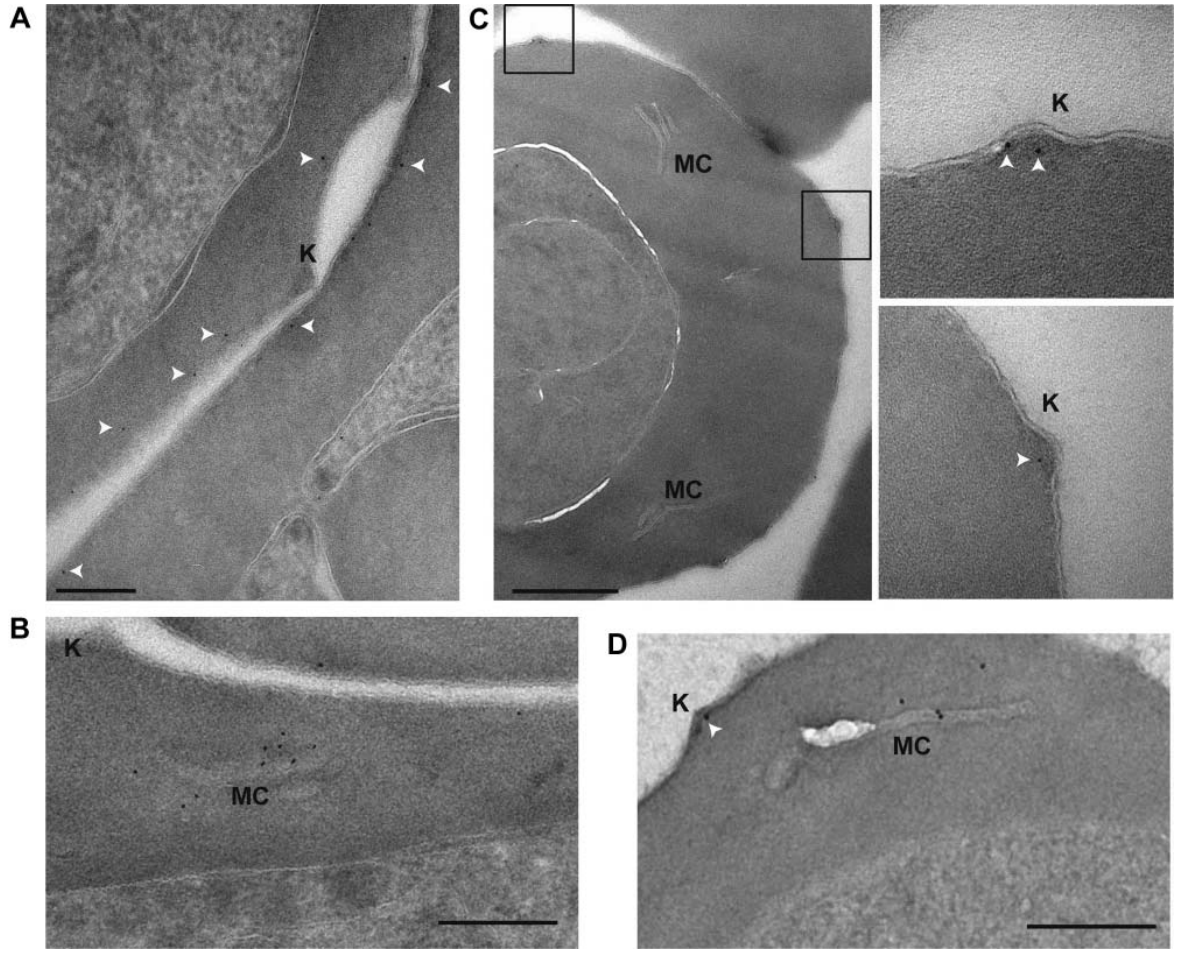

Figure 3. PFE1605w localizes to knobs. Shown here are postembedding immunoelectron microscopy images of iRBCs expressing PFI1780w-GFP (*A*, *B*), PFE1605w-HA (*C*), and PFE1605w-GFP (*D*). Insets: enlarged views of boxed sections. White arrows, 5 nM gold. Knobs (K) and Maurer's clefts (MC) are labeled. Scale bars = 200 nm (*A*); 500 nm (*C*); 250 nm (*B*, *D*).

within the parasite cytosol (Supplemental Fig. S2*A*, top panel). In young trophozoites PFE1605w and MAHRP1 colocalized to Maurer's clefts with a partial overlap of signals, suggesting subdomains in Maurer's clefts as described previously for MAHRP1 and PfEMP1 (54). This is also evidence for PFE1605w transport to already formed Maurer's clefts and proof that cargo arrives at clefts independent of their formation as reported previously (54, 55). At later stages, PFE1605w dissociates from Maurer's clefts and is transported to the iRBC membrane or knobs (Supplemental Fig. S2*A*, panel 3).

In contrast to PFE1605w and PFI1780w, MAL8P1.4, which does not interact with the ATS domain (Fig. 1*A*), showed persistent Maurer's cleft localization in IFAs (Supplemental Fig. S2*B*).

PHIST domains compete for a conserved epitope at the ATS C terminus

Despite our efforts, the PFE1605w PHIST domain evaded crystallization alone or in complex with ATS fragments and was unsuitable for extensive NMR analysis due to limited solubility. Thus, we turned to PFI1780w, which also interacts with ATS, to gain information on the PHIST-ATS complex. To delineate the specific PHIST-ATS interaction site, we performed NMR titrations of $^{13}C/^{15}N$-enriched ATS PF08_0141 (32) with the unenriched PFI1780w PHIST domain (residues 98–247). As shown in **Fig. 5*A*–*C***, the largest chemical shift perturbations, indicative of complex formation, span a wide region at the flexible C terminus of the ATS. Although sequence similarity across the C terminus of PfEMP1 intracellular segments is relatively low (32), ~75% of the amino acids most perturbed on PFI1780w binding are conserved (I311, I313, I330, L331, D336, I338, Y339, Y340, and W391) or conservatively substituted (T329, D332, E335, I372, and V390) in the majority of members of the PfEMP1 family (Supplemental Fig. S1*A*). We were able to perform similar experiments on $^{13}C/^{15}N$-enriched ATS with unenriched PFE1605w under dilute conditions and recorded the loss of ATS resonance intensity in the

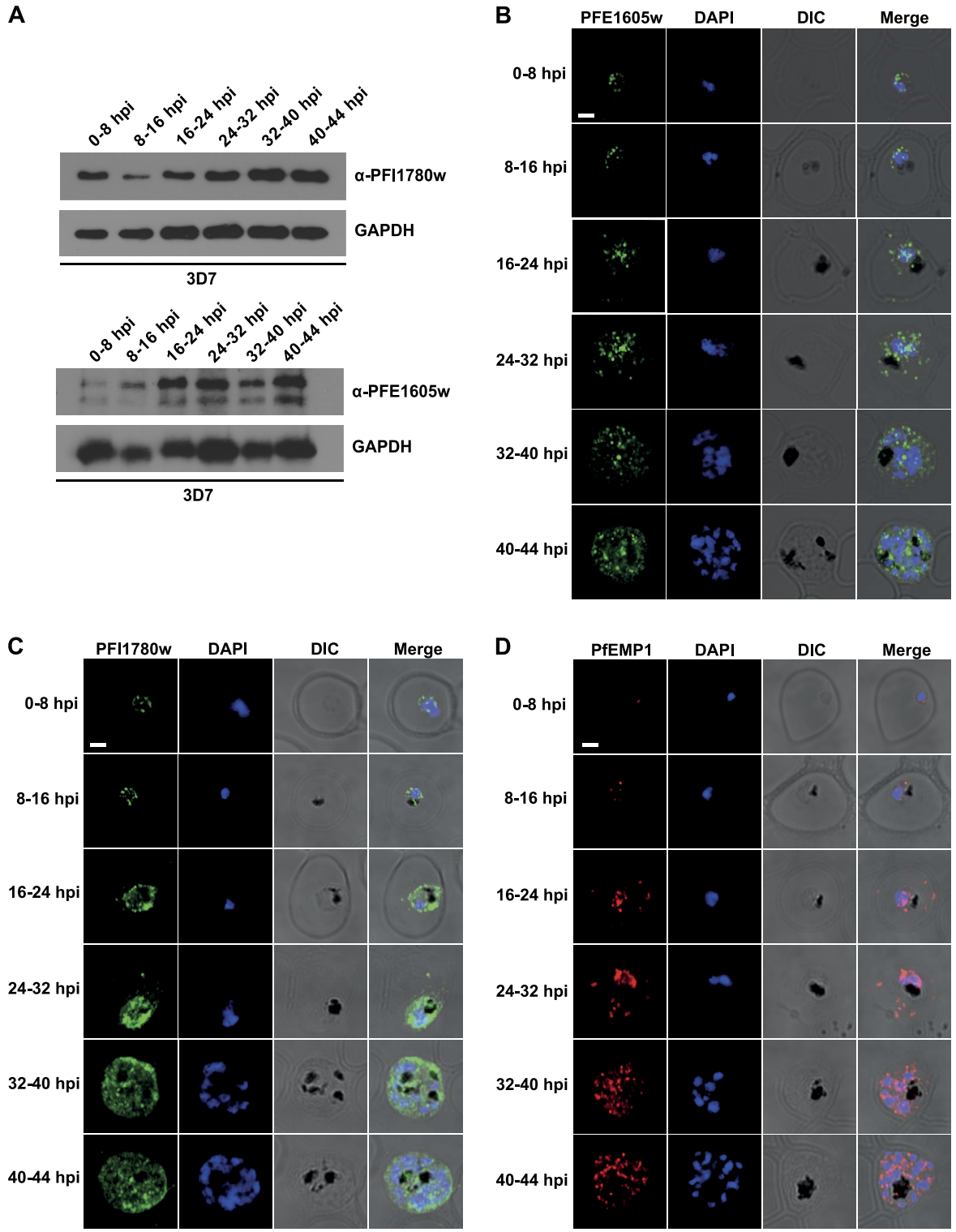

Figure 4. PFE1605w is cotranslocated with PfEMP1. *A*) Western blot with extracts from stage-specific parasites (hpi indicated for each lane). GAPDH was used as loading control. *B*–*D*) Confocal immunofluorescence analysis of tightly synchronized 3D7 parasites. Samples were collected at 8-h intervals and stained with antibodies recognizing PFE1605w (*B*), PFI1780w (*C*), or ATS (*D*) and costained with DAPI. Scale bars = 2 μm. DIC, differential interference contrast microscopy.

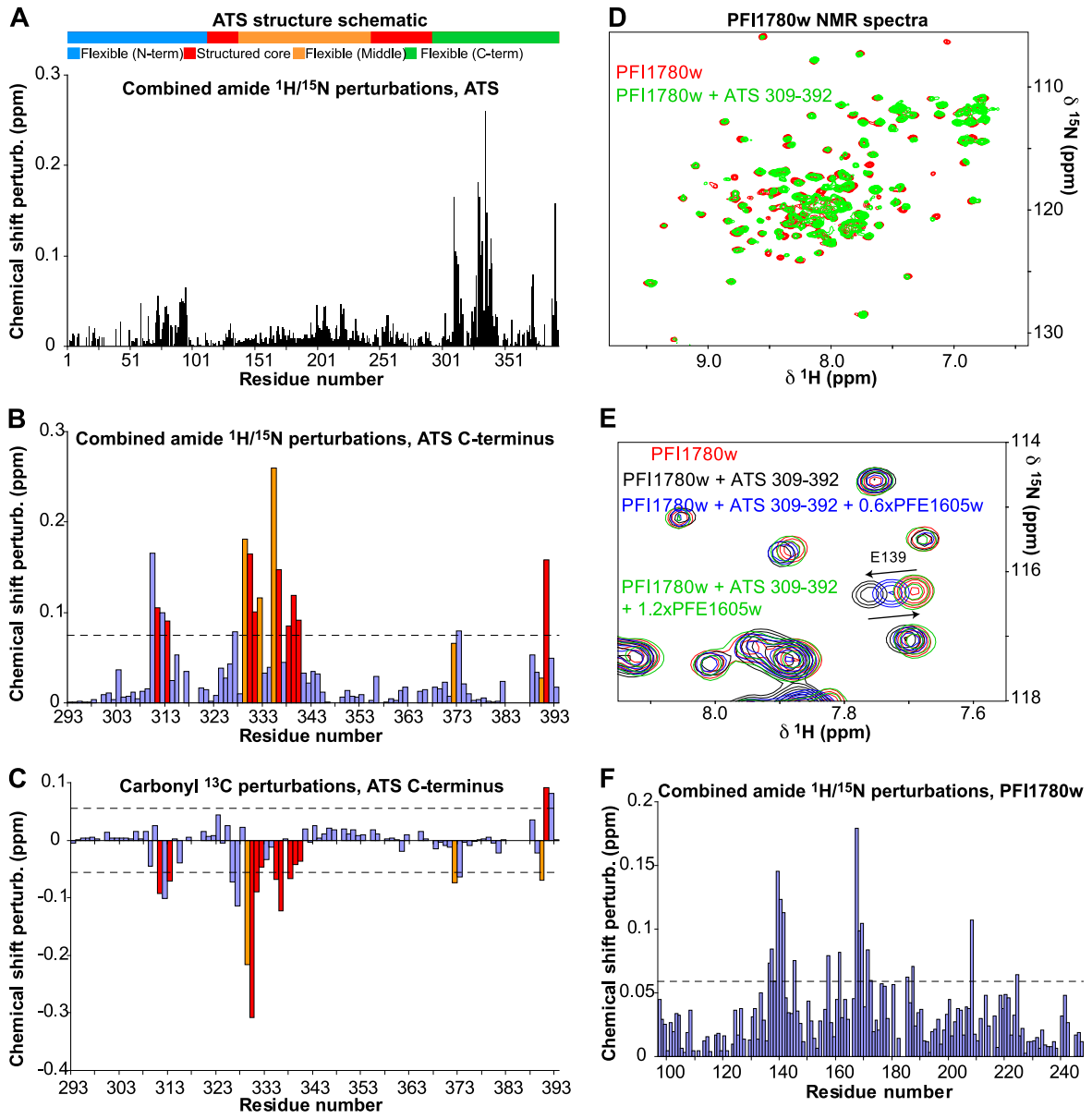

Figure 5. NMR analysis of the PFI1780w-ATS interaction. *A*) Combined perturbations of backbone amide nuclei of 0.1 mM $^{13}C/^{15}N$-enriched ATS on titration with 0.2 mM unenriched PFI1780w PHIST domain. Data were recorded at 10°C and pH 7.0. Schematic representation of ATS structure (32) is shown at top. *B*) Expansion of panel *A* for the ATS C-terminal section. Dashed line denotes the level of average perturbation plus 1 SD; residues with perturbations above this line are considered as significantly affected. *C*) Carbonyl perturbations of the same ATS region as in panel *B*. Residues judged as significantly affected in either amide or carbonyl perturbations are colored based on their conservation: red if identical or orange if conservatively substituted in ≥75% of PfEMP1 members in *P. falciparum* isolate 3D7. *D*) ^{15}N-heteronuclear single quantum coherence spectra overlay from 0.1 mM ^{15}N-enriched PFI1780w PHIST domain alone (red) or in the presence of 0.2 mM unenriched ATS C-terminal fragment (residues 309–392, green). Spectra were recorded at 37°C and pH 6.5. Perturbations in peak positions show formation of the PFI1780w-ATS complex. *E*) Expansion of overlaid spectra from 50 μM PFI1780w PHIST domain alone (red), in the presence of 50 μM ATS residues 309–392 (black), after addition of 0.6× stoichiometric ratio of unenriched PFE1605w PHIST domain (blue), or after addition of 1.2× stoichiometric ratio of PFE1605w (green). PFE1605w addition reverses PFI1780w perturbations caused by ATS binding, suggesting that the 2 PHIST proteins compete for the same ATS binding site. *F*) Per-residue combined perturbations of backbone amide ^{1}H and ^{15}N nuclei from the PFI1780w spectra shown in panel *D*. Dashed line identifies significantly perturbed residues as in panel *B*.

presence of PFE1605w (Supplemental Fig. S3*A*). Mapping interaction interfaces using this type of information is less sequence specific than that with the chemical shift perturbations observed with PFI1780w, as loss of resonance intensity may reflect interactions by a specific residue or its neighbors. Nonetheless, the data (Supplemental Fig. S3*B*) suggest that PFE1605w affects a wide span of the ATS C terminus that includes the PFI1780w interaction epitope (Fig. 5*B, C*). In addition, PFE1605w makes additional contacts with the ATS C terminus that span residues 303–309 and 353–362; these additional contacts may contribute to the higher ATS affinity of this PHIST variant.

To confirm that the 2 PHIST proteins compete for the same ATS interaction epitope, we performed NMR experiments using ^{15}N-enriched PFI1780w and unenriched ATS C terminus and PFE1605w (Fig. 5*D*). Perturbations on PFI1780w resonances caused by ATS are reversed by PFE1605w (Fig. 5*E*), which supports the competition between these PHIST domains.

Structure of the PFI1780w PHIST domain

We obtained crystals of a PFI1780w fragment spanning residues 85–247 and solved the resulting structure to 2.35-Å resolution (Supplemental Table S1). The final model showed 2 protein chains forming a tight helix-swapped dimer in the crystal (**Fig. 6*A***); however, AUC velocity experiments showed that PFI1780w is monomeric in solution under physiological conditions (Fig. 6*B*). Thus, we concluded that the dimer is a crystallization artifact and consider only the monomeric unit of the PHIST domain.

PFI1780w residues 98–247 adopted a highly α-helical configuration (Fig. 6*C*), in agreement with structure predictions (19) and circular dichroism data (32). A short initial helix (α1) is followed by an antiparallel bundle of 3 long helices (α2−α4), which are up to 51 aa in length. The PFI1780w triple-helical bundle is of length (~6.5 nm) comparable to that of a spectrin repeat; however, in contrast to spectrin, it adopts a right-handed twist (Fig. 6*D*). PHIST domains show remarkable sequence divergence, and PFI1780w belongs to the most variable PHISTc subtype of this family (19). Alignment of the PFI1780w PHIST domain with its 5 closest relatives showed just 4% identical and 20.7% conservatively substituted residues (Supplemental Fig. S1*B*). The vast majority of these conserved amino acids, including all tryptophans characteristic of the PHIST family (19), are involved in the protein hydrophobic core and do not form a continuous surface area. Nonetheless, the PFI1780w structural model

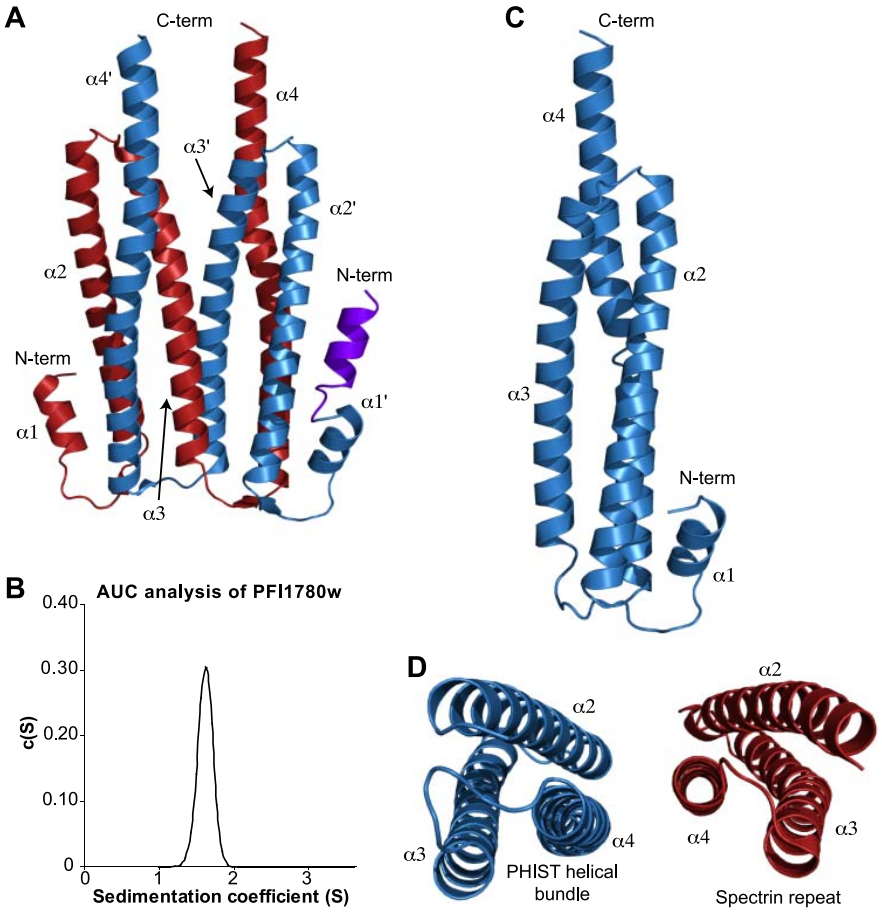

Figure 6. Structure of PFI1780w. *A*) Crystallographic model of the PFI1780w PHIST domain, showing the dimer (blue and red chains). Residues 85–97 (purple) are visible in only one polypeptide chain. *B*) AUC velocity experiment of PFI1780w residues 85–247. Data analysis yielded a narrow distribution at 1.65 S, with best friction ratio of 1.61 and 19,919 Da corresponding molecular mass. *C*) Monomeric model of the PFI1780w PHIST domain. *D*) Twist of the triple-helix bundle for PFI1780w and spectrin (RCSB 3KBT). Both models are visualized with their C termini below the page.

is sufficient to model with 98–100% confidence the domain structures for all members of this family using automated prediction pipelines.

Structural analysis of the PHIST-ATS interaction

The chemical shift perturbations of PFI1780w on ATS binding allowed us to map the binding site on the PHIST structure (Fig. 5*F*). The most significant changes localized at the middle of the PFI1780w triple-helical bundle, and, in particular, over a continuous surface on helices α2 and α3 (**Fig. 7*C*** and Supplemental Fig. S1*B*). The amino acids forming this ATS-binding interface (K136, E138, E139, H167, F168, and Q171) are not conserved between PFI1780w and PFE1605w, which probably contributes to the different ATS affinities of these proteins. Nonetheless, because PFI1780w and PFE1605w compete for the same ATS epitope, we reasoned that an analysis of the PFI1780w-ATS interaction may provide a partial model of the high-affinity complex.

The number of ATS-binding residues on PFI1780w is remarkably small compared with the broad span of perturbations observed on the ATS C terminus (Fig. 5*A*). In particular, the continuous surface identified on PFI1780w α2–α3 can only accommodate approximately 6 aa in an extended conformation. To understand how these observations relate, we predicted the transient structure adopted by the ATS C-terminal epitope (residues 306–346) on PFI1780w binding using CS-Rosetta (41). As shown in Fig. 7*A*, *B*, the structure prediction converged to a single β sheet formed by ATS residues 311–314 (β1), 320–324 (β2), 328–334 (β3), and 337–343 (β4). Formation of a single β sheet by ATS residues 306–346 may explain the widespread chemical shift changes seen in this construct on PFI1780w binding, as nearly all residues would transit from a random coil to an extended conformation. Yet, at the same time, the single ATS β sheet could provide a relatively narrow interaction interface with PFI1780w along the β-sheet edge. Thus, we propose that an ATS associates along one β-sheet edge with PFI1780w (Fig. 7*D*).

DISCUSSION

The extensive remodeling of host erythrocytes by invading *Plasmodia* is an impressive feat of biological engineering necessary for the parasites to grow, replicate, and evade the immune system; thus, it has clear implications for the human host. The unique alterations induced by *P. falciparum* resulting in iRBC cytoadherence are linked to disease severity (7). Yet our understanding of this process is largely incomplete, especially at a mechanistic level. Although iRBC remodeling involves hundreds of proteins, few interactions and even fewer structures have been examined in detail. Here, we present the first structural-functional insights on PHIST proteins, which comprise a large subset of the *P. falciparum* exportome (4, 19). Notably, our study suggests strong links between a specific PHIST member and PfEMP1, the parasite receptor responsible for cytoadherence.

PHIST domains, as demonstrated here by PFI1780w (Fig. 6), are characterized by a relatively simple α-heli-

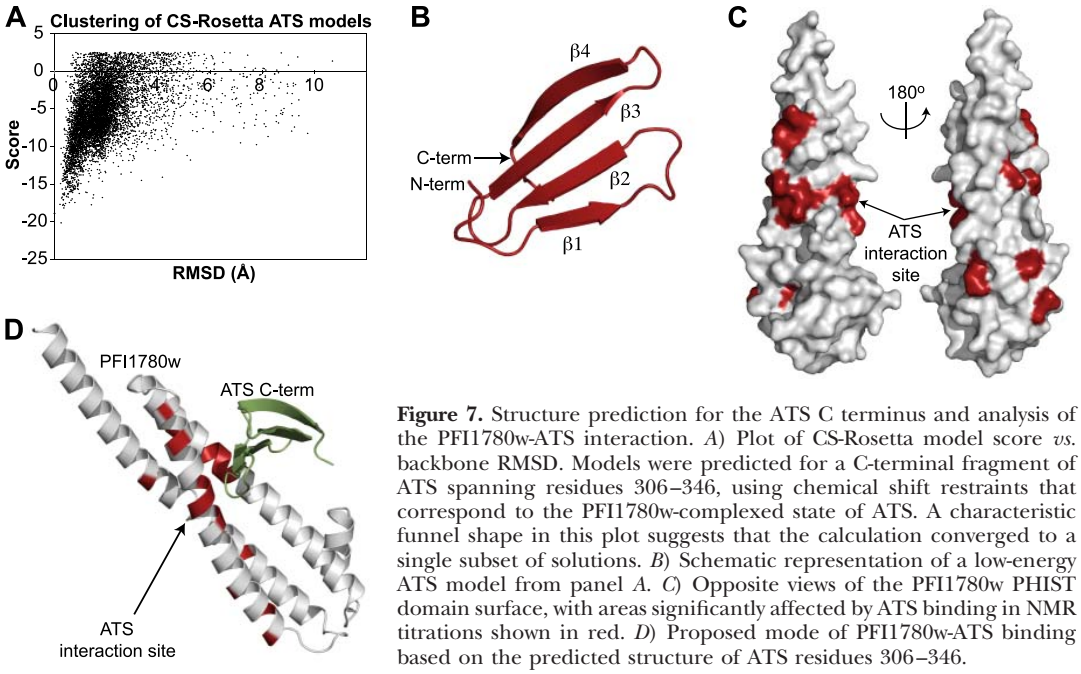

Figure 7. Structure prediction for the ATS C terminus and analysis of the PFI1780w-ATS interaction. *A*) Plot of CS-Rosetta model score *vs.* backbone RMSD. Models were predicted for a C-terminal fragment of ATS spanning residues 306–346, using chemical shift restraints that correspond to the PFI1780w-complexed state of ATS. A characteristic funnel shape in this plot suggests that the calculation converged to a single subset of solutions. *B*) Schematic representation of a low-energy ATS model from panel *A*. *C*) Opposite views of the PFI1780w PHIST domain surface, with areas significantly affected by ATS binding in NMR titrations shown in red. *D*) Proposed mode of PFI1780w-ATS binding based on the predicted structure of ATS residues 306–346.

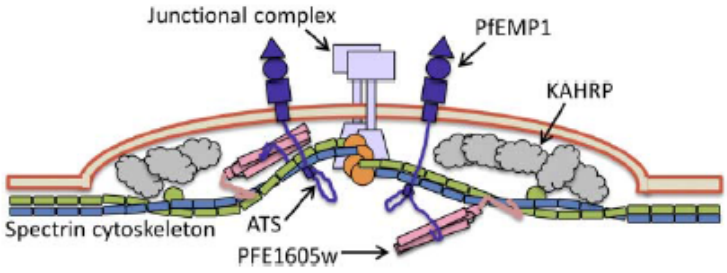

Figure 8. Schematic representation of an iRBC knob. Our proposed mechanism of PFE1605w function, connecting the C terminus of PfEMP1 ATS to the cytoskeleton, is illustrated.

seem to have a variety of functions in the parasite (4, 20, 21, 26, 30), but this might reflect their role as interaction hubs that can bind flexible protein segments, as shown here for ATS (Fig. 7). Thus far, the molecular evidence of PHIST-mediated interactions presented here and elsewhere (20, 21, 56) involves only ~10% of all family members, and high-throughput molecular methods may provide a clearer picture of the PHIST interactome.

What is the relationship of PHIST proteins with PfEMP1? In a limited set of PHIST variants, we identified 2 members, PFI1780w and PFE1605w, that bound the PfEMP1 intracellular segment (Fig. 1*A*); it is likely that additional PfEMP1-binding PHIST domains can be found among the 72 members of this family. Both PHIST proteins described here interact with the same PfEMP1 epitope but with significantly different affinities. Furthermore, substantial variation in binding strength was observed, depending on specific PHIST/PfEMP1 combinations (Fig. 1*B*), which leads us to propose that individual PHIST variants might have been optimized for different groups of PfEMP1 molecules. This proposal is strongly supported by transcriptomic evidence of a specific PHISTa member (PF14_0472) up-regulated in parasites expressing PfEMP1 variants binding human brain endothelial cells (26). Similarly, we observed that both PfEMP1-binding PHIST proteins localized to the iRBC membrane (Fig. 2*B*), but only PFE1605w was coexported with PfEMP1 and localized in knobs (Fig. 3).

Very recently Proellocks *et al.* (56) showed that disruption of PFE1605w, termed LyMP in their study, reduced iRBC cytoadherence to CD36 by 55%, while retaining knob formation and PfEMP1 surface localization. Further, they identified an interaction between inside-out vesicles prepared from uninfected human erythrocytes and the PFE1605w positively charged C terminus, but not its PHIST domain. Together with the data presented here, we can now suggest at least one mechanistic role for PFE1605w and potentially for other PHIST proteins in cytoadherence (**Fig. 8**). We propose that PFE1605w tightly binds to the PfEMP1 intracellular segment (Fig. 1) soon after export from the parasite and remains bound during trafficking to Maurer's clefts (Fig. 4) and eventually knobs (Fig. 3). When in knobs, the C-terminal segment of PFE1605w links PfEMP1 with the host cytoskeleton. The PFE1605w-ATS interaction (Fig. 7) probably complements direct ATS-cytoskeletal binding (57) and ensures mechanical robustness against shear forces exerted by blood flow, thereby allowing strong cytoadherence.

In summary, we present here the first structural insights on members of the PHIST family and how they function as protein interaction modules. The interaction properties of specific members could be linked to their cellular localization and trafficking pattern alongside the well characterized PfEMP1, allowing the proposition of a mechanistic model of the function of PHIST molecules in cytoadherence. FJ

The authors are grateful to David Staunton, Nick Soffe, Edward Lowe, and Philip Fowler for the upkeep of the supporting facilities at Oxford Biochemistry and to Henning Stahlberg and his team at the Center for Cellular Imaging and NanoAnalytics (C-CINA) and the Image Core Facility, Biozentrum, University of Basel, for the access and support. The authors acknowledge the Diamond Light Source (Harwell, UK) for access to synchrotron beamlines and the Oxford Protein Production Facility (Harwell, UK) for assistance with expression of PHIST domains. This work received support from the Wellcome Trust for the Oxford Biochemistry NMR facility (grant 094872/Z/10/Z, grant 088497/Z/09/Z to I.V., and a Ph.D. studentship to E.C.). The cell biological part of this study was supported by the Swiss National Science Foundation (grants 31003A_132709/1 and 31003A_149297/1).

REFERENCES

1. Mundwiler-Pachlatko, E., and Beck, H. P. (2013) Maurer's clefts, the enigma of *Plasmodium falciparum*. *Proc. Natl. Acad. Sci. U. S. A.* **110,** 19987–19994
2. Nguitragool, W., Bokhari, A. A., Pillai, A. D., Rayavara, K., Sharma, P., Turpin, B., Aravind, L., and Desai, S. A. (2011) Malaria parasite clag3 genes determine channel-mediated nutrient uptake by infected red blood cells. *Cell* **145,** 665–677
3. Cooke, B. M., Mohandas, N., and Coppel, R. L. (2001) The malaria-infected red blood cell: structural and functional changes. *Adv. Parasitol.* **50,** 1–86
4. Maier, A. G., Rug, M., O'Neill, M. T., Brown, M., Chakravorty, S., Szestak, T., Chesson, J., Wu, Y., Hughes, K., Coppel, R. L., Newbold, C., Beeson, J. G., Craig, A., Crabb, B. S., and Cowman, A. F. (2008) Exported proteins required for virulence and rigidity of *Plasmodium falciparum*-infected human erythrocytes. *Cell* **134,** 48–61
5. Kyes, S., Horrocks, P., and Newbold, C. (2001) Antigenic variation at the infected red cell surface in malaria. *Annu. Rev. Microbiol.* **55,** 673–707
6. Baruch, D. I., Pasloske, B. L., Singh, H. B., Bi, X., Ma, X. C., Feldman, M., Taraschi, T. F., and Howard, R. J. (1995) Cloning the *P. falciparum* gene encoding PfEMP1, a malarial variant antigen and adherence receptor on the surface of parasitized human erythrocytes. *Cell* **82,** 77–87
7. Chen, Q., Schlichtherle, M., and Wahlgren, M. (2000) Molecular aspects of severe malaria. *Clin. Microbiol. Rev.* **13,** 439–450

6. Baruch, D. I., Pasloske, B. L., Singh, H. B., Bi, X., Ma, X. C., Feldman, M., Taraschi, T. F., and Howard, R. J. (1995) Cloning the *P. falciparum* gene encoding PfEMP1, a malarial variant antigen and adherence receptor on the surface of parasitized human erythrocytes. *Cell* **82,** 77–87
7. Chen, Q., Schlichtherle, M., and Wahlgren, M. (2000) Molecular aspects of severe malaria. *Clin. Microbiol. Rev.* **13,** 439–450
8. Marti, M., Good, R. T., Rug, M., Knuepfer, E., and Cowman, A. F. (2004) Targeting malaria virulence and remodeling proteins to the host erythrocyte. *Science* **306,** 1930–1933
9. Hiller, N. L., Bhattacharjee, S., van Ooij, C., Liolios, K., Harrison, T., Lopez-Estrano, C., and Haldar, K. (2004) A host-targeting signal in virulence proteins reveals a secretome in malarial infection. *Science* **306,** 1934–1937
10. Heiber, A., Kruse, F., Pick, C., Gruring, C., Flemming, S., Oberli, A., Schoeler, H., Retzlaff, S., Mesen-Ramirez, P., Hiss, J. A., Kadekoppala, M., Hecht, L., Holder, A. A., Gilberger, T. W., and Spielmann, T. (2013) Identification of new PNEPs indicates a substantial non-PEXEL exportome and underpins common features in Plasmodium falciparum protein export. *PLoS Pathog.* **9,** e1003546
11. De Koning-Ward, T. F., Gilson, P. R., Boddey, J. A., Rug, M., Smith, B. J., Papenfuss, A. T., Sanders, P. R., Lundie, R. J., Maier, A. G., Cowman, A. F., and Crabb, B. S. (2009) A newly discovered protein export machine in malaria parasites. *Nature* **459,** 945–949
12. Wickham, M. E., Rug, M., Ralph, S. A., Klonis, N., McFadden, G. I., Tilley, L., and Cowman, A. F. (2001) Trafficking and assembly of the cytoadherence complex in Plasmodium falciparum-infected human erythrocytes. *EMBO J.* **20,** 5636–5649
13. Knuepfer, E., Rug, M., Klonis, N., Tilley, L., and Cowman, A. F. (2005) Trafficking determinants for PfEMP3 export and assembly under the *Plasmodium falciparum*-infected red blood cell membrane. *Mol. Microbiol.* **58,** 1039–1053
14. Magowan, C., Nunomura, W., Waller, K. L., Yeung, J., Liang, J., Van Dort, H., Low, P. S., Coppel, R. L., and Mohandas, N. (2000) *Plasmodium falciparum* histidine-rich protein 1 associates with the band 3 binding domain of ankyrin in the infected red cell membrane. *Biochim. Biophys. Acta* **1502,** 461–470
15. Taylor, D. W., Parra, M., Chapman, G. B., Stearns, M. E., Rener, J., Aikawa, M., Uni, S., Aley, S. B., Panton, L. J., and Howard, R. J. (1987) Localization of *Plasmodium falciparum* histidine-rich protein 1 in the erythrocyte skeleton under knobs. *Mol. Biochem. Parasitol.* **25,** 165–174
16. Weng, H., Guo, X., Papoin, J., Wang, J., Coppel, R., Mohandas, N., and An, X. (2014) Interaction of *Plasmodium falciparum* knob-associated histidine-rich protein (KAHRP) with erythrocyte ankyrin R is required for its attachment to the erythrocyte membrane. *Biochim. Biophys. Acta* **1838,** 185–192
17. Cooke, B. M., Buckingham, D. W., Glenister, F. K., Fernandez, K. M., Bannister, L. H., Marti, M., Mohandas, N., and Coppel, R. L. (2006) A Maurer's cleft-associated protein is essential for expression of the major malaria virulence antigen on the surface of infected red blood cells. *J. Cell Biol.* **172,** 899–908
18. Spycher, C., Rug, M., Pachlatko, E., Hanssen, E., Ferguson, D., Cowman, A. F., Tilley, L., and Beck, H. P. (2008) The Maurer's cleft protein MAHRP1 is essential for trafficking of PfEMP1 to the surface of *Plasmodium falciparum*-infected erythrocytes. *Mol. Microbiol.* **68,** 1300–1314
19. Sargeant, T. J., Marti, M., Caler, E., Carlton, J. M., Simpson, K., Speed, T. P., and Cowman, A. F. (2006) Lineage-specific expansion of proteins exported to erythrocytes in malaria parasites. *Genome Biol.* **7,** R12
20. LaCount, D. J., Vignali, M., Chettier, R., Phansalkar, A., Bell, R., Hesselberth, J. R., Schoenfeld, L. W., Ota, I., Sahasrabudhe, S., Kurschner, C., Fields, S., and Hughes, R. E. (2005) A protein interaction network of the malaria parasite *Plasmodium falciparum*. *Nature* **438,** 103–107
21. Parish, L. A., Mai, D. W., Jones, M. L., Kitson, E. L., and Rayner, J. C. (2013) A member of the *Plasmodium falciparum* PHIST family binds to the erythrocyte cytoskeleton component band 4.1. *Malar. J.* **12,** 160
22. Young, J. A., Fivelman, Q. L., Blair, P. L., de la Vega, P., Le Roch, K. G., Zhou, Y., Carucci, D. J., Baker, D. A., and Winzeler, E. A. (2005) The *Plasmodium falciparum* sexual development transcriptome: a microarray analysis using ontology-based pattern identification. *Mol. Biochem. Parasitol.* **143,** 67–79
23. Silvestrini, F., Bozdech, Z., Lanfrancotti, A., Di Giulio, E., Bultrini, E., Picci, L., Derisi, J. L., Pizzi, E., and Alano, P. (2005) Genome-wide identification of genes upregulated at the onset of gametocytogenesis in *Plasmodium falciparum*. *Mol. Biochem. Parasitol.* **143,** 100–110
24. Eksi, S., Haile, Y., Furuya, T., Ma, L., Su, X., and Williamson, K. C. (2005) Identification of a subtelomeric gene family expressed during the asexual-sexual stage transition in *Plasmodium falciparum*. *Mol. Biochem. Parasitol.* **143,** 90–99
25. Rovira-Graells, N., Gupta, A. P., Planet, E., Crowley, V. M., Mok, S., Ribas de Pouplana, L., Preiser, P. R., Bozdech, Z., and Cortes, A. (2012) Transcriptional variation in the malaria parasite *Plasmodium falciparum*. *Genome Res.* **22,** 925–938
26. Claessens, A., Adams, Y., Ghumra, A., Lindergard, G., Buchan, C. C., Andisi, C., Bull, P. C., Mok, S., Gupta, A. P., Wang, C. W., Turner, L., Arman, M., Raza, A., Bozdech, Z., and Rowe, J. A. (2012) A subset of group A-like var genes encodes the malaria parasite ligands for binding to human brain endothelial cells. *Proc. Natl. Acad. Sci. U. S. A.* **109,** E1772–E1781
27. Florens, L., Liu, X., Wang, Y., Yang, S., Schwartz, O., Peglar, M., Carucci, D. J., Yates, J. R., 3rd, and Wub, Y. (2004) Proteomics approach reveals novel proteins on the surface of malaria-infected erythrocytes. *Mol. Biochem. Parasitol.* **135,** 1–11
28. Florens, L., Washburn, M. P., Raine, J. D., Anthony, R. M., Grainger, M., Haynes, J. D., Moch, J. K., Muster, N., Sacci, J. B., Tabb, D. L., Witney, A. A., Wolters, D., Wu, Y., Gardner, M. J., Holder, A. A., Sinden, R. E., Yates, J. R., and Carucci, D. J. (2002) A proteomic view of the *Plasmodium falciparum* life cycle. *Nature* **419,** 520–526
29. Lasonder, E., Ishihama, Y., Andersen, J. S., Vermunt, A. M., Pain, A., Sauerwein, R. W., Eling, W. M., Hall, N., Waters, A. P., Stunnenberg, H. G., and Mann, M. (2002) Analysis of the *Plasmodium falciparum* proteome by high-accuracy mass spectrometry. *Nature* **419,** 537–542
30. Regev-Rudzki, N., Wilson, D. W., Carvalho, T. G., Sisquella, X., Coleman, B. M., Rug, M., Bursac, D., Angrisano, F., Gee, M., Hill, A. F., Baum, J., and Cowman, A. F. (2013) Cell-cell communication between malaria-infected red blood cells via exosome-like vesicles. *Cell* **153,** 1120−1133.
31. Sanders, P. R., Gilson, P. R., Cantin, G. T., Greenbaum, D. C., Nebl, T., Carucci, D. J., McConville, M. J., Schofield, L., Hodder, A. N., Yates, J. R., 3rd, and Crabb, B. S. (2005) Distinct protein classes including novel merozoite surface antigens in Raft-like membranes of *Plasmodium falciparum*. *J. Biol. Chem.* **280,** 40169–40176
32. Mayer, C., Slater, L., Erat, M. C., Konrat, R., and Vakonakis, I. (2012) Structural analysis of the *plasmodium falciparum* erythrocyte membrane protein 1 (PfEMP1) intracellular domain reveals a conserved interaction epitope. *J. Biol. Chem.* **287,** 7182–7189
33. Schuck, P. (2000) Size-distribution analysis of macromolecules by sedimentation velocity ultracentrifugation and Lamm equation modeling. *Biophys. J.* **78,** 1606–1619
34. Kabsch, W. (2010) Xds. *Acta Crystallogr. D Biol. Crystallogr.* **66,** 125–132
35. Evans, P. (2006) Scaling and assessment of data quality. *Acta Crystallogr. D Biol. Crystallogr.* **62,** 72–82
36. Adams, P. D., Grosse-Kunstleve, R. W., Hung, L. W., Ioerger, T. R., McCoy, A. J., Moriarty, N. W., Read, R. J., Sacchettini, J. C., Sauter, N. K., and Terwilliger, T. C. (2002) PHENIX: building new software for automated crystallographic structure determination. *Acta Crystallogr. D Biol. Crystallogr.* **58,** 1948–1954
37. Emsley, P., and Cowtan, K. (2004) Coot: model-building tools for molecular graphics. *Acta Crystallogr. D Biol. Crystallogr.* **60,** 2126–2132
38. Bricogne, G., Blanc, E., Brandl, M., C., F., Keller, P., Paciorek, W., Roversi, P., Sharff, A., Smart, O. S., Vonrhein, C., and Womack, T. O. (2011) *BUSTER version 2.10*. Global Phasing Ltd., Cambridge, UK
39. Chen, V. B., Arendall, W. B., 3rd, Headd, J. J., Keedy, D. A., Immormino, R. M., Kapral, G. J., Murray, L. W., Richardson, J. S., and Richardson, D. C. (2010) MolProbity: all-atom structure validation for macromolecular crystallography. *Acta Crystallogr. D Biol. Crystallogr.* **66,** 12–21
40. DeLano, W. L. (2002) *The PyMOL Molecular Graphics System*, DeLano Scientific, San Carlos, CA, USA

41. Shen, Y., Lange, O., Delaglio, F., Rossi, P., Aramini, J. M., Liu, G., Eletsky, A., Wu, Y., Singarapu, K. K., Lemak, A., Ignatchenko, A., Arrowsmith, C. H., Szyperski, T., Montelione, G. T., Baker, D., and Bax, A. (2008) Consistent blind protein structure generation from NMR chemical shift data. *Proc. Natl. Acad. Sci. U. S. A.* **105,** 4685–4690
42. Shen, Y., Delaglio, F., Cornilescu, G., and Bax, A. (2009) TALOS+: a hybrid method for predicting protein backbone torsion angles from NMR chemical shifts. *J. Biomol. NMR* **44,** 213–223
43. Crabb, B. S., Rug, M., Gilberger, T. W., Thompson, J. K., Triglia, T., Maier, A. G., and Cowman, A. F. (2004) Transfection of the human malaria parasite *Plasmodium falciparum*. *Methods Mol. Biol.* **270,** 263–276
44. Flueck, C., Bartfai, R., Volz, J., Niederwieser, I., Salcedo-Amaya, A. M., Alako, B. T., Ehlgen, F., Ralph, S. A., Cowman, A. F., Bozdech, Z., Stunnenberg, H. G., and Voss, T. S. (2009) *Plasmodium falciparum* heterochromatin protein 1 marks genomic loci linked to phenotypic variation of exported virulence factors. *PLoS Pathog.* **5,** e1000569
45. Trager, W., and Jensen, J. B. (1976) Human malaria parasites in continuous culture. *Science* **193,** 673–675
46. Pachlatko, E., Rusch, S., Muller, A., Hemphill, A., Tilley, L., Hanssen, E., and Beck, H. P. (2010) MAHRP2, an exported protein of *Plasmodium falciparum*, is an essential component of Maurer's cleft tethers. *Mol. Microbiol.* **77,** 1136–1152
47. Spielmann, T., Fergusen, D. J., and Beck, H. P. (2003) *etramps*, a new *Plasmodium falciparum* gene family coding for developmentally regulated and highly charged membrane proteins located at the parasite-host cell interface. *Mol. Biol. Cell* **14,** 1529–1544
48. Maier, A. G., Rug, M., O'Neill, M. T., Beeson, J. G., Marti, M., Reeder, J., and Cowman, A. F. (2007) Skeleton-binding protein 1 functions at the parasitophorous vacuole membrane to traffic PfEMP1 to the *Plasmodium falciparum*-infected erythrocyte surface. *Blood* **109,** 1289–1297
49. Gruring, C., and Spielmann, T. (2012) Imaging of live malaria blood stage parasites. *Methods Enzymol.* **506,** 81–92
50. Tokuyasu, K. T. (1973) A technique for ultracryotomy of cell suspensions and tissues. *J. Cell Biol.* **57,** 551–565
51. Spycher, C., Klonis, N., Spielmann, T., Kump, E., Steiger, S., Tilley, L., and Beck, H. P. (2003) MAHRP-1, a novel *Plasmodium falciparum* histidine-rich protein, binds ferriprotoporphyrin IX and localizes to the Maurer's clefts. *J. Biol. Chem.* **278,** 35373–35383
52. Bozdech, Z., Llinas, M., Pulliam, B. L., Wong, E. D., Zhu, J., and DeRisi, J. L. (2003) The transcriptome of the intraerythrocytic developmental cycle of *Plasmodium falciparum*. *PLoS. Biol.* **1,** E5
53. Le Roch, K. G., Zhou, Y., Blair, P. L., Grainger, M., Moch, J. K., Haynes, J. D., De La Vega, P., Holder, A. A., Batalov, S., Carucci, D. J., and Winzeler, E. A. (2003) Discovery of gene function by expression profiling of the malaria parasite life cycle. *Science* **301,** 1503–1508
54. McMillan, P. J., Millet, C., Batinovic, S., Maiorca, M., Hanssen, E., Kenny, S., Muhle, R. A., Melcher, M., Fidock, D. A., Smith, J. D., Dixon, M. W., and Tilley, L. (2013) Spatial and temporal mapping of the PfEMP1 export pathway in *Plasmodium falciparum*. *Cell. Microbiol.* **15,** 1401–1418
55. Gruring, C., Heiber, A., Kruse, F., Ungefehr, J., Gilberger, T. W., and Spielmann, T. (2011) Development and host cell modifications of *Plasmodium falciparum* blood stages in four dimensions. *Nat. Commun.* **2,** 165
56. Proellocks, N. I., Herrmann, S., Buckingham, D. W., Hanssen, E., Hodges, E. K., Elsworth, B., Morahan, B. J., Coppel, R. L., and Cooke, B. M. (2014) A lysine-rich membrane-associated PHISTb protein involved in alteration of the cytoadhesive properties of *Plasmodium falciparum*-infected red blood cells. *FASEB J.* **28,** 3103−3113
57. Oh, S. S., Voigt, S., Fisher, D., Yi, S. J., LeRoy, P. J., Derick, L. H., Liu, S., and Chishti, A. H. (2000) *Plasmodium falciparum* erythrocyte membrane protein 1 is anchored to the actin-spectrin junction and knob-associated histidine-rich protein in the erythrocyte skeleton. *Mol. Biochem. Parasitol.* **108,** 237–247

Received for publication May 8, 2014.
Accepted for publication June 16, 2014.

Figure S1

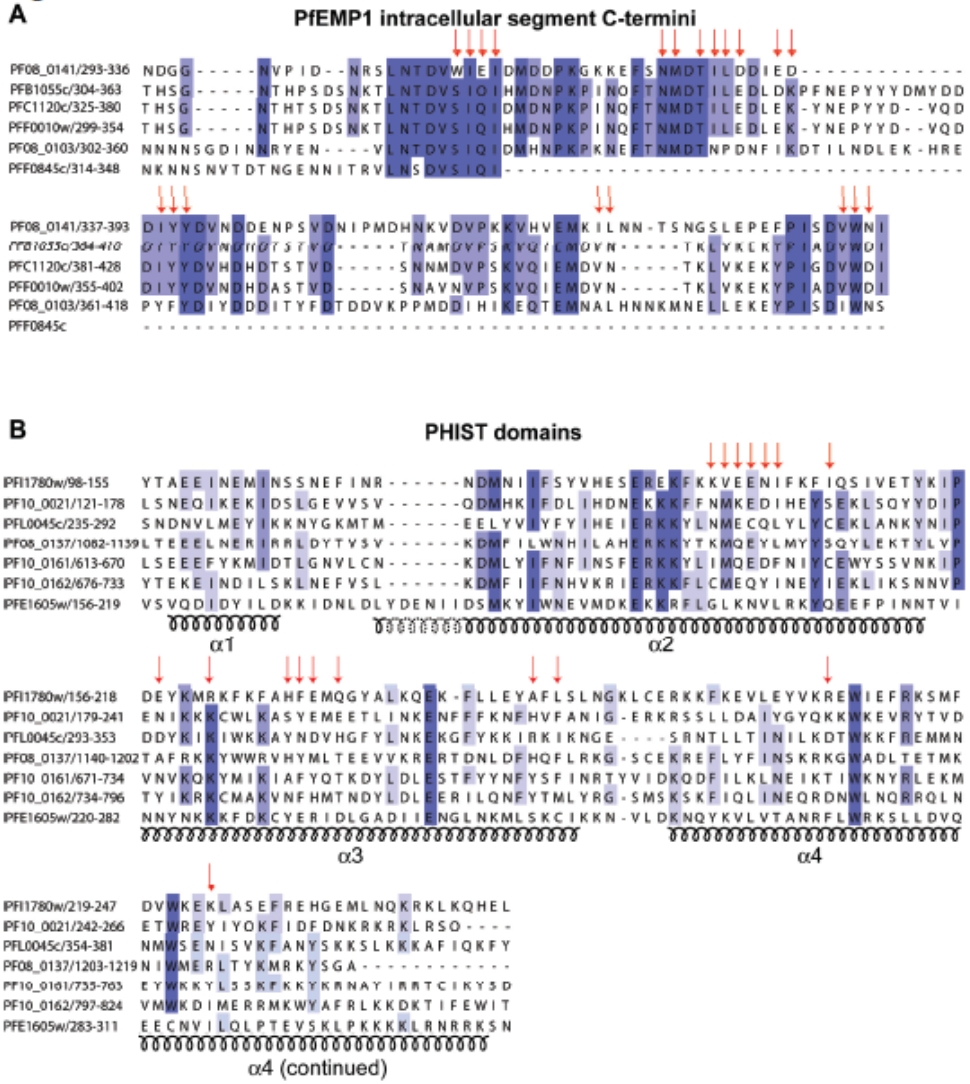

Figure S1: ClustalW2 (1) sequence alignment. A) Alignment of the intracellular segment C-termini from six PfEMP1 members with substantial sequence divergence (2, 3). Residues are coloured by conservation. Red arrows denote residues significantly affected in NMR titrations with PFI1780w PHIST domain (Fig. 6 in the main manuscript). Note that the intracellular segment of PfEMP1 variant PFF0845c is severely truncated. B) Similar alignment of the PHIST domains from PFI1780w, its five closest homologues and PFE1605w. Secondary structure elements inferred from the PFI1780w crystallographic structure are denoted below the alignment.

1. Larkin, M. A., Blackshields, G., Brown, N. P., Chenna, R., McGettigan, P. A., McWilliam, H., Valentin, F., Wallace, I. M., Wilm, A., Lopez, R., Thompson, J. D., Gibson, T. J., and Higgins, D. G. (2007) Clustal W and Clustal X version 2.0. *Bioinformatics* **23**, 2947-2948
2. Lavstsen, T., Salanti, A., Jensen, A. T., Arnot, D. E., and Theander, T. G. (2003) Sub-grouping of Plasmodium falciparum 3D7 var genes based on sequence analysis of coding and non-coding regions. *Malar J* **2**, 27
3. Mayer, C., Slater, L., Erat, M. C., Konrat, R., and Vakonakis, I. (2012) Structural analysis of the plasmodium falciparum Erythrocyte membrane protein 1 (PfEMP1) intracellular domain reveals a conserved interaction epitope. *J Biol Chem* **287**, 7182-7189

Figure S2

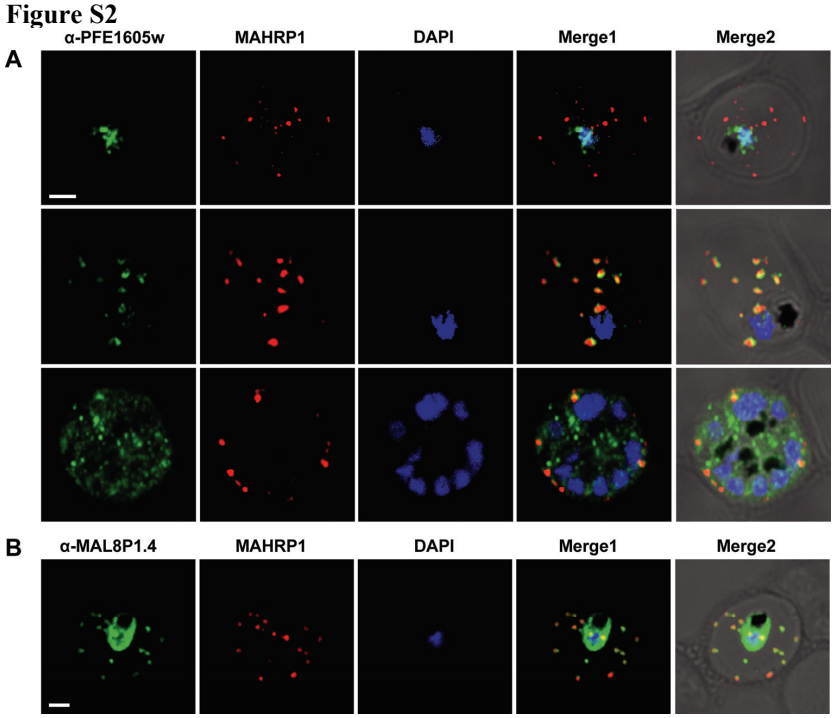

Figure S2: PFE1605w associates transiently with Maurer's clefts and is exported to the iRBC. A) Co-localization IFA of acetone-fixed 3D7 parasites with antibodies recognizing MAHRP1 and PFE1605w. DAPI was used to stain nuclei. Scale bar, 2 µm. B) Similar IFA using antibodies recognizing MAHRP1 and MAL8P1.4.

Figure S3

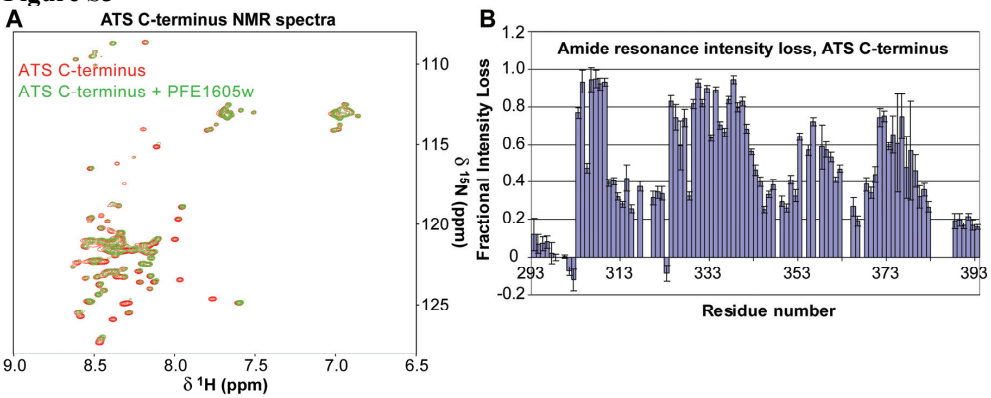

Figure S3: NMR analysis of the PFE1605w – ATS interaction. A) ^{1}H-^{15}N spectra overlay from 50 µM $^{13}C/^{15}N$-enriched ATS C-terminus alone (red) or in the presence of equimolar amount of unenriched PFE1605w PHIST domain (green). Spectra were recorded at 10°C and pH 6.5. Specific loss of resonance intensity suggests formation of a PFE1605w – ATS complex. B) Plot of fractional intensity loss versus residue number for the ATS C-terminus. Compared to the PFI1780w interaction (Fig. 5B,C), PFE1605w shows additional contacts to ATS residues 303-309 and 353-362.

Table S1: Crystallographic data collection and refinement statistics

Protein	*PFI1780w*	*PFI1780w (I3C[a]-derivative)*
PDB entry ID	4JLE	–
Space group	$P3_1\,2\,1$	$P3_1\,2\,1$

Unit cell (Å)	a = 71.04;
	b = 71.03;
	c = 146.40
		a = 71.11;
		b = 71.11;
		c = 154.42

Beamline	DLS/I04	DLS/I04
Wavelength (Å)	0.9795	1.6531
Resolution range (Å) High resolution shell (Å)	146.40-2.35 2.48-2.35	56.71-2.44 2.57-2.44
R_{Merge}[b]	0.063 (0.494)	0.087 (0.431)
R_{Pim}[b]	0.038 (0.300)	0.057 (0.280)
Completeness[b] (%)	99.9 (100)	97.5 (93.0)
Multiplicity[b]	3.6 (3.7)	5.8 (5.7)
$I/\sigma(I)$[b]	11.8 (2.4)	14.9 (4.3)
Phasing		
No. of I sites	–	27
Resolution	–	56.71-2.44
FOM *initial*[c]	–	0.51
FOM *DM*[d]	–	0.81
Refinement statistics		
R_{work} (reflections)	0.2055 (17490)	–
R_{free}(reflections)	0.2480 (947)	–
Number of atoms		
Protein atoms	2694	–
Ligands	10	–
Waters	47	–
Average B factors (Å^2)		
Protein atoms	66.6	–
Water	58.0	–
RMSD from ideal values		
Bonds / angles (Å/°)	0.010 / 0.95	–
Protein statistics[e]		
Ramachandran favored (%)	99.67	–
Ramachandran disallowed (%)	0.0	–
Clashscore (percentile)	2.61 (100%)	–
MolProbity score (percentile)	1.05 (100%)	–

[a] 5-amino-2,4,6-triiodoisophthalic acid
[b] Values in parentheses correspond to the high resolution shell
[c] From PHASER (1)
[d] From RESOLVE (2)
[e] From MolProbity (3)

1. McCoy, A. J., Grosse-Kunstleve, R. W., Adams, P. D., Winn, M. D., Storoni, L. C., and Read, R. J. (2007) Phaser crystallographic software. *J. Appl. Crystallogr.* **40**, 658 - 674
2. Terwilliger, T. C. (2000) Maximum-likelihood density modification. *Acta Crystallogr D Biol Crystallogr* **56**, 965-972
3. Chen, V. B., Arendall, W. B., 3rd, Headd, J. J., Keedy, D. A., Immormino, R. M., Kapral, G. J., Murray, L. W., Richardson, J. S., and Richardson, D. C. (2010) MolProbity: all-atom structure validation for macromolecular crystallography. *Acta Crystallogr D Biol Crystallogr* **66**, 12-21

Chapter 3

Plasmodium falciparum Plasmodium helical interspersed subtelomeric proteins contribute to cytoadherence and anchor *P. falciparum* erythrocyte membrane protein 1 to the host cell cytoskeleton

Alexander Oberli[1,2], Laura Zurbrügg[1,2], Sebastian Rusch[1,2], Françoise Brand[1,2], Madeleine E. Butler[3], Jemma L. Day[3], Erin E. Cutts[3], Thomas Lavstsen[4], Ioannis Vakonakis[3] and Hans-Peter Beck[1,2,*]

Affiliation of authors:

[1] Swiss Tropical and Public Health Institute, Basel, Switzerland

[2] University of Basel, Basel, Switzerland

[3] Department of Biochemistry, University of Oxford, Oxford, United Kingdom

[4] Centre for Medical Parasitology, Department of International Health, Immunology, and Microbiology, University of Copenhagen and Department of Infectious Diseases, Rigshospitalet, Copenhagen, Denmark

[*] Corresponding author:

Molecular Parasitology Unit, Swiss Tropical and Public Health Institute, Socinstrasse 57, CH 4002 Basel, Switzerland, +41 6128 48116, e-mail: hans-peter.beck@unibas.ch

This article has been published in

Cellular Microbiology, Volume 18, Issue 10, Pages 1415-1428, April 2016

Cellular Microbiology (2016) **18**(10), 1415–1428
doi:10.1111/cmi.12583
First published online 26 April 2016

Plasmodium falciparum Plasmodium helical interspersed subtelomeric proteins contribute to cytoadherence and anchor *P. falciparum* erythrocyte membrane protein 1 to the host cell cytoskeleton

Alexander Oberli,[1,2] Laura Zurbrügg,[1,2] Sebastian Rusch,[1,2] Françoise Brand,[1,2] Madeleine E. Butler,[3] Jemma L. Day,[3] Erin E. Cutts,[3] Thomas Lavstsen,[4,5] Ioannis Vakonakis[3] and Hans-Peter Beck[1,2*]

[1]*Swiss Tropical and Public Health Institute, Basel, Switzerland.*
[2]*University of Basel, Basel, Switzerland.*
[3]*Department of Biochemistry, University of Oxford, Oxford, UK.*
[4]*Centre for Medical Parasitology, Department of International Health, Immunology, and Microbiology, University of Copenhagen, Copenhagen, Denmark.*
[5]*Department of Infectious Diseases, Rigshospitalet, Copenhagen, Denmark.*

Summary

Adherence of *Plasmodium falciparum*-infected erythrocytes to host endothelium is conferred through the parasite-derived virulence factor *P. falciparum* erythrocyte membrane protein 1 (PfEMP1), the major contributor to malaria severity. PfEMP1 located at knob structures on the erythrocyte surface is anchored to the cytoskeleton, and the *Plasmodium* helical interspersed subtelomeric (PHIST) gene family plays a role in many host cell modifications including binding the intracellular domain of PfEMP1. Here, we show that conditional reduction of the PHIST protein PFE1605w strongly reduces adhesion of infected erythrocytes to the endothelial receptor CD36. Adhesion to other endothelial receptors was less affected or even unaltered by PFE1605w depletion, suggesting that PHIST proteins might be optimized for subsets of PfEMP1 variants. PFE1605w does not play a role in PfEMP1 transport, but it directly interacts with both the intracellular segment of PfEMP1 and with cytoskeletal components. This is the first report of a PHIST protein interacting with key molecules of the cytoadherence complex and the host cytoskeleton, and this functional role seems to play an essential role in the pathology of *P. falciparum*.

Received 12 January, 2016; revised 15 February, 2016; accepted 21 February, 2016. *For correspondence. E-mail hans-peter.beck@unibas.ch; tel. +41-61-284 8116; Fax +41-61-284 8101.

Introduction

After invading the human erythrocyte, the malaria parasite *Plasmodium falciparum* refurbishes its host cell dramatically. The most important changes lead to sequestration of infected cells to the microvasculature of human organs – the sole cause of morbidity and mortality in malaria tropica. These changes also allow the malaria parasite to grow in a parasitophorous vacuole inside the erythrocyte and enable nutrient uptake. The parasite invests approximately 10% of its proteome to refurbish the host cell in this way. Hundreds of exported parasite proteins fall into one of two groups (Spillman *et al.*, 2015). The first group is well defined and consists of proteins containing a pentameric motif, termed PEXEL/HT (*Plasmodium* export element/host targeting signal) (Hiller *et al.*, 2004; Marti *et al.*, 2004), which allows the establishment of a *P. falciparum* exportome with approximately 400 proteins (Sargeant *et al.*, 2006). A second group of exported proteins, which do not contain a PEXEL/HT motif or any other identifiable export motif, has also been observed (PEXEL-negative exported proteins). It is difficult to predict the true number of PEXEL-negative exported proteins and hence the total number of exported proteins (Heiber *et al.*, 2013). The export of both groups of proteins results in profound structural and morphological changes in the erythrocyte. For example it causes the formation of electron-dense protrusions on the erythrocyte surface, called knobs (Watermeyer *et al.*, 2016), alters red blood cell (RBC) rigidity (Maier *et al.*, 2008) and increases membrane permeability (Nguitragool *et al.*, 2011).

A key molecule and ligand for binding infected red blood cells (iRBCs) to host cell receptors on the vascular endothelium is the *P. falciparum* erythrocyte membrane protein 1 (PfEMP1). This major parasite virulence factor is

embedded in the knobs through a transmembrane helix and comprises a highly variable ectodomain and a semiconserved intracellular segment, the acidic terminal segment (ATS) (Lavstsen *et al*., 2003; Mayer *et al*., 2012). The extracellular part of PfEMP1 consists of multiple adhesion domains, enabling the infected cell to bind to host adhesins including CD36, intercellular adhesion molecule-1 (ICAM-1) and chondroitin sulfate A (CSA). This binding leads to iRBC sequestration within the microvasculature (Kraemer and Smith, 2006). In contrast, the cytoplasmic domain is relatively conserved and was previously thought to interact with the knob-associated histidine-rich protein (KAHRP) (Crabb *et al*., 1997) and, potentially, with the erythrocyte cytoskeleton components actin and spectrin (Kilejian *et al*., 1991; Waller *et al*., 1999, 2002; Oh *et al*., 2000). Recent data, however, do not support a direct ATS–KAHRP interaction but rather an ATS interaction with PHIST proteins PFI1780w and PFE1605w (Mayer *et al*., 2012; Oberli *et al*., 2014).

The proteins encoded by the *phist* multigene family are defined by the presence of a 150-amino acid domain consisting of four consecutive α-helices. Almost all members include a signal sequence and a PEXEL motif (Sargeant *et al*., 2006). The *phist* family underwent dramatic lineage-specific proliferation in *P. falciparum* and is suspected of playing a major role in host cell modifications in cytoplasmic protein associations (Sargeant *et al*., 2006; Oakley *et al*., 2007; Frech and Chen, 2013). To date, only a few PHIST proteins have been partially characterized and almost no molecular functions have been assigned, despite their wide distribution within the iRBC. So far, members of the PHIST protein family have been implicated in knob formation (Maier *et al*., 2008), in altered host cell rigidity (Mills *et al*., 2007; Maier *et al*., 2008), in trafficking of and interaction with PfEMP1 (Maier *et al*., 2008; Mayer *et al*., 2012; Oberli *et al*., 2014) and in iRBC adhesion to the brain microvasculature (Daily *et al*., 2005; Claessens *et al*., 2012). Moreover, PHIST proteins have been shown to localize to the iRBC periphery (Tarr *et al*., 2014), possibly binding erythrocyte cytoskeletal components (Kilili and LaCount, 2011; Parish *et al*., 2013; Proellocks *et al*., 2014). They have also been found in detergent-resistant membrane fractions (Sanders, 2005) and in exosomes mediating cell–cell communication (Regev-Rudzki *et al*., 2013).

Previously, we showed that PFE1605w, another member of the PHIST protein family, is exported to knobs and binds directly to the PfEMP1 ATS domain, displaying similar temporal and spatial export as PfEMP1 (Oberli *et al*., 2014). This finding differs somewhat from those of Proellocks *et al*. (2014), who suggested an alternative localization. Fluorescence polarization experiments using PFE1605w and a set of ATS domains from different PfEMP1 molecules showed substantial variation in binding affinity, suggesting that different PHIST proteins might have been optimized for different PfEMP1 members (Oberli *et al*., 2014). Here we present the first functional analysis of a PHIST protein by using inducible downregulation of PFE1605w and also a unique controlled system that blocks PFE1605w at Maurer's clefts. Both approaches showed that reduced levels of PFE1605w within the knobs lead to strongly reduced adhesion of iRBC to endothelial receptors, but that PFE1605w plays no role in transporting PfEMP1 or its surface exposure. PFE1605w directly binds the C-terminus of different ATS domains *in vitro* and in iRBC and interacts with components of band 3 and junctional complexes at the erythrocyte membrane. This is the first report of a functional role for PFE1605w, which anchors a variety of PfEMP1 variants to the cytoskeleton of the iRBC.

Results

Inducible regulation of PFE1605w

To investigate the function of PFE1605w, we generated a parasite cell line that allowed a conditional expression of the endogenous protein by using the human FK506 binding protein (FKBP) destabilization domain (DD) technique (Banaszynski *et al*., 2006; Armstrong and Goldberg, 2007). For this, parasites were generated that expressed endogenous PFE1605w as a C-terminally tagged green fluorescent protein–DD fusion protein and whose PFE1605w–DD was rapidly degraded if not stabilized by Shield-1. The integration of the plasmid containing the coding sequence for the PFE1605w–DD construct at the correct locus was confirmed by Southern blot (Fig. S1A). Immunofluorescence assays (IFAs) showed the expected localization of tagged PFE1605w at Maurer's clefts and at the iRBC membrane (Fig. 1A) as previously shown with non-modified protein (Oberli *et al*., 2014). In parasites grown for 96 h without Shield-1 (PFE1605w^{OFF}), PFE1605w levels were highly reduced and the residual protein was visible only within the parasite. Parasites grown for 96 h under the presence of Shield-1 (PFE1605w^{ON}) displayed normal levels and distribution of PFE1605w. Western blot analysis of synchronized PFE1605w^{ON}/PFE1605w^{OFF} parasites with polyclonal antibodies against PFE1605w showed significantly reduced levels of PFE1605w in PFE1605w^{OFF} parasites compared with PFE1605w^{ON} and 3D7 wild-type parasites (Fig. 1B). To test the PFE1605w^{ON}/PFE1605w^{OFF} parasites' adherence to recombinant CD36, a semistatic adhesion assay was performed. PFE1605w^{OFF} parasites showed a 50% (±9%, $n=3$) decrease in adhesion to CD36 (Fig. 1C) compared with PFE1605w^{ON} parasites, a result similar to that observed with a PFE1605w gene disruption (Proellocks *et al*., 2014). Subsequent addition of Shield-1 to the cultures (PFE1605w^{RES}) restored adhesion to CD36 to the same

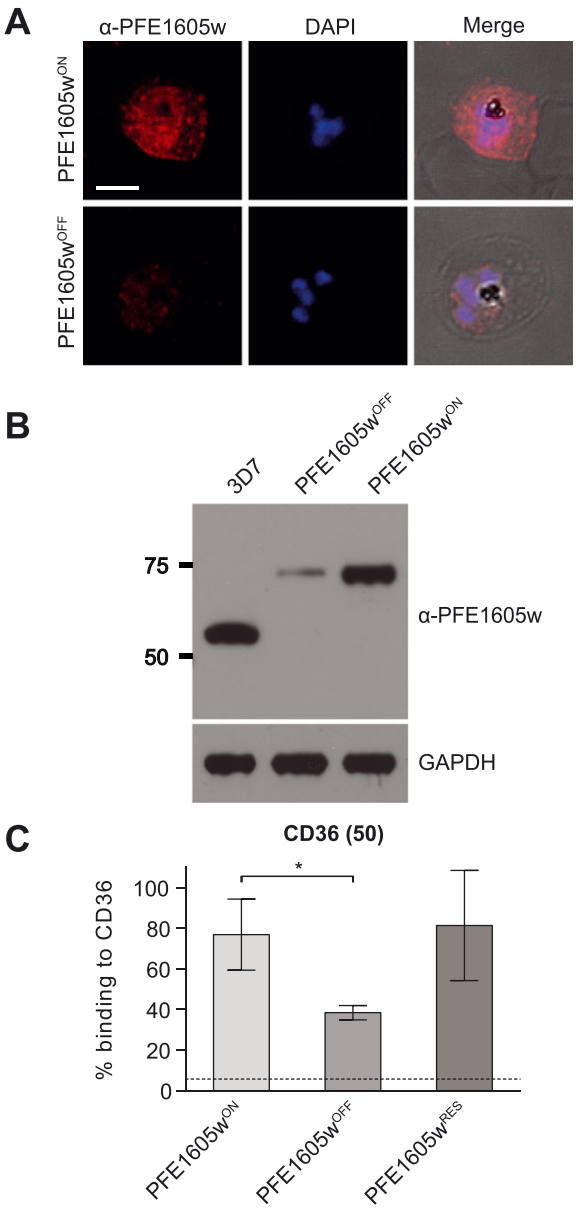

Fig. 1. Conditional depletion of PFE1605w. Confocal immunofluorescence and Western blot analysis of synchronized 3D7 parasites expressing endogenous PFE1605w as a C-terminally tagged DD fusion protein grown for 96 h in the presence (PFE1605w^{ON}) or absence (PFE1605w^{OFF}) of 625 nM Shield-1.
A. Confocal immunofluorescence.
B. Western blot. The specificity of affinity-purified polyclonal α-PFE1605w antibodies is described in Fig. S1B. The nuclei were stained with DAPI. Scale bar = 3 μm. GAPDH was used as loading control.
C. Semistatic adhesion assay of RBCs infected with PFE1605w^{ON}/PFE1605w^{OFF} parasites to immobilized recombinant CD36 at 50 μg ml^{-1}. The graph displays mean values across triplicate samples normalized to 3D7 wild-type parasite binding. The error bars represent SDs of three independent experiments. An arbitrary threshold (dashed line) for unspecific binding was calculated as the mean level of iRBC binding to 1% w/v BSA plus 2 SDs. *P* values were calculated by using a two-tailed Student's *t*-test, asterisk indicates $P \leq 0.05$.

level as that for PFE1605w^{ON} parasites (Fig. 1C). This indicates that reduced levels of exported PFE1605w results in a significant reduction of adhesion of iRBCs.

Inducible tethering of PFE1605w at Maurer's clefts

To confirm the importance of PFE1605w presence in knobs for cytoadherence, an alternative approach was used. By conditionally tethering PFE1605w to the cytoplasmic domain of a Maurer's cleft protein, we prevented its transport to the knobs, thereby blocking the presence of PFE1605w at the knob structure. The technique is based on the heterodimerization of the FKBP12 to the FKBP-rapamycin binding (FRB) domain of human mechanistic target of rapamycin in the presence of rapamycin (Haruki *et al.*, 2008; Busch *et al.*, 2009; Robinson *et al.*, 2010; Xu *et al.*, 2010). First, we generated parasites that expressed PFE1605w C-terminally fused to FKBP under the control of the endogenous promoter (Fig. S1A). These parasites were subsequently transfected with a plasmid that episomally expressed membrane-associated histidine-rich protein 1 (MAHRP1) fused to an mCherry tag and an FRB domain under the mal7 promoter (Figs 2A and S1C). In ring-stage parasites, the MAHRP1–FRB fusion protein was exported to the Maurer's clefts, whereas the FKBP-tagged PFE1605w still resided within the parasite (Fig. 2B). In trophozoite and schizont parasites, PFE1605w–FKBP was correctly exported to Maurer's clefts and to knobs as previously described (Oberli *et al.*, 2014). Upon adding 100 nM rapalog (a rapamycin analogue) to ring-stage parasites, a ternary complex at the Maurer's clefts composed of MAHRP1–FRB, rapalog and PFE1605w–FKBP was formed as soon as PFE1605w–FKBP was exported to Maurer's clefts (Fig. 2B) and PFE1605w–FKBP was blocked from localizing in the knobs. Next, we tested the cytoadhesive properties of parasites grown in the presence or absence of rapalog (PFE1605w^{+RAP}/PFE1605w^{-RAP}) to recombinant CD36. Parasites cultured in the presence of rapalog (PFE1605w^{+RAP}) showed a 62% (±9%, $n = 3$) reduction in binding to CD36 compared with parasites grown without rapalog (PFE1605w^{-RAP}) (Fig. 2C). To demonstrate that endogenous untagged PFE1605w does not bind MAHRP1–FRP upon addition of the rapalogue, 3D7 wild-type parasites were transfected with the MAHRP1–FRB plasmid. In both cases (control^{+RAP}/control^{-RAP}), the parasites showed comparable levels of binding to CD36, indicating that no heterodimerization occurred (Fig. 2C).

PFE1605w has no significant role in P. falciparum *erythrocyte membrane protein 1 transport*

To test whether PFE1605w reduction or tethering impairs transport of other well-characterized exported proteins, we analysed the PFE1605w^{ON}/PFE1605w^{OFF}/PFE1605w^{+RAP}/PFE1605w^{-RAP} parasites by IFA by using antibodies against PfEMP1, PfEMP3, KAHRP,

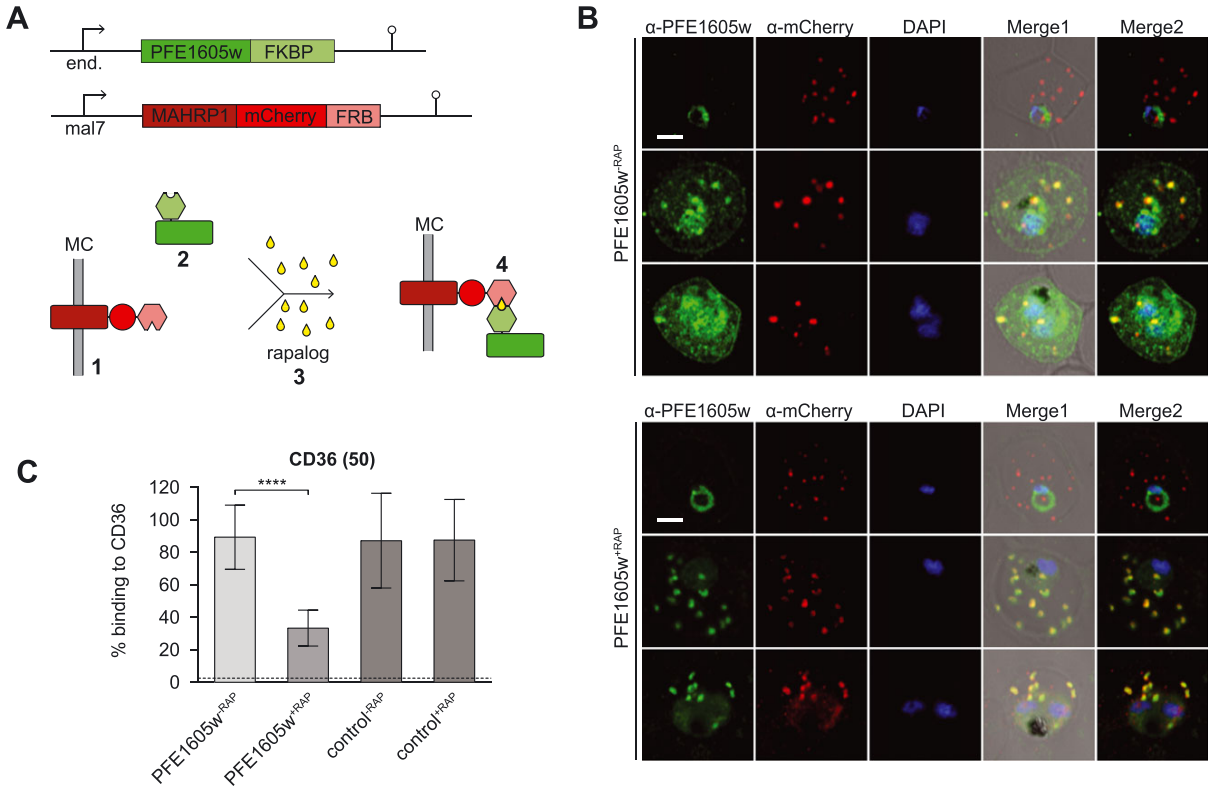

Fig. 2. Controlled tethering of PFE1605w at Maurer's clefts.
A. Schematic representation of controlled PFE1605w tethering. The episomally expressed MAHRP1-FRB fusion protein is exported to Maurer's clefts (1) prior to the export of C-terminally FKBP-tagged PFE1605w (2). Upon close proximity of the two fusion proteins and addition of rapalog (3), heterodimerization of the FKBP domain and the FRB domain occurs (4) and PFE1605w is immobilized at Maurer's clefts.
B. Confocal immunofluorescence analysis of parasites grown in the absence (PFE1605w^{-RAP}) or presence (PFE1605w^{+RAP}) of 100 nM rapalog. The nuclei were stained with DAPI. Scale bar = 2 μm.
C. Semistatic adhesion assay of PFE1605w^{-RAP}/PFE1605w^{+RAP} parasites to immobilized recombinant CD36 protein at 50 μg ml^{-1} concentration. The graph displays mean values across triplicate samples, and the error bars represent the SDs of three independent experiments. An arbitrary threshold (dashed line) for unspecific binding was calculated as the mean level of iRBC binding to 1% w/v BSA plus two SDs. *P* values were calculated by using a two-tailed Student's *t*-test; the asterisks indicate $P \leq 0.0001$.

mature parasite-infected erythrocyte surface antigen (MESA), ring-infected erythrocyte surface antigen (RESA), MAHRP1, MAHRP2 and HSP70x. All tested proteins revealed correct subcellular localization in parasites (data shown for PFE1605w^{ON}/PFE1605w^{OFF} parasites; Fig. S2).

To test whether the observed reduction in CD36 binding was due to a reduction of PfEMP1 surface exposure, we treated iRBCs with trypsin. In all parasite cultures, PfEMP1 was correctly displayed on the iRBC surface (Fig. 3A and B) as evident by PfEMP1 proteolysis that yields intact ATS domains. The trypsin cleavage assay also revealed that the size of PfEMP1 in all parasites were identical, suggesting that the same PfEMP1 variant was expressed in the parasite lines compared. Scanning electron microscopy (SEM) showed the presence of knobs in all parasite cell lines (Fig. S3); thus, the reduction in cytoadherence observed in PFE1605w^{OFF} and PFE1605w^{+RAP} parasites was not due to decreased knob formation.

Cytoadhesive properties of infected red blood cells expressing different P. falciparum *erythrocyte membrane protein 1 in the absence of PFE1605w*

Previously, we showed that the recombinant PHIST domain of PFE1605w interacted with six different ATS variants with up to 25-fold differences in affinity (Oberli *et al.*, 2014). This suggested that PFE1605w might be optimized for binding to a subset of PfEMP1 variants; hence, it might be relevant only for iRBC binding to a subset of endothelial receptors. Therefore, we selected parasites expressing PFE1605w–DD on different host receptors, including CD36, ICAM-1 and CSA, in order to isolate parasites expressing different PfEMP1 molecules. After four rounds of pre-selection, we obtained parasites binding to CD36, ICAM-1, or CSA (Fig. 4). Expression of *var* genes in all the pre-selected parasite lines was tested by quantitative PCR (qPCR) and showed a clear differential expression of *var* genes, suggesting the

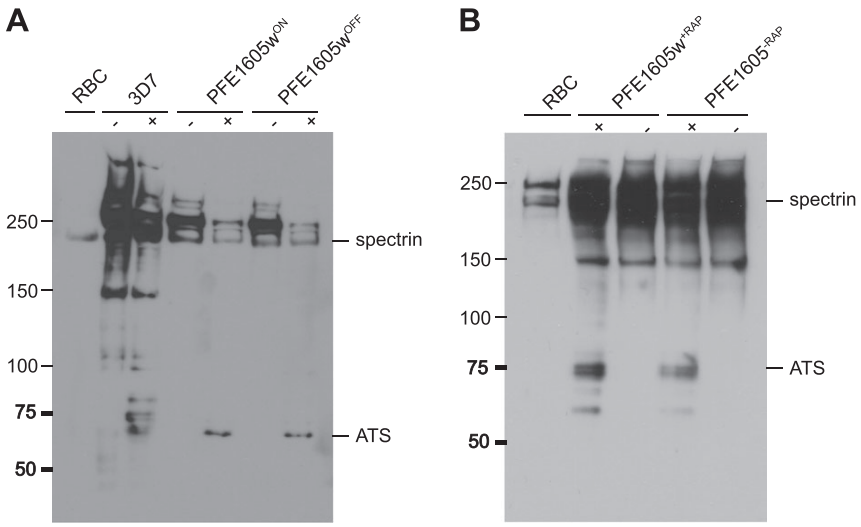

Fig. 3. PfEMP1 surface exposure is not impaired upon PFE1605w depletion in knobs. Determination of PfEMP1 surface exposure by detecting trypsin cleavage in 3D7 wild type, PFE1605w^{ON}/PFE1605w^{OFF} and PFE1605w^{+RAP}/PFE1605w^{-RAP} parasites.
A. PFE1605w^{ON}/PFE1605w^{OFF}.
B. PFE1605w^{+RAP}/PFE1605w^{-RAP} parasites. Trophozoites of each parasite line were treated with trypsin (+) or without trypsin (−), and the extracts were analysed by Western blot by using antibodies against ATS domains.

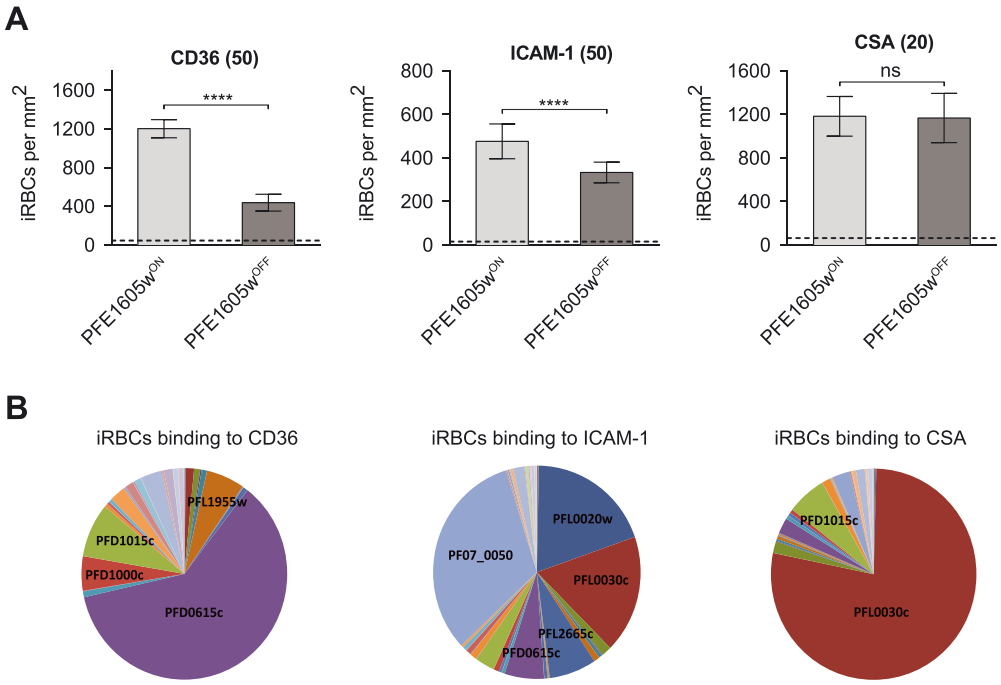

Fig. 4. iRBCs expressing a different PfEMP1 variant show different level of reduction in cytoadherence upon conditional depletion of PFE1605w.
A. Preselected iRBCs binding to either recombinant CD36, ICAM-1 or CSA immobilized on tissue-treated glass slides at 50 μg ml^{-1} (CD36, ICAM-1) or 20 μg ml^{-1} (CSA) concentrations. Parasites expressing PFE1605w as a C-terminally tagged DD fusion protein were grown for 96 h in the presence (PFE1605w^{ON}) or absence (PFE1605w^{OFF}) of 625 nM Shield-1. The graphs display overall mean values across triplicate experiments using linear regression with a random effect for experiment. The error bars represent the SDs of the triplicate experiments. An arbitrary threshold (dashed line) for unspecific binding was calculated as the mean level of iRBC binding to 1% w/v BSA plus two SDs. *P* values were calculated by using a two-tailed Student's *t*-test. The asterisks indicate $P \leq 0.0001$. 'ns' indicates $P \geq 0.05$.
B. Pie charts show the *var* transcript distribution in the selected lines. qPCR was performed with specific primers for each *var* gene as previously reported.

display of a distinct PfEMP1 variant on the iRBC surface (Fig. 4B). Pre-selected parasites were grown with and without Shield-1 and after 96 h they were allowed to bind to their respective receptor in a semistatic adhesion assay. Parasites grown in the absence of Shield-1 showed an approximately 64% reduction in binding to

CD36 (Fig. 4A). Binding to ICAM-1 was reduced by 30% and binding to CSA showed no reduction at all (Fig. 4A), indicating that PFE1605w plays no role in CSA-mediated cytoadherence.

PFE1605w binds the C-terminal part of the acidic terminal segment

Previously, we showed that the recombinant PHIST domain of PFE1605w binds with low-micromolar affinity to the C-terminal part of the ATS domain (ATS-C) of PfEMP1 variant PF08_0141 (Oberli *et al.*, 2014). Sequence conservation among ATS domains suggested that ATS-C provides the PFE1605w binding epitope in most PfEMP1 variants. To test this, we performed *in vitro* fluorescence polarization binding experiments by using the PFE1605w PHIST domain and fluorescein-labelled recombinant ATS-C fragments from PfEMP1 variants dominantly expressed in preselected parasites (Figs 4B and S4A). In almost all cases, we observed direct PFE1605w–ATS-C binding with dissociation constants (K_d) in the 4–90 μM range (Fig. 5A).

To test whether PFE1605w binds to ATS-C in *P. falciparum* iRBCs, we designed two mini-PfEMP1 constructs consisting of an N-terminal part of a PEXEL protein (PF13_0275) including a signal sequence and a PEXEL motif, the ATS-C of two PfEMP1 variants and a 3xHA tag to allow detection (Figs 5B and S4B). The PfEMP1 variants selected, PF08_0141 and PFF0010w, display approximately 13-fold difference in *in vitro* affinity (5 and 65 μM K_d respectively) for the PHIST domain of PFE1605w (Oberli *et al.*, 2014). Because the fusion proteins were expressed under the *crt* promoter, they were found early in the life cycle. Due to the lack of a TM domain, the mini-PfEMP1 was soluble and exported to the erythrocyte cytosol with the predicted size (Fig. S1D). Potential ATS-C interaction partners were detected by co-immunoprecipitation (Co-IP) followed by mass spectrometry (MS) for protein identification. Trophozoite extracts from parasites expressing a mini-PfEMP1 fusion protein were used to isolate potential

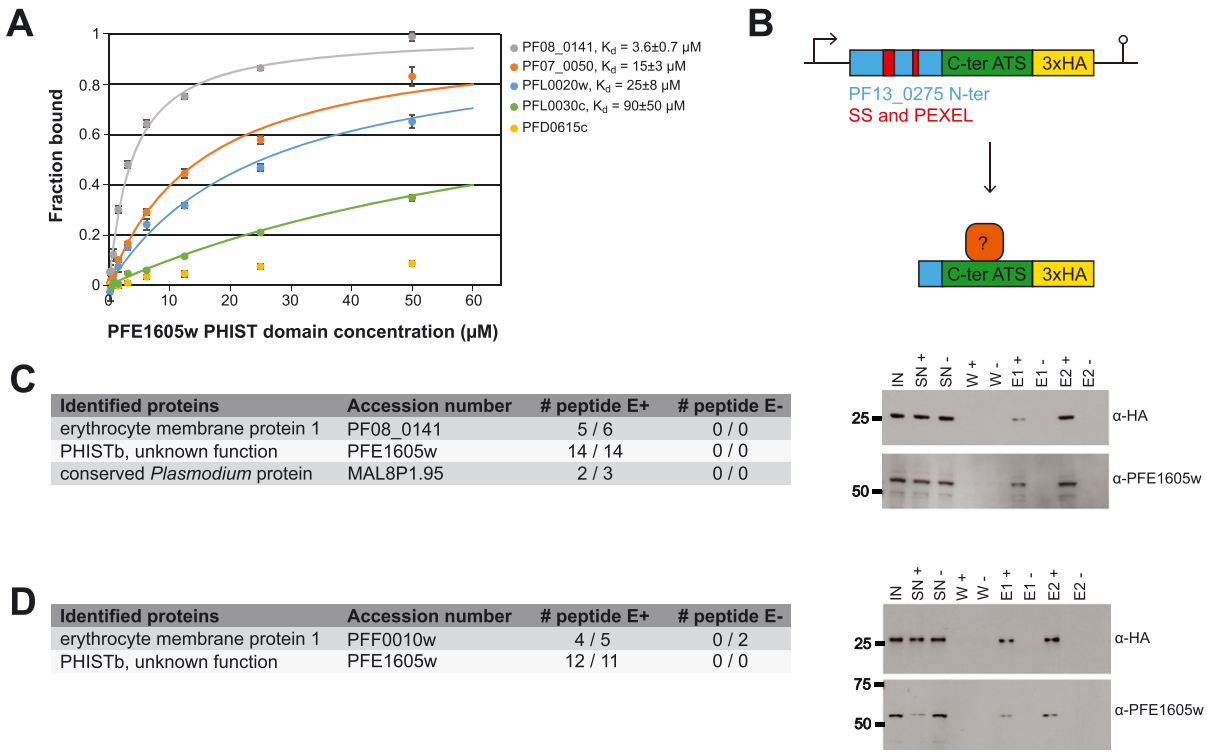

C

Identified proteins	Accession number	# peptide E+	# peptide E-
erythrocyte membrane protein 1	PF08_0141	5 / 6	0 / 0
PHISTb, unknown function	PFE1605w	14 / 14	0 / 0
conserved *Plasmodium* protein	MAL8P1.95	2 / 3	0 / 0

D

Identified proteins	Accession number	# peptide E+	# peptide E-
erythrocyte membrane protein 1	PFF0010w	4 / 5	0 / 2
PHISTb, unknown function	PFE1605w	12 / 11	0 / 0

Fig. 5. PFE1605w directly binds the ATS C-terminus.
A. Fluorescence polarization titrations of 5-FAM-labelled ATS-C constructs from PfEMP1 variants (Fig. S4A) with unlabelled PFE1605w PHIST domain. Data points, normalized to the fraction of ATS-C bound at each PFE1605w concentration, are shown as coloured circles. The error bars were derived from four technical replicates. The solid lines correspond to data fitted with a single-site association model. Equilibrium dissociation constants (K_d) for the PFE1605w–ATS-C interaction are shown. The interaction of PfEMP1 variant PFD0615c with PFE1605w could not be fitted.
B. Schematic representation of the mini-PfEMP1 construct for Co-IP experiments. C and D. LC-ESI-MS/MS results of two independent Co-IP experiments using parasites expressing mini-PfEMP1 constructs composed of the C-terminal part of PF08_0141 (C) or PFF0010w (D). Only peptide hits detected in both of the duplicate experiments are shown. Samples were also analysed by Western blot with α-HA and α-PFE1605w antibodies. IN, input; SN, supernatant; W, wash; E, elution.

interacting proteins through an hemagglutinin (HA)-affinity matrix. As a negative control, parasite extract with an excess of soluble HA peptide was added during the affinity-matrix binding of the mini-PfEMP1 fusion proteins. Western blot analysis confirmed that the mini-PfEMP1 fusion proteins were successfully purified and that PFE1605w was coeluted with both mini-PfEMP1 constructs (Fig. 5C and D). In addition, from duplicate Co-IP experiments, the liquid chromatography–mass spectrometry (LC-MS)/MS analysis detected from both mini-PfEMP1 constructs more than 10 peptide hits for PFE1605w (Fig. 5C and D). These results demonstrate a direct protein–protein interaction of PFE1605w with the C-terminal part of the ATS domain of different PfEMP1 variants.

Potential PFE1605w interaction partners

To detect other potential PFE1605w interaction partners, we performed Co-IP experiments with parasites expressing the PFE1605w–3xHA fusion protein, followed by MS-based protein identification. Different components of the human erythrocyte cytoskeleton were detected, in addition to two *Plasmodium* proteins of unknown function (Fig. 6A).

To confirm these potential PFE1605w interaction partners from the human cytoskeleton, we performed reverse Co-IP experiments with 3D7 wild-type parasite lysate and specific antibodies against human bands 3 and 4.2, both of which locate equally at band 3 and junctional complexes (Mankelow *et al.*, 2012), and ankyrin 1. From the elution of reverse Co-IP with antibodies against human band 4.2, Western blots detected a dominant band, identified as PFE1605w (Fig. 6C). MS identified other components of band 3 and junctional complexes, including band 3, band 4.2, band 4.1, the α- and β-chains of spectrin and ankyrin, but no other *Plasmodium* protein except PFE1605w (Fig. 6B), again suggesting that PFE1605w interacts with one or several cytoskeletal components.

A

Identified proteins	Accession number	# peptide E+	# peptide E-
PHISTb, unknown function	PFE1605w	8 / 9	0 / 2
conserved *Plasmodium* protein	MAL8P1.95	2 / 2	0 / 0
conserved *Plasmodium* protein	PF08_0091	2	0
erythrocyte band 3	B3AT_HUMAN	3	0
ankyrin 1	ANK1_HUMAN	2	0
erythrocyte band 4.2 isoform 1	EPB42_HUMAN	2	0
erythrocyte band 7	STOM_HUMAN	2	0

B

Identified proteins	Accession number	# peptide E+	# peptide E-
spectrin alpha chain	SPTA1_HUMAN	272 / 225	10 / 3
spectrin beta chain	SPTB1_HUMAN	238 / 208	9 / 2
ankyrin 1	ANK1_HUMAN	141 / 124	29 / 10
erythrocyte band 4.2 isoform 1	EPB42_HUMAN	56 / 50	13 / 5
erythrocyte band 4.1	41_HUMAN	55 / 47	4 / 0
erythrocyte band 3	B3AT_HUMAN	50 / 45	19 / 17
erythrocyte band 7	STOM_HUMAN	24 / 23	4 / 3
PHISTb, unknown function	PFE1605w	20 / 13	0 / 2
erythroid membrane-as. protein	ERMAP_HUMAN	9 / 8	0 / 0

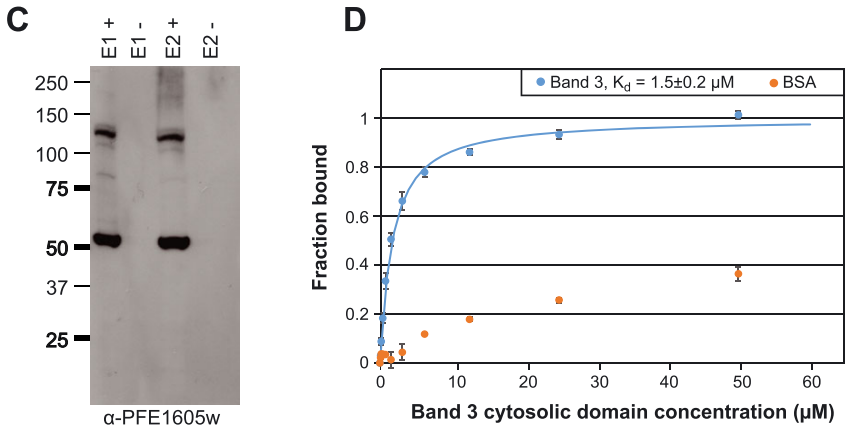

Fig. 6. PFE1605w binds to the RBC cytoskeleton.
A. LC-ESI-MS/MS results of two independent Co-IP experiments using parasites expressing PFE1605w-HA.
B. LC-ESI-MS/MS results of two independent reverse Co-IP experiments with α-band 4.2 antibodies coupled to protein G Dynabeads. All experiments were performed twice.
C. Elution fractions of the reverse Co-IP experiment were also analysed by Western blot with α-PFE1605w antibodies.
D. Fluorescence polarization titrations of 5-FAM-labelled PFE1605w-C with unlabelled band 3 cytosolic domain or BSA as a negative control. Data points, normalized to the fraction of PFE1605w-C bound at each titrant concentration, are shown as coloured circles. The error bars were derived from three replicates. The fit to a single-site association model is shown as solid line. The interaction of PFE1605w-C with BSA could not be fitted.

To further probe the cytoskeletal interactions of PFE1605w, we produced a fluorescein-labelled recombinant PFE1605w fragment (PFE1605w-C) comprising the C-terminal tail of this protein that follows the PHIST domain. PFE1605w-C was previously shown to bind to inside-out vesicles prepared from uninfected erythrocytes (Proellocks *et al*., 2014). In the fluorescence–polarization binding experiments, PFE1605w-C interacted with recombinant band 3 with approximately 1.5 μM K_d (Fig. 6D). This result demonstrates the direct interaction of PFE1605w with a specific cytoskeletal protein, although we do not exclude the possibility that PFE1605w partakes in a larger multiprotein complex.

Discussion

The remarkable number of exported PHIST proteins predicted and the dramatic lineage-specific proliferation of this multigene family in *P. falciparum* only (Sargeant *et al*., 2006) suggest an important role for PHIST proteins in host cell modifications. These modifications lead to the dramatic morbidity and mortality observed with this parasite. This observation is reflected in the number of recent publications showing that PHIST proteins are involved in altering host cell rigidity (Mills *et al*., 2007; Maier *et al*., 2008), binding erythrocyte components (Silva *et al*., 2005; Mills *et al*., 2007; Pei *et al*., 2007a; Parish *et al*., 2013; Proellocks *et al*., 2014), reducing cytoadherence under flow (Maier *et al*., 2008; Proellocks *et al*., 2014), mediating cell–cell communication (Regev-Rudzki *et al*., 2013), cytoskeletal association (Tarr *et al*., 2014) and elevated transcript levels of some *phist* genes in patients (Daily *et al*., 2005; Mok *et al*., 2007; Claessens *et al*., 2012). Although it has been assumed that most PHIST proteins contain one or more interaction epitopes (Sargeant *et al*., 2006), to the best of our knowledge, no detailed characterization of protein interactions directly linked to the functional role of a PHIST protein has been reported.

Here, we have functionally characterized PFE1605w, which has been shown to bind to the ATS domain of PfEMP1, comigrates with PfEMP1 in space and time and localizes to Maurer's clefts and knobs (Oberli *et al*., 2014), although an alternative localization has been suggested (Proellocks *et al*., 2014). In addition to the well-known and frequently used conditional post-translational regulation using an FKBP DD, we applied a 'knock-sideways' or 'anchor-away' system (Haruki *et al*., 2008; Busch *et al*., 2009; Robinson *et al*., 2010; Xu *et al*., 2010). With this method, we took advantage of the rapalog-induced heterodimerization of the FKBP12 and FRB domains to tether PFE1605w at Maurer's clefts, the transient location for a variety of parasite proteins destined to the iRBC membrane and surface. The tethering technique is a powerful way of revealing the function of an exported protein in host cell refurbishment and helps to dissect the role of these proteins within the export pathway. Both methods, tethering of PFE1605w at Maurer's clefts and protein destabilization, confirmed that mislocalization or depletion of PFE1605w did not result in reduced surface exposed PfEMP1, suggesting no obvious role for PFE1605w in PfEMP1 transport. At the same time, however, both methods of PFE1605w depletion from knobs resulted in large reduction of cytoadherence to CD36.

The different levels of reduction in parasite cytoadherence to specific endothelial receptors upon PFE1605w depletion suggest a highly specialized role for this protein. Previously, we tested six PfEMP1 ATS variants for binding the PHIST domain of PFE1605w (Oberli *et al*., 2014) and revealed up to 25-fold differences in binding affinities. This suggests that sequence variation in ATS has optimized PFE1605w for binding to a PfEMP1 subset and that perhaps other PHIST proteins might have coevolved with specific ATS domains to create interaction pairs with maximum binding strength. In this simplified model, differences in the PFE1605w–ATS binding affinity might be expected to account for differences in the cytoadherence phenotype upon PFE1605w depletion.

Our assays partly support this model of PFE1605w function, as evidenced by the lack of an effect of PFE1605w depletion on cytoadherence observed for CSA-binding parasites, where the ATS-C fragment of the dominantly expressed PfEMP1 variant (PFL0030c, VAR2CSA) had a very weak binding affinity to the PFE1605w PHIST domain ($K_d \sim 90$ μM). In contrast, the ATS-C fragments of PfEMP1 variants most often found in ICAM-1-binding parasites, PF07_0050 and PFL0020w, have up to sixfold higher PFE1605w affinity, and ICAM-1 parasite cytoadherence is reduced by 30% upon PFE1605w depletion.

The complete picture, however, is more nuanced. Co-IP assays coupled with MS robustly detected the *in vivo* association of PFE1605w with two mini-PfEMP1 constructs encompassing the ATS-C fragment of two PfEMP1 variants. These variants represent the two main subtypes of PfEMP1 ATS, groups A (PF08_0141) and B (PFF0010w). The *in vitro* affinity of these ATS domains for the PFE1605w PHIST, however, varies by more than 10-fold. We also observed that the ATS-C fragment of the PfEMP1 variant dominantly expressed in CD36-binding parasites, PFD0615c, displays essentially no direct affinity for PFE1605w, despite the large decrease in CD36 cytoadherence upon PFE1605w depletion. The result seems to contradict the simple PFE1605w functional model presented above.

To reconcile these results, we must consider the following: PFE1605w directly binds the majority of ATS

domains tested here and in previous studies (Oberli *et al.*, 2014). This interaction is present *in vivo* for both strongly and weakly associated PFE1605w–ATS pairs. PFE1605w does not affect PfEMP1 transport and it colocalizes to knobs with PfEMP1 (Oberli *et al.*, 2014). Indeed, the significant reduction in receptor binding upon tethering PFE1605w to Maurer's clefts strongly indicates that this protein exercises its functional role in knobs. There, PFE1605w is likely to be joined by (and might act together with) other ATS-binding PHIST proteins such as PFI1780w (Mayer *et al.*, 2012; Oberli *et al.*, 2014), thereby accounting for the partial disruption of cytoadherence upon PFE1605w depletion. Further, in certain PfEMP1 variants, such as the CD36-binding PFD0615c, the PFE1605w–ATS interaction might be mediated or strongly reinforced by other PHIST proteins. Because most of the PHIST proteins are expressed simultaneously, it seems that partnering must occur in the cytosol of the host or directly at the periphery (Fig. 7). Transcriptome analyses of all selected cell lines grown with or without shield excluded a possible upregulation of certain PHIST (data not shown).

To date, only a few direct interactions of exported proteins with cytoskeletal components of erythrocytes have been described and confirmed, e.g. KAHRP (Pei *et al.*, 2005; Weng *et al.*, 2014), PfEMP3 (Pei *et al.*, 2007b), RESA (Pei *et al.*, 2007a) and MESA (Magowan *et al.*, 2000). Both KAHRP and PfEMP3 are required for correct trafficking and functional PfEMP1 display on the erythrocyte surface (Crabb *et al.*, 1997; Waterkeyn *et al.*, 2000), while PFE1605w is not. Co-IP experiments with the full-length PFE1605w–HA fusion protein identified a number of host integral membrane proteins and components of the erythrocyte cytoskeleton as putative binders, and fluorescence polarization experiments confirmed the direct interaction of the PFE1605w C-terminus with the cytosolic domain of band 3. Thus, we have now shown the presence of two interaction epitopes within PFE1605w, at its PHIST domain and the C-terminus, making it an anchoring molecule between PfEMP1 and the host cytoskeleton. The findings are consistent with previous assays suggesting an association of PFE1605w C-terminal fragments with erythrocyte-derived inside-out vesicles (Proellocks *et al.*, 2014). Both co-IP and *in vitro* experiments suggest that PFE1605w, and thus PfEMP1, targets the host's band 3 and junctional complexes, while, interestingly, PFE1605w was the only parasite protein detected. The next step would be to map the exact interaction epitopes of PFE1605w with band 3 and possibly other cytoskeletal proteins. In addition to eluci-

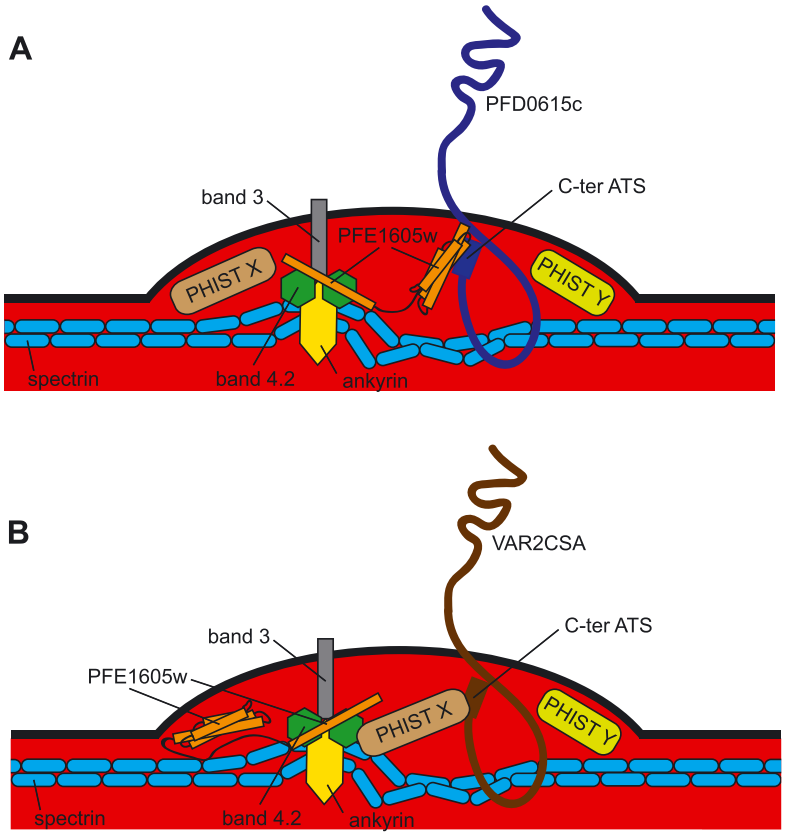

Fig. 7. Schematic representation of the proposed functional role of PFE1605w within the iRBC knob structure.
A. Both Co-IP experiments and *in vivo* experiments showed that the PHIST domain of PFE1605w binds the C-terminal part of different ATS domains and the C-terminal part of PFE1605w targets the host band 3 and junctional complexes, thus making it an anchoring molecule between PfEMP1 and the host cytoskeleton.
B. As various PHIST domains interacted with the same PfEMP1 epitope but with different affinities, it is conceivable that another PHIST protein might take over the function of PFE1605w depending on the surface exposed PfEMP1 molecule.

dating the complex that anchors PfEMP1 to the cytoskeleton, it would be valuable to study whether other PHIST proteins might bind PfEMP1 variants, in particular VAR2CSA, where CSA cytoadherence was not reduced upon depletion of PFE1605w. The PHIST interactome invites further studies to fully understand the remodelling of the host cell leading to pathology.

In summary, we show that the PHIST protein PFE1605w binds not only to PfEMP1 but also to members of band 3 and junctional complexes of the host cell. PFE1605w, however, plays no role in the transport of PfEMP1. We also show that various PfEMP1 molecules interact differently with PFE1605w and binding to endothelial receptors is partially disrupted upon conditional knock-down or misplacement of PFE1605w. A profound analysis of other exported PHIST proteins and their interaction partners should help to reveal key components of the cytoadherence complex.

Experimental procedures

Parasite culture and transfection

Plasmodium falciparum 3D7 cell culture and transfection were performed according to standard procedures (Ljungström *et al*., 2008). Transfected parasites were grown in the presence of the indicated combinations of 10 nM WR99210 (Jacobs Pharmaceuticals, Cologne, Germany), 2.5 mg ml^{-1} blasticidin (Life Technologies, Zug, Switzerland), 625 nM Shield-1 and 100 nM A/C Heterodimerizer (Clontech).

Plasmid constructs

Primers 5′-ATTTGGATCCATGAGGTTTACTAATTCATTATATTCG-3′ and 5′-ATATGCTAGCATTTTTTTTTTTATTTTCTTTTCCAGA TTTG-3′ were used to clone full-length PFE1605w into pBcamR–3xHA (Flueck *et al*., 2009) via BamHI and NheI restriction sites. To fuse the FKBP DD to the C-terminus of PFE1605w in 3D7 wild-type parasites, a 785 bp flank of the 3′ end of PFE1605w was cloned into pARL-DD via BglII and AvrII restriction sites by using the primers 5′-ATATAGATCTTAACAGCAAATAGATTTT TATGGAG-3′ and 5′-ATATCCTAGGATTTTTTTTTTTATTTTCTTTTCCAGATTTG-3′. MAHRP1 was cloned into mal7–mCherry–FRB (kindly provided by Tobias Spielmann (Grüring *et al*., 2011)) via XhoI and KpnI restriction sites by using the primers 5′-ATATCTCGAGATGGCAGAGCAA GCAGC-3′ and 5′-CAGCGGTA CCATTATCTTTTTTTTCTTGTT CTAATTTTGC-3′. Mini-PfEMP1 constructs were synthesized (Fig. S4B) and cloned into pBcamR-3xHA via NcoI and NheI restriction sites.

Western blot analysis

Parasite proteins were obtained as previously described (Oberli *et al*., 2014), and samples were run on 12% w/v polyacrylamide bis-Tris, 4–12% w/v polyacrylamide bis-Tris or 3–8% w/v polyacrylamide Tris-acetate NuPAGE gels (Invitrogen). Proteins were detected by using rabbit antibodies directed against the PFE1605w PHIST domain (α-PFE1605w) (Pacific Immunology Inc.) (Fig. S1B), rabbit α-HA (Roche 1:100), mouse α-glyceraldehyde-3-phosphate dehydrogenase (α-GAPDH) (1:20 000), rat α-mCherry (Life Technologies; 1:1000) and mouse α-ATS (1:500). PfEMP1 was extracted as described (Van Schravendijk *et al*., 1993) and detected with the mouse α-ATS (1:500) antibody.

Southern blot analysis

Genomic DNA of saponin-lysed parasites was isolated as previously described (Beck, 2002). DNA was digested with AflII and XhoI restriction enzymes (New England Biolabs), separated on a 0.8% w/v agarose gel and transferred to a Amersham Hybond–N$^+$ membrane (GE Healthcare). The blot was probed with [^{32}P]-dATP-labelled h*dhfr* PCR fragments.

Fluorescence microscopy

Immunofluorescence assays were performed on acetone-fixed blood smears of infected parasite cultures (Spielmann *et al*., 2003) and blocked with 3% v/w BSA. Primary antibodies included rabbit α-PFE1605w (1:200), mouse α-KAHRP (1:200), mouse α-RESA (1:250), rabbit α-MESA (1:250), mouse α-ATS (1:100), mouse α-PfEMP3 (1:100), rabbit α-MAHRP1 (1:200), rabbit α-HSP70x (1:500) and rat α-mCherry (Life Technologies; 1:200). Secondary antibodies (goat α-rabbit Alexa 594, goat α-mouse Alexa 594, goat α-rabbit Alexa 488, goat α-rat Alexa 594; Invitrogen) were incubated with 1 μg ml^{-1} 4,6-diamidino-2-phenylindole (DAPI; Roche) at 1:200 dilution. Images were taken with a Zeiss LSM 700 confocal microscope (Carl Zeiss GmbH, Jena, Germany), with ×63 oil-immersion lens (1.4 numerical aperture) and processed in PHOTOSHOP CS6.

Scanning electron microscopy

After knob selection and Percoll purification, the erythrocytes/iRBCs were fixed in 2% v/v glutaraldehyde in phosphate buffer for 1 h at room temperature. After three washes in PBS, the samples were transferred to coverslips preliminary coated with poly-L-lysine (Sigma), dehydrated in increasing concentration of ethanol (10% v/v, 25% v/v, 50% v/v, 75% v/v, 90% v/v and 2× 100% v/v, 10 min each) and dried at the critical point. Finally, coverslips were mounted onto stubs, sputtered with 5 nm platinum (LEICA EM ACE600) and imaged at 5 kV with a SEM Versa 3D (FEI). The micrographs were coloured in PHOTOSHOP CS6.

Trypsin cleavage assay

For trypsin cleavage, Percoll-purified trophozoite stage parasites were incubated either in L-(tosylamido-2-phenyl) ethyl chloromethyl ketone-treated trypsin (Sigma, 100 μg ml^{-1} in PBS) or in trypsin and 1 mg ml^{-1} soybean trypsin inhibitor (Sigma, 1 mg ml^{-1} in PBS) for 15 min at 37°C. The digest was stopped by the addition of soybean trypsin inhibitor to a final concentration of 1 mg ml^{-1}. PfEMP1 extraction and subsequent analysis was done as previously described (Van Schravendijk *et al*., 1993; Waterkeyn *et al*., 2000).

Selection for receptor binding with recombinant protein

Subpopulations of parasites were selected by panning the parental parasite cell line (3D7) over purified human recombinant CD36 (50 μg ml^{-1}), CD31 (50 μg ml^{-1}), ICAM-1 (50 μg ml^{-1}), Thrombospondin-1 (50 μg ml^{-1}), endothelial protein C receptor (50 μg ml^{-1}) and CSA (20 μg ml^{-1}) according to Ockenhouse *et al*. (1991). Recombinant proteins were dissolved in double-distilled H_2O to the indicated final concentration and absorbed to a six-well tissue culture plate (Falcon 353045, Corning, NY, USA) overnight at 4°C. The wells were blocked with 1% w/v BSA in RPMI medium for 1 h at 37°C. and the parasite culture was added for 2 h with a gentle shake of the tissue culture plate every 15 min. Unbound parasites were removed by five gentle washes with RPMI-Hepes and uninfected RBCs (5% haematocrit) were added. After 24 h of incubation allowing late-stage parasites to release merozoites to invade new RBCs, the newly invaded RBCs were transferred into continuous cell culture. The panning procedure was repeated four times prior to RNA isolation and cytoadhesion assays.

Cytoadhesion assay

Purified recombinant protein was spotted on wells of an eight-chamber polystyrene vessel tissue culture-treated glass slide (Falcon, Big Flats, NY, USA) with concentrations as indicated and coated overnight at 4°C to allow proteins to absorb to the surface. The wells were blocked with 1% w/v BSA in RPMI medium for 1 h at 37°C. Selected parasite cell lines were split and cultured separately with or without 500 nM Shield-1 for 96 h. Parasites were washed twice with RPMI-Hepes and spotted onto immobilized recombinant protein and cultured for 2 h under continuous and simultaneous shaking (140 r.p.m., proBlot 25 Rocker; Labnet International Inc., NY, USA) (105 r.p.m., Lab-Therm LT-W, Kühner, Switzerland) at 37°C. Non-bound erythrocytes were removed by gently flooding each well with RPMI-Hepes six times with simultaneous shaking for 2 min. Bound iRBCs were fixed with 2% v/v glutaraldehyde in RPMI-Hepes overnight and stained with Giemsa for 1 h and microscopically quantified. Results are shown as mean number of parasites bound per square millimetre and normalized to 1% parasitaemia.

Quantitative PCR for P. falciparum *erythrocyte membrane protein 1 expression*

Synchronized cultures of PFE1605w–DD expressing parasites preselected to bind CD36, ICAM-1 or CSA were split and cultured 96 h in the presence (+) or absence (−) of Shield-1, and ring-stage parasites were used for *var* transcript profiling, as previously described (Dahlbäck *et al*., 2007). Transcript abundance of each 3D7 *var* gene was determined relative to internal control transcripts by qPCR by using gene-specific primers and complementary DNA synthesized from total RNA extracted from pelleted infected erythrocytes dissolved in TRIzol.

Recombinant protein expression

Codon-optimized genes encoding the ATS-C fragments of PfEMP1 variants (Fig. S4A) were cloned in a modified pET-16 vector (Merc Millipore). Gene fragments coding for amino acids 300–528 of PFE1605w (PFE1605w-C) or amino acids 1–379 of human erythrocytic band 3 were cloned in a pFloat2 vector (Rogala *et al*., 2015), which provides an N-terminal His_6 tag.

Purification and fluorescent labelling of ATS-C and PFE1605w-C was performed as previously described (Mayer *et al*., 2012); briefly, clones were transformed in *Escherichia coli* strain BL21 (DE3), grown in Luria–Bertani medium and protein expression was induced with 0.1 mM isopropyl β-D-1-thiogalactopyranoside. Cells were lysed by sonication, and proteins were purified from lysate supernatants by using metal-affinity, ion-exchange and size-exclusion chromatography. Fluorescent labelling was performed by *N*-(5-fluoresceinyl)maleimide (5-FAM; Invitrogen) conjugating to a single cysteine residue at the protein N-terminus that was added during cloning. Labelled ATS-C and unreacted dye were separated by size-exclusion chromatography. Protein identity and 5-FAM labelling was confirmed by electrospray ionisation (ESI) MS.

Purification of the PFE1605w PHIST domain and the cytosolic band 3 domain was performed as previously described (Zhang *et al*., 2000; Oberli *et al*., 2014).

Fluorescence polarization binding assays

Fluorescence polarization measurements were recorded at 20°C by using a CLARIOStar fluorimeter (BMG Labtech; λ_{ex} = 485 nm, λ_{em} = 520 nm). Five hundred nanomolar 5-FAM-labelled ATS-C variants in 50 mM NaCl, 20 mM Na_2HPO_4 pH 6.5 buffer were titrated with defined concentrations of PFE1605w PHIST domain in the same buffer. For the band 3–PFE1605w-C interaction, 0.5 μM 5-FAM-labelled PFE1605w-C in 50 mM NaCl, 20 mM Na_2HPO_4 pH 7.0 buffer was titrated with unlabelled band 3. Changes in fluorescence polarization were fitted by using a single binding model in the program ORIGIN (OriginLab).

Coimmunoprecipitation experiments

Three hundred millilitres of cell culture (5% haematocrit, 5-8% parasitaemia) of 3D7 parasites or 3D7 parasites episomally expressing PFE1605w–3xHA/mini-PfEMP1 was cross-linked in 1% v/v formaldehyde. The reaction was stopped after 10 min by adding 2.5 M glycine. Immunoprecipitation was performed as previously described (Dietz *et al*., 2014). For the Co-IP experiments with the mini-PfEMP1 fusion protein, Pierce α-HA magnetic beads (Thermo Scientific) were used. For the reverse Co-IP with α-band 4.2 antibodies, Dynabeads Protein G were used together with the cross-linking reagent BS3 to avoid coelution of antibodies, according to the manufacturer's protocol (Life Technologies). The eluted fraction was analysed on a 4–12% w/v polyacrylamide bis-Tris gel (Invitrogen) and fractions of it or TCA precipitated pellets were sent to the central core facility for LC-MS/MS analysis.

Acknowledgements

The authors are grateful to Tobias Spielmann for sharing the mal7–mCherry–FRB vector. We would like to thank the following colleagues for sharing antibodies: Brian Cooke (anti-ATS), Claudia Daubenberger (anti-GAPDH), Jude Przyborski (anti-HSP70x), Diane Taylor (anti-KAHRP), Ross Coppel (anti-MESA) and Alex Maier (anti-PfEMP3). We thank Henning Stahlberg and his team at the C-CINA and the Image Core Facility, Biozentrum, University of Basel, for the access and support for confocal and electron microscopy work and David Stanton for maintenance of the Oxford Biochemistry biophysics facility. We are grateful to Dirk Reiter for assistance with experiments.

This work was supported by the Swiss National Science Foundation (http://www.snf.ch) (Grant 31003A_149297/1 to HPB), the Wellcome Trust (http://www.wellcome.ac.uk) (RCD fellowship 088497/Z/09/Z to IV and PhD studentship to JLD and EEC) as well as by the Lundbeck Foundation (http://www.lundbeckfoundation.com) and the Danish Council for Independent Research, Medical Sciences, Sapere Aude program (http://ufm.dk/en/research-and-innovation/councils-and-commissions/the-danish-council-for-independent-research) (DFF–4004-00624B to TL). The funders had no role in the study design, data collection and analysis, the decision to publish or the preparation of the manuscript.

Conflict of interest

The authors declare no conflict of interest.

Author contributions

AO, LZ and SR performed the cell biological experiments; FB performed the electron microscopy experiments; MEB, JLD and EEC performed the biophysical interaction experiments; TL analysed the *var* gene expression and AO, JV and HPB conceived the experiments and wrote the paper.

References

Armstrong, C.M., and Goldberg, D.E. (2007) An FKBP destabilization domain modulates protein levels in *Plasmodium falciparum*. *Nat Methods* **4**: 1007–1009.

Banaszynski, L.A., Chen, L., Maynard-Smith, L.A., Ooi, A.G.L., and Wandless, T.J. (2006) A rapid, reversible, and tunable method to regulate protein function in living cells using synthetic small molecules. *Cell* **126**: 995–1004.

Beck, H.-P. (2002) Extraction and purification of plasmodium pDNA. In *Malaria Methods and Protocols*. Doolan, D. (ed). Totowa, New Jersey: Humana Press, pp. 159–163.

Busch, A., Kiel, T., and Hübner, S. (2009) Quantification of nuclear protein transport using induced heterodimerization. *Traffic* **10**: 1221–1227.

Claessens, A., Adams, Y., Ghumra, A., Lindergard, G., Buchan, C.C., Andisi, C., *et al.* (2012) A subset of group A-like *var* genes encodes the malaria parasite ligands for binding to human brain endothelial cells. *Proc Natl Acad Sci* **109**: E1772–E1781.

Crabb, B.S., Cooke, B.M., Reeder, J.C., Waller, R.F., Caruana, S.R., Davern, K.M., *et al.* (1997) Targeted gene disruption shows that knobs enable malaria-infected red cells to cytoadhere under physiological shear stress. *Cell* **89**: 287–296.

Dahlbäck, M., Lavstsen, T., Salanti, A., Hviid, L., Arnot, D.E., Theander, T.G., and Nielsen, M.A. (2007) Changes in *var* gene mRNA levels during erythrocytic development in two phenotypically distinct *Plasmodium falciparum* parasites. *Malar J* **6**: 78.

Daily, J.P., Le Roch, K.G., Sarr, O., Ndiaye, D., Lukens, A., Zhou, Y., *et al.* (2005) In vivo transcriptome of *Plasmodium falciparum* reveals overexpression of transcripts that encode surface proteins. *J Infect Dis* **191**: 1196–1203.

Dietz, O., Rusch, S., Brand, F., Mundwiler-Pachlatko, E., Gaida, A., Voss, T., and Beck, H.-P. (2014) Characterization of the small exported *Plasmodium falciparum* membrane protein SEMP1. *PLoS One* **9** e103272.

Flueck, C., Bartfai, R., Volz, J., Niederwieser, I., Salcedo-Amaya, A.M., Alako, B.T.F., *et al.* (2009) *Plasmodium falciparum* heterochromatin protein 1 marks genomic loci linked to phenotypic variation of exported virulence factors. *PLoS Pathog* **5** e1000569.

Frech, C., and Chen, N. (2013) Variant surface antigens of malaria parasites: functional and evolutionary insights from comparative gene family classification and analysis. *BMC Genomics* **14**: 427.

Grüring, C., Heiber, A., Kruse, F., Ungefehr, J., Gilberger, T.-W., and Spielmann, T. (2011) Development and host cell modifications of *Plasmodium falciparum* blood stages in four dimensions. *Nat Commun* **2**: 165.

Haruki, H., Nishikawa, J., and Laemmli, U.K. (2008) The anchor-away technique: rapid, conditional establishment of yeast mutant phenotypes. *Mol Cell* **31**: 925–932.

Heiber, A., Kruse, F., Pick, C., Grüring, C., Flemming, S., Oberli, A., *et al.* (2013) Identification of new PNEPs indicates a substantial non-PEXEL exportome and underpins common features in *Plasmodium falciparum* protein export. *PLoS Pathog* **9** e1003546.

Hiller, N.L., Bhattacharjee, S., van Ooij, C., Liolios, K., Harrison, T., Lopez-Estrano, C., and Haldar, K. (2004) A host-targeting signal in virulence proteins reveals a secretome in malarial infection. *Science* **306**: 1934–1937.

Ljungström, I., Moll, K., Perlmann, H., Scherf, A., and Wahlgren, M. (2008). Methods in malaria research (MR4/ATCC).

Kilejian, A., Rashid, M.A., Aikawa, M., Aji, T., and Yang, Y.-F. (1991) Selective association of a fragment of the knob protein with spectrin, actin and the red cell membrane. *Mol Biochem Parasitol* **44**: 175–181.

Kilili, G.K., and LaCount, D.J. (2011) An erythrocyte cytoskeleton-binding motif in exported *Plasmodium falciparum* proteins. *Eukaryot Cell* **10**: 1439–1447.

Kraemer, S.M., and Smith, J.D. (2006) A family affair: *var* genes, PfEMP1 binding, and malaria disease. *Curr Opin Microbiol* **9**: 374–380.

Lavstsen, T., Salanti, A., Jensen, A.T., Arnot, D.E., and Theander, T.G. (2003) Sub-grouping of *Plasmodium falciparum* 3D7 *var* genes based on sequence analysis of coding and non-coding regions. *Malar J* **2**: 27.

Magowan, C., Nunomura, W., Waller, K.L., Yeung, J., Liang, J., Van Dort, H., *et al.* (2000) *Plasmodium falciparum* histidine-rich protein 1 associates with the band 3 binding domain of ankyrin in the infected red cell membrane. *Biochim Biophys Acta BBA-Mol Basis Dis* **1502**: 461–470.

Maier, A.G., Rug, M., O'Neill, M.T., Brown, M., Chakravorty, S., Szestak, T., *et al.* (2008) Exported proteins required for virulence and rigidity of *Plasmodium falciparum*-infected human erythrocytes. *Cell* **134**: 48–61.

Mankelow, T.J., Satchwell, T.J., and Burton, N.M. (2012) Refined views of multi-protein complexes in the erythrocyte membrane. *Blood Cells Mol Dis* **49**: 1–10.

Marti, M., Good, R.T., Rug, M., Knuepfer, E., and Cowman, A.F. (2004) Targeting malaria virulence and remodeling proteins to the host erythrocyte. *Science* **306**: 1930–1933.

Mayer, C., Slater, L., Erat, M.C., Konrat, R., and Vakonakis, I. (2012) Structural analysis of the *Plasmodium falciparum* erythrocyte membrane protein 1 (PfEMP1) intracellular domain reveals a conserved interaction epitope. *J Biol Chem* **287**: 7182–7189.

Mills, J.P., Diez-Silva, M., Quinn, D.J., Dao, M., Lang, M.J., Tan, K.S.W., *et al.* (2007) Effect of plasmodial RESA protein on deformability of human red blood cells harboring *Plasmodium falciparum*. *Proc Natl Acad Sci* **104**: 9213–9217.

Mok, B.W., Ribacke, U., Winter, G., Yip, B.H., Tan, C.-S., Fernandez, V., *et al.* (2007) Comparative transcriptomal analysis of isogenic *Plasmodium falciparum* clones of distinct antigenic and adhesive phenotypes. *Mol Biochem Parasitol* **151**: 184–192.

Nguitragool, W., Bokhari, A.A.B., Pillai, A.D., Rayavara, K., Sharma, P., Turpin, B., *et al.* (2011) Malaria parasite *clag3* genes determine channel-mediated nutrient uptake by infected red blood cells. *Cell* **145**: 665–677.

Oakley, M.S.M., Kumar, S., Anantharaman, V., Zheng, H., Mahajan, B., Haynes, J.D., *et al.* (2007) Molecular factors and biochemical pathways induced by febrile temperature in intraerythrocytic *Plasmodium falciparum* parasites. *Infect Immun* **75**: 2012–2025.

Oberli, A., Slater, L.M., Cutts, E., Brand, F., Mundwiler-Pachlatko, E., Rusch, S., *et al.* (2014) A *Plasmodium falciparum* PHIST protein binds the virulence factor PfEMP1 and comigrates to knobs on the host cell surface. *FASEB J* **28**: 4420–4433.

Ockenhouse, C.F., Ho, M., Tandon, N.N., Van Seventer, G.A., Shaw, S., White, N.J., *et al.* (1991) Molecular basis of sequestration in severe and uncomplicated *Plasmodium falciparum* malaria: differential adhesion of infected erythrocytes to CD36 and ICAM-l. *J Infect Dis* **164**: 163–169.

Oh, S.S., Voigt, S., Fisher, D., Yi, S.J., LeRoy, P.J., Derick, L.H., *et al.* (2000) *Plasmodium falciparum* erythrocyte membrane protein 1 is anchored to the actin–spectrin junction and knob-associated histidine-rich protein in the erythrocyte skeleton. *Mol Biochem Parasitol* **108**: 237–247.

Parish, L.A., Mai, D.W., Jones, M.L., Kitson, E.L., and Rayner, J.C. (2013) A member of the *Plasmodium falciparum* PHIST family binds to the erythrocyte cytoskeleton component band 4.1. *Malar J* **12**: 1–9.

Pei, X., An, X., Guo, X., Tarnawski, M., Coppel, R., and Mohandas, N. (2005) Structural and Functional studies of interaction between *Plasmodium falciparum* knob-associated histidine-rich protein (KAHRP) and erythrocyte spectrin. *J Biol Chem* **280**: 31166–31171.

Pei, X., Guo, X., Coppel, R., Bhattacharjee, S., Haldar, K., Gratzer, W., *et al.* (2007a) The ring-infected erythrocyte surface antigen (RESA) of *Plasmodium falciparum* stabilizes spectrin tetramers and suppresses further invasion. *Blood* **110**: 1036–1042.

Pei, X., Guo, X., Coppel, R., Mohandas, N., and An, X. (2007b) *Plasmodium falciparum* erythrocyte membrane protein 3 (PfEMP3) destabilizes erythrocyte membrane skeleton. *J Biol Chem* **282**: 26754–26758.

Proellocks, N.I., Herrmann, S., Buckingham, D.W., Hanssen, E., Hodges, E.K., Elsworth, B., *et al.* (2014) A lysine-rich membrane-associated PHISTb protein involved in alteration of the cytoadhesive properties of *Plasmodium falciparum*-infected red blood cells. *FASEB J* **28**: 3103–3113.

Regev-Rudzki, N., Wilson, D.W., Carvalho, T.G., Sisquella, X., Coleman, B.M., Rug, M., *et al.* (2013) Cell–cell communication between malaria-infected red blood cells via exosome-like vesicles. *Cell* **153**: 1120–1133.

Robinson, M.S., Sahlender, D.A., and Foster, S.D. (2010) Rapid inactivation of proteins by rapamycin-induced rerouting to mitochondria. *Dev Cell* **18**: 324–331.

Rogala, K.B., Dynes, N.J., Hatzopoulos, G.N., Yan, J., Pong, S.K., Robinson, C.V., *et al.* (2015) The *Caenorhabditis elegans* protein SAS-5 forms large oligomeric assemblies critical for centriole formation. *eLife* **4**.

Sanders, P.R. (2005) Distinct protein classes including novel merozoite surface antigens in raft-like membranes of *Plasmodium falciparum*. *J Biol Chem* **280**: 40169–40176.

Sargeant, T.J., Marti, M., Caler, E., Carlton, J.M., Simpson, K., Speed, T.P., and Cowman, A.F. (2006) Lineage-specific expansion of proteins exported to erythrocytes in malaria parasites. *Genome Biol* **7**: R12.

Van Schravendijk, M., Pasloske, B., Baruch, D., Handunnetti, S., and Howard, R. (1993) Immunochemical characterization and differentiation of two approximately 300-kD erythrocyte membrane-associated proteins of *Plasmodium falciparum*, PfEMP1 and PfEMP3. *Am J Trop Med Hyg* **49**: 552–565.

Silva, M.D., Cooke, B.M., Guillotte, M., Buckingham, D.W., Sauzet, J.-P., Scanf, C.L., *et al.* (2005) A role for the *Plasmodium falciparum* RESA protein in resistance against heat shock demonstrated using gene disruption: phenotyping resa-KO *Plasmodium falciparum* parasites. *Mol Microbiol* **56**: 990–1003.

Spielmann, T., Fergusen, D.J., and Beck, H.-P. (2003) etramps, a new *Plasmodium falciparum* gene family coding for developmentally regulated and highly charged membrane proteins located at the parasite–host cell interface. *Mol Biol Cell* **14**: 1529–1544.

Spillman, N.J., Beck, J.R., and Goldberg, D.E. (2015) Protein export into malaria parasite–infected erythrocytes: mechanisms and functional consequences. *Annu Rev Biochem* **84**: 813–841.

Tarr, S.J., Moon, R.W., Hardege, I., and Osborne, A.R. (2014) A conserved domain targets exported PHISTb family proteins to the periphery of *Plasmodium* infected erythrocytes. *Mol Biochem Parasitol* **196**: 29–40.

Waller, K.L., Cooke, B.M., Nunomura, W., Mohandas, N., and Coppel, R.L. (1999) Mapping the binding domains involved in the interaction between the *Plasmodium falciparum* knob-associated histidine-rich protein (KAHRP) and the cytoadherence ligand *P. falciparum* erythrocyte membrane protein 1 (PfEMP1). *J Biol Chem* **274**: 23808–23813.

Waller, K.L., Nunomura, W., Cooke, B.M., Mohandas, N., and Coppel, R.L. (2002) Mapping the domains of the cytoadherence ligand *Plasmodium falciparum* erythrocyte membrane protein 1 (PfEMP1) that bind to the knob-associated histidine-rich protein (KAHRP). *Mol Biochem Parasitol* **119**: 125–129.

Waterkeyn, J.G., Wickham, M.E., Davern, K.M., Cooke, B.M., Coppel, R.L., Reeder, J.C., *et al.* (2000) Targeted mutagenesis of *Plasmodium falciparum* erythrocyte membrane protein 3 (PfEMP3) disrupts cytoadherence of malaria-infected red blood cells. *EMBO J* **19**: 2813–2823.

Watermeyer, J.M., Hale, V.L., Hackett, F., Clare, D.K., Cutts, E.E., Vakonakis, I., *et al.* (2016) A spiral scaffold underlies cytoadherent knobs in *Plasmodium falciparum*-infected erythrocytes. *Blood* **127**: 343–351.

Weng, H., Guo, X., Papoin, J., Wang, J., Coppel, R., Mohandas, N., and An, X. (2014) Interaction of *Plasmodium falciparum* knob-associated histidine-rich protein (KAHRP) with erythrocyte ankyrin R is required for its attachment to the erythrocyte membrane. *Biochim Biophys Acta Biomembr* **1838**: 185–192.

Xu, T., Johnson, C.A., Gestwicki, J.E., and Kumar, A. (2010) Conditionally controlling nuclear trafficking in yeast by chemical-induced protein dimerization. *Nat Protoc* **5**: 1831–1843.

Zhang, D., Kiyatkin, A., Bolin, J.T., and Low, P.S. (2000) Crystallographic structure and functional interpretation of the cytoplasmic domain of erythrocyte membrane band 3. *Blood* **96**: 2925–2933.

Supporting information

Additional Supporting information may be found in the online version of this article at the publisher's web-site:

Fig. S1. Plasmid maps, Southern blot and Western blots of extracts from cell lines used in this study.
Fig. S2. Localization of well-characterized exported proteins upon PFE1605w reduction.
Fig. S3. Reduced levels of PFE1605w do not alter knob formation.
Fig. S4. ATS-C and mini-PfEMP1 constructs.

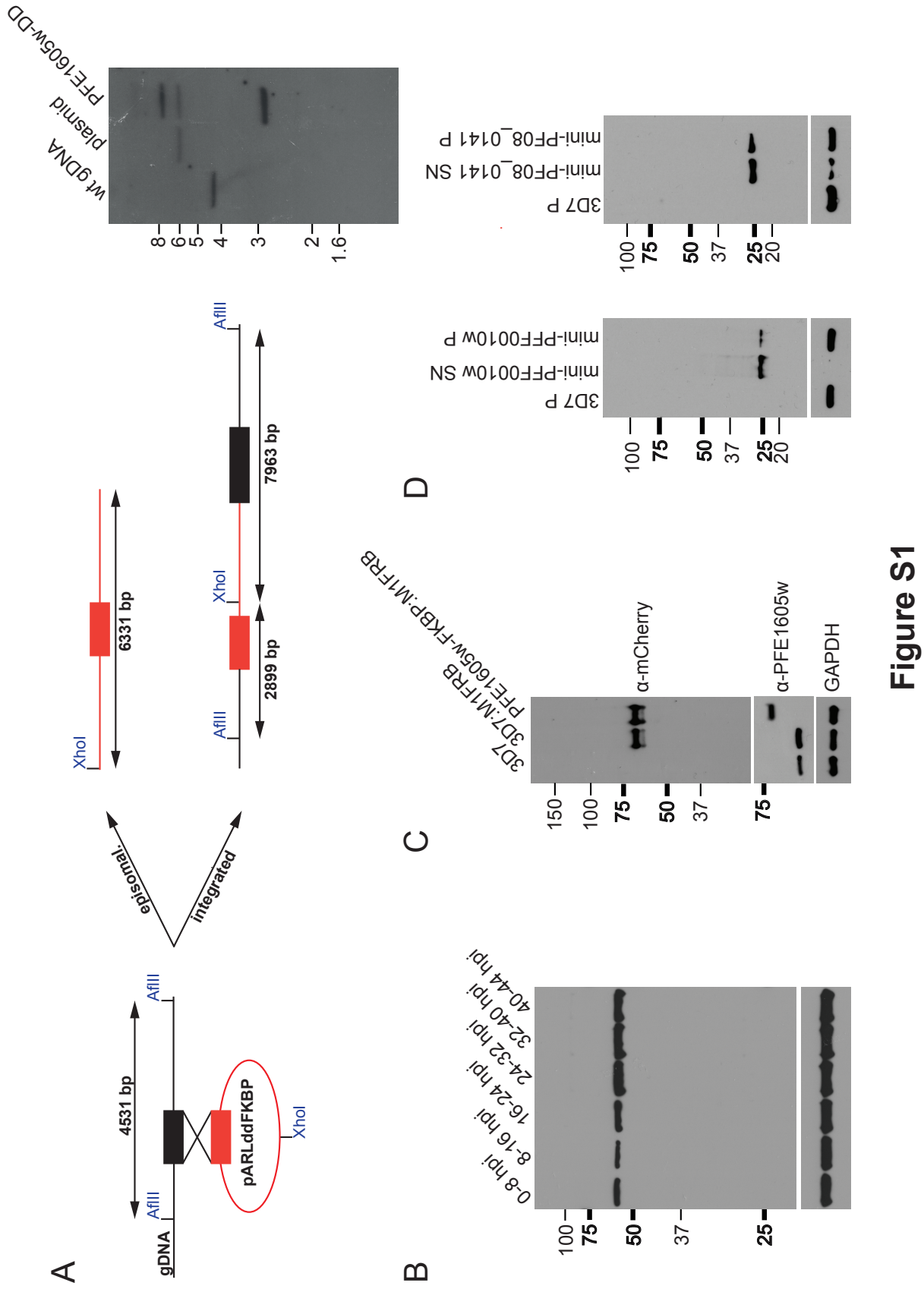
A
gDNA
AflII
AflII
4531 bp
pARLddFKBP
XhoI
episomal
integrated
XhoI
6331 bp
AflII
XhoI
AflII
7963 bp
2899 bp
B
100
75
50
37
25
0-8 hpi
8-16 hpi
16-24 hpi
24-32 hpi
32-40 hpi
40-44 hpi
C
3D7
3D7:M1FRB
PFE1605w-FKBP:M1FRB
150
100
75
50
37
75
α-mCherry
α-PFE1605w
GAPDH
D
100
75
50
37
25
20
3D7 P
mini-PFF0010w SN
mini-PFF0010w P
100
75
50
37
25
20
3D7 P
mini-PFO8_0141 SN
mini-PFO8_0141 P
wt gDNA
plasmid
PFE1605w-DD
8
6
5
4
3
2
1.6

Figure S1

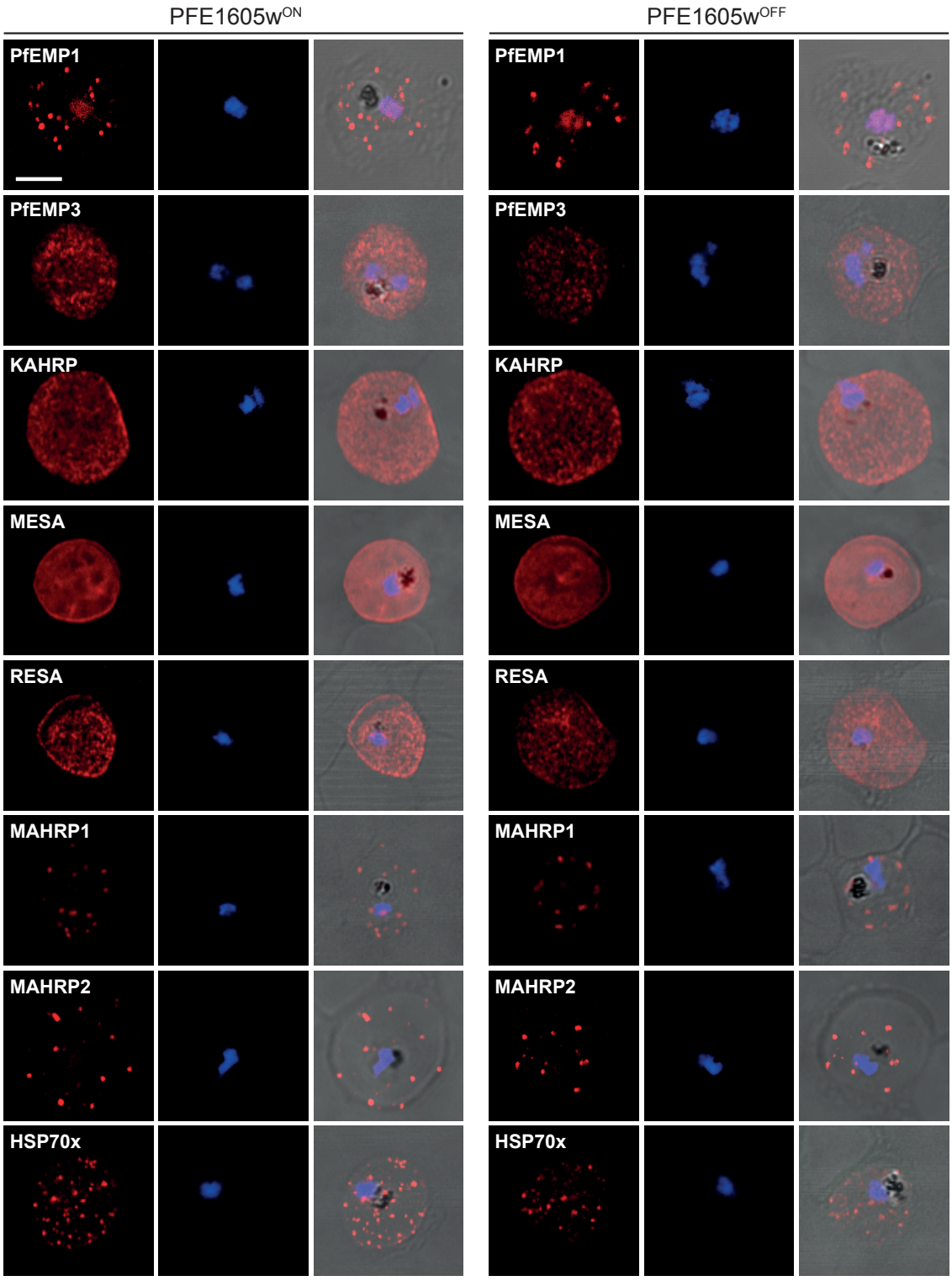
PFE1605w^ON
PFE1605w^OFF
PfEMP1
PfEMP3
KAHRP
MESA
RESA
MAHRP1
MAHRP2
HSP70x

Figure S2

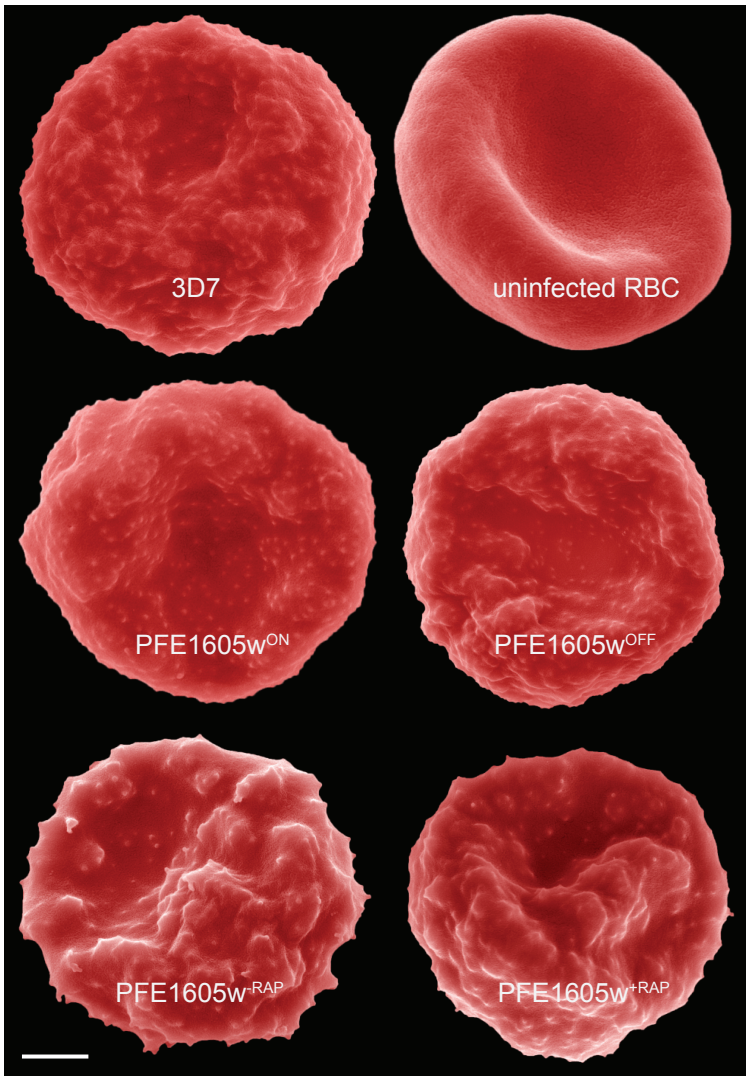
3D7
uninfected RBC
PFE1605w^ON
PFE1605w^OFF
PFE1605w^-RAP
PFE1605w^+RAP

Figure S3

A

ATS-C constructs

PF08_0141
```
  1 GPLGSCNDGG NVPIDNRSLN TDVWIEIDMD DPKGKKEFSN MDTILDDIED DIYYDVNDDE 60
 61 NPSVDNIPMD HNKVDVPKKV HVEMKILNNT SNGSLEPEFP ISDVWNI               107
```

PF07_0050
```
  1 GPLGSCTHSG NTHPSDSNKT LNTDVSIQIH MDDPKPINQF TNMDTILEDL EKYNEPYYDV 60
 61 QDDIYYDVND HDTSTADSNA MDVPSKVQIE MDVNTKLVKE KYPIADVWDI            110
```

PFL0020w
```
  1 GPLGSCTHSG NTHPSDSNKT LNTDVSIQIH MDNPKPINQF TNMDTILEDL EKYNEPYYDV 60
 61 QDDIYYDVND HDASTVDSNN MDVPSKVQIE MDVNTKLVKE KYPIADVWDI            110
```

PFL0030c
```
  1 GPLGSCRKEY LLDIQPSTLD DIHKINDETY NIISTNNIYD HPSQETPLQL LGSTNIIPSY 60
 61 ITTEQNNGLR TNISMDTYID ETNNNNVVAT SIIGDDQMEN SYNS                  104
```

PFD0615c
```
  1 GPLGSCTHSG NKHNGIQSNI PSSDIHPSDI HSGKLSDTPS DNNIHSDIPY VLNSDVSIQI 60
 61 HMDNPKPTNE DNVVDSNPVG NNIYVDNNPN QTFPSNPNPV ENNTYVNAPT NVQIEMDVNN 120
121 HKVVKEKYPI SDMLDI                                               136
```

B

Mini-PfEMP1 constructs

PF08_0141
```
  1 MKTYNSLNNI MGFQGEHNST VPSYNKSSME KSSNIRNNRG RVYSFHFLVK IFACSLFIWT 60
 61 LYVSHNGNVS TNVDVVNTTQ GLSKGRILTQ GDHHEETEDV NHKAHHTGER TSNDGGNVPI 120
121 DNRSLNTDVW IEIDMDDPKG KKEFSNMDTI LDDIEDDIYY DVNDDENPSV DNIPMDHNKV 180
181 DVPKKVHVEM KILNNTSNGS LEPEFPISDV WNI                              213
```

PFF0010w
```
  1 MKTYNSLNNI MGFQGEHNST VPSYNKSSME KSSNIRNNRG RVYSFHFLVK IFACSLFIWT 60
 61 LYVSHNGNVS TNVDVVNTTQ GLSKGRILTQ GDHHEETEDV NHKAHHTGER TSTHSGNTHP 120
121 SDSNKTLNTD VSIQIHMDNP KPINQFTNMD TILEDLEKYN EPYYDVQDDI YYDVNDHDAS 180
181 TVDSNAVNVP SKVQIEMDVN TKLVKEKYPI ADVWDI                          216
```

Figure S4

Figure legends

Figure S1: Plasmid maps, Southern blot and Western blots of extracts from cell lines used in this study

(A) Schematic map of the endogenous *pfe1605w* locus before and after plasmid integration in PFE1605w^{ON} parasites. *Afl*II and *Xho*I restriction sites are indicated in blue and pARLddFKBP vector is indicated in red. Southern blot shows integration into the endogenous *pfe1605w* locus. 3D7 wild-type gDNA was used as a control. (B) Specificity of the polyclonal affinity-purified α-PFE1605w antibody. α-PFE1605w Western blot with extracts from stage-specific 3D7 wild-type parasites (hours post-invasion indicated for each lane). GAPDH was used as a loading control. (C) Western blot of extracts from 3D7 wild-type parasites, 3D7 parasites episomally expressing MAHRP1-FRB fusion protein and of double transfected parasites expressing PFE1605w C-terminally fused to FKBP but also the MAHRP1-FRB fusion protein. Decoration of the same Western blot with α-PFE1605w (different molecular weight is due to the successful integration of the FKBP domain) and α-GAPDH as loading control is shown at the bottom. (D) Western blots of saponin-lysed parasites expressing PF08_0141 and PFF0010w mini-PfEMP1 constructs. SN= supernatant after saponin lysis, P= pellet after saponin lysis.

Figure S2: Localization of well-characterized exported proteins upon PFE1605w reduction

Confocal immunofluorescence analysis of 3D7 parasites expressing endogenous PFE1605w as a C-terminally tagged GFP-DD fusion protein grown for 96 hours in presence (PFE1605w^{ON}) or absence (PFE1605w^{OFF}) of 625 nM Shield-1. Nuclei were stained with DAPI. Scale bar = 3 µm.

Figure S3: Reduced levels of PFE1605w do not alter knob formation

Scanning electron microscopy of an uninfected RBC, an iRBC with a 3D7 wild-type parasite and iRBCs with PFE1605w^{ON}/PFE1605w^{OFF}/PFE1605w^{+RAP}/ PFE1605w^{-RAP} parasites. Scale bar= 1 µm.

Figure S4: ATS-C and mini-PfEMP1 constructs

(A) Protein sequences of ATS-C constructs used in this study. Constructs were cloned in a modified pET16 vector for recombinant expression in *E. coli*, leading to the inclusion of a six amino acid cloning artefact at the construct N-terminus (illustrated in blue) in the final purified material. The ATS-C sequence, derived from the indicated PfEMP1 variant, is illustrated in green. In all cases fluorescent labelling of ATS-C was performed by 5-FAM conjugation to amino acid C6 of each construct. To avoid the inclusion of multiple 5-FAM labels existing cysteines in the ATS-C sequences of variants PFL0030c and PFD0615c were conservatively substituted to serine; the substituted amino acids are underlined. (B) Protein sequences of the mini-PfEMP1 constructs cloned into pBcamR_3xHA. The N-terminus of PF13_0275 includes a SS and PEXEL motif and is indicated in blue. The C-termini of ATS domains from PF08_0141 and PFF0010w are illustrated in green.

Chapter 4

Plasmodium falciparum blood stage parasites selected for binding to ICAM-1 express *var* group B PfEMP1

Alexander Oberli[1,2], Thomas Lavstsen[3] and Hans-Peter Beck[1,2,*]

Affiliation of authors:

[1] Swiss Tropical and Public Health Institute, Basel, Switzerland

[2] University of Basel, Basel, Switzerland

[3] Centre for Medical Parasitology, Department of International Health, Immunology, and Microbiology, University of Copenhagen and Department of Infectious Diseases, Rigshospitalet, Copenhagen, Denmark

[*] Corresponding author:

Molecular Parasitology Unit, Swiss Tropical and Public Health Institute, Socinstrasse 57, CH 4002 Basel, Switzerland, +41 6128 48116, e-mail: hans-peter.beck@unibas.ch

Manuscript in preparation for submission

Abstract

Sequestration of red blood cells infected with the malaria parasite *Plasmodium falciparum* to host endothelial cells has been associated with severe forms of the disease. This phenomenon is mediated by a number of host endothelial receptors and PfEMP1, parasite-derived variant antigens expressed on the surface of the infected red blood cell (iRBC). An important host receptor is the intercellular adhesion molecule-1 (ICAM-1) and there is evidence that ICAM-1 play a role in the pathology of cerebral malaria. The current study examined the PfEMP1 expression and ICAM-1 binding phenotype of 3D7 parasites. We show that PFL0020w, a group B PfEMP1 variant, binds ICAM-1 through the DBLβ domain. Moreover, for the first time we provide direct evidence for a dual binding affinity of an identified PfEMP1 variant to different endothelial receptors in 3D7 *in vitro* culture. Overall, this study contributes to the understanding of ICAM-1 binding domains and its relevance to disease.

Introduction

Sequestration of infected red blood cells (iRBCs) in the microvasculature of human organs is key to the pathogenesis of severe *Plasmodium falciparum* malaria. This process is mediated by the interaction between the antigenic variable parasite adherence ligand *Plasmodium falciparum* erythrocyte membrane protein 1 (PfEMP1) on the surface of the iRBC and host receptors on vascular endothelium. Severe malaria is associated with parasites expressing a particular subset of PfEMP1 (Jensen, 2004; Lavstsen et al., 2012; Turner et al., 2013), which elicit severe symptoms probably by conferring a particularly strong and/or detrimental host receptor interaction. Several human receptors have been suggested as interaction partners for PfEMP1 associated with severe disease, but evidence from studies of parasite binding *ex vivo* is for most candidates scarce and often ambiguous (Rowe et al., 2009). Instead, answers to the question of which PfEMP1-human receptor interaction characterizes severe malaria infections has emerged from studies focussing on typing *var/*PfEMP1 sequences and relating these to expression in patients and specific receptor interactions (Jensen et al., 2004; Lavstsen et al., 2012; Nielsen et al., 2002). PfEMP1 molecules have acquired an extraordinary large sequence diversity, but consist of relatively ordered compositions of Duffy binding like (DBL) domains and two cysteine-rich inter-domain regions (CIDR) (Rowe et al., 2009). Based on N-terminal untranslated upstream regions and DBL-CIDR domains, PfEMP1 can be divided into two main groups: A (having DBLα1-CIDRα1, β,γ or δ domains) or B/C (having DBLα0-CIDR2-6 domains). Evidence from studies of *var* expression in patients, protein-protein interactions and phenotype selected parasite clones converges towards the notion that a subset of group A PfEMP1 with CIDRα1 domains elicite severe malaria (Turner et al., 2013). This appears to be mediated by binding to endothelial protein C receptor (EPCR), while parasites expressing group B/C PfEMP1 molecules bind CD36 via CIDRα2-6 domains and rarely cause severe malaria symptoms (Cabrera et al., 2014). However, all PfEMP1 contain 2-7 additional DBL or CIDR domains, and it remains unknown what role other domains might play in cytoadhesion or pathogenicity. In particular, the intercellular adhesion molecule 1 (ICAM-1) has been suggested to play a role in iRBC binding to cerebral blood vessels (Joergensen et al., 2010; Oleinikov et al., 2009) leading to cerebral malaria, although an association with severe malaria and PfEMP1 expression phenotype has remained unclear. ICAM-1 binding has been mapped to different DBLβ domains found in group A and B/C genes

(Joergensen et al., 2010; Oleinikov et al., 2009; Smith et al., 1995) based mainly on studies of recombinant proteins. A few parasites, including both group A and B PfEMP1 expressing lines, have been demonstrated to bind ICAM-1 (Bengtsson et al., 2013). In the current study, we investigated the *var/*PfEMP1 expression and binding phenotypes of ICAM-1 selected 3D7 parasite lines to identify which PfEMP1 types readily mediate binding to ICAM-1. We show that ICAM-1 binding selects for parasites that express group B PfEMP1, which bind ICAM-1 through their DBLβ domain.

Results

iRBC binding to ICAM-1 and CD36

To create a set of parasite populations with well-defined ICAM-1 binding characteristics, *P. falciparum* 3D7 parasites were selected by sequential panning on either recombinant ICAM-1 or CD36. After four rounds of selection RNA was collected and qPCR with specific primers for all 3D7 *var* gene variants was performed. The *var* transcript profiling after the repetitive selection for CD36 or ICAM-1 binding revealed a single dominant transcript from gene PFD0615c for parasites binding to CD36 (Fig. 1B) and predominantly from genes PF07_0050 and PFL0020w for the parasites selected for binding to ICAM-1 (Fig. 1C; referred to as 3D7_ICAM-1_1st). In order to generate a single PfEMP1 expressing parasite population, antibodies raised against a recombinant protein covering the DBLγ14-DBLζ5-DBLε4 region of PFL0020w (Fig. 1A) was used to select PFL0020w expressing parasites. When tested after four rounds of selection a PFL0020w transcript dominated the *var* transcript profile (Fig. 1D; referred to as 3D7_ICAM-1_PFL0020w). To characterize the binding properties of these parasites binding to immobilized recombinant ICAM-1, CD36, EPCR and CSA was assayed under semi-static conditions. Overall, these parasites showed binding to recombinant ICAM-1 and CD36 but no significant binding to EPCR and CSA could be observed (Fig. 2A). In a similar approach parasites selected for CD36 binding expressing mainly PFD0615c showed binding only to recombinant CD36 but no significant binding to either ICAM-1, EPCR or CSA (Fig. 2B).

ICAM-1 inhibition assay

Both PFL0020w and PF07_0050 are group B genes containing a DBL domain C-terminally to their DBLα-CIDRα domains. To detect whether ICAM-1 binding of PFL0020w and PF07_0050

was mediated by the DBLβ domains as predicted from previous studies (Bengtsson et al., 2013; Howell et al., 2008) the ICAM-1 binding inhibitory effect of antibodies raised against recombinant DBLβ domain (SM11/12) of PFL0020w were tested. As control served antibodies raised against the DBLγ14-DBLζ5-DBLε4 region (51/56) of PFL0020w and a mix of antibodies raised binding to the DBLδ3, DBLβ6 and 3 domain head of PF11_0521. PF11_0521 is not expressed in any of the tested parasite cultures (indicated as control). The binding of 3D7_ICAM-1_1st (expressing both PF07_0050 and PFL0020w) to ICAM1 was reduced by 27.2% (n=3) by anti-DBLβ antibodies, whereas no reduction in binding was seen using any of the control antibodies (Fig. 2C). Similarly, only anti-DBLβ antibodies showed a strong inhibitory effect on ICAM1 binding of 3D7_ICAM-1_PFL0020w parasites, reducing binding by 80.05% (n=3) (Fig. 2D) clearly indicating that the major binding epitope of PFL0020w to ICAM-1 is located at least partly in the DBLβ domain of this PfEMP1 molecule.

Discussion

Despite recent advances in unravelling PfEMP1 mediated host-parasite interactions in *P. falciparum* malaria, the full interactome of the PfEMP1 protein family is yet to be described and the relative clinical importance of different established receptor interactions resolved. To begin answering these questions it is important to establish strong associations between PfEMP1 domain variants and human receptor binding capabilities. Studies of patient isolates are challenged both by the difficulty of identifying the PfEMP1 mediating an observed binding phenotype, lack of knowledge on which receptor interaction to test and how to recapitulate the *in vivo* conditions of parasite binding to endothelial cells. One of the best studied interactions is the binding to ICAM-1 via PfEMP1 DBLβ domains (Howell et al., 2008; Janes et al., 2011; Smith et al., 2000). ICAM-1 binding has been demonstrated from very diverse DBLβ domains subtypes unique to either of group A (DBLβ3) and group B/C (DBLβ5) PfEMP1 (Oleinikov et al., 2009). The association of ICAM1 binding with severe malaria has been unclear. It is thought that a first wave of cerebral sequestration is mediated by EPCR-binding PfEMP1 (Turner et al., 2013) causing down-regulation of EPCR and thrombomodulin on the endothelium (Moxon et al., 2013). EPCR loss and probably pro-inflammatory responses to iRBC binding causes upregulation of ICAM-1 (Moxon et al., 2013; Tripathi et al., 2007), which leads to adhesion of iRBCs expressing ICAM-1-binding group A PfEMP1 molecules. It is possible that these ambiguous results reflect binding of parasites often

causing severe pathology (group A PfEMP1 expressing) as well as parasites that rarely lead to severe symptoms (group B PfEMP1 expressing). Our current study expands our understanding of which PfEMP1 variants bind ICAM-1. The successful selection of group B type PfEMP1 suggests that parasites expressing these variants have also a high affinity for ICAM-1. However, group A PfEMP1s are often very scarcely expressed in long term established *in vitro* parasite cultures, and it is possible that insufficient group A PfEMP1 were expressed. However, it is also possible that the static ICAM-1 binding assay, also commonly used in field studies, preferentially selects for the smaller group B PfEMP1 molecules. Nevertheless, our results add to the detailed list of PfEMP1 with validated ICAM-1 binding capability.

Interestingly, the parasite line expressing PFL0020w also exhibited strong capability to bind CD36. Although these data cannot show that the same parasites could bind both receptors, it is the most likely explanation given the uniform expression of PFL0020w. This cooperative binding has previously been suggested (Ockenhouse 1992; McCormick, 1997; Yipp, 2007; Rowe, 2009), and is in agreement with the prediction of CD36 binding of the PFL0020w CIDRα domain. To our knowledge, these data are the first to provide experimental proof of a specific PfEMP1 molecule involved in a dual receptor binding. Current data support involvement of group A PfEMP1 (and the group A like DC8 PfEMP1) in severe malaria (Lavstsen et al., 2012), suggesting that parasites expressing CD36-binding PfEMP1 and possibly ICAM-1-binding PfEMP1 rarely lead to severe malaria. However, *var* transcript analysis of patient isolates based on PCR assays have been unable to target this type of PfEMP1 specifically, and more studies are required to elucidate if PfEMP1 predicted with this phenotype are associated with SM.

Single parasites express only one PfEMP1 variant at the time, although one particular 3D7 clone has been reported to express multiple variants. Within a population of parasites different PfEMP1 variants will be expressed. The qPCR results of ICAM-1 1st (Fig. 1C) suggests a population of parasites expressing two to three PfEMP1 variants including two upsB group var genes with a DBLβ domain. Further selection with specific antibody binding to the DBLβ domain of PFL0020w led to the ICAM-1 binding 3D7_ICAM-1_PFL0020w which is mainly expressing PFL0020w (Fig. 1D). The binding of the preselected parasite cell line 3D7_ICAM-1_PFL0020w to ICAM-1 was strongly inhibited with antibodies targeting the DBLβ

domain of PFL0020w, indicating that the interaction can be mapped to the DBLβ domain of PFL0020w. The small amount of iRBCs binding to ICAM-1 might be explained by binding of iRBCs expressing PFL2665c (Fig. 1D). Notably, the inhibition of binding 3D7_ICAM-1_1st was only reduced by 27.2% compared to the same parasite culture in absence of the SM11/12 Abs. This smaller amount of reduction most probably is referred to the subpopulation of parasites expressing PFL0020w.

In summary our study shows that the DBLβ domain of PFL0020w is associated with recombinant ICAM-1 binding as specific blocking antibodies resulted in strong inhibition of ICAM-1 binding. We provide the first experimental proof for dual receptor binding of a PfEMP1 variant as parasites expressing PFL0020w revealed comparable binding levels to ICAM-1 and CD36. Overall this study adds to the effort to map binding domains and thus to functionally define PfEMP1 molecules and their involvement in the various disease presentations.

Materials and Methods

Parasite culture

P. falciparum 3D7 parasites were cultured in human AB+ erythrocytes (5% haematocrit) using complete RPMI medium with 0.5% Albumax according to standard procedures (Ljungström et al., 2008). All binding assays were performed three weeks after selection and PCR confirmation was done with the identical material.

Selection for receptor binding with recombinant protein

Subpopulations of parasites were selected by panning the parental cell line over purified human recombinant CD36 (50µg/ml, Life Tech., 10752-H08H) and ICAM-1 (50µg/ml, Life Tech., 10346-H03H) according to Ockenhouse et al. (Ockenhouse et al., 1991). Briefly, recombinant proteins were dissolved in ddH_2O to the indicated final concentration and absorbed to a 6 well tissue culture plate (Falcon 353045, Corning, NY, USA) overnight at 4°C in a humid chamber. Unbound sites were blocked with 3%BSA in RPMI medium for 1h at 37°C and parasite culture was added for 2h, by gently shaking the tissue culture pate every 15 min. Unbound parasite were removed by five gentle washes with RPMI-HEPES and uninfected RBCs were added. After 24h of incubation allowing late stage parasites to release merozoite to invade unbound RBCs, the newly invaded RBCs were removed from the culture

plate and placed into continuous cell culture. This panning procedure was done four times prior to RNA isolation and adhesion assays.

Selection for receptor binding with specific antibodies

Additionally, a subset of parasites was selected for expressing a specific PfEMP1 variant on the surface of the iRBC using the following var gene domain specific antibodies: rat anti-PFL0020w DBLγ14-DBLζ5-DBLε4 (51/56), rabbit anti-PFL0020w DBLβ (SM11/12), rabbit anti-PF11_0521 DBLδ3, rabbit anti-PF11_0521 DBLβ6, rabbit anti-PF11_0521 3 domain head. For this, 200 µl of parasite culture was washed twice with RPMI-HEPES and resuspended in 2ml filter-sterilized RPMI-HEPES with 100µl antibodies. After incubation of 40 min at 37°C under shaking conditions the parasite culture was washed twice with washing medium (RPMI+gentamycin). The RBCs were resuspended in 2ml RPMI-HEPES including 50µl Biotin-conjugated anti-rat antibodies (B7139 Sigma) and incubated for 35 min at 37°C under shaking conditions. After washing 50µl streptavidin coated dynabeads (M280 Sigma) were added and incubated for 15min at 37°C under shaking conditions. The parasite expressing the specific PfEMP1 variant on the surface were collected by a magnet allowing the beads to stick. Unbound parasites were removed by washing the beads for six times with washing medium. The parasites bound to the beads were then placed into continuous cell culture. The panning procedure was done four times prior to all performed experiments.

Quantitative PCR

Ring stage cultures of parasites preselected to bind either CD36 or ICAM-1 were used as template for *var* transcript profiling, as previous described (Dahlbäck et al., 2007). The transcript abundance of each 3D7 *var* gene was determined relative to internal control transcripts by quantitative PCR using gene specific primers and cDNA synthesized from total RNA extracted from pelleted infected erythrocytes dissolved in TRIzol.

Cytoahesion assay

Purified recombinant protein was spotted on wells of 8 chamber polystyrene vessel tissue culture treated glass slide (Falcon, Big Flats, NY, USA) with concentrations as indicated and coated overnight at 4°C to allow proteins to absorb to the surface. Unbound sites were blocked with 1% BSA in RPMI medium for 1h at 37°C. The parasite cell line obtained by the repeated panning procedures were washed twice with RPMI-HEPES and spotted onto

immobilized recombinant protein and cultured under continuous and simultaneous shaking (140 rpm, proBlot 25 Rocker, Labnet International Inc, NY, USA) (105 rpm, Lab-Therm LT-W, Kühner, Switzerland) at 37°C by fixing the ProBlot 25 Rocker onto the shaking plate of the Lab-Therm shaking incubator for continuous suspension of the parasite culture over the 2h incubation time. Non-bound RBCs were removed by gently flooding each well with RPMI-HEPES and simultaneous shaking for 2 min in a total of six times. For quantification, bound RBCs were fixed with 2% glutaraldehyde in RPMI-HEPES overnight and stained with 10% Giemsa for 1h. The results are shown as mean number of parasites bound per mm^2 and 1% parasitemia or as percentage of the control binding.

Acknowledgements

The authors are grateful to Louise Turner for sharing antibodies. This work was supported by the Swiss National Science Foundation (grant 31003A_149297/1) as well as by the Lundbeck Foundation and the Danish Council for Independent Research, Medical Sciences, Sapere Aude program (DFF–4004-00624B).

References

Bengtsson, A., Joergensen, L., Rask, T.S., Olsen, R.W., Andersen, M.A., Turner, L., Theander, T.G., Hviid, L., Higgins, M.K., Craig, A., et al. (2013). A Novel Domain Cassette Identifies Plasmodium falciparum PfEMP1 Proteins Binding ICAM-1 and Is a Target of Cross-Reactive, Adhesion-Inhibitory Antibodies. J. Immunol. Author Choice *190*, 240–249.

Cabrera, A., Neculai, D., and Kain, K.C. CD36 and malaria: friends or foes? A decade of data provides some answers. Trends Parasitol. *30*, 436–444.

Dahlbäck, M., Lavstsen, T., Salanti, A., Hviid, L., Arnot, D.E., Theander, T.G., and Nielsen, M.A. (2007). Changes in var gene mRNA levels during erythrocytic development in two phenotypically distinct Plasmodium falciparum parasites. Malar. J. *6*, 78.

Howell, D.P.-G., Levin, E.A., Springer, A.L., Kraemer, S.M., Phippard, D.J., Schief, W.R., and Smith, J.D. (2008). Mapping a common interaction site used by Plasmodium falciparum Duffy binding-like domains to bind diverse host receptors: Interaction site for DBLβ−C2 and ICAM-1. Mol. Microbiol. *67*, 78–87.

Ljungström, Moll, K., Perlmann, H., Scherf, A., and Wahlgren, M. (2008). Methods in malaria research (MR4/ATCC).

Janes, J.H., Wang, C.P., Levin-Edens, E., Vigan-Womas, I., Guillotte, M., Melcher, M., Mercereau-Puijalon, O., and Smith, J.D. (2011). Investigating the Host Binding Signature on the Plasmodium falciparum PfEMP1 Protein Family. PLoS Pathog. *7*, e1002032.

Jensen, A.T.R. (2004). Plasmodium falciparum Associated with Severe Childhood Malaria Preferentially Expresses PfEMP1 Encoded by Group A var Genes. J. Exp. Med. *199*, 1179–1190.

Joergensen, L., Bengtsson, D.C., Bengtsson, A., Ronander, E., Berger, S.S., Turner, L., Dalgaard, M.B., Cham, G.K.K., Victor, M.E., Lavstsen, T., et al. (2010). Surface Co-Expression of Two Different PfEMP1 Antigens on Single Plasmodium falciparum-Infected Erythrocytes Facilitates Binding to ICAM1 and PECAM1. PLoS Pathog. *6*, e1001083.

Lavstsen, T., Turner, L., Saguti, F., Magistrado, P., Rask, T.S., Jespersen, J.S., Wang, C.W., Berger, S.S., Baraka, V., Marquard, A.M., et al. (2012). Plasmodium falciparum erythrocyte membrane protein 1 domain cassettes 8 and 13 are associated with severe malaria in children. Proc. Natl. Acad. Sci. *109*, E1791–E1800.

Moxon, C.A., Wassmer, S.C., Milner, D.A., Chisala, N.V., Taylor, T.E., Seydel, K.B., Molyneux, M.E., Faragher, B., Esmon, C.T., Downey, C., et al. (2013). Loss of endothelial protein C receptors links coagulation and inflammation to parasite sequestration in cerebral malaria in African children. Blood *122*, 842–851.

Nielsen, M.A., Staalsoe, T., Kurtzhals, J.A.L., Goka, B.Q., Dodoo, D., Alifrangis, M., Theander, T.G., Akanmori, B.D., and Hviid, L. (2002). Plasmodium falciparum Variant Surface Antigen Expression Varies Between Isolates Causing Severe and Nonsevere Malaria and Is Modified by Acquired Immunity. J. Immunol. *168*, 3444–3450.

Ockenhouse, C.F., Ho, M., Tandon, N.N., Van Seventer, G.A., Shaw, S., White, N.J., Jamieson, G. A., Chulay, J.D., and Webster, H.K. (1991). Molecular Basis of Sequestration in Severe and Uncomplicated Plasmodium falciparum Malaria: Differential Adhesion of Infected Erythrocytes to CD36 and ICAM-l. J. Infect. Dis. *164*, 163–169.

Oleinikov, A.V., Amos, E., Frye, I.T., Rossnagle, E., Mutabingwa, T.K., Fried, M., and Duffy, P.E. (2009). High Throughput Functional Assays of the Variant Antigen PfEMP1 Reveal a Single Domain in the 3D7 Plasmodium falciparum Genome that Binds ICAM1 with High Affinity and Is Targeted by Naturally Acquired Neutralizing Antibodies. PLoS Pathog. *5*, e1000386.

Rowe, J.A., Claessens, A., Corrigan, R.A., and Arman, M. (2009). Adhesion of Plasmodium falciparum-infected erythrocytes to human cells: molecular mechanisms and therapeutic implications. Expert Rev. Mol. Med. *11*, e16.

Smith, J.D., Chitnis, C.E., Craig, A.G., Roberts, D.J., Hudson-Taylor, D.E., Peterson, D.S., Pinches, R., Newbold, C.I., and Miller, L.H. (1995). Switches in Expression of Plasmodium falciparum var Genes Correlate with Changes in Antigenic and Cytoadherent Phenotypes of Infected Erythrocytes. Cell *82*, 101–110.

Smith, J.D., Craig, A.G., Kriek, N., Hudson-Taylor, D., Kyes, S., Fagen, T., Pinches, R., Baruch, D.I., Newbold, C.I., and Miller, L.H. (2000). Identification of a Plasmodium falciparum intercellular adhesion molecule-1 binding domain: A parasite adhesion trait implicated in cerebral malaria. Proc. Natl. Acad. Sci. *97*, 1766–1771.

Tripathi, A.K., Sullivan, D.J., and Stins, M.F. (2007). Plasmodium falciparum—Infected Erythrocytes Decrease the Integrity of Human Blood-Brain Barrier Endothelial Cell Monolayers. J. Infect. Dis. *195*, 942–950.

Turner, L., Lavstsen, T., Berger, S.S., Wang, C.W., Petersen, J.E.V., Avril, M., Brazier, A.J., Freeth, J., Jespersen, J.S., Nielsen, M.A., et al. (2013). Severe malaria is associated with parasite binding to endothelial protein C receptor. Nature *498*, 502–505.

Figure legends

Figure 1: Selection for iRBCs expressing PfEMP1 variants binding to ICAM-1 and CD36. (A) Schematic presentation of detected 3D7 var gene ectodomains and the corresponding antibody epitopes. (B-D) qPCR results of 3D7 parasites selected for binding to recombinant CD36 (B) ICAM-1 (C) or specific PFL0020w antibodies (D). All selection experiments were performed four times prior to RNA extraction.

Figure 2: Binding of selected iRBCs to different endothelial surface proteins. Binding of iRBCs to different endothelial receptors selected for expressing PFL0020w (A), or PFD0615c (B). The results show the mean of binding (iRBC/ mm^2/ 1% parasitemia). The effect of a set of antibodies binding to different domains of PFL0020w on the binding of iRBCs selected to express (C) PF07_0050 and PFL0020w or (D) only PFL0020w (also see Fig. 1C/1D). The results are expressed as the percentage of binding of the selected population to ICAM-1 against the percentage of the binding to ICAM-1 without antibodies (% of reference binding). The bar graphs display overall mean values across triplicate experiments using linear regression with a random effect for experiment and error bars represent the s.d. of triplicate experiments. An arbitrary threshold (black dashed line) for unspecific binding was calculated as the mean level of iRBC binding to 1% BSA plus two s.d. All recombinant proteins were immobilized in 20µl spots at 50µg/ml except for CSA (20µg/ml).

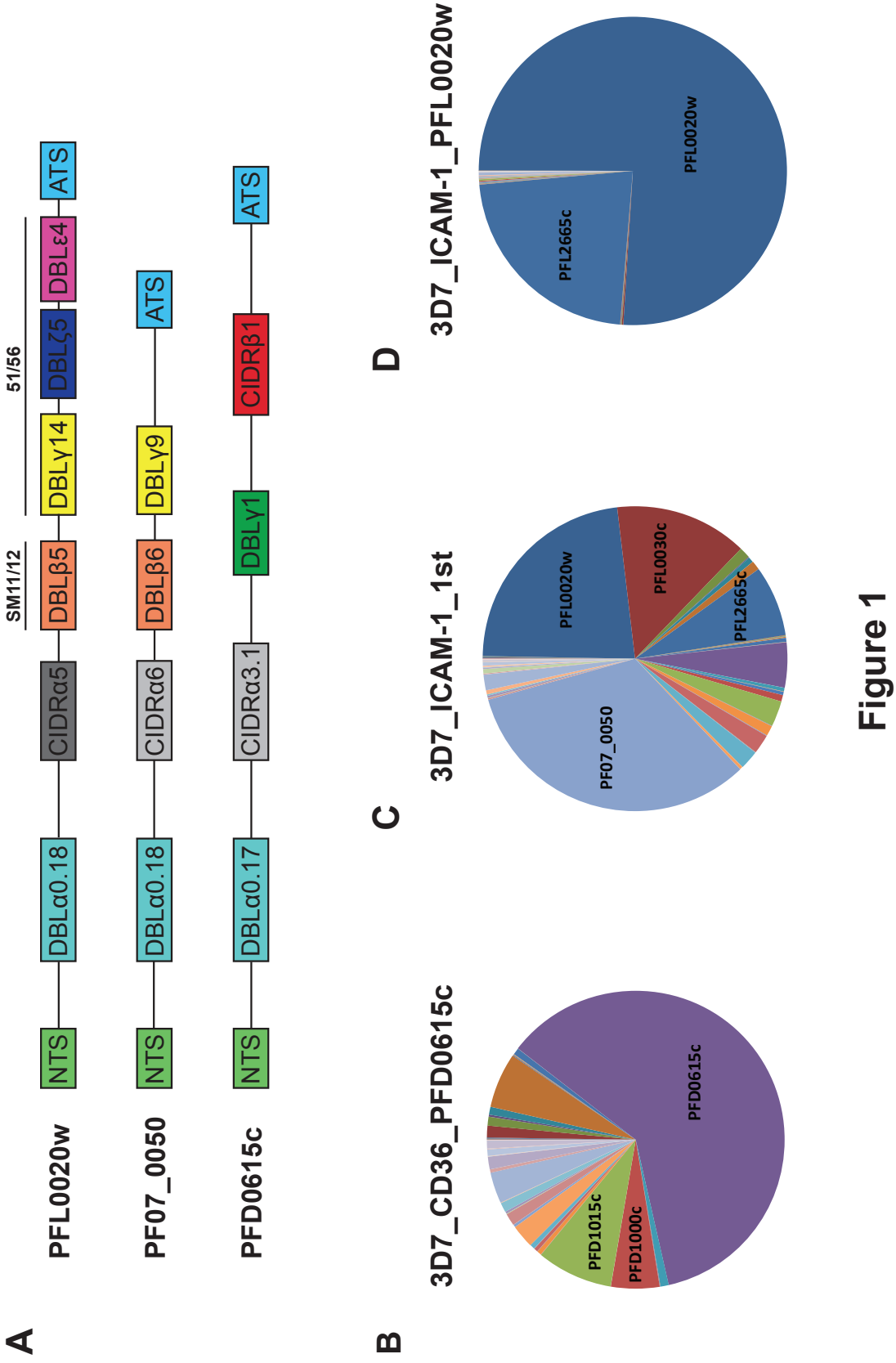
A
PFL0020w
NTS
DBLα0.18
CIDRα5
DBLβ5
DBLγ14
DBLζ5
DBLε4
ATS
SM11/12
51/56
PF07_0050
NTS
DBLα0.18
CIDRα6
DBLβ6
DBLγ9
ATS
PFD0615c
NTS
DBLα0.17
CIDRα3.1
DBLγ1
CIDRβ1
ATS
B
3D7_CD36_PFD0615c
PFD0615c
PFD1000c
PFD1015c
C
3D7_ICAM-1_1st
PFL0020w
PFL0030c
PFL2665c
PF07_0050
D
3D7_ICAM-1_PFL0020w
PFL0020w
PFL2665c

Figure 1

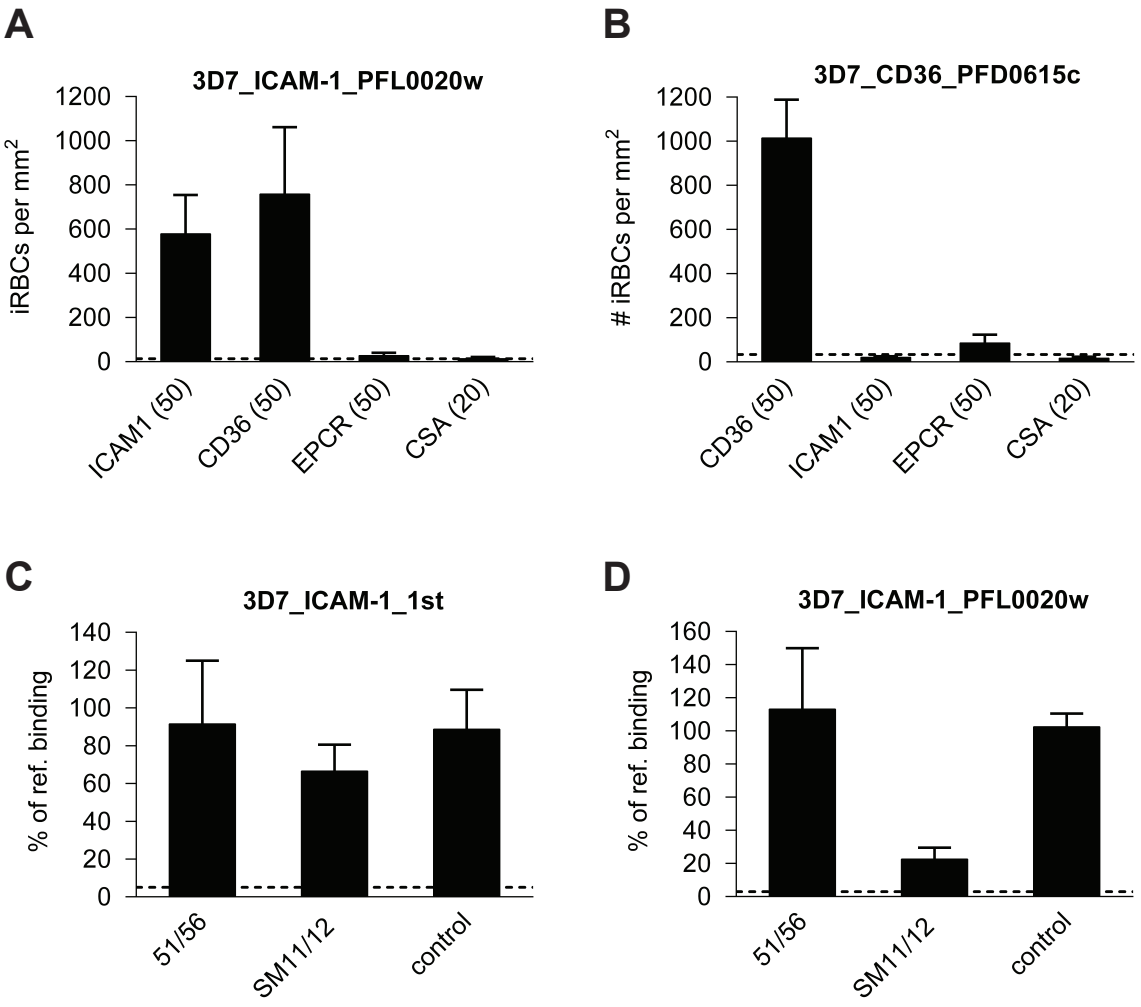
A
3D7_ICAM-1_PFL0020w
iRBCs per mm2
1200
1000
800
600
400
200
0
ICAM1 (50)
CD36 (50)
EPCR (50)
CSA (20)
B
3D7_CD36_PFD0615c
iRBCs per mm2
1200
1000
800
600
400
200
0
CD36 (50)
ICAM1 (50)
EPCR (50)
CSA (20)
C
3D7_ICAM-1_1st
% of ref. binding
140
120
100
80
60
40
20
0
51/56
SM11/12
control
D
3D7_ICAM-1_PFL0020w
% of ref. binding
160
140
120
100
80
60
40
20
0
51/56
SM11/12
control

Figure 2

Chapter 5

General Discussion

General discussion

Despite global efforts towards control and elimination of the disease, the deadliest form of malaria caused by *Plasmodium falciparum* is still responsible for approximately 580,000 deaths every year, most of them children under 5 year of age (WHO, 2014). All pathology observed is exclusively attributable to the asexual red blood cell stages of the parasite. As the erythrocyte neither possess internal organelles nor a protein export system, the parasite extensively remodels its host cell. The parasite exports a large number of proteins and generates membranous structures like Maurer's clefts, which are important structural components of the protein export system. Maurer's clefts may be a major gateway through which both soluble and membrane proteins reach the RBC membrane. Moreover the parasite induces formation of characteristic knob-like surface protrusions, which harbor the major virulence factor, *Plasmodium falciparum* erythrocyte membrane protein 1 (PfEMP1). The surface exposure of PfEMP1 mediates binding to endothelial receptors leading to adherence and sequestration of iRBCs. The subsequent obstruction of blood vessels leads to severe forms of malaria including organ failure and cerebral malaria. Recently, the conserved intracellular ATS domain of PfEMP1 was found to be a conserved protein interaction epitope (Mayer et al., 2012). It was shown that this epitope interacts with the PHIST domain of PFI1780w, a member of the *Plasmodium* Helical Interspersed Sub-Telomeric (PHIST) protein family. Therefore, Mayer and colleagues proposed that PHIST domains facilitate protein interactions and that the conserved ATS epitope may be targeted to disrupt the parasite cytoadherence (Mayer et al., 2012).

Previous work in our lab showed that the Membrane Associated Histidine-Rich Protein 2 (MAHRP2) was found to be located at Maurer's clefts tethers (Pachlatko et al., 2010). Co-immunoprecipitation experiments identified several potential interaction partners of MAHRP2 and among these, four belonged to the PHIST protein family. The initial aim of this dissertation was to reveal the potential interaction network of a subset of PHIST proteins, their function in host cell refurbishment and their influence on the transport of PfEMP1 to the iRBC surface.

Despite recent progress in functional studies using forward or reverse genetics in combination with phenotypic read-out strategies, little is known about the role of exported proteins and their relevance to disease. In a recent study, Sargeant et al. developed an

algorithm for the prediction of exported proteins in the genus *Plasmodium* (Sargeant et al., 2006). This software, termed ExportPred, uses a hidden Markov model to simultaneously model the PEXEL motif and SS features required for transport beyond the parasite's confines. This model allowed clustering of exported *Plasmodium* proteins and identified the PHIST protein family. Several studies further contributed to the classification of PHIST proteins (Frech and Chen, 2013; Oakley et al., 2007) resulting in currently 89 paralogs in *P. falciparum*, subgrouped into 28 PHISTa, 6 PHISTa-like, 24 PHISTb, 7 PHISTb DnaJ, 18 PHISTc and 6 PHIST proteins without sub-classification (own research, unpublished). Future structure prediction of exported *Plasmodium* proteins might result even in a higher number of PHIST proteins as structural similarities of proteins are difficult to detect on the basis of primary amino acid sequences. Currently, the *P. falciparum* exportome is predicted to comprise of about 550 proteins (Spielmann & Gilberger, 2015) and therefore the PHIST proteins account for approximately 16% of all exported proteins. The growing body of information on PHIST proteins suggests that they are mainly involved in two processes: cytoadherence and host cell remodeling during asexual development.

In this dissertation I focused on the characterization of the PHISTb protein PFE1605w, which is localizing to knobs, is found in membrane fractions of lysed iRBCs, interacts with the intracellular ATS domain of PfEMP1 and co-migrates with PfEMP1 in a temporal and spatial manner (Oberli et al., 2014). Initially, the objective of the thesis was to elucidate the function of four PHIST proteins, namely MAL8P1.4, PF08_0137, MAL7P1.172 and PFE1605w. However, work on MAL8P1.4 was embedded in a Master thesis (J. Warncke) and PF08_0137 had been identified to be located in J-dots, and was not further followed up. MAL7P1.172 had already been studied and reported by Maier and colleagues (Maier et al., 2008).

MAL8P1.4 was shown to be a soluble protein mainly localized in the RBC cytosol. Moreover, a faint focal pattern along the periphery of the RBC cytoplasm was detected (Warncke et al., unpublished). Interestingly, the PHIST domain of MAL8P1.4 was not shown to interact with the ATS domain of PfEMP1 (Oberli et al., 2014). PF08_0137, a PHISTc and the longest of all PHIST protein in terms of amino acid sequence was found to co-localize with HSP70x, suggesting localization to J-dots. Another PHISTc protein, MAL7P1.172 or also termed PfEMP1 trafficking protein 2 (PTP2) was shown to localize to the Maurer's clefts lumen and gene disruption resulted in a reduced level of PfEMP1 exposure on the RBC surface (Maier et

al., 2008). Moreover, in a follow-up study PTP2 was found to localize to exosomes, a newly discovered means of *P. falciparum* communication by plasmid transfer between iRBCs (Regev-Rudzki et al., 2013). Already the localization and function of the PHIST proteins of this small subset of four proteins illustrates the diverse distribution and highlights the important role of PHIST proteins in host cell refurbishment and cytoadherence.

As the PHISTc protein PFI1780w was found to biophysically interact with the ATS domain of PfEMP1 (Mayer et al., 2012) and a GFP tagged N-terminal PFI1780w reporter construct revealed a localization in the RBC cytosol (Sargeant et al., 2006) we decided to include this protein in our list of PHIST proteins to be characterized within the framework of this thesis.

Live cell imaging and solubility assays with both PFI1780w-GFP and PFE1605w-GFP expressing parasites suggested for both proteins a localization close or adjacent to the iRBC membrane. Post-embedding immunoelectron microscopy and immunofluorescence analysis of tightly synchronized 3D7 parasites revealed that both PFE1605w and PfEMP1 is exported at approximately 16-24 hpi to Maurer's clefts prior to localize to knobs, suggesting a co-transport of PFE1605w with PfEMP1. The hypothesis of PHIST proteins to function as chaperones for protein translocation emerged from the first description and report of PHIST proteins (Prajapati & Singh, 2013; Sargeant et al., 2006). This assumption probably emerged because a subset of PHISTb feature a DnaJ domain, which is a cardinal characteristic of HSP40 chaperones and is thought to mediate translocation of proteins beyond the parasite's confines. Notably, studies to unravel the export mechanism of PfEMP1 transport also indicated a possible role of a soluble chaperone complex (Knuepfer, 2005; Papakrivos et al., 2004).

With inducible down-regulation of PFE1605w but also with inducible tethering of PFE1605w at Maurer's clefts we could show that in absence of PFE1605w in knobs PfEMP1 is still exposed on the iRBC membrane, suggesting no significant role of PFE1605w in PfEMP1 transport. These findings are in accordance to previous results reported by Proellocks and colleagues, as ablation of PFE1605w in 3D7 parasites showed no change in the surface exposure of PfEMP1 compared to wild-type 3D7 parasites (Proellocks et al., 2014). Using cryo-immunoelectron microscopy, the authors suggest that PFE1605w localizes exclusively to regions of the iRBC membrane between knobs even though they mentioned the detection of one single gold particle at a knob. As the published EM image of iRBCs expressing

PFI1780w-HA displays atypical knob structures, the proposed localization of PFE1605w by Proellocks and colleagues is debatable.

In contrast to the knob localization of PFE1605w, we detected PFI1780w in close proximity to the RBC membrane but clearly absent in knobs, indicating a different functional role for PFI1780w. Moreover we could not observe an intermediate step of protein translocation from the parasite confine to the RBC membrane and inducible destabilization of PFI1780w upon Shield-1 removal was achieved to a limited amount only. Despite the different timing of export for PFI1780w and PfEMP1, it might be possible that PFI1780w is involved in trafficking of PfEMP1 as we detected a moderate binding affinity of the PHIST domain with the ATS domain of a subset of PfEMP1 variants. As competitional binding experiments with PFE1605w, which has a stronger binding affinity to ATS, showed that PFE1605w is able to dissolve the PFI1780w-ATS interaction upon addition, one could think of PFI1780w being involved in PfEMP1 transport to the RBC membrane and then being replaced by PFE1605w, which anchors PfEMP1 to the RBC cytoskeleton. As we have tested only five PHIST domains for direct binding of the PfEMP1 intracellular segment, it is likely that among the 89 detected PHIST proteins other PHIST domains show binding affinity to PfEMP1. Moreover, as we have shown that PFE1605w displays up to 25-fold differences in binding affinity to different C-terminal ATS domains of different PfEMP1 variants, different PHIST/PfEMP1 combinations may have emerged influencing the cytoadhesive properties of the iRBC and therefore affecting pathology. However, we have no experimental proof to corroborate this theory and further work is needed to reveal the function of PFI1780w.

The PEXEL motif of PFI1780w deviates from the canonical pattern by having K at position 1 (KSLAE) and therefore referred to as non-canonical PEXEL (Pick et al., 2011) which was considered not to be functional in *P. falciparum* (Boddey et al., 2013; Sleebs et al., 2014). Our full-length PFI1780w-GFP fusion protein was exported to the iRBC cytosol as previously reported for a GFP-tagged PFI1780w N-terminus reporter construct (Sargeant et al., 2006), but additionally revealed a localization adjacent to the RBC membrane. A recent study on the export of non-canonical PEXEL proteins included the expression of truncated reporter as GFP fusion proteins in *P. falciparum* (Schulze et al., 2015). The study demonstrates that the PFI1780w PEXEL motif is correctly cleaved and N-acetylated indicating that non-canonical PEXEL proteins are functional in accordance with a supportive sequence environment.

Changing K at position 1 to A (ASLAE) led to processing further downstream at an unknown site, indicating PEXEL independent translocation. Substitution of K with E (ESLAE) resulted in an unprocessed and not exported fusion protein. Interestingly, the N-terminal truncated PFI1780w reporter fusion protein comprised of aa 1-383 revealed a similar fluorescent pattern as we observed with the full-length fusion protein, but the reporter protein including aa 1-90 showed uniform RBC cytosol localization. These findings lead to the assumption that the aa 90-383 region mediates aggregation at the RBC membrane and may contain a protein interaction epitope to bind iRBC membrane/cytoskeleton components. Interestingly, the PHIST domain of PFI1780w comprises aa 98-247 and therefore might be responsible for the RBC membrane localization of the reporter construct.

As PHIST proteins are shown to play a role in host cell modification and cytoadherence, it might be possible that PFI1780w or other PHIST proteins not only bind the intracellular ATS domain of PfEMP1 but also other intracellular domains of variant surface antigens (VSA), like RIFIN, STEVOR and PfMC-2TM, which are shown to be exposed on the RBC surface (Bachmann et al., 2015; Fernandez et al., 1999; Niang et al., 2009). Besides the well-studied PfEMP1, the smaller VSA families RIFIN, STEVOR and PfMC-2TM are also assumed to play an important role in pathogenicity of malaria. Recently STEVORs were shown to bind glycophorin C on erythrocytes, therefore mediating rosetting (Niang et al., 2014) and also RIFINs were detected to be involved in sequestration and rossetting of blood group A iRBCs (Goel et al., 2015). Structural predictions of the three large protein families suggested that the variable domains are exposed on the iRBC surface and the conserved N-terminal part protrudes into the RBC cytosol (Cheng et al., 1998; Sam-Yellowe et al., 2004). Therefore, it might be possible that PHIST proteins or other exported proteins bind the conserved domains of different VSAs and anchor these molecules to the RBC cytoskeleton alike PFE1605w anchors different PfEMP1 variants to the RBC cytoskeleton. However, there is no experimental evidence for this hypothesis and an improved structure prediction algorithm for most RIFIN proteins suggests that the conserved N-terminal is exposed on the surface of the iRBC (Bultrini et al., 2009). As the conditional regulation of PFI1780w by the use of the destabilization domain was only partially successful, classical knockout strategies and tethering of PFI1780w using the knocksideway technique will hopefully reveal the exact function of PFI1780w.

Recent work on the subcellular localization of a subset of PHISTb proteins showed a predominant and uniform localization at the RBC periphery (Tarr et al., 2014). Within this subset, only one GFP-tagged PHISTb protein did not depict a peripheral localization. However, originally annotated as a PHISTb protein (Sargeant et al., 2006) it has recently been classified as a PHISTc protein (Frech & Chen, 2013). Moreover, Tarr et al. postulate that the PRESAN domain (PHIST domain with extended amino residues) is the target sequence for correct localization of these proteins in the RBC periphery. Truncated version of two PHISTb proteins, namely PFD0080c and RESA indicated that both PRESAN domains with an additional N-terminal sequence mediate peripheral localization in the iRBC periphery (Tarr et al., 2014). Current work in our lab to reveal the localization of a set of 12 PHISTb proteins also showed a peripheral localization for all GFP-fusion proteins (Jan Warncke, unpublished data). Even though little is known about the function of PHISTb proteins, the few existing functional data and localization studies suggest or show interaction with host cytoskeleton components either directly or in a protein complex.

The MESA erythrocyte cytoskeleton-binding (MEC) motif was found to be present in 14 *P. falciparum* proteins which are predicted to be exported. This motif is suggested to act as a protein module responsible for linking exported *P. falciparum* proteins to the RBC membrane (Kilili & LaCount, 2011). Notably, nine of the 14 proteins comprising the MEC motif belong to the PHISTb protein family. Moreover, six proteins with a MEC motif were shown to bind inside-out vesicles (IOVs) and half of them belong to the PHISTb family. These findings further support the hypothesis that PHISTb proteins are exported to the iRBC membrane and are involved in host cell remodeling and cytoadhesion by binding to components of the RBC cytoskeleton and to the intracellular part of RBC transmembrane proteins.

Members of large gene families of apicomplexan parasites are mostly encoded at chromosome ends and are often involved in antigenic variation or undergo diversification (Brayton et al., 2007; Gardner et al., 2002). This is also the case for *phist* genes which are encoded in the sub-telomeric regions of the chromosomes (except chromosome 3). A few studies showed that the variation in expression of this large gene family is regulated by reversible modifications to chromatin and not by copy number variation (Flueck et al., 2009; Lopez-Rubio et al., 2009; Rovira-Graells et al., 2012; Salcedo-Amaya et al., 2009). Thus,

epigenetic processes may control the expression of these genes to allow the parasite to rapidly respond to changes in the environment such as antibody recognition, reduction of nutrients or changes in the host cell ligand. As we hypothesized that there are different PHIST/PfEMP1 combinations depending on the PfEMP1 variant expressed, we performed microarray analysis to detect whether changes in *phist* expression has been observed as a response by the parasite to the expression of a different PfEMP1 variant and the conditional reduction of PFE1605w level (Fig. 1A&B, Appendix). Comparative transcriptional profiling of all three selected PFE1605w^{ON}/PFE1605w^{OFF} parasite lines revealed no increase or decrease of *phist* or *var* gene expression upon conditional depletion of PFE1605w. These findings are not very surprising as the parasite would need a feedback mechanism in order to respond to the lack of PFE1605w in knobs by either up-regulation of *pfe1605w* transcription as the parasite would try to maintain the status quo or by expressing another *phist* gene which would then take over the function of the missing *pfe1605w* gene product. However, such a feedback mechanism has never been reported in *P. falciparum* and is unlikely to exist.

To find *phist* genes differentially expressed due to selection of a specific PfEMP1 molecule, the fold change in *phist* genes between parasites binding to CD36, ICAM-1 and CSA should be compared. Interestingly, for some *phist* genes such changes were detected (Fig. 1A, Appendix). However, we cannot state that the observed transcriptional variation in the preselected parasite lines is due to switching in expression of PfEMP1 as we profiled RNA from ring stage parasites and the time point of RNA harvesting may vary between the different samples. Thus, the different preselected parasite lines cannot be compared against one another. Nevertheless, the detection of few dominantly expressed *var* genes is in accordance to our qPCR results shown in chapter 3 (Fig. 1B, Appendix).

It may also be that the cell-culture adapted parasite does not epigenetically control the expression of many exported proteins during the RBC cell cycle but rather exports a controlled basic amount of a variety of proteins regardless of the expenses for this massive amount of exported proteins and the need of these proteins in the RBC cytoplasm. This might be different *in vivo* as there are only limited resources available. It may be that several PHIST proteins have the same or a comparable affinity for a specific PfEMP1 variant and therefore another exported PHIST protein might take over the function of PFE1605w, resulting in no significant reduction of cytoadherence upon reduction of PFE1605w levels, as

seen for parasite selected to bind to CSA. One could argue that the time period of Shield-1 removal (96 hours) was too short and therefore no significant change of transcription was observed comparing the +/- Shield-1 parasite cultures. However, the inducible degradation of PFE1605w occurs fast and previous studies highlighted that transcriptional changes in parasite cultures upon removal of proteins or induced heat shocks occur rapidly (Rovira-Graells et al., 2012; Silva et al., 2005).

Different transcriptional studies showed that the PHISTa protein PF14_0752 was dramatically up-regulated after selection for binding to CD36 (Mok et al., 2007), in field isolates (Daily et al., 2005) and in 3D7 gametocytes (Eksi et al., 2005). PF14_0752 has a transcriptional peak in ring stages and therefore may be translated before the particular PfEMP1 variant is exposed on the surface of the iRBC (Le Roch et al., 2004).

So far PFE1605w is the only protein of the PHIST family reported to localize to knobs. However, the growing amount of information about PHIST proteins and unpublished data on the constituents of knobs, namely the “knobosome”, suggests a temporal or residential localization of a variety of PHIST proteins to knobs. PHISTb or PHIST proteins in general are suggested to be involved in the structural organization of knobs, as disruption of PFD1170c resulted in a knobless iRBC surface and a partial reduction of cytoadherence under flow conditions (Maier et al., 2008). This reduced cytoadhesive properties of RBCs infected with parasites lacking PFD1170c is most probably the result of absent knob structures as we showed no association of the PHIST domain of PFD1170c with the ATS domain of PfEMP1 (Oberli et al., 2014).

The knob structure appears as an electron-dense nanoscale protrusion on the iRBC surface and it is assumed that besides KAHRP, PfEMP1, PfEMP3 and MESA (Cooke et al., 2002) many other parasite-encoded proteins localize to knobs. Interestingly , a very recent study showed that the knob density on the iRBC surface depends on the PfEMP1 variant expressed (Subramani et al., 2015). Therefore it might be that knob organization and PfEMP1 expression are evolutionary related phenotypes. These findings would suggest that variable but specific requirements for PfEMP1 surface presentation and structural organization of the knobs exist. This would then provide optimal receptor affinities in different tissues with different needs for the iRBC such as speed of blood flow or abundance of the receptor molecules. This would be in accordance with our hypothesis that different PHIST/PfEMP1

combinations may have emerged. The results in chapter 3 show that down-regulation of PFE1605w levels in parasites expressing different molecules resulted in strong differences in cytoadherence, except for parasites preselected to bind CSA. Furthermore, the ATS-C fragment of VAR2CSA has a weak binding affinity to the PFE1605w PHIST domain ($K_d \sim 40$ µM) compared to other ATS-C fragments of other PfEMP1 molecules. Taken into account that the blood flow in the placenta is very low compared to other human body tissues and CSA is very abundant, only moderate anchoring of VAR2CSA might be required within the knob. In contrast, adhesion to infrequent receptors in organs with high speed blood flow needs stronger anchoring and better presentation of this specific PfEMP1 variant. As it is shown that PHIST domains bind different PfEMP1 variants with different affinities, such PHIST/PfEMP1 combination may have evolved due to different needs of surface exposure and already small differences in the semi-conserved ATS sequence may influence the capacity to bind PHIST proteins and impact the organization of knobs and therefore the anchorage of the corresponding PfEMP1 variant.

The cytoadherence complex is essential for structurally insert PfEMP1 in the iRBC membrane and is composed of different exported proteins (Wickham et al., 2001). The best-studies and probably the main structural component of knobs is KAHRP. KAHRP is shown to interact with spectrin , actin and ankyrin (Chishti et al., 1992; Kilejian et al., 1991; Magowan et al., 2000; Oh et al., 2000) and is essential for the formation of knobs (Crabb et al., 1997). Infected RBCs loaded with recombinant fragments of spectrin or ankyrin led to a diffuse distribution of KAHRP throughout the iRBC cytosol, indicating that the interaction with spectrin and ankyrin is necessary for appropriate membrane localization of KAHRP (Pei et al., 2005; Weng et al., 2014). Parasites lacking KAHRP do not form knobs but still express PfEMP1 on the RBC surface but display reduced levels of rigidity and adhesion compared to wild-type parasites (Crabb et al., 1997; Maier et al., 2008; Rug et al., 2006). Different studies with recombinant ATS and KAHRP fragments showed an interaction when immobilized on a surface (Oh et al., 2000; Waller et al., 1999, 2002). Thus, the ATS-KAHRP interaction is widely accepted in the malaria field even though no direct biophysical studies or in vivo data support the ATS-KAHRP association. Recent NMR and fluorescence anisotropy experiments under physiological conditions do not support this interaction (Mayer et al., 2012). Nevertheless, a very weak interaction with an affinity constant in the mM range cannot be excluded.

However, such an interaction would be 1,000 times weaker as previously reported with experiments using recombinant ATS and KAHRP (Oh et al., 2000; Waller et al., 1999, 2002) and therefore the physical relevance of this interaction is questionable.

It is undisputed that knob formation and therefore KAHRP is important for PfEMP1-mediated cytoadherence. However, loss of KAHRP does not reduce PfEMP1 trafficking to the iRBC surface but it dramatically reduce cytoadherence under physiological flow conditions. This is consistent with the suggestion that KAHRP does not directly bind the ATS domain of PfEMP1. As KAHRP is the main constituent of knobs, it might be that KAHRP generates the structural matrix of the knobs but shows no direct interaction to the ATS domain within the cytoadherence complex. Therefore it is likely that other molecules are involved in linking PfEMP1 to the iRBC cytoskeleton. As we report that PFE1605w directly interacts with the ATS domain of PfEMP1 but also cytoskeletal components of the host cell we suggest that PFE1605w and maybe other PHIST proteins anchor a variety of PfEMP1 molecules to cytoskeleton components of the band 3 and the 4.1R complex in the knob structures.

Adhesion of iRBC to host endothelial cells has been associated with severe form of the disease. This phenomenon is mediated by the variable ectodomain of PfEMP1 and a number of endothelial receptors which have been described in detail (Craig & Scherf, 2001). Berendt and colleagues identified ICAM-1 as an adhesion receptor for iRBCs (Berendt et al., 1989) and sequestration of iRBCs binding to ICAM-1 has repeatedly been implicated in cerebral malaria pathogenesis (Turner et al., 1994). The binding of PfEMP1 to ICAM-1 is shown to occur via one of seven Duffy-binding-like (DBLβ) domains and from diverse DBLβ domain subtypes which are unique to group A (DBLβ3) and group B/C (DBLβ5) PfEMP1 (Oleinikov et al., 2009). The knowledge of the binding site for PfEMP1 on ICAM-1 DBLβ interaction mainly derives from studies using recombinant proteins or binding adhesion studies with isolates from patients (Howell et al., 2008; Janes et al., 2011; Madkhali et al., 2014; Oleinikov et al., 2009; Smith et al., 2000; Springer et al., 2004).

The successful selection of group B type PfEMP1 in 3D7 parasite culture suggests that parasites expressing PF07_0050 and PFL0020w had the highest affinity for ICAM-1. However, it could be that group A PfEMP1s are underrepresented in long term *in vitro* parasite culture or that in static/semi-static ICAM-1 adhesion assays ICAM-1 is preferentially bound by group B PfEMP1. Moreover, a very recent study compared different *in vitro* cultivation conditions

and showed that iRBC cultured with AlbuMAX displayed a stronger reduction in cytoadhesion to endothelial receptors than iRBCs cultured with human serum (Tilly et al., 2015).

Interestingly, iRBCs expressing PFL0020w showed strong capability to bind CD36. Such a synergistic interaction between ICAM-1 and CD36 in mediating iRBC binding was previously reported using human dermal microvascular endothelial cells (HDMEC) which express both ICAM-1 and CD36 (McCormick et al., 1997). Mc Cormick and colleagues claimed that this synergistic interaction only occurs on endothelial cells and fails when the chosen adhesion molecules are immobilized on plastic. We could show that parasites expressing PFL0020w revealed binding to both ICAM-1 and CD36 even though we cannot definite be sure that the exact same parasites can bind both receptors, as we also detected moderate *pfl2665c* transcripts in the 3D7_ICAM-1_PFL0020w parasite line. Even though this CD36 binding was predictable, as PFL0020w comprises a CIDRα5 domain and binding to CD36 is known to be mediated by CIDR$\alpha_{2\text{-}6}$ domains (Smith et al., 2003), this is the first experimental proof of a specific PfEMP1 molecule involved in dual receptor binding in 3D7 *in vitro* culture. Such a dual selection for binding both CD36 and ICAM-1 has been reported for different parasite lines (Cooke et al., 1994; Janes et al., 2011). The CD36 adhesion phenotype is associated with uncomplicated malaria (Ochola et al., 2011) and it may be that these dual receptor binding PfEMP1 molecules evolved to adhere in tissues other than the brain as CD36 is absent on cerebral endothelium (Wassmer et al., 2011). This theory might explain the equivocal mechanism of cerebral malaria with the involvement of a combination of endothelial surface moieties (Esser et al., 2014).

In this thesis we show that members of the PHIST protein family bind the intracellular domain of PfEMP1 through their PHIST domain. Moreover, in collaboration we resolved the first crystallographic structure of a PHIST protein and derived a partial model of the PHIST-ATS interaction from NMR measures. This allowed us to propose a mechanistic model of the function of PHIST molecules in cytodherence. In a cell biological approach we were able to show that the PHISTb protein PFE1605w is exported to knobs, binds the C-terminal part of the ATS domain and further interacts with components of the RBC cytoskeleton. Inducible regulation of PFE1605w but also controlled tethering at Maurer's clefts resulted in reduced

adhesion of iRBCs to CD36 but did not ablate PfEMP1 surface exposure. Down-regulation of PFE1605w levels in parasites expressing different PfEMP1 molecules resulted in strong differences in cytoadherence suggesting (i) different affinities for different ATS / PfEMP1 combinations or (ii) different roles for proteins of the cytoadherence complex in anchoring PfEMP1 in knobs, depending on the expressed PfEMP1 variant.

We also investigated the var expression and binding phenotypes of ICAM-1 selected parasite lines and showed that ICAM-1 binding selects for parasites expressing PFL0020w, a group B PfEMP1, and binding is mediated through the DBLβ domain. Furthermore we show a dual binding affinity of PFL0020w to different endothelial receptors.

In conclusion, we report for the first time that a PHIST protein interacts with both PfEMP1 and the host cytoskeleton and propose a functional role of PFE1605w in anchoring different PfEMP1 molecules to the cytoskeleton thus influencing the cytoadhesive properties of iRBCs. It remains to be elucidated how other PHIST proteins and other key molecules of the cytoadherence complex further contribute to sequestration of iRBCs.

References

Bachmann, A., Scholz, J., JanSZen, M., Klinkert, M.-Q., Tannich, E., Bruchhaus, I., and Petter, M. (2015). A comparative study of the localization and membrane topology of members of the RIFIN, STEVOR and PfMC-2TM protein families in Plasmodium falciparum-infected erythrocytes. Malar. J. *14*, 274.

Berendt, A.R., Simmons, D.L., Tansey, J., Newbold, C.I., and Marsh, K. (1989). Intercellular adhesion molecule-1 is an endothelial cell adhesion receptor for Plasmodium falciparum. Nature *341*, 57–59.

Boddey, J.A., Carvalho, T.G., Hodder, A.N., Sargeant, T.J., Sleebs, B.E., Marapana, D., Lopaticki, S., Nebl, T., and Cowman, A.F. (2013). Role of Plasmepsin V in Export of Diverse Protein Families from the *Plasmodium falciparum* Exportome: Substrate Specificity of Plasmepsin V. Traffic *14*, 532–550.

Brayton, K.A., Lau, A.O.T., Herndon, D.R., Hannick, L., Kappmeyer, L.S., Berens, S.J., Bidwell, S.L., Brown, W.C., Crabtree, J., Fadrosh, D., et al. (2007). Genome Sequence of Babesia bovis and Comparative Analysis of Apicomplexan Hemoprotozoa. PLoS Pathog *3*, e148.

Bultrini, E., Brick, K., Mukherjee, S., Zhang, Y., Silvestrini, F., Alano, P., and Pizzi, E. (2009). Revisiting the Plasmodium falciparum RIFIN family: from comparative genomics to 3D-model prediction. BMC Genomics *10*, 445.

Cheng, Q., Cloonan, N., Fischer, K., Thompson, J., Waine, G., Lanzer, M., and Saul, A. (1998). stevor and rif are Plasmodium falciparum multicopy gene families which potentially encode variant antigens. Mol. Biochem. Parasitol. *97*, 161–176.

Chishti, A.H., Andrabi, K.I., Derick, L.H., Palek, J., and Liu, S.-C. (1992). Isolation of skeleton-associated knobs from human red blood cells infected with malaria parasite Plasmodium falciparum. Mol. Biochem. Parasitol. *52*, 283 – 287.

Cooke, B.M., Berendt, A.R., Craig, A.G., MacGregor, J., Newbold, C.I., and Nash, G.B. (1994). Rolling and stationary cytoadhesion of red blood cells parasitized by Plasmodium falciparum: separate roles for ICAM-1, CD36 and thrombospondin. Br. J. Haematol. *87*, 162–170.

Cooke, B.M., Glenister, F.K., Mohandas, N., and Coppel, R.L. (2002). Assignment of functional roles to parasite proteins in malaria-infected red blood cells by competitive flow-based adhesion assay. Br. J. Haematol. *117*, 203–211.

Crabb, B.S., Cooke, B.M., Reeder, J.C., Waller, R.F., Caruana, S.R., Davern, K.M., Wickham, M.E., Brown, G.V., Coppel, R.L., and Cowman, A.F. (1997). Targeted Gene Disruption Shows That Knobs Enable Malaria-Infected Red Cells to Cytoadhere under Physiological Shear Stress. Cell *89*, 287 – 296.

Craig, A., and Scherf, A. (2001). Molecules on the surface of the Plasmodium falciparum infected erythrocyte and their role in malaria pathogenesis and immune evasion. Mol. Biochem. Parasitol. *115*, 129 – 143.

Daily, J.P., Le Roch, K.G., Sarr, O., Ndiaye, D., Lukens, A., Zhou, Y., Ndir, O., Mboup, S., Sultan, A., Winzeler, E.A., et al. (2005). In Vivo Transcriptome of *Plasmodium falciparum* Reveals Overexpression of Transcripts That Encode Surface Proteins. J. Infect. Dis. *191*, 1196–1203.

Eksi, S., Haile, Y., Furuya, T., Ma, L., Su, X., and Williamson, K.C. (2005). Identification of a subtelomeric gene family expressed during the asexual–sexual stage transition in Plasmodium falciparum. Mol. Biochem. Parasitol. *143*, 90–99.

Esser, C., Bachmann, A., Kuhn, D., Schuldt, K., Förster, B., Thiel, M., May, J., Koch-Nolte, F., Yáñez-Mó, M., Sánchez-Madrid, F., et al. (2014). Evidence of promiscuous endothelial binding by Plasmodium falciparum-infected erythrocytes. Cell. Microbiol. *16*, 701–708.

Fernandez, V., Hommel, M., Chen, Q., Hagblom, P., and Wahlgren, M. (1999). Small, Clonally Variant Antigens Expressed on the Surface of the Plasmodium falciparum–Infected Erythrocyte Are Encoded by the rif Gene Family and Are the Target of Human Immune Responses. J. Exp. Med. *190*, 1393–1404.

Flueck, C., Bartfai, R., Volz, J., Niederwieser, I., Salcedo-Amaya, A.M., Alako, B.T.F., Ehlgen, F., Ralph, S.A., Cowman, A.F., Bozdech, Z., et al. (2009). Plasmodium falciparum Heterochromatin Protein 1 Marks Genomic Loci Linked to Phenotypic Variation of Exported Virulence Factors. PLoS Pathog *5*, e1000569.

Frech, C., and Chen, N. (2013). Variant surface antigens of malaria parasites: functional and evolutionary insights from comparative gene family classification and analysis. BMC Genomics *14*, 427.

Gardner, M.J., Hall, N., Fung, E., White, O., Berriman, M., Hyman, R.W., Carlton, J.M., Pain, A., Nelson, K.E., Bowman, S., et al. (2002). Genome sequence of the human malaria parasite Plasmodium falciparum. Nature *419*, 498–511.

Goel, S., Palmkvist, M., Moll, K., Joannin, N., Lara, P., R Akhouri, R., Moradi, N., Ojemalm, K., Westman, M., Angeletti, D., et al. (2015). RIFINs are adhesins implicated in severe Plasmodium falciparum malaria. Nat Med *21*, 314–317.

Howell, D.P.-G., Levin, E.A., Springer, A.L., Kraemer, S.M., Phippard, D.J., Schief, W.R., and Smith, J.D. (2008). Mapping a common interaction site used by Plasmodium falciparum Duffy binding-like domains to bind diverse host receptors. Mol. Microbiol. *67*, 78–87.

Janes, J.H., Wang, C.P., Levin-Edens, E., Vigan-Womas, I., Guillotte, M., Melcher, M., Mercereau-Puijalon, O., and Smith, J.D. (2011). Investigating the Host Binding Signature on the Plasmodium falciparum PfEMP1 Protein Family. PLoS Pathog. *7*, e1002032.

Kilejian, A., Rashid, M.A., Aikawa, M., Aji, T., and Yang, Y.-F. (1991). Selective association of a fragment of the knob protein with spectrin, actin and the red cell membrane. Mol. Biochem. Parasitol. *44*, 175–181.

Kilili, G.K., and LaCount, D.J. (2011). An Erythrocyte Cytoskeleton-Binding Motif in Exported Plasmodium falciparum Proteins. Eukaryot. Cell *10*, 1439–1447.

Knuepfer, E. (2005). Trafficking of the major virulence factor to the surface of transfected P falciparum-infected erythrocytes. Blood *105*, 4078–4087.

Lopez-Rubio, J.-J., Mancio-Silva, L., and Scherf, A. (2009). Genome-wide Analysis of Heterochromatin Associates Clonally Variant Gene Regulation with Perinuclear Repressive Centers in Malaria Parasites. Cell Host Microbe *5*, 179–190.

Madkhali, A.M., Alkurbi, M.O., Szestak, T., Bengtsson, A., Patil, P.R., Wu, Y., Alharthi, S., Jensen, A.T.R., Pleass, R., and Craig, A.G. (2014). An Analysis of the Binding Characteristics of a Panel of Recently Selected ICAM-1 Binding Plasmodium falciparum Patient Isolates. PLoS ONE *9*, e111518.

Magowan, C., Nunomura, W., Waller, K.L., Yeung, J., Liang, J., Dort, H.V., Low, P.S., Coppel, R.L., and Mohandas, N. (2000). Plasmodium falciparum histidine-rich protein 1 associates with the band 3 binding domain of ankyrin in the infected red cell membrane. Biochim. Biophys. Acta BBA - Mol. Basis Dis. *1502*, 461 – 470.

Maier, A.G., Rug, M., O'Neill, M.T., Brown, M., Chakravorty, S., Szestak, T., Chesson, J., Wu, Y., Hughes, K., Coppel, R.L., et al. (2008). Exported Proteins Required for Virulence and Rigidity of Plasmodium falciparum-Infected Human Erythrocytes. Cell *134*, 48–61.

Mayer, C., Slater, L., Erat, M.C., Konrat, R., and Vakonakis, I. (2012). Structural Analysis of the Plasmodium falciparum Erythrocyte Membrane Protein 1 (PfEMP1) Intracellular Domain Reveals a Conserved Interaction Epitope. J. Biol. Chem. *287*, 7182–7189.

McCormick, C.J., Craig, A., Roberts, D., Newbold, C.I., and Berendt, A.R. (1997). Intercellular adhesion molecule-1 and CD36 synergize to mediate adherence of Plasmodium falciparum-infected erythrocytes to cultured human microvascular endothelial cells. J. Clin. Invest. *100*, 2521.

Mok, B.W., Ribacke, U., Winter, G., Yip, B.H., Tan, C.-S., Fernandez, V., Chen, Q., Nilsson, P., and Wahlgren, M. (2007). Comparative transcriptomal analysis of isogenic Plasmodium falciparum clones of distinct antigenic and adhesive phenotypes. Mol. Biochem. Parasitol. *151*, 184–192.

Niang, M., Yan Yam, X., and Preiser, P.R. (2009). The Plasmodium falciparum STEVOR Multigene Family Mediates Antigenic Variation of the Infected Erythrocyte. PLoS Pathog *5*, e1000307.

Niang, M., Bei, A.K., Madnani, K.G., Pelly, S., Dankwa, S., Kanjee, U., Gunalan, K., Amaladoss, A., Yeo, K.P., Bob, N.S., et al. (2014). STEVOR Is a Plasmodium falciparum Erythrocyte Binding Protein that Mediates Merozoite Invasion and Rosetting. Cell Host Microbe *16*, 81–93.

Oakley, M.S.M., Kumar, S., Anantharaman, V., Zheng, H., Mahajan, B., Haynes, J.D., Moch, J.K., Fairhurst, R., McCutchan, T.F., and Aravind, L. (2007). Molecular Factors and Biochemical Pathways Induced by Febrile Temperature in Intraerythrocytic Plasmodium falciparum Parasites. Infect. Immun. *75*, 2012–2025.

Oberli, A., Slater, L.M., Cutts, E., Brand, F., Mundwiler-Pachlatko, E., Rusch, S., Masik, M.F.G., Erat, M.C., Beck, H.-P., and Vakonakis, I. (2014). A Plasmodium falciparum PHIST protein binds the virulence factor PfEMP1 and comigrates to knobs on the host cell surface. FASEB J. *28*, 4420–4433.

Ochola, L.B., Siddondo, B.R., Ocholla, H., Nkya, S., Kimani, E.N., Williams, T.N., Makale, J.O., Liljander, A., Urban, B.C., Bull, P.C., et al. (2011). Specific Receptor Usage in Plasmodium falciparum Cytoadherence Is Associated with Disease Outcome. PLoS ONE *6*, e14741.

Oh, S.S., Voigt, S., Fisher, D., Yi, S.J., LeRoy, P.J., Derick, L.H., Liu, S.-C., and Chishti, A.H. (2000). Plasmodium falciparum erythrocyte membrane protein 1 is anchored to the actin–spectrin junction and knob-associated histidine-rich protein in the erythrocyte skeleton. Mol. Biochem. Parasitol. *108*, 237–247.

Oleinikov, A.V., Amos, E., Frye, I.T., Rossnagle, E., Mutabingwa, T.K., Fried, M., and Duffy, P.E. (2009). High Throughput Functional Assays of the Variant Antigen PfEMP1 Reveal a Single Domain in the 3D7 Plasmodium falciparum Genome that Binds ICAM1 with High Affinity and Is Targeted by Naturally Acquired Neutralizing Antibodies. PLoS Pathog. *5*, e1000386.

Pachlatko, E., Rusch, S., Müller, A., Hemphill, A., Tilley, L., Hanssen, E., and Beck, H.-P. (2010). MAHRP2, an exported protein of Plasmodium falciparum, is an essential component of Maurer's cleft tethers: MAHRP2 is a component of P. falciparum tethers. Mol. Microbiol. *77*, 1136–1152.

Papakrivos, J., Newbold, C.I., and Lingelbach, K. (2004). A potential novel mechanism for the insertion of a membrane protein revealed by a biochemical analysis of the Plasmodium falciparum cytoadherence molecule PfEMP-1: Membrane association of PfEMP-1. Mol. Microbiol. *55*, 1272–1284.

Pei, X., An, X., Guo, X., Tarnawski, M., Coppel, R., and Mohandas, N. (2005). Structural and Functional Studies of Interaction between Plasmodium falciparum Knob-associated Histidine-rich Protein (KAHRP) and Erythrocyte Spectrin. J. Biol. Chem. *280*, 31166–31171.

Pick, C., Ebersberger, I., Spielmann, T., Bruchhaus, I., and Burmester, T. (2011). Phylogenomic analyses of malaria parasites and evolution of their exported proteins. BMC Evol. Biol. *11*, 167.

Prajapati, S.K., and Singh, O.P. (2013). Remodeling of human red cells infected with Plasmodium falciparum and the impact of PHIST proteins. Blood Cells. Mol. Dis. *51*, 195–202.

Proellocks, N.I., Herrmann, S., Buckingham, D.W., Hanssen, E., Hodges, E.K., Elsworth, B., Morahan, B.J., Coppel, R.L., and Cooke, B.M. (2014). A lysine-rich membrane-associated PHISTb protein involved in alteration of the cytoadhesive properties of Plasmodium falciparum-infected red blood cells. FASEB J. *28*, 3103–3113.

Regev-Rudzki, N., Wilson, D.W., Carvalho, T.G., Sisquella, X., Coleman, B.M., Rug, M., Bursac, D., Angrisano, F., Gee, M., Hill, A.F., et al. (2013). Cell-Cell Communication between Malaria-Infected Red Blood Cells via Exosome-like Vesicles. Cell *153*, 1120–1133.

Le Roch, K.G., Johnson, J.R., Florens, L., Zhou, Y., Santrosyan, A., Grainger, M., Yan, S.F., Williamson, K.C., Holder, A.A., Carucci, D.J., et al. (2004). Global analysis of transcript and protein levels across the Plasmodium falciparum life cycle. Genome Res. *14*, 2308–2318.

Rovira-Graells, N., Gupta, A.P., Planet, E., Crowley, V.M., Mok, S., Ribas de Pouplana, L., Preiser, P.R., Bozdech, Z., and Cortes, A. (2012). Transcriptional variation in the malaria parasite Plasmodium falciparum. Genome Res. *22*, 925–938.

Rug, M., Prescott, S.W., Fernandez, K.M., Cooke, B.M., and Cowman, A.F. (2006). The role of KAHRP domains in knob formation and cytoadherence of P falciparum-infected human erythrocytes. Blood *108*, 370–378.

Salcedo-Amaya, A.M., van Driel, M.A., Alako, B.T., Trelle, M.B., van den Elzen, A.M., Cohen, A.M., Janssen-Megens, E.M., van de Vegte-Bolmer, M., Selzer, R.R., Iniguez, A.L., et al. (2009). Dynamic histone H3 epigenome marking during the intraerythrocytic cycle of Plasmodium falciparum. Proc. Natl. Acad. Sci. *106*, 9655–9660.

Sam-Yellowe, T.Y., Florens, L., Johnson, J.R., Wang, T., Drazba, J.A., Le Roch, K.G., Zhou, Y., Batalov, S., Carucci, D.J., Winzeler, E.A., et al. (2004). A Plasmodium Gene Family Encoding Maurer's Cleft Membrane Proteins: Structural Properties and Expression Profiling. Genome Res. *14*, 1052–1059.

Sargeant, T.J., Marti, M., Caler, E., Carlton, J.M., Simpson, K., Speed, T.P., and Cowman, A.F. (2006). Lineage-specific expansion of proteins exported to erythrocytes in malaria parasites. Genome Biol. *7*, R12.

Schulze, J., Kwiatkowski, M., Borner, J., Schlüter, H., Bruchhaus, I., Burmester, T., Spielmann, T., and Pick, C. (2015). The *P lasmodium falciparum* exportome contains non-canonical PEXEL/HT proteins: PEXEL/HT plasticity. Mol. Microbiol. *97*, 301–314.

Silva, M.D., Cooke, B.M., Guillotte, M., Buckingham, D.W., Sauzet, J.-P., Scanf, C.L., Contamin, H., David, P., Mercereau-Puijalon, O., and Bonnefoy, S. (2005). A role for the Plasmodium falciparum RESA protein in resistance against heat shock demonstrated using gene disruption: Phenotyping resa-KO Plasmodium falciparum parasites. Mol. Microbiol. *56*, 990–1003.

Sleebs, B.E., Lopaticki, S., Marapana, D.S., O'Neill, M.T., Rajasekaran, P., Gazdik, M., Günther, S., Whitehead, L.W., Lowes, K.N., Barfod, L., et al. (2014). Inhibition of Plasmepsin V Activity Demonstrates Its Essential Role in Protein Export, PfEMP1 Display, and Survival of Malaria Parasites. PLoS Biol. *12*, e1001897.

Smith, J.D., Craig, A.G., Kriek, N., Hudson-Taylor, D., Kyes, S., Fagen, T., Pinches, R., Baruch, D.I., Newbold, C.I., and Miller, L.H. (2000). Identification of a Plasmodium falciparum intercellular adhesion molecule-1 binding domain: A parasite adhesion trait implicated in cerebral malaria. Proc. Natl. Acad. Sci. *97*, 1766–1771.

Smith, T.G., Serghides, L., Patel, S.N., Febbraio, M., Silverstein, R.L., and Kain, K.C. (2003). CD36-Mediated Nonopsonic Phagocytosis of Erythrocytes Infected with Stage I and IIA Gametocytes of Plasmodium falciparum. Infect. Immun. *71*, 393–400.

Spielmann, T., and Gilberger, T.-W. (2015). Critical Steps in Protein Export of Plasmodium falciparum Blood Stages. Trends Parasitol. *31*, 514–525.

Springer, A.L., Smith, L.M., Mackay, D.Q., Nelson, S.O., and Smith, J.D. (2004). Functional interdependence of the DBLβ domain and c2 region for binding of the Plasmodium falciparum variant antigen to ICAM-1. Mol. Biochem. Parasitol. *137*, 55 – 64.

Subramani, R., Quadt, K., Jeppesen, A.E., Hempel, C., Petersen, J.E.V., Hassenkam, T., Hviid, L., and Barfod, L. (2015). *Plasmodium falciparum* -Infected Erythrocyte Knob Density Is Linked to the PfEMP1 Variant Expressed. mBio *6*, e01456–15.

Tarr, S.J., Moon, R.W., Hardege, I., and Osborne, A.R. (2014). A conserved domain targets exported PHISTb family proteins to the periphery of Plasmodium infected erythrocytes. Mol. Biochem. Parasitol. *196*, 29–40.

Tilly, A.-K., Thiede, J., Metwally, N., Lubiana, P., Bachmann, A., Roeder, T., Rockliffe, N., Lorenzen, S., Tannich, E., Gutsmann, T., et al. (2015). Type of in vitro cultivation influences cytoadhesion, knob structure, protein localization and transcriptome profile of Plasmodium falciparum. Sci. Rep. *5*, 16766.

Turner, G.D.H., Morrison, H., Jones, M., Davis, T.M.E., Looareesuwan, S., Buley, I.D., Gatter, K.C., Newbold, C.I., Pukritayakamee, S., Nagachinta, B., et al. (1994). An Immunohistochemical Study of the Pathology of Fatal Malaria: Evidence for Widespread Endothelial Activation and a Potential Role for Intercellular Adhesion Molecule-1 in Cerebral Sequestration. Am. J. Pathol. *145*, 1057–1069.

Waller, K.L., Cooke, B.M., Nunomura, W., Mohandas, N., and Coppel, R.L. (1999). Mapping the Binding Domains Involved in the Interaction between the Plasmodium falciparum Knob-associated Histidine-rich Protein (KAHRP) and the Cytoadherence Ligand P. falciparumErythrocyte Membrane Protein 1 (PfEMP1). J. Biol. Chem. *274*, 23808–23813.

Waller, K.L., Nunomura, W., Cooke, B.M., Mohandas, N., and Coppel, R.L. (2002). Mapping the domains of the cytoadherence ligand Plasmodium falciparum erythrocyte membrane protein 1 (PfEMP1) that bind to the knob-associated histidine-rich protein (KAHRP). Mol. Biochem. Parasitol. *119*, 125–129.

Wassmer, S.C., Moxon, C.A., Taylor, T., Grau, G.E., Molyneux, M.E., and Craig, A.G. (2011). Vascular endothelial cells cultured from patients with cerebral or uncomplicated malaria exhibit differential reactivity to TNF. Cell. Microbiol. *13*, 198–209.

Weng, H., Guo, X., Papoin, J., Wang, J., Coppel, R., Mohandas, N., and An, X. (2014). Interaction of Plasmodium falciparum knob-associated histidine-rich protein (KAHRP) with erythrocyte ankyrin R is required for its attachment to the erythrocyte membrane. Biochim. Biophys. Acta BBA - Biomembr. *1838*, 185–192.

Wickham, M.E., Rug, M., Ralph, S.A., Klonis, N., McFadden, G.I., Tilley, L., and Cowman, A.F. (2001). Trafficking and assembly of the cytoadherence complex in Plasmodium falciparum-infected human erythrocytes. EMBO J. *20*, 5636–5649.

WHO, Global Malaria Programme, and World Health Organization (2014). World Malaria Report 2014.

Outlook

In this dissertation we have identified the PHISTb protein PFE1605w to play a functional role in cytoadherence of iRBC by anchoring different PfEMP1 variants to cytoskeletal components of the host cell. Furthermore, we resolved the first crystallographic structure of a PHIST protein confirming the predicted α-helical conformation of the PHIST domain and derived a model of the PHIST-PfEMP1 interaction. Although this thesis contributes to the better understanding of the cytoadhesion process and sheds light on protein interactions at the host-parasite interface, additional work remains to validate and elucidate the overall role of PHIST proteins in cytoadherence and host cell refurbishment.

First, the different levels of reduction in cytoadherence detected upon reduction of PFE1605w levels in parasite lines preselected to express a particular PfEMP1 variant on the surface of the iRBC should be explained. For this purpose we selected a cell biological and a biochemical approach. With exported mini-PfEMP1 constructs consisting of a PEXEL/SS motif, the ATS domain of the detected PfEMP1 variants (PFD0615c, PF07_0050, PFL0020w, PFL0030c) and a tag, proteins interacting with the ATS domain of the particular PfEMP1 molecule should be detected. This approach could lead to the detection of potential PHIST/PfEMP1 combinations.

Co-IP and reverse Co-IP experiments with PFE1605w and α-band 4.2 antibodies respectively, revealed different components of the band 3 complex and the 4.1R complex as potential interaction partners of PFE1605w. In a next step these different potential interaction partners should be tested for a direct interaction with PFE1605w and may be mapped to specific residues or a specific domain of PFE1605w.

As Co-IP experiments with components normally enriched at the interface of the iRBC membrane/cytoskeleton are complex and a challenging task we plan to generate a construct encompassing the human erythrocyte band 4.2 protein. The construct would be similar to our mini-PfEMP1 constructs but instead of the ATS-C fragment of PfEMP1 the fusion protein comprises a full-length human erythrocyte band 4.2 fragment. Thus, the idea would be that the parasite exports soluble *P. falciparum* codon-optimized full-length human erythrocyte band 4.2 fragments and Co-IP experiments coupled with mass spectrometry would enable us to detect potential band 4.2 interaction partners. If successful, we could replace the band

4.2 sequence by any other *P. falciparum* codon-optimized sequence or fragment of a component of the host cytoskeleton.

Third, the function of PFI1780w should be identified. As the PFI1780w-DD fusion protein could not be degraded upon Shield-1 removal I would suggest to tether PFI1780w at the PVM by using the knocksideways technique (e.g. heterodimerization with Exp1) to dissect the transport and to reveal the function of PFI1780w. Furthermore one could try to tether PFI1780w at Maurer's clefts (e.g. heterodimerization with MAHRP1) even though no transient localization of PFI1780w at Maurer's clefts has been observed so far. In addition, further attempts to generate a PFI1780w knockout parasite line should be made.

Newly established methods like transfection of merozoites, CRISPR/Cas9 and the knocksideways technique in our lab has opened the door to faster identify and target parasite gene products that may play a role in pathogenesis and disease outcome. Thus, instead of focusing on the characterization of a single protein, a selection of related proteins can simultaneously be analyzed and characterized.

A large-screen approach to test the interaction of different PHIST domains with the ATS domain of PfEMP1 may identify additional members of the PHIST protein family to bind PfEMP1. Here, the focus would be on members of the PHISTb and PHISTc subclass, as many PHISTb/c proteins were shown to localize to the periphery of the iRBC. Moreover, potential binding of PHIST domains to the semi-conserved intracellular domain of other variant surface antigens like RIFINs and STEVORs should be tested.

The work in this dissertation focused on asexual RBC stages of *P. falciparum*. Recent work indicates that parasite protein export profoundly marks early sexual differentiation and *P. falciparum* gametocyte-exported proteins (PfGEXPs) contribute to host cell remodeling. Recent data on a PHISTc protein, namely PfGEXP5, being early exported from gametocytes into the host cell cytoplasm and transcriptional upregulation of some *phista* genes in gametocytes indicate that members of the PHIST protein family might contribute to host cell refurbishment in this phase of the lifecycle. Therefore it would be important to unravel the function of PHIST proteins in gametocytes.

Appendix

Transcriptional changes upon conditional depletion of PFE1605w

Method

Synchronized cultures of PFE1605w-DD expressing parasites preselected to bind either CD36, ICAM-1 or CSA were split and cultured 96 hours in presence (^{ON}) or absence (^{OFF}) of Shield-1. Subsequently, when the parasites became ring stage parasites, RNA was isolated from 30ml culture (5% haematocrit, 2-5% parasitemia) using RiboZol RNA extraction reagent (Amresco) and cDNA synthesis was carried out as described (Bozdech et al., 2003). Cy5-labeled cDNA was hybridized against a Cy3-labeled 3D7 cDNA reference pool generated from mixed stages from five consecutive timepoints of the RBC cell cycle. Equal amounts of Cy5- and Cy3-samples were hybridized on an Agilent *P. falciparum* glass slide microarray as described (Painter et al., 2013). Slides were washed twice with 6xSSPE/0.005% SDS, once in 0.06xSSPE/0.005% SDS, dried and scanned using a GenePix 4000B microarray scanner and GenePix pro 7 software. Normalization and background elimination was performed with Acuity 4.1 software. Heatmaps were generated using TreeView software.

Lack of transcriptional changes in absence of PFE1605w

We formulated the hypothesis that specific combinations of PHIST and PfEMP1 variants might have evolved to anchor PfEMP1 within the knobs. To test this proposition we conducted comparative transcriptional profiling of all pre-selected PFE1605w^{ON}/PFE1605w^{OFF} parasites. We profiled RNA from the same batch of parasites that were tested in binding assays. To identify genes differentially expressed in direct response to selection we focussed our analysis on the members of the *phist* (Fig. 1A) and *var* gene families (Fig. 1B). No significant increase or decrease of *phist* gene expression upon conditional depletion of PFE1605w was observed. The detection of few dominantly expressed *var* genes are in accordance to our performed qPCR results shown in chapter 3.

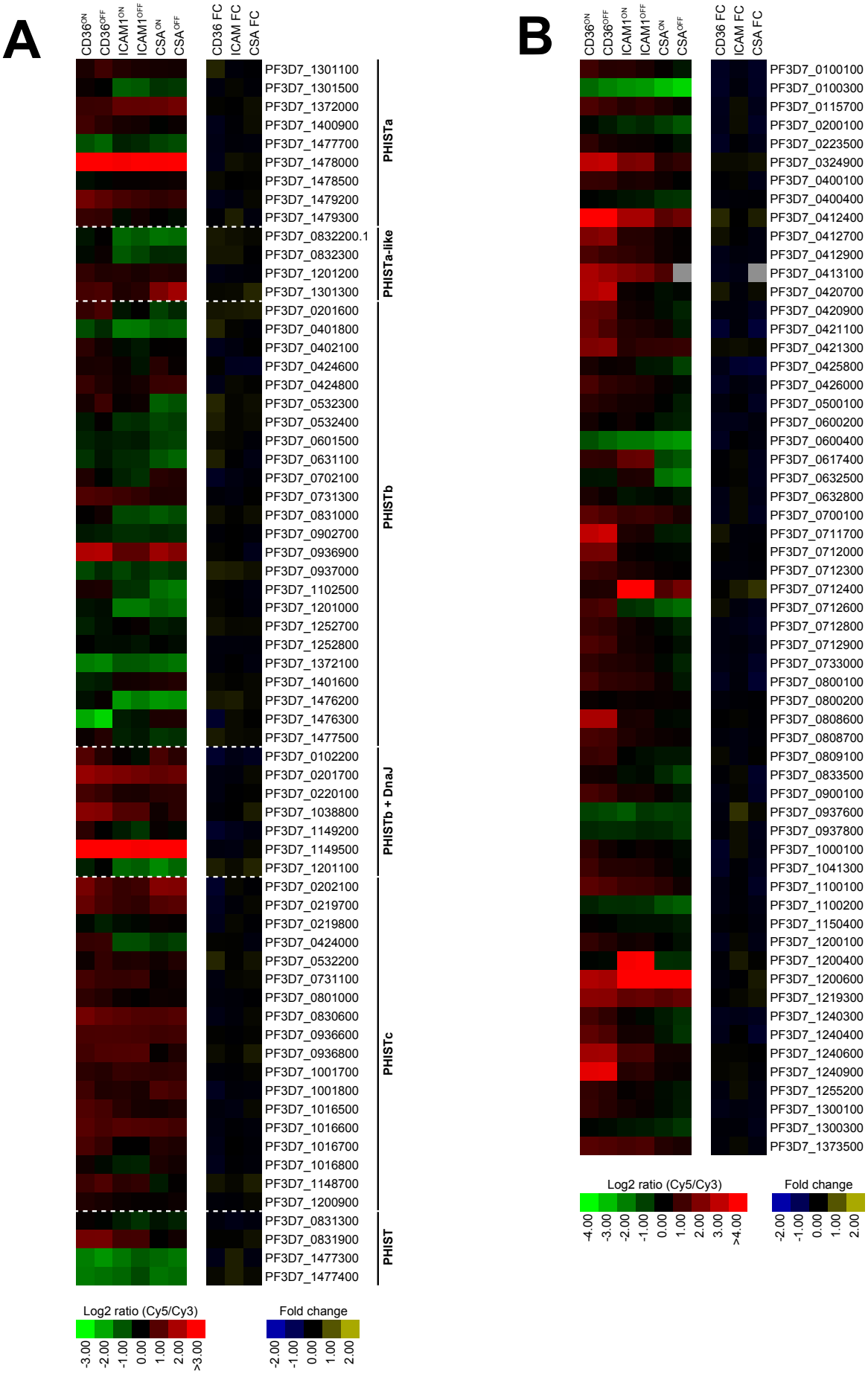
A
CD36ON
CD36OFF
ICAM1ON
ICAM1OFF
CSAON
CSAOFF
CD36 FC
ICAM FC
CSA FC
PF3D7_1301100
PF3D7_1301500
PF3D7_1372000
PF3D7_1400900
PF3D7_1477700
PF3D7_1478000
PF3D7_1478500
PF3D7_1479200
PF3D7_1479300
PF3D7_0832200.1
PF3D7_0832300
PF3D7_1201200
PF3D7_1301300
PF3D7_0201600
PF3D7_0401800
PF3D7_0402100
PF3D7_0424600
PF3D7_0424800
PF3D7_0532300
PF3D7_0532400
PF3D7_0601500
PF3D7_0631100
PF3D7_0702100
PF3D7_0731300
PF3D7_0831000
PF3D7_0902700
PF3D7_0936900
PF3D7_0937000
PF3D7_1102500
PF3D7_1201000
PF3D7_1252700
PF3D7_1252800
PF3D7_1372100
PF3D7_1401600
PF3D7_1476200
PF3D7_1476300
PF3D7_1477500
PF3D7_0102200
PF3D7_0201700
PF3D7_0220100
PF3D7_1038800
PF3D7_1149200
PF3D7_1149500
PF3D7_1201100
PF3D7_0202100
PF3D7_0219700
PF3D7_0219800
PF3D7_0424000
PF3D7_0532200
PF3D7_0731100
PF3D7_0801000
PF3D7_0830600
PF3D7_0936600
PF3D7_0936800
PF3D7_1001700
PF3D7_1001800
PF3D7_1016500
PF3D7_1016600
PF3D7_1016700
PF3D7_1016800
PF3D7_1148700
PF3D7_1200900
PF3D7_0831300
PF3D7_0831900
PF3D7_1477300
PF3D7_1477400
PHISTa
PHISTa-like
PHISTb
PHISTb + DnaJ
PHISTc
PHIST
Log2 ratio (Cy5/Cy3)
-3.00
-2.00
-1.00
0.00
1.00
2.00
>3.00
Fold change
-2.00
-1.00
0.00
1.00
2.00
B
CD36ON
CD36OFF
ICAM1ON
ICAM1OFF
CSAON
CSAOFF
CD36 FC
ICAM FC
CSA FC
PF3D7_0100100
PF3D7_0100300
PF3D7_0115700
PF3D7_0200100
PF3D7_0223500
PF3D7_0324900
PF3D7_0400100
PF3D7_0400400
PF3D7_0412400
PF3D7_0412700
PF3D7_0412900
PF3D7_0413100
PF3D7_0420700
PF3D7_0420900
PF3D7_0421100
PF3D7_0421300
PF3D7_0425800
PF3D7_0426000
PF3D7_0500100
PF3D7_0600200
PF3D7_0600400
PF3D7_0617400
PF3D7_0632500
PF3D7_0632800
PF3D7_0700100
PF3D7_0711700
PF3D7_0712000
PF3D7_0712300
PF3D7_0712400
PF3D7_0712600
PF3D7_0712800
PF3D7_0712900
PF3D7_0733000
PF3D7_0800100
PF3D7_0800200
PF3D7_0808600
PF3D7_0808700
PF3D7_0809100
PF3D7_0833500
PF3D7_0900100
PF3D7_0937600
PF3D7_0937800
PF3D7_1000100
PF3D7_1041300
PF3D7_1100100
PF3D7_1100200
PF3D7_1150400
PF3D7_1200100
PF3D7_1200400
PF3D7_1200600
PF3D7_1219300
PF3D7_1240300
PF3D7_1240400
PF3D7_1240600
PF3D7_1240900
PF3D7_1255200
PF3D7_1300100
PF3D7_1300300
PF3D7_1373500
Log2 ratio (Cy5/Cy3)
-4.00
-3.00
-2.00
-1.00
0.00
1.00
2.00
3.00
>4.00
Fold change
-2.00
-1.00
0.00
1.00
2.00

Figure 1: Conditional depletion of PFE1605w in parasites expressing a particular PfEMP1 variant does not alter *phist* expression

Relative expression profiles (Cy5/Cy3 log2 ratios) and fold change (FC) in gene expression of all *phist* (A) and *var* (B) genes in parasites selected for binding to either recombinant CD36, ICAM-1 or CSA. Parasites expressing PFE1605w-DD were grown for 96 hours in presence (e.g. $CD36^{ON}$) or absence (e.g $CD36^{OFF}$) of 625 nM Shield-1.

References

Bozdech, Z., Llinás, M., Pulliam, B.L., Wong, E.D., Zhu, J., and DeRisi, J.L. (2003). The transcriptome of the intraerythrocytic developmental cycle of Plasmodium falciparum. PLoS Biol *1*, e5.

Painter, H., Altenhofen, L., Kafsack, B.C., and Llinás, M. (2013). Whole-Genome Analysis of Plasmodium spp. Utilizing a New Agilent Technologies DNA Microarray Platform. In Malaria, R. Ménard, ed. (Humana Press), pp. 213–219